



**HAL**  
open science

# Development of safe and efficient aav vectors for retinal gene therapy

Hanen Khabou

► **To cite this version:**

Hanen Khabou. Development of safe and efficient aav vectors for retinal gene therapy. *Neurons and Cognition* [q-bio.NC]. Sorbonne Université, 2018. English. NNT : 2018SORUS460 . tel-02926062

**HAL Id: tel-02926062**

**<https://theses.hal.science/tel-02926062>**

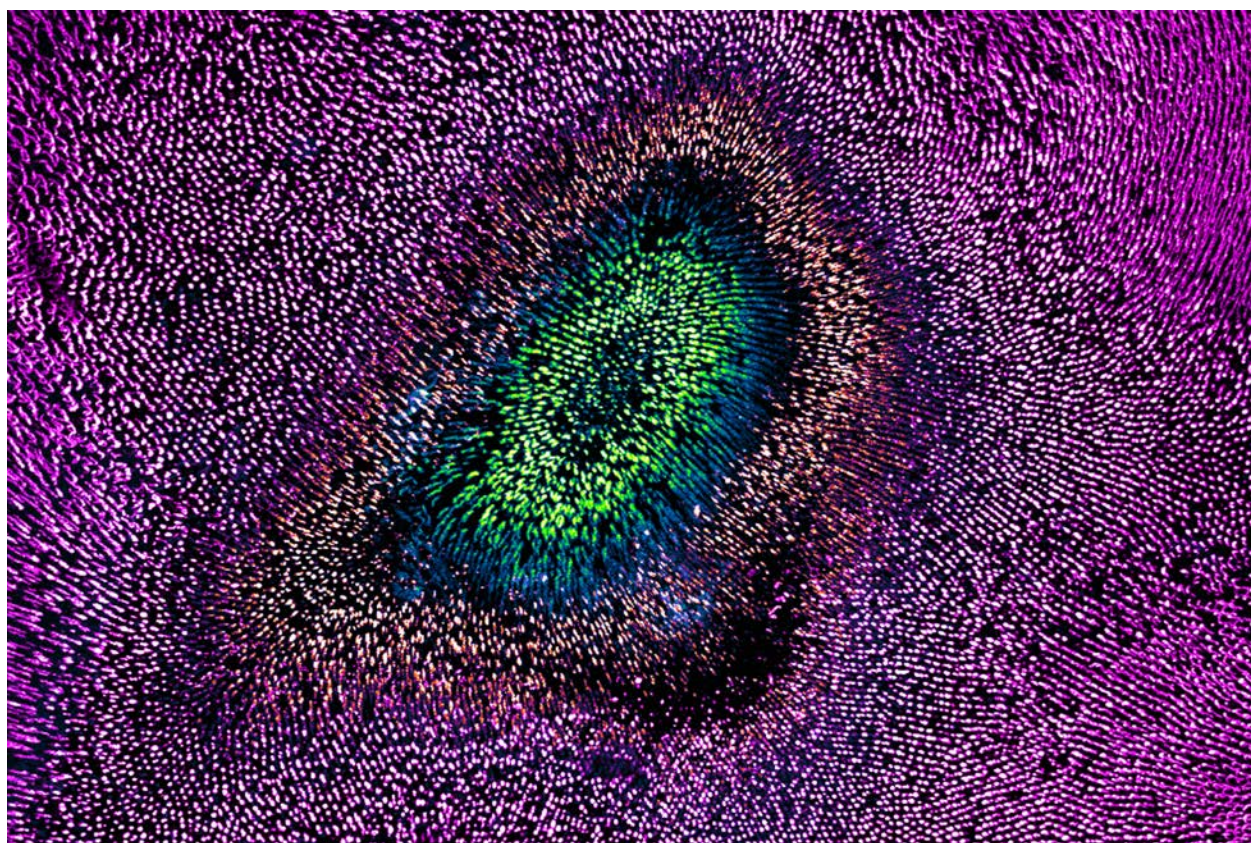
Submitted on 31 Aug 2020

**HAL** is a multi-disciplinary open access archive for the deposit and dissemination of scientific research documents, whether they are published or not. The documents may come from teaching and research institutions in France or abroad, or from public or private research centers.

L'archive ouverte pluridisciplinaire **HAL**, est destinée au dépôt et à la diffusion de documents scientifiques de niveau recherche, publiés ou non, émanant des établissements d'enseignement et de recherche français ou étrangers, des laboratoires publics ou privés.

# Development of safe and efficient AAV vectors for retinal gene therapy

Thèse de doctorat présentée par Hanen Khabou  
Pour obtenir le grade de docteur de Sorbonne Universités-UPMC  
Sciences de la Vie, spécialité Neurosciences



Soutenance de thèse le 13 avril 2018, devant un jury composé de:

Pr. Philippe Ravassard	Directeur de Recherches CNRS, France	Examineur
Dr. Leah Byrne	Chercheuse à l'Université de Pittsburgh, Etats-Unis	Rapporteuse
Pr. Dominik Fischer	Professeur à l'Université de Tübingen, Allemagne	Rapporteur
Dr. Deniz Dalkara	Chargée de Recherches INSERM, France	Directrice de thèse



*To my family,*

*And to my previous teachers and supervisors, from school to university.*

*Thank you for everything*



# Acknowledgments/Remerciements

*To all the people that contributed to this work and helped me during my thesis, thank you! I sincerely enjoyed working with all of you.*

*I thank Pr Fischer and Dr Byrne, for accepting to evaluate my work; and Pr Ravassard as well –who also took part in my ‘half-thesis’ committees. Thank you Sylvain for your feedback in these committees as well.*

*I met Deniz when she gave a talk at the the Brain and Spine Institute in Paris where I was doing a master internship in Claire Wyart’s team. This is when all this work started! I take the opportunity here to thank my previous research internships’ supervisors, with whom I learned so much and made me love science and research even more. Thank you Laura and Marco; thank you Céline, Lydia, and Claire for your support and all that you taught me!*

Je remercie le Pr Sahel grâce à qui j’ai pu m’inscrire en thèse puisque Deniz n’avait pas encore son HDR il y a quelques années.

Deniz, merci de m’avoir accueilli dans ton équipe en stage de M2, puis en thèse; merci de m’avoir fait confiance et de ton soutien tout au long de ces années ! J’ai énormément appris à tes côtés. Merci aussi pour tes conseils et critiques qui m’ont permis de m’améliorer. Merci également de m’avoir encadrée comme tu l’as fait: c’est-à-dire avec beaucoup de liberté, mais tout en étant aussi très disponible et à l’écoute.

Merci à toute l’équipe, qui a bien changé au fil du temps ! Merci à la fois aux anciens et aux membres actuels: Peggy et Adeline, Eleonore, Arthur, Catherine, Muge.

Merci Mélissa et Céline W pour toute votre aide en bio mol, surtout pour les clonages,  
Merci Emilie et Camille, pour toutes les “prods” d’AAVs !

*Marcela, I wanted to write this in Spanish, but since you don’t even notice the difference anymore when I write to you in English or Spanish it’s useless ;) It was really great to work together, and I am happy that our joint efforts led to our publication. Your strength and courage are inspiring. I sincerely wish you all the best for your future directions!*

Merci Laure G et Fiona pour tous les organoïdes.

Merci Cardillia, en particulier pour ton aide précieuse sur les manips de comportement.

*Thank you Diane, for all our discussions and post-lab meeting lunches!*

Merci également aux étudiants que j’ai encadrés, en particulier Chloé, pour ton sérieux et ton enthousiasme pendant tes deux stages de M1 et M2; et Laure P. pour ton implication lorsque nous avons continué ce même projet.

Merci à chacun de vous pour tous les bons moments au labo et hors du labo; et d'avoir fait de la team "S15" une équipe où il est si agréable de travailler. Bonne chance pour avancer et finir vos projets respectifs, et pour la suite !

Merci également à toutes les personnes des plateformes de l'IdV ! Stéphane F, merci pour ton aide et ta disponibilité au confocal à chaque fois que j'ai eu un problème... Merci Valérie, pour ta disponibilité et ta gentillesse, surtout pour les dissections de dernière minute pour nous tous à l'IdV, et pour m'avoir montré la culture de rétines de primates. Merci également à tous les membres de l'animalerie IdV, en particulier Manu, Julie D et Quénot qui sont toujours disponibles pour aider ou résoudre un problème de manip... Plus généralement, merci à vous tous aux animaleries de l'IdV et de Mircen qui prenez soin des animaux !

Ce travail n'aurait pas vu voir le jour sans nos collaborateurs au sein et hors de l'IdV: Merci beaucoup à Antoine, pour toutes les manip de patch sur ces rétines si précieuses !! -ainsi qu'à Jens. Céline N, Stéphane B, Elena, Claire-Maëlle, Joanna, merci pour les manip à Mircen ! Merci à Sacha, Olivier G et Amélie; à Gwenaëlle et Alexis au CEA; ainsi que Sylvain, Julie V et Gaëlle à Généthon. Merci aussi à Romain et Olivier M pour m'avoir appris les bases du MEA. Merci Giulia pour ton aide, et pour tout les moments partagés pendant nos années de thèse !

Merci à toutes les autres personnes de l'IdV avec qui j'ai eu l'occasion de travailler: Alvaro, ainsi que Pierre et Annabelle.

Merci aussi à l'AFM-Téléthon, qui a financé ma thèse durant ces 4 années.

Et parce que les moments les plus difficiles de la thèse ont été le début et la fin, et la révision des articles, j'adresse un merci tout particulier aux personnes qui ont été présentes dans ces moments-là ! Merci à Mélissa et Céline W pour votre expertise en bio mol; merci à Marie, Adeline et Peggy pour leur aide durant mes premières manip à l'animalerie.

*Last but not least, thank God I have the best family in the world!* A ma mère, et à mon père, merci pour votre soutien constant. Merci à mes trois 'petites' soeurs, Anwaar (pardon, Anwaâr !) et Marwa pour tous les fous rires et tout le reste. Merci aussi pour toutes les répétitions des oraux (et surtout pour les re re répétitions) ! Et Tassou, merci d'être le rayon de soleil de la famille, tout simplement !







# Index

<b>Acknowledgments/Remerciements</b> .....	<b>5</b>
<b>Index of Figures</b> .....	<b>11</b>
<b>List of abbreviations</b> .....	<b>13</b>
<b>Introduction</b> .....	<b>15</b>
<b>I. Introduction to the visual system</b> .....	<b>17</b>
i. Visual system and the retina .....	17
1. Anatomy of the visual system.....	17
2. Structure of the retina .....	18
ii. Structure and properties of mammalian photoreceptors .....	22
1. Interspecies differences in photoreceptor function and distribution .....	22
2. Functional properties of photoreceptors .....	25
3. Retinal circuitry after activation of the phototransduction cascade .....	26
iii. The fovea, responsible for high acuity vision in primates .....	27
1. Human visual field .....	27
2. Structure of the fovea .....	28
3. Development of the fovea .....	29
4. Foveal cones .....	29
<b>II. Gene therapy and retinal diseases: a successful combination?</b> .....	<b>31</b>
i. Retinal disorders .....	31
1. Complexity and heterogeneity of retinal disorders .....	31
2. Retinitis Pigmentosa, the most common form of inherited retinal degeneration	32
ii. Current versus emerging ocular gene therapies, and future challenges .....	34
1. General principle of gene therapy and advantages of the eye as a target organ	34
2. Gene augmentation strategies .....	35
3. Mutation-independent gene therapy approaches.....	39
<b>III. Vectorology: the puzzle of gene therapy</b> .....	<b>43</b>
i. How to transfer a DNA drug safely to the retina in the long-term? .....	43
1. Non-viral vectors.....	43
2. Adenoviral and retroviral vectors .....	44
3. Adeno-associated vectors .....	44
4. Safety and long-lasting effects of AAV vectors .....	48
ii. How to deliver genes specifically to cone photoreceptors? .....	49
1. Choosing the appropriate administration route .....	49
2. Choosing the appropriate capsid.....	52
3. Selection of cell-type specific promoters .....	54
iii. How to maximize AAV vector efficiency?.....	54
1. Optimizing the expression cassette.....	54

2. Other ways of enhancing gene transfer efficiency .....	55
iv. Translation of gene therapy from rodents to primates .....	56
<b>IV. Objectives of the PhD project: gene delivery to cones for mutation</b>	
<b>independent gene therapy .....</b>	<b>59</b>
i. Therapeutic objectives .....	59
ii. Specific objectives and steps of my thesis.....	61
<b>Results .....</b>	<b>63</b>
<b>I. Toxicity study of AAV vectors at high-input doses.....</b>	<b>65</b>
<b>II. Design and characterization of enhanced capsids for photoreceptor</b>	
<b>transduction 91</b>	
<b>III. Translational aspects: noninvasive foveal targeting and efficient vision</b>	
<b>restoration .....</b>	<b>107</b>
<b>IV. Combined gene therapies for longer lasting vision restoration.....</b>	<b>127</b>
iii. Aims and methodology .....	127
iv. Evaluation of the therapeutic benefits of RdCVF <i>in vivo</i> .....	129
v. Restorative optogenetic therapy using Jaws in blind mice .....	130
vi. Progress made towards the initial aim and next steps.....	133
<b>Discussion &amp; Perspectives .....</b>	<b>135</b>
<b>Bibliography.....</b>	<b>141</b>
<b>Annexes .....</b>	<b>151</b>
<b>I. Supplementary results of Chapter I.....</b>	<b>152</b>
<b>II. Supplementary results of Chapter II.....</b>	<b>154</b>
<b>III. Supplementary results of Chapter III.....</b>	<b>160</b>
<b>Abstract.....</b>	<b>173</b>
<b>Résumé .....</b>	<b>174</b>

# Index of Figures

Figure 1: Visual perception of patients affected by various retinal disorders .....	16
Figure 2: Structure of the visual system .....	17
Figure 3: Structure of the retina and the light-sensitive photoreceptors .....	18
Figure 4: Importance of retinal interneurons in visual processing. ....	20
Figure 5: Importance of non-neuronal cell types in retinal homeostasis. ....	21
Figure 6: Opsins and human color vision .....	22
Figure 7: Types of photoreceptors and their distribution in the mouse versus human retina .....	23
Figure 8 : Calyceal processes of the primate retina .....	24
Figure 9: Differences between mouse and primate visual system and the resulting visual perception. .....	24
Figure 10: Schematic representation of the phototransduction cascade in cones .....	26
Figure 11: Retinal circuit activation in response to light stimulus. ....	27
Figure 12 : Differentiable areas and angles for perception of motion, colors, shapes and texts.....	28
Figure 13: Structure of the fovea. ....	28
Figure 14: Structure of the foveal avascular zone (FAZ).....	29
Figure 15: Properties of the peripheral versus foveal retinal circuitr .....	31
Figure 17 : Eye fundus images of a healthy retina versus Retinitis Pigmentosa (RP) patient retinas .....	32
Figure 18: Description of Retinitis Pigmentosa (RP) .....	33
Figure 19: Principle of vector and DNA combination for gene therapy with the example of adeno- associated viral vectors. ....	34
Figure 20: Rods feed cones to promote their survival through RdCVF secretion. ....	40
Figure 21: Optogenetic tools from microbial origin used for vision restoration.....	41
Figure 22: Optogenetic therapy proof-of-concept studies with different target cells .....	41
Figure 23: Goggles compatible with optogenetic reactivation .....	42
Figure 24: Vectors for gene delivery .....	45
Figure 25: Diversity of gene delivery vector sizes and shapes .....	45
Figure 26: Structure of AAV capsid proteins .....	47
Figure 27: Delivery of gene therapy drug to the primate retina using subretinal or intravitreal injections. ....	50
Figure 28: Barriers to retinal transduction after intravitreal AAV delivery.....	51
Figure 29: Directed evolution process to select for best variants to transduce outer retinal layers. .	53
Figure 30: AAV2-7m8 enhanced retinal gene delivery properties.....	54
Figure 31: Summary of methods used to improve gene delivery using AAV vectors.....	56
Figure 32: Structure and thickness of the inner limiting membrane (ILM), an important barrier to AAV particles and determinant of transduction patterns .....	57
Figure 33: Differences between mouse and primate eyes .....	58
Figure 34 : Gene therapy strategies to treat the fovea.....	60
Figure 35: Optokinetics reflex is improved after early AAV-RdCVF administration in rd10 pups....	129
Figure 36: Effect of RdCVF on cones in the long-term.....	130
Figure 37: Evaluation of vision restoration in Jaws injected animals .....	131
Figure 38: Ex-vivo recordings of retinal activity after injection with Jaws or GFP .....	132

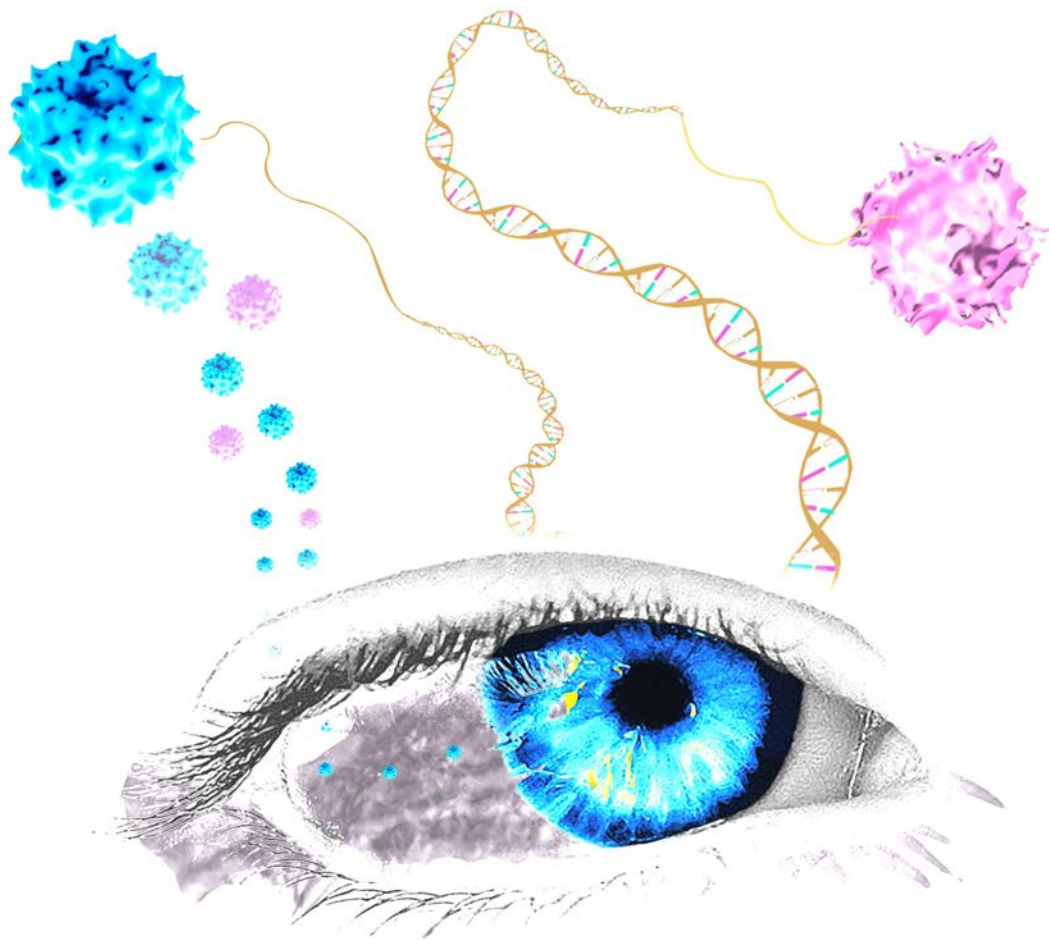


# List of abbreviations

<b>AAV</b>	Adeno-Associated Virus
<b>AMD</b>	Age-related Macular Degeneration
<b>CAG promoter</b>	Cytomegalovirus early enhancer/chicken $\beta$ actin promoter
<b>cDNA</b>	complementary DNA
<b>ChR</b>	Channelrhodopsin
<b>cGMP</b>	cyclic Guanosine MonoPhosphate
<b>CMV</b>	Cytomegalovirus promoter
<b>CNG</b>	Cyclic-Nucleotide Gated channel
<b>ELM</b>	External Limiting Membrane
<b>FAZ</b>	Foveal Avascular Zone
<b>GFP</b>	Green Fluorescent Protein
<b>HEK</b>	Human Embryonic Kidney
<b>HSPG</b>	Heparan Sulfate ProteoGlycans
<b>ILM</b>	Inner Limiting Membrane
<b>INL</b>	Inner Nuclear Layer
<b>ITRs</b>	Inverted Terminal Repeats
<b>LCA</b>	Leber Congenital Amaurosis
<b>LGN</b>	Laterate Geniculate Nucleus
<b>NHP</b>	Non-Human Primate
<b>NpHR</b>	Halorhodopsin
<b>OLM</b>	Outer Limiting Membrane
<b>ONL</b>	Outer Nuclear Layer
<b>ORF</b>	Open Reading Frame
<b>OS</b>	Outer Segments
<b>POS</b>	Photoreceptor Outer Segments
<b>PDE</b>	Phosphodiesterase
<b>PRs</b>	Photoreceptors
<b>RP</b>	Retinitis Pigmentosa
<b>qPCR</b>	quantitative Polymerase Chain Reaction
<b>rAAV</b>	recombinant Adeno-Associated Virus
<b>RdCVF</b>	Rod-derived Cone Viability Factor
<b>RGCs</b>	Retinal Ganglion Cells
<b>RPE</b>	Retinal Pigmented Epithelium
<b>sc</b>	self-complementary Adeno-Associated Virus
<b>ss</b>	single-stranded Adeno-Associated Virus
<b>vg</b>	viral genome
<b>VP1, VP2, VP3</b>	Viral Protein 1, Viral Protein 2, Viral Protein 3



# Introduction



©D. Dalkara



## Context

The eye is an ideal organ for the development of gene-based therapies as it is easily accessible for surgical injection and it responds well to local treatments without systemic effects. Moreover, the retina is a post-mitotic tissue where gene transfer can provide long-term production of a therapeutic protein. It is perhaps due to these favorable properties of the eye that the first examples of clinical success in gene therapy have been obtained ten years ago for the treatment of Leber Congenital Amaurosis, a rare retinal degenerative disease. This has been achieved with the use of adeno-associated viral vectors that efficiently carry and deliver therapeutic genes to the retina. Since, the human eye is in the forefront of future gene therapy clinical trials and there is now an urgent need to develop new viral variants more efficient for retinal gene delivery. Optimization of gene therapy vectors is expected to help us spare and save sight in more patients suffering from retinal disease in the years to come.

Photoreceptor degenerative disorders like retinitis pigmentosa and other rod-cone dystrophies are characterized by a central island of surviving neuronal tissue until the fifth decade of life, and to save this area —i.e. the fovea, from further degeneration or reanimate it using vision restoration strategies would be the obvious target for next generation gene therapies. Indeed, the fovea is the region of the primate retina responsible for high acuity daylight vision and the distinction of colors, and it is crucial to activities such as reading, driving and recognizing faces.

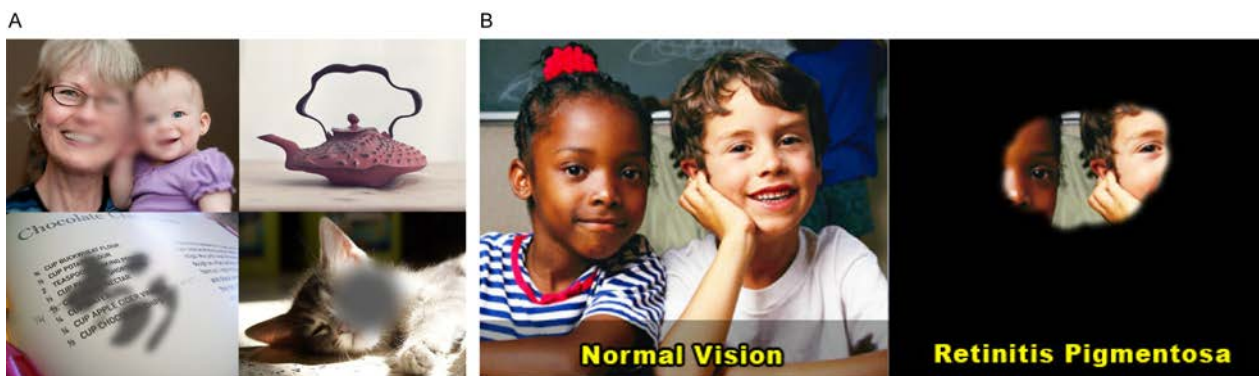


**Figure 1: Visual perception of patients affected by various retinal disorders.** (A) Blurry or distorted images, and blind spots are perceived by patients with Age-Related Macular Degeneration (AMD) that affects the fovea. Adapted from <http://www.scienceofamd.org>. (B) Other pathologies however, first lead to peripheral vision loss. Resulting 'tunnel vision' is typically observed for Retinitis Pigmentosa where the fovea is preserved. End-stage disease development leads to blindness. Adapted from <http://herbalcareproductstreatment.wordpress.com>.

My thesis objective was to design new gene delivery vectors to non-invasively target cone photoreceptors in the fovea, to enable mutation independent gene therapies such as vision restoration using optogenetics and neuroprotection. To place my PhD project in context, I will first present the structure of the eye and the retina. Second, inherited retinal disorders and their causes will be exposed, together with current therapeutic options to fight these diseases. Finally, I will stress the importance of viral vector design to obtain efficacious treatments, and the different available methods to obtain such vectors.

## I. Introduction to the visual system

### i. Visual system and the retina

#### 1. Anatomy of the visual system

The visual system is composed of two major organs: the eye, a sensory organ, and the brain. They are directly connected via the optic nerve (Figure 2). The lateral geniculate nucleus (LGN) is the main central connection between the eye and the visual cortex. The LGN –located in the thalamus– is thus a relay center for the visual pathway, and projects to the primary visual cortex (V1) at the back of the head in the occipital lobe. Afterwards, complex cortico-cortical connexions between other visual areas of the brain allow representation of movements, colors, shapes, etc. For example, in the mouse visual system there are seven functionally different visual areas that encode a unique information (1).

The retina –lining the back of the eye– is the light sensor of the visual system. Light passes through pupil, lens and vitreous before reaching the light-sensitive retina. The fovea of primates, responsible for high acuity vision, is located in the central region of the retina, referred to as the macula (Figure 2).

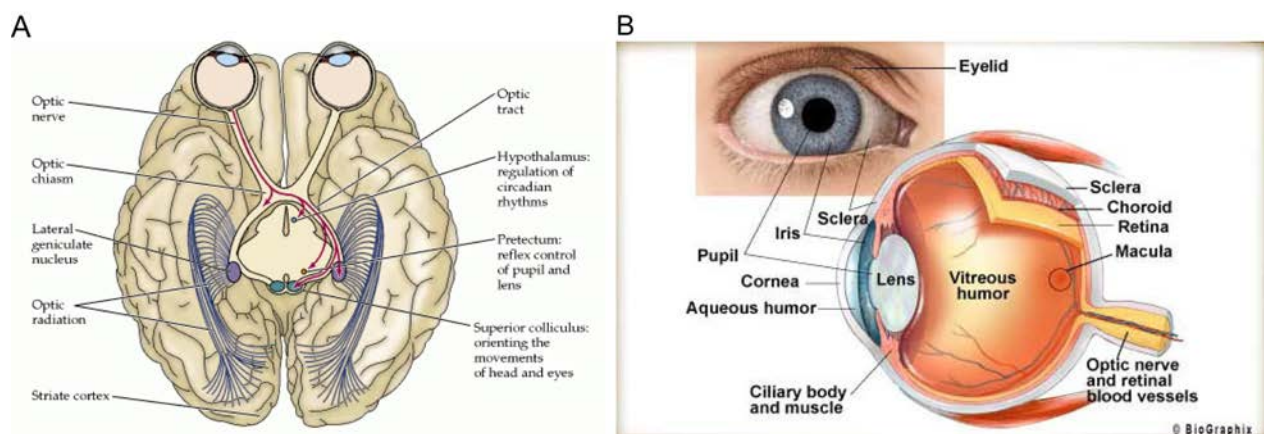


**Figure 2: Structure of the visual system.** (A) The eye is connected to the brain via the optic nerve, which projects to different structures, including the lateral geniculate nucleus (LGN) in the thalamus, the superior colliculus, the pretectum and the hypothalamus. Projections of the LGN end in the primary visual cortex (V1) also known as the striate cortex. Adapted from *Neuroscience*, Sinauer Associates, 2001. (B) Schematic representation of the eye. The retina is the light sensor of the eye and is located at the back of the eye. The fovea is located at the center of the macula.

## 2. Structure of the retina

The retina is a complex and fragile neural tissue composed of five main types of neurons (Figure 3). Photoreceptors (PRs) are the primary neurons of the retina that capture light and convert it into electrical and chemical signals. There are two types of PRs: first, rods that allow night and peripheral vision. Cones however, allow daylight, color vision and in primates, they are also necessary for central, high acuity vision. Rod and cone PRs sense light with their outer segments (OS) to which they owe their name (Figure 3). OS are filled with stacks of membranes containing visual pigments such as rhodopsins or cone opsins that absorb photons, which lead to activation of PRs.

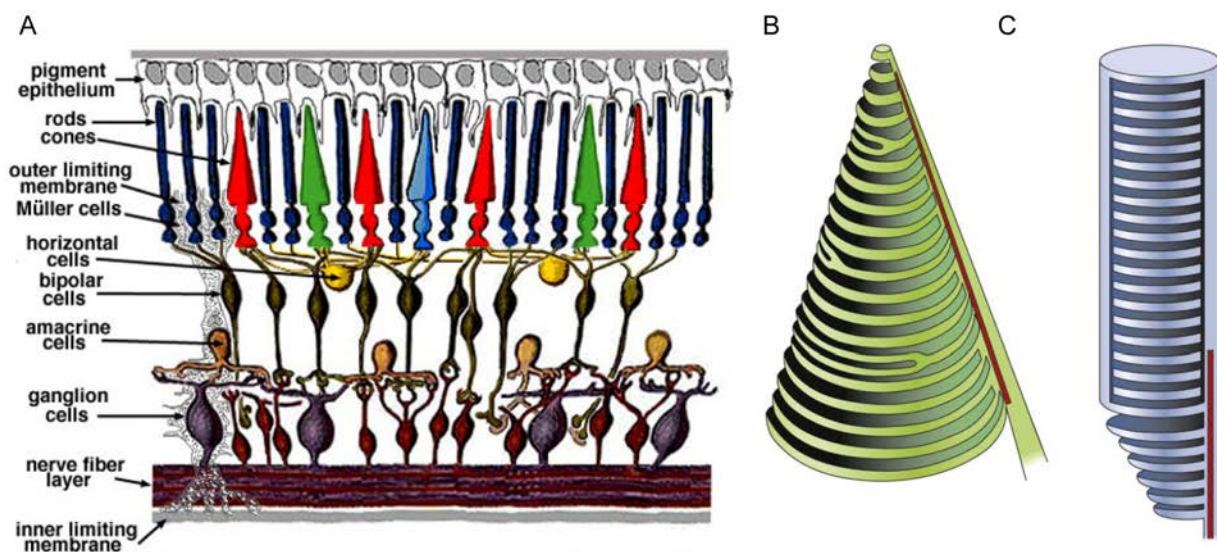


**Figure 3: Structure of the retina and the light-sensitive photoreceptors.** (A) Schematic representation of major retinal cell types. Adapted from <http://www.webvision.med.utah.edu>. (B) Schematic representation of cone photoreceptor outer segments, where cone opsins are located. Adapted from (2). (C) Schematic representation of rod photoreceptor outer segments, where rhodopsin is located. Adapted from (2).

Signals sent by PRs are processed by retinal bipolar cells (3), and finally reach retinal ganglion cells (RGCs) (Figure 3) whose axons form the optic nerve connecting the eye to the brain (Figure 2). Importantly, horizontal and amacrine cells control and modulate these signals (4). The cone-bipolar-horizontal cell synapse constitutes the first synapse of the retina. Horizontal cells makes us able to look at both bright and dim objects at the same time, by measuring and modulating the levels of illumination that fall upon different regions of the retinal surface (Figure 4 and (4, 5)). On the other hand, amacrine cells are controllers of ganglion cell responses and have diverse functions –which are mostly unknown (4). An example of their role in motion object detection is shown in Figure 4. While there are only 5 main types of neurons, altogether more than 60 subtypes are found in the mammalian retina (4). Retinal circuitry and visual processing is highly complex and not fully understood.

Apart from these neurons there are other retinal cell types important for retinal functioning such as cells of the retinal pigment epithelium (RPE). The RPE is a melanin containing epithelium that lines the back of the eye (Figures 3 and 5). RPE cells are the most distant cells to the light that enters the pupil. The RPE not only allows backscattering the light that enters the eye, but also actively participates to the visual cycle by its involvement in the phototransduction, an enzyme cascade following photon capture by visual pigments. Moreover, to maintain normal vision, RPE cells constantly renew photoreceptor outer segments through phagocytosis (6).

Retinal glia also play vital roles to the health of neurons. Glial cells include astrocytes, microglial cells and Müller cells. Astrocytes are located in the RGC layer and are part of the blood retinal-barrier. Microglial cells fulfil a key role in controlling immune responses. Finally, Müller cells are the major type of glial cells in the retina (Figure 3) responsible for homeostasis, metabolic support and neuroprotection (7). They are also more directly involved in synaptic activity by the uptake of glutamate. Interestingly, Müller cells also form architectural support and act as living optic fibers that guide light from the vitreous side to the photoreceptors (8) with their peculiar morphology (Figure 5). Cell bodies of Müller cells are located in the inner nuclear layer (INL) while they extend to both RGC side and PR side (Figure 3). One endfeet ends at the level at the external limiting membrane (ELM) while the other end forms the inner limiting membrane (ILM). Finally, Müller glial cells are involved in the formation and maintenance the blood-retinal barrier, and in the uptake of nutrients and disposal of metabolites under physiological conditions (9).

Blood and oxygen supply of the retina is ensured by the choroid (Figure 5) -located under the RPE- whose vessels irrigate the retina (10, 11). The fovea is an exception to that as it is avascular (Figure 5), but the minor thickness of this region permits its oxygenation via the choroidal circulation (11).

I will now focus on the structural and functional properties of retinal light-sensitive neurons: the photoreceptors, particularly the cones.

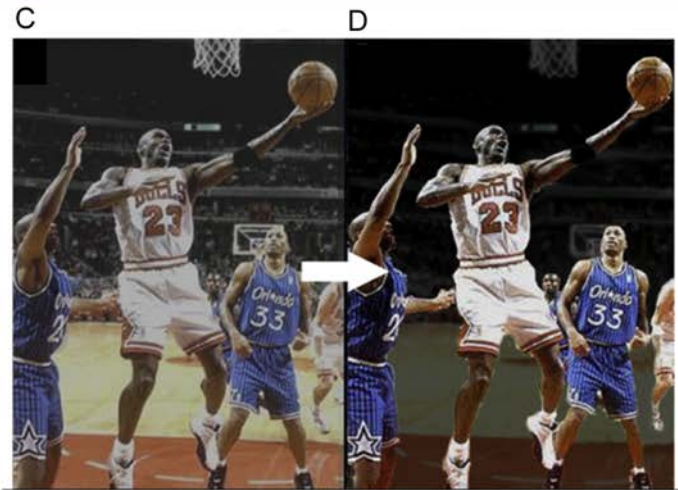
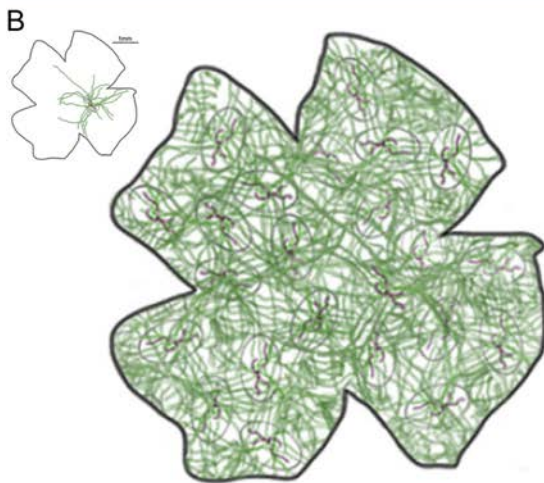
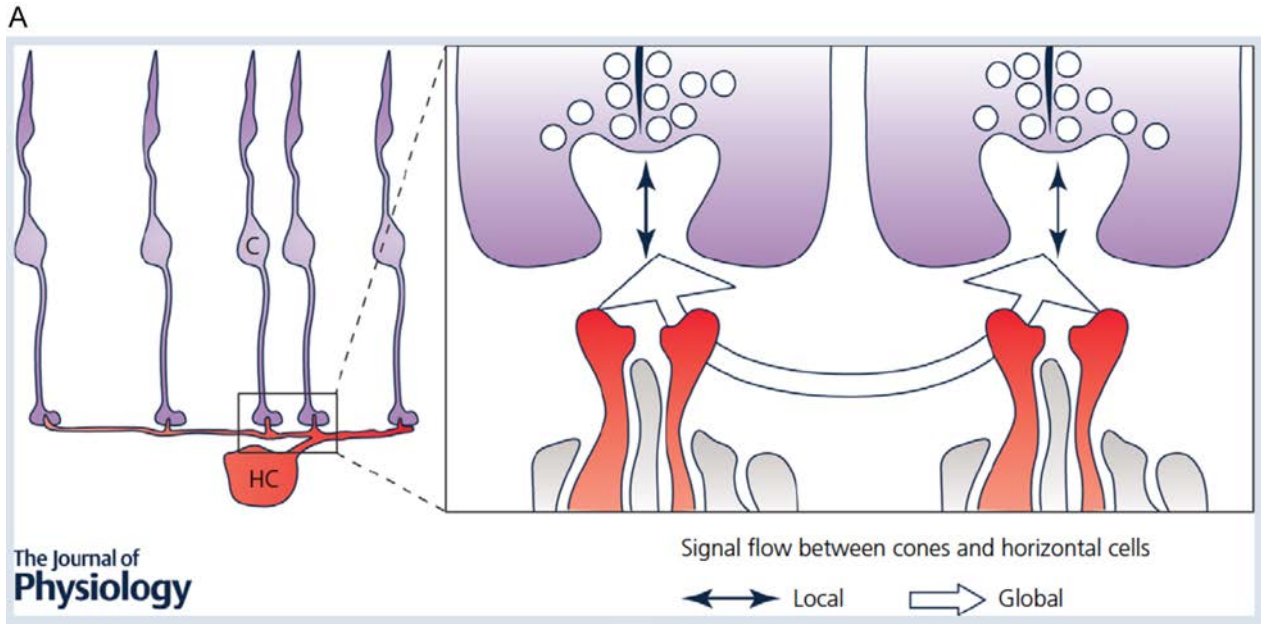


**Figure 4: Importance of retinal interneurons in visual processing.** (A) Horizontal cells modulate both local and global signal flows coming from cones (5). (B) Widefield amacrine cell morphology (inset) shows that a single widefield amacrine cell covers a large area of the retina (4). A few number of those cells is sufficient to cover the whole retinal surface. (C-D) Object motion detection enhancement by widefield amacrine cells. (C) Native image. (D) Image transmitted to the brain after object motion enhancement. Widefield amacrine cells involved in motion detection stress on perception of moving parts of the visual scenes only, by making retinal ganglion cells respond most strongly to objects that are moving relative to stationary surroundings.

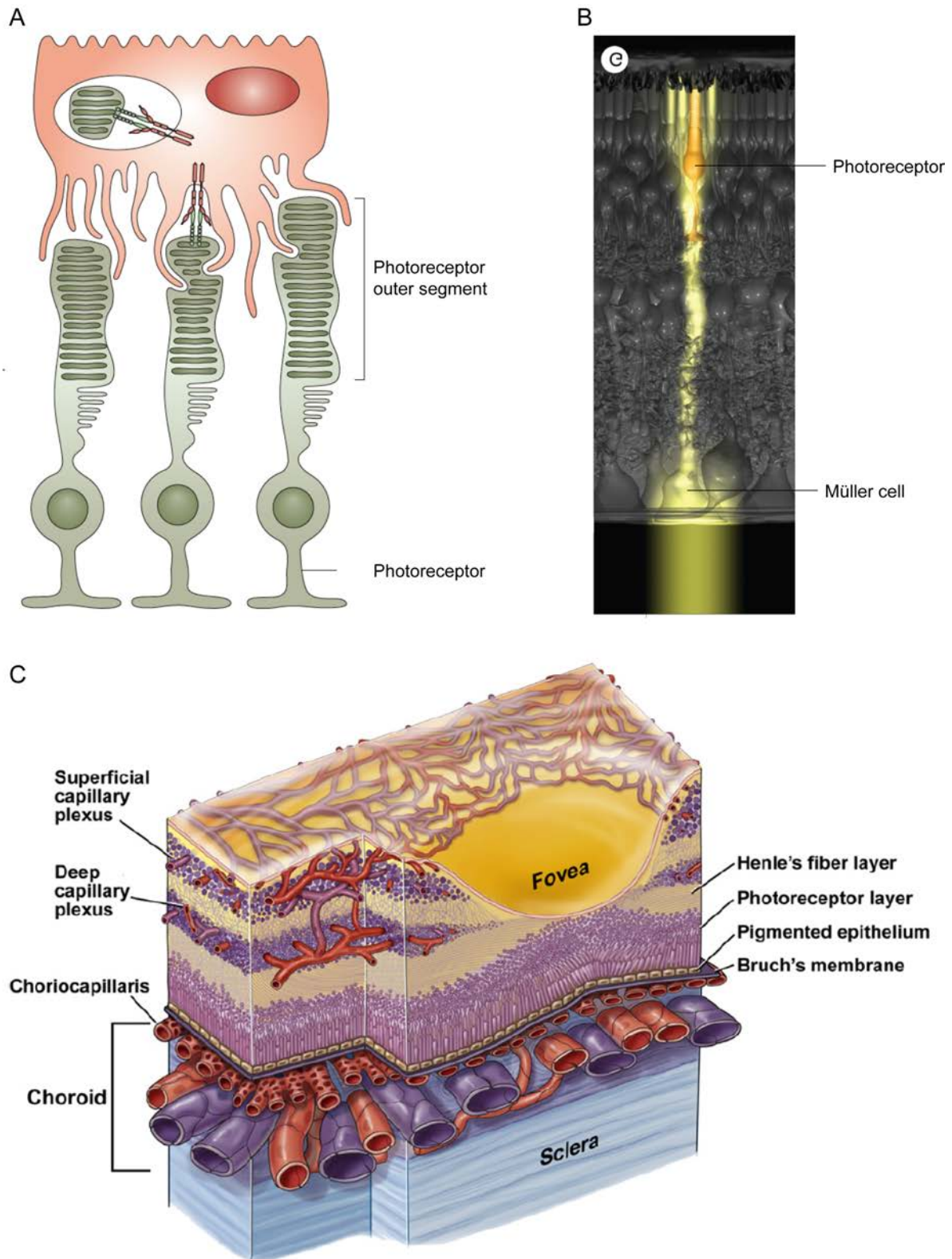


**Figure 5: Importance of non-neuronal cell types in retinal homeostasis.** (A) Retinal pigment epithelium (RPE) cells closely interact with photoreceptors and allow photoreceptor outer segment (POS) renewal by phagocytosis of POS tips. Adapted from (12). (B) Müller cells form living optic fibers that guide light to the photoreceptor layer –among other numerous functions. Adapted from (7). (C) Choroid is essential for blood supply to the retina, providing nutrients and oxygen. Adapted from (11).

## ii. Structure and properties of mammalian photoreceptors

### 1. Interspecies differences in photoreceptor function and distribution

Although retinal morphology is similar among many vertebrate species, important differences exist. Rods are the sensors of low light levels and can sense as low as one single photon (13, 14). They are responsible for night vision, while cones are responsible for daylight and color vision –although a recent study shows that rods also contribute to daylight vision (15).

Nocturnal animals such as rodents have rod-dominated retinas, with 97% of rods versus 3% of cones only, containing about 180,000 cones for 6.4 million rods (16). Diurnal species however, have higher number of cones. In the human retina there are approximately 6 million cones and 100 million rods (i.e. 6% versus 94%, respectively) (17). Rods sense light with the photopigment rhodopsin.

Color vision is possible because there are several subtypes of cones; each associated to an opsin that is sensitive to a different wavelength range (Figure 6). There are two cone subtypes in rodents: S- and M-cones, which stands for short wavelength and middle wavelength cones, or blue and green cones. It is sometimes said that mice have a third cone subtype which co-expresses S and M opsins (18). Primates have three subtypes of cones: like mice we have S- and M-cones, but we also have L-cones –long-wavelength opsin– that are sensitive to red light.

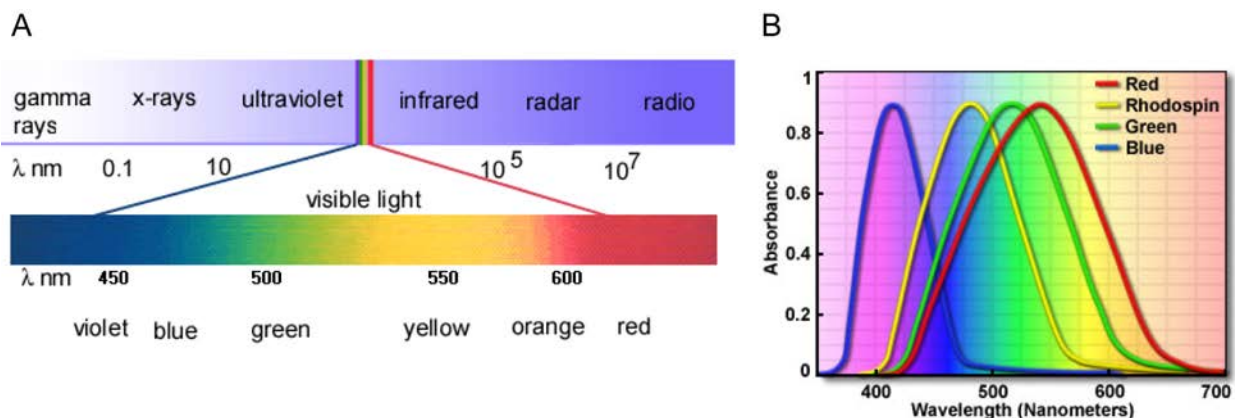
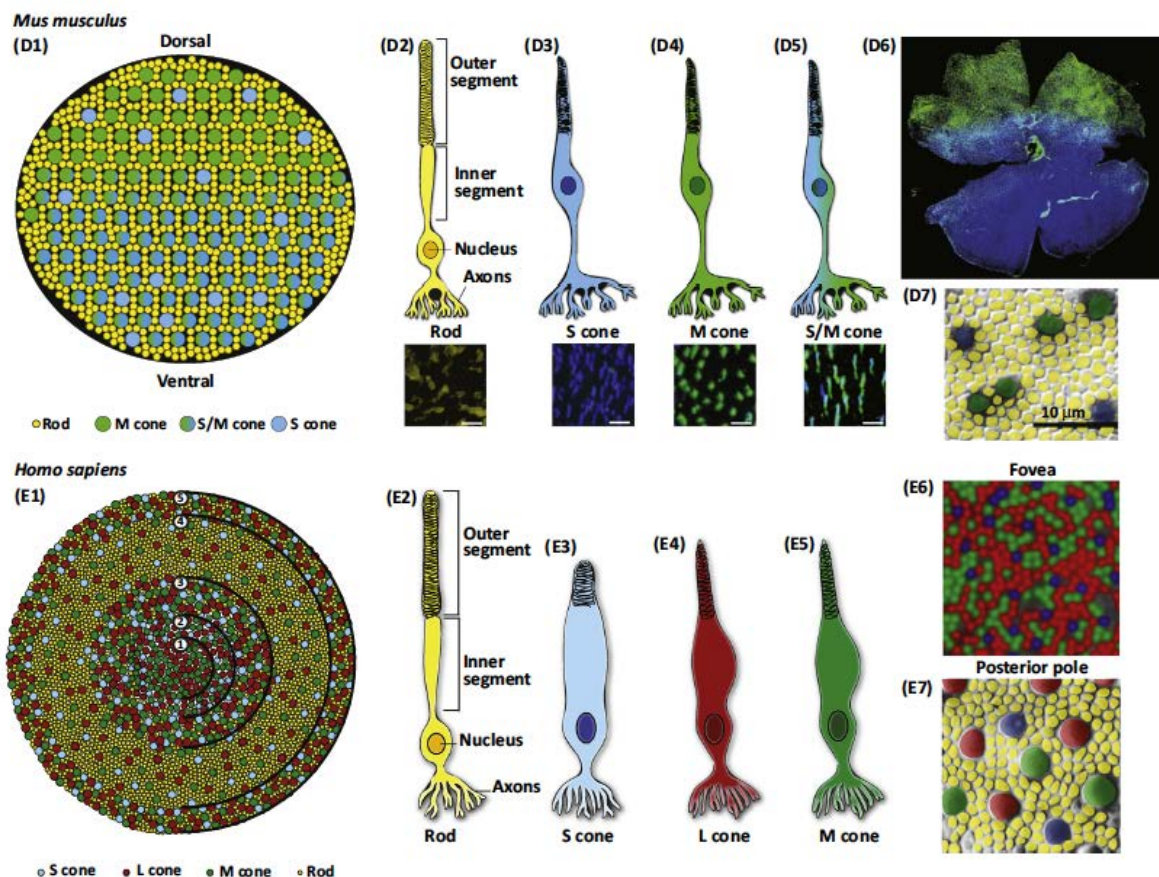


**Figure 6: Opsins and human color vision.** (A) Visible spectrum perceived by our visual system. Modified from <http://www.archives.library.illinois.edu>. (B) Absorption spectra of human opsins allow color vision. Rods express only one type of opsin: the rhodopsin. Adapted from <http://www.physics.stackexchange.com>

An additional difference in the properties of photoreceptors between rodents and primates is their distribution across the retina (Figure 7). In mice, the ventral part of mouse retina encodes preferentially dark contrast through blue cones and could be the sky sensors of bird preys (19) –when mice look up the image is sensed with the ventral retina. The dorsal part of the retina, composed mainly of green cones, is the ground sensor (19). In primates, the difference is even more striking, as cone density is much higher in the central retina while rods density is higher in the periphery. The highest density of cones is found in the fovea. Mice have no fovea and no high acuity vision.



Trends in Genetics

Figure 7: Types of photoreceptors and their distribution in the mouse (top panels) versus human (bottom panels) retina. Adapted from (18).

Anatomical differences between mouse and primate photoreceptors also exist. In primates there are calyceal processes in the intermediate region between the outer and inner segments of both rods and cones (Figure 8). These processes are long microvilli that emerge from the apical region of the inner segment and ensheath the basal part of the outer segment. Their role is still unknown but mutation in proteins found in the calyceal processes are associated to syndromic Retinitis Pigmentosa (20) (as the ocular phenotype of Usher syndrome, associated to deafness).



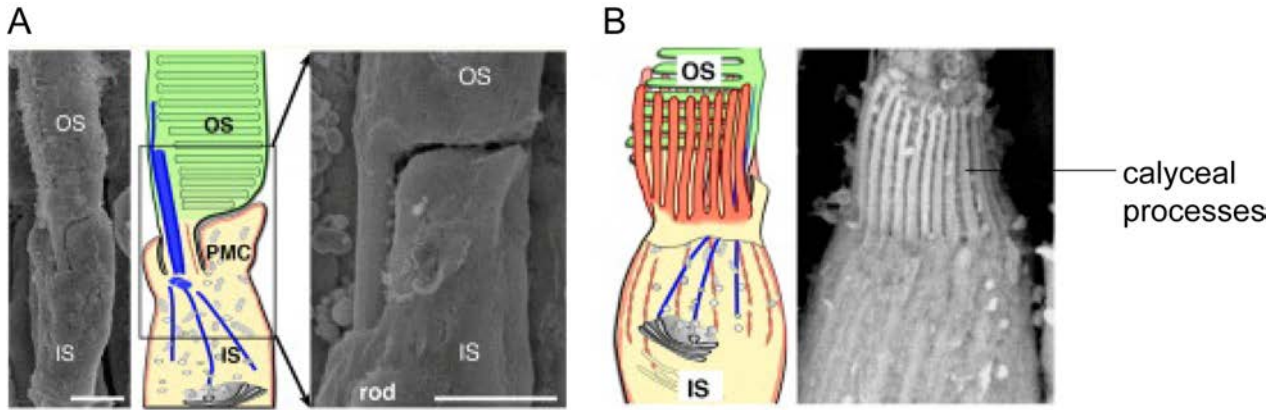


**Figure 8 : Calyceal processes of the primate retina.** (A) Mouse photoreceptors are devoid of calyceal processes. (B) Calyceal processes of the macaque retina emerging from the inner segments and ensheathing the outer segment. OS: Outer Segment; IS: Inner Segment. Adapted from (20).

All of these differences between rodent and primate retinas together with differences in cortical structure and complexity are responsible for the difference in visual perception, and question the pertinence of mouse models for vision science and therapeutics development (Figure 9).

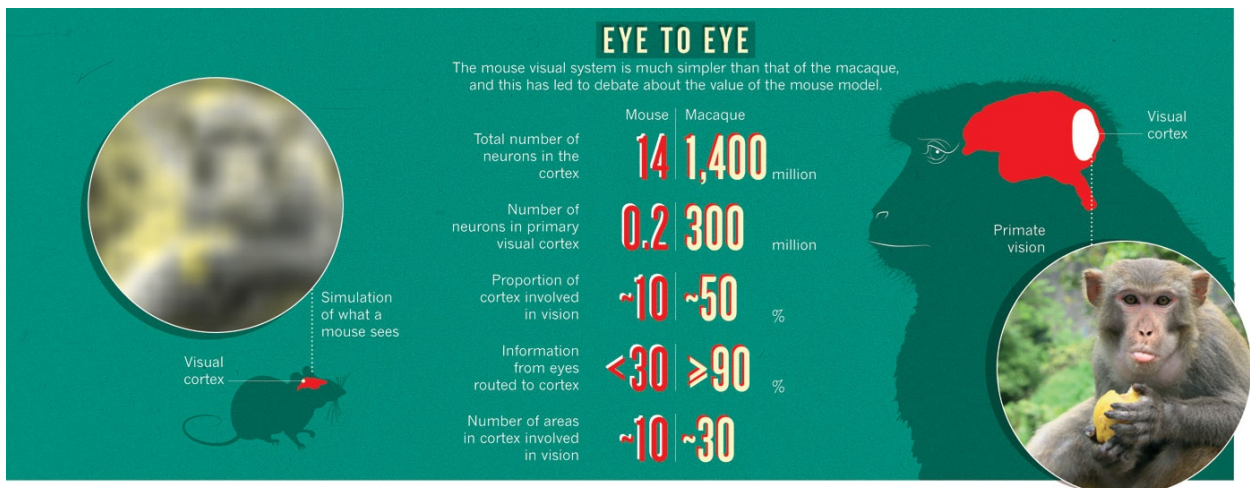


**Figure 9: Differences between mouse and primate visual system and the resulting visual perception.** Adapted from (21).

## 2. Functional properties of photoreceptors

The conversion of light into electrical and chemical signals occurs in the outer segments of photoreceptors.

In absence of light, all components of the phototransduction cascade are in a dark-adapted state. The cyclic-nucleotide gated (CNG) channels are cyclic guanosine monophosphate (cGMP)-gated. When cGMP binds to CNG channels, it causes the channels to open, which allows sodium ( $\text{Na}^+$ ) and calcium ( $\text{Ca}^{2+}$ ) ions to flow into the cell. The photoreceptor depolarizes (Figure 10).

In presence of light, the phototransduction results from a series of three steps:

**Step 1:** Light activates the photopigments.

Activation of the phototransduction cascade begins with absorption of a photon. The opsin is composed of two parts: a proteic part, which is located within the disc membranes; and a light-absorbing part, which is the retinal –a derivative of the vitamin A. Light absorption leads to 11-cis-retinal (dark-adapted state) isomerization into the all-trans-retinal isomer configuration (light-adapted state). As a result, the opsin conformation is modified and becomes catalytically active.

**Step 2:** Activation of the photopigments reduces the cGMP concentration.

The transducin -a member of the G protein family- binds the opsin. Its  $\alpha$ -subunit is activated by the replacement of GDP by GTP. Then, the  $\alpha$ -subunit dissociates from the  $\beta$ - $\gamma$  subunits to activate the membrane-associated phosphodiesterase 6 (PDE) by removing its two regulatory ( $\gamma$ ) subunits. The activated phosphodiesterase hydrolyses cGMP in GMP.

**Step 3:** The reduction of cGMP concentration closes CNG channels: the photoreceptor is hyperpolarized.

When cGMP is reduced, CNG channels close. Cation entry is stopped, which induces photoreceptor hyperpolarization and activation.

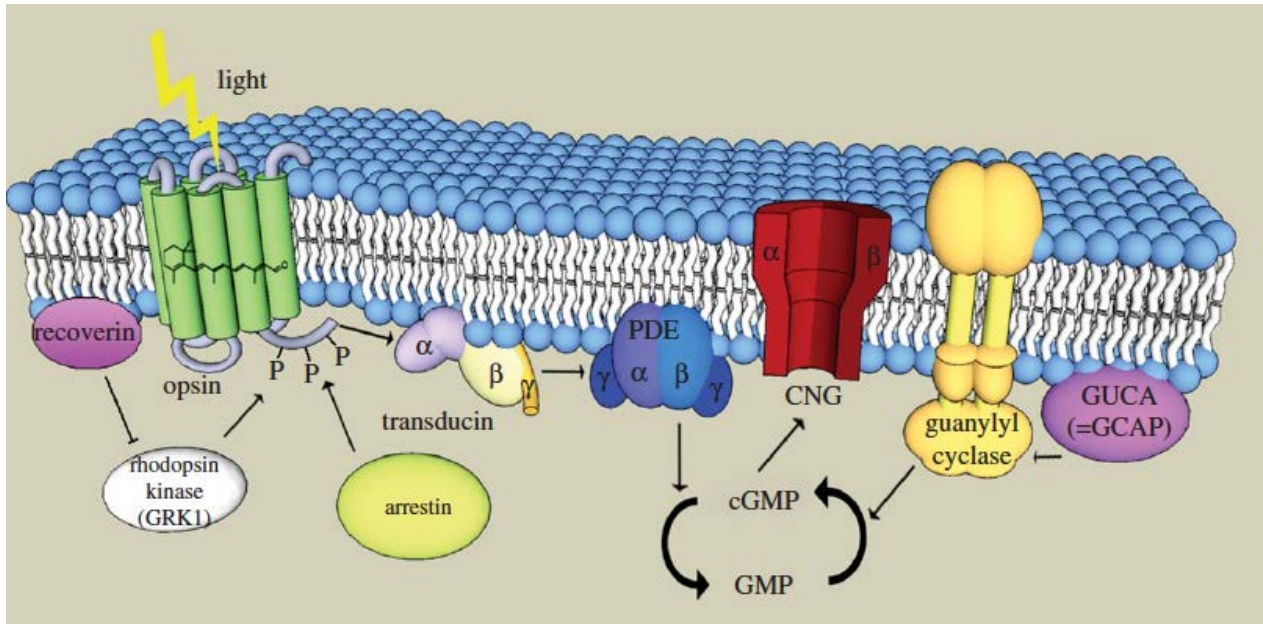


**Figure 10: Schematic representation of the phototransduction cascade in cones** (22). *P*: phosphate ; *PDE*: phosphodiesterase ; *CNG* : cyclic-nucleotide gated channel, *cGMP* : cyclic guanosine monophosphate, *GUCA*: plays a role in the recovery of retinal photoreceptors from photobleaching.

After activation, the phototransduction cascade is deactivated. Without this deactivation, the photoreceptor will not be able to answer to another light stimulus. Two mechanisms terminate light response: the transducin inactivates itself by hydrolyzing bound GTP. Second, the rhodopsin kinase phosphorylates the opsin and this phosphorylated opsin interacts with the regulatory protein arrestin, leading to its rapid inactivation (23).

It is the combination of the different isoforms of phototransduction cascade proteins, together with the structure of outer segments, that are responsible for the better light sensitivity of rods compared to cones (24).

### 3. Retinal circuitry after activation of the phototransduction cascade

After activation of the visual phototransduction cascade by light, signals are then transmitted to the second order neurons -namely bipolar cells- and eventually reach RGCs (Figure 11). After hyperpolarization of cones, their synaptic vesicles release less glutamate, which activate bipolar cells, and then activate ganglion cells. Eventually, retinal output represents a first integration level. The brain then allows visual representation.

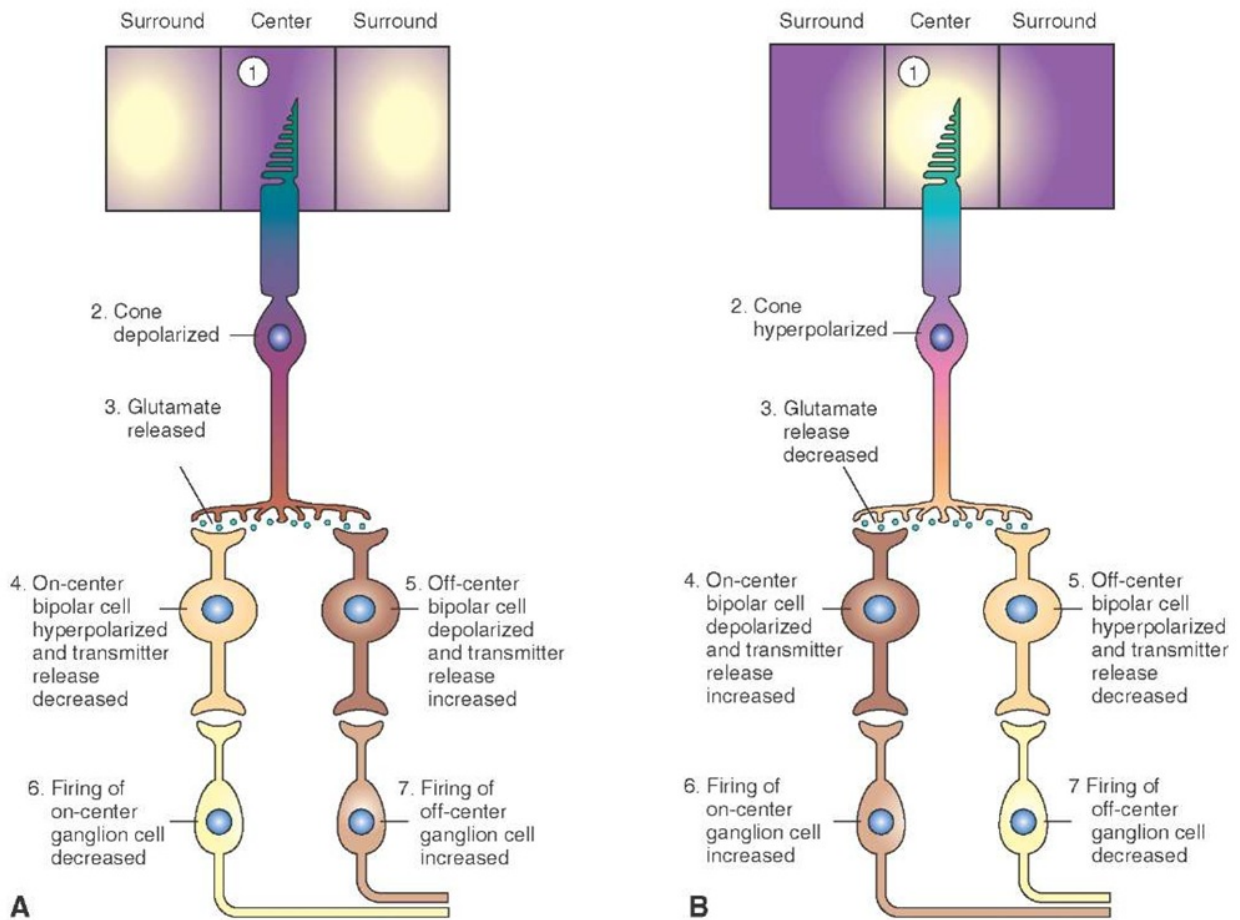


**Figure 11: Retinal circuit activation in response to light stimulus.** Adapted from <http://www.what-when-how.com>

### iii. The fovea, responsible for high acuity vision in primates

The fovea is the region of the retina responsible for high acuity vision in primates. What are the properties of this peculiar and important structure?

#### 1. Human visual field

Most obvious changes in the visual field are motion, which can be perceived with the whole field of view, from the periphery to the center (Figure 12). Color is perceivable in a smaller angle. However, perception of shapes and especially texts is perceivable in much smaller angles. This is directly linked to the distribution of rods and cones in the retina, and the presence of the fovea.

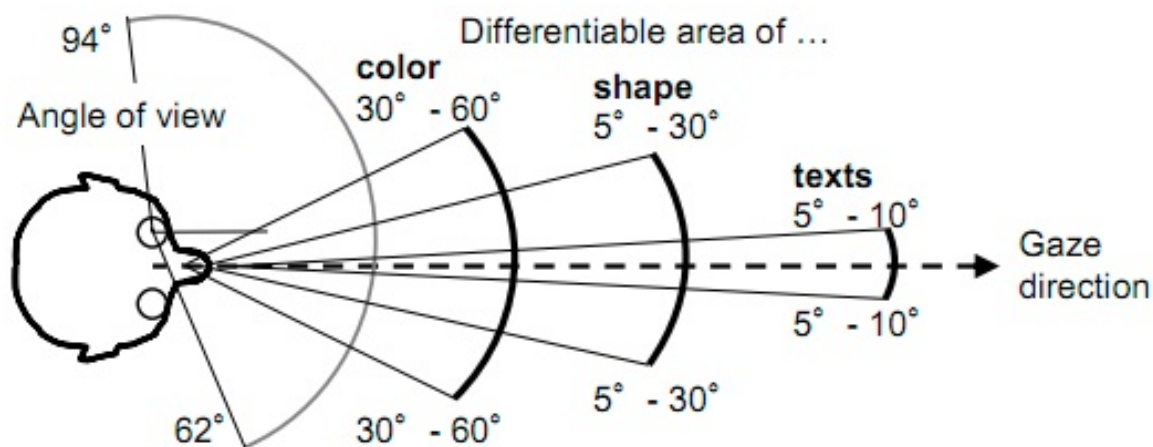


Figure 12 : Differentiable areas and angles for perception of motion, colors, shapes and texts. Adapted from <http://technologyreview.com>.

## 2. Structure of the fovea

Amongst mammals, only primates possess a fovea. It is located in the central retina and represents less than 1% of the total retinal surface area (25). Yet it is a crucial structure as it provides the input to more than 50% of the visual cortex. The foveola, located at the center of the fovea, contains only cones (Figure 13), and corresponds to the area with peak cone density (26).

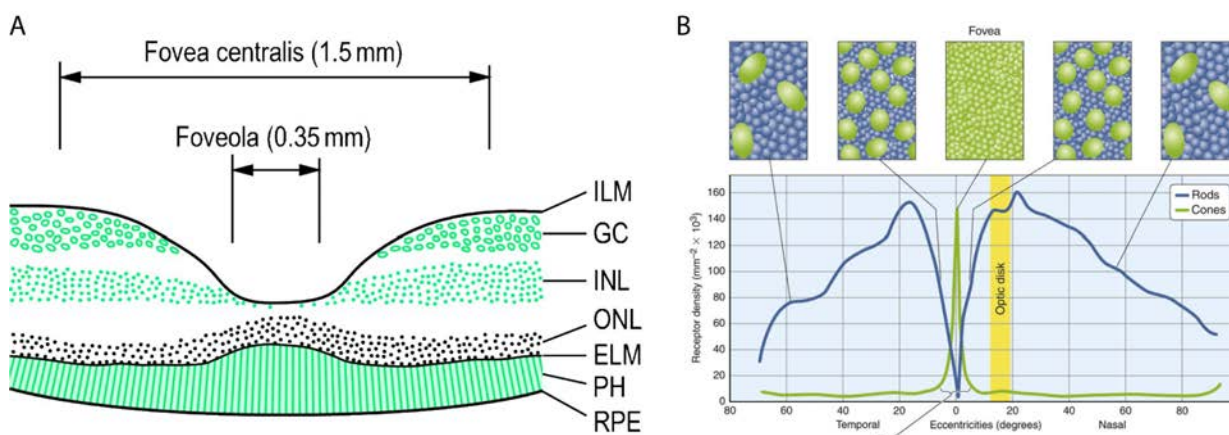
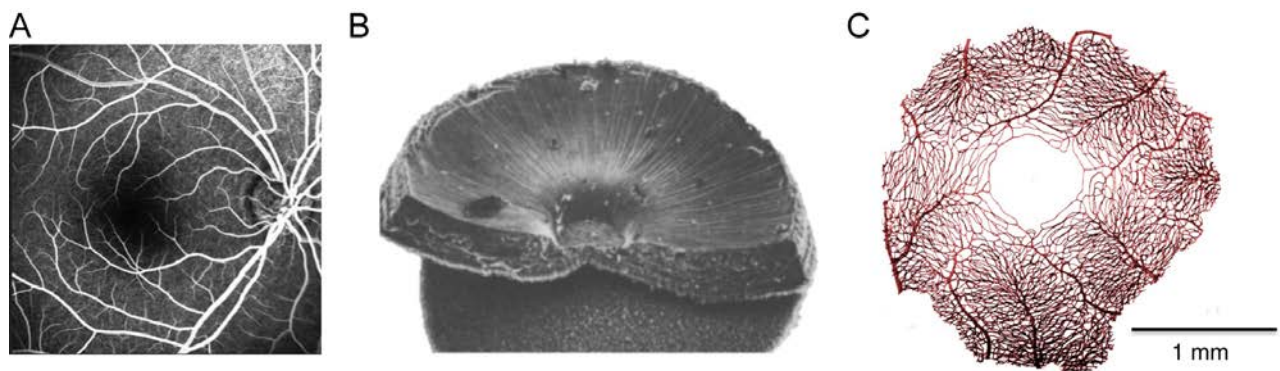


Figure 13: Structure of the fovea. (A) The foveola, at the center of the fovea, contains only cones. Adapted from *Dictionary of Optometry and Visual Science, 7th edition, Butterworth-Heinemann*. (B) Rod and cone density in the retina. Adapted from (2).

### 3. Development of the fovea

Development of the fovea is not fully understood, probably because it is present only in primates, which made it difficult to study its development. We now know that foveal development requires the definition of a foveal avascular zone (FAZ) (Figure 14), defined by absence of retinal blood vessels (27). Then local factors expressed by ganglion cells prevent the migration of astrocytes into the central retina and formation of blood vessels. After birth, size of the FAZ reduces and capillaries surrounding the fovea form.



**Figure 14: Structure of the foveal avascular zone (FAZ).** (A) Human eye fundus image following angiography with injection of a agent to visualize retinal blood vessels (28). (B) Close-up to the fovea seen with electron microscopy, with the typical foveal pit or foveal slope seen at its center where no blood vessels are found. Adapted from (29) (C) Schematic representation of retinal blood vessels and capillaries surrounding, but absent from the fovea. Adapted from (29) and reprinted from (26).

### 4. Foveal cones

What is responsible for high acuity vision and high spatial resolution, allowed by the fovea? It seems that this retinal area has several features that are optimal for high spatial resolution. First, highest cone density and elongated shape enables them to pack more closely and to act as more efficient waveguides (26). The fovea is a rod- and blue cone-free zone, and is also characterized by a lack of vasculature and nerves (30, 31). High acuity performance is also related to foveal circuitry itself, which is different from the peripheral circuitry. Within the fovea, the 'midget' circuitry predominates (32), characterized by a one to one relationship where a single cone is connected to a single bipolar cell then connected to a single ganglion cell (Figure 15). Also, there are few lateral connections in the central, inner retina and foveal midget ganglion cells receive little or no synaptic inhibition (33).

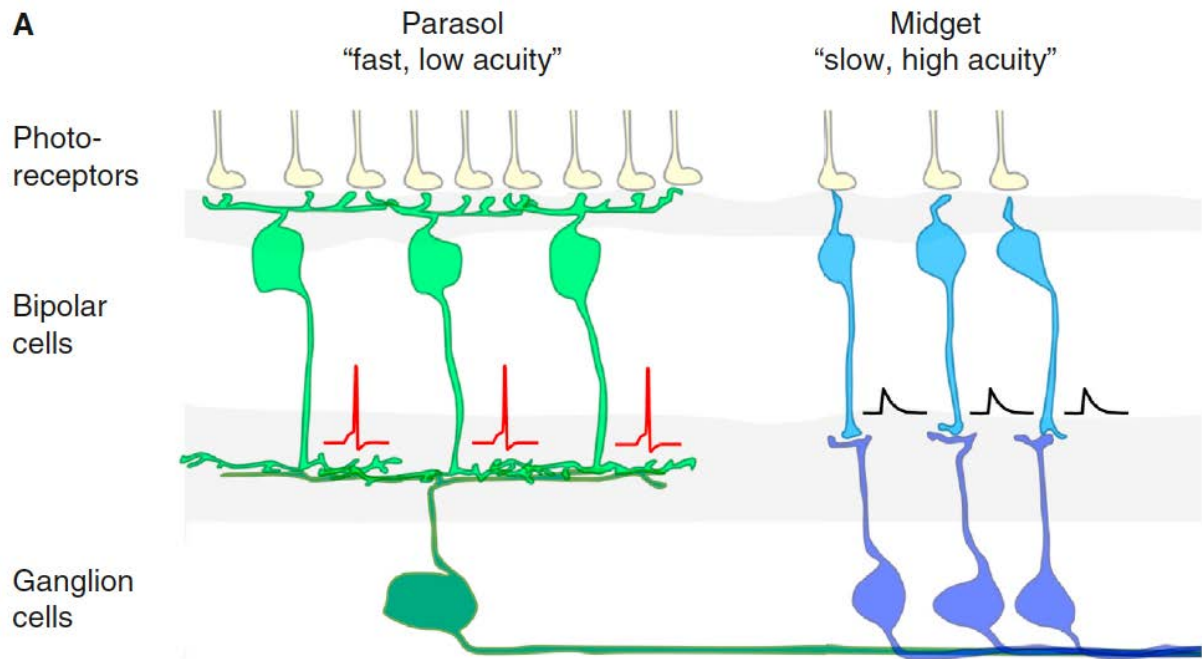


*Figure 15: Properties of the peripheral versus foveal retinal circuitry. Adapted from (32).*

The retina is a fragile tissue whose alteration can lead to partial or total blindness. In particular, defects in the phototransduction cascade or in proteins involved in communication between different retinal neurons can lead to retinal dysfunction and/or degeneration. What are the characteristics of retinal diseases and the mechanisms of photoreceptor dysfunction or death?

## II. Gene therapy and retinal diseases: a successful combination?

Vision is of our most valuable sense and its loss is a feared handicap. Retinal degenerative diseases can have a huge impact on the quality of life. One of the current most promising strategies for treating retinal disorders is gene therapy.

### i. Retinal disorders

#### 1. Complexity and heterogeneity of retinal disorders

Blindness is not always due to defects in the retina. The leading cause of vision loss worldwide is cataract (due to opacification of the lens). Retinal diseases are due to defects or loss of retinal cells. Loss of RGCs leads to glaucoma and is the second cause of vision loss worldwide (34, 35). In industrialized countries, the most frequent cause of vision loss is the progressive loss of photoreceptors and in particular macular degeneration. Age-related Macular Degeneration (AMD) is the first cause of blindness in the elderly over 50, and affects >30% people over 75 years old (36). AMD is a multifactorial disease caused by environmental factors and influenced by many genes (37).

Inherited forms of retinal degeneration are also common causes of vision loss with a prevalence of 1 in 3,000. There has been major progress in the discovery of loci and genes involved in retinal diseases in the last 20 years (Figure 16). We have today a list of more than 250 identified genes (38). In parallel, there has also been an improved understanding of pathophysiological mechanisms involved in such disorders. Besides, numerous proof of concept studies in small and large animal models and clinical studies for the treatment of retinal diseases, in particular gene therapies, have been developed.

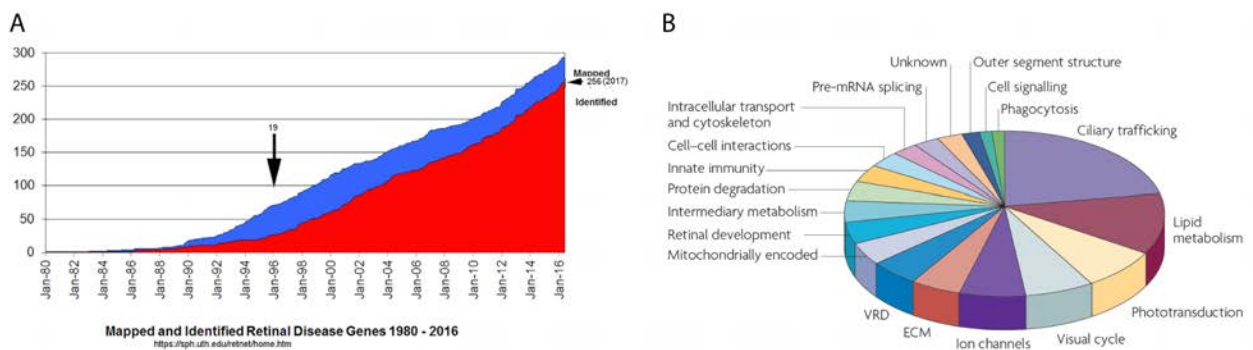


**Figure 16: Genetic complexity of retinal disorders.** (A) Number of identified genes involved in retinal disorders has considerably increased the last 20 years. Adapted from (38). (B) Functional categorization of genes involved in photoreceptor degeneration. Those genes are involved in numerous and diverse cell and tissue functions. Adapted from (36).



## 2. Retinitis Pigmentosa, the most common form of inherited retinal degeneration

The most frequent inherited retinal degeneration –but still a rare disease– is Retinitis Pigmentosa (RP), that represents 40% of inherited retinal degeneration cases. RP prevalence is 1 in 3,500 to 4,000. RP is most of the time a rod-cone dystrophy, where a primary loss of rods occurs which leads to night and peripheral blindness. A secondary loss of cones then happens. At this point visual field slowly constricts until it spares only the macula (Figure 17B), which leads to a ‘tunnel vision’ (Figure 1). At late stages, the macula is also affected, eventually causing total blindness (Figure 17C). Patients can be affected from early to middle adulthood, between 20 and 64 years (39). Rapidity of disease development and vision loss is also variable. Today there is no long-treatment available for this disease, current treatments only include slowing down vision loss with sunlight protection and vitaminotherapy (40).

There is a promising approach developed for end-stage RP, namely retinal implants that electrically target surviving retinal circuit. They are composed of a photosensitive part (e.g. cameras), a processing step that transforms the visual information into electrical signals, and an array of electrodes that deliver the electrical signals to target cells. The first commercialized visual implant was Argus II device, developed by Second Sight Medical Products. Such implants restored light perception in a significant ratio of patients, who could achieve visually guided tasks such as object localization and motion discrimination (41).

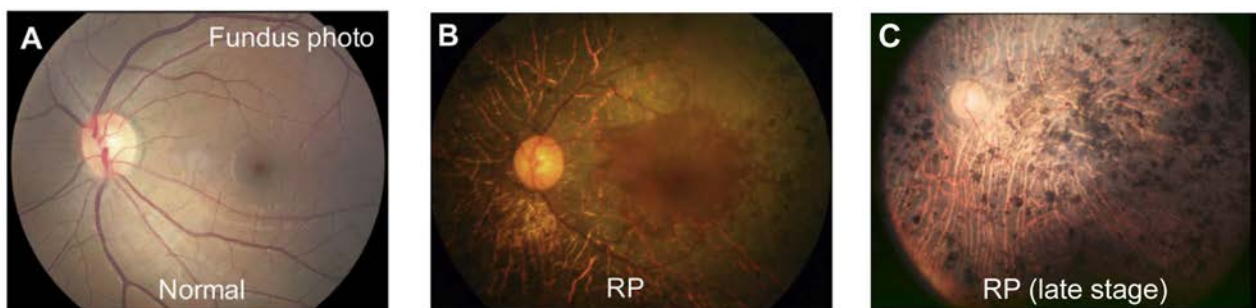


**Figure 17 : Eye fundus images of a healthy retina versus Retinitis Pigmentosa (RP) patient retinas. (A)** Normal eye fundus image. Adapted from (40). **(B)** Mid-stage RP patient eye fundus image. Presence of retinal deposits and abnormal vessels, except in the macula. This lead to tunnel vision as only central retina is preserved. Adapted from (40) **(C)** Late-stage RP patient eye fundus image. Presence of retinal deposits, abnormal vessels, even in the macula, and pale optic disk. Modified from (42).

RP is an extremely complex and heterogeneous group of retinal diseases at the genetic level. Cases are classified as autosomal dominant (24%), autosomal recessive (41%) and X-linked (22%), and the remaining 12% of cases are presumed to result from non-genetic factors, non-Mendelian inheritance (for example, mitochondrial or de novo mutations) or complex inheritance (36). There is an important number of genes involved in RP (Figure 19).

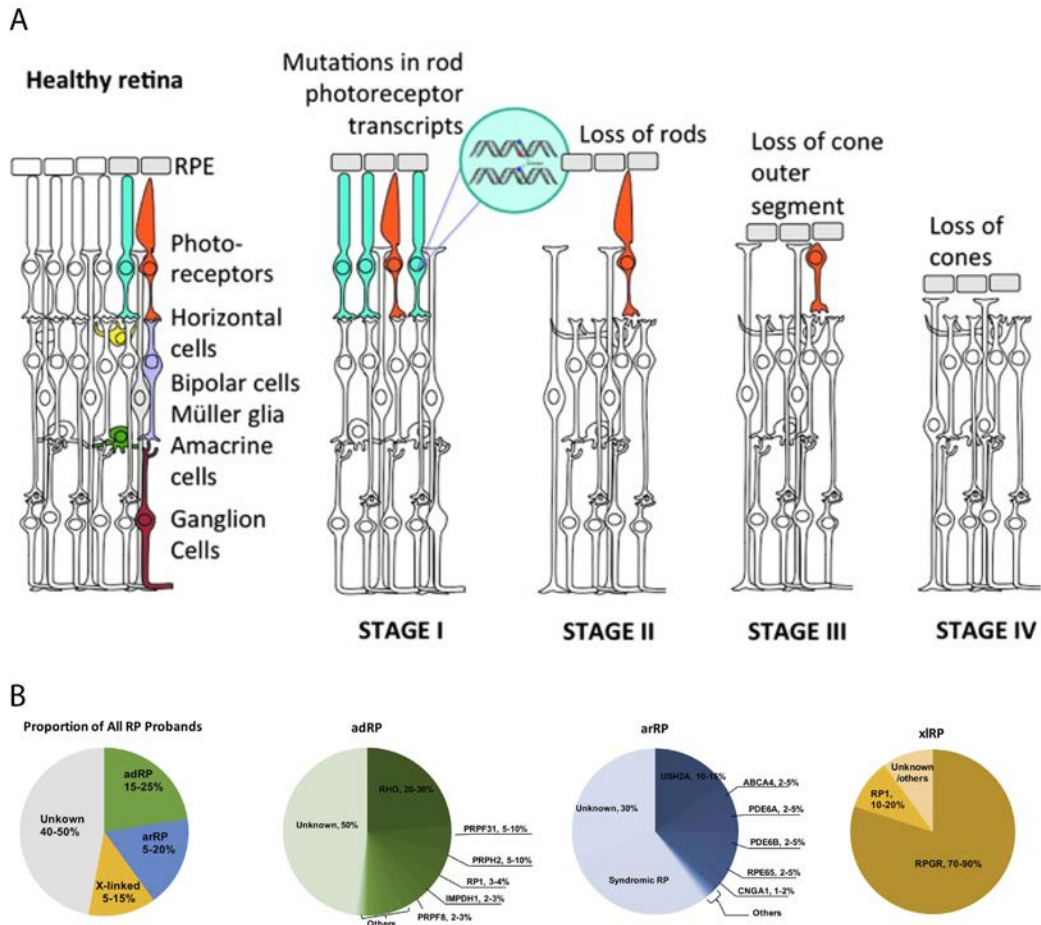


**Figure 18: Description of Retinitis Pigmentosa (RP).** (A) Timecourse of cell death and vision loss in RP. Adapted from (43). (B) Genetic forms of RP inheritance and diversity of genes involved. Adapted from (42). adRP : autosomal dominant RP ; arRP : autosomal recessive RP ; xIRP : x-linked RP.

In spite of this genetic complexity, there is a common phenotype in these rod-cone dystrophies. Usually, the first clinical observation in RP patients is night vision disturbance, because mutations lead to loss of rods but not cones. However, in the longer term, when most of the rods are lost, cones start to die too. Why are cones lost if the underlying mutations do not affect them? Several hypotheses have been proposed to explain cone cell death following rod cell death (44). The first explanation is related to the toxicity of dying rods for neighboring cones, through the release of toxic substances. A second explanation is the reduction of trophic support from rods to cones. There are evidence that a trophic factor released by rods promotes cone and outer segment survival (45–49). When absent, this factor referred to as Rod-derived Cone Viability Factor (RdCVF), leads to cone degeneration. A third hypothesis is that the oxidative stress resulting from rod cell death causes cone cell death. It is likely that a combination of both loss of trophic support and increase of oxidative stress are responsible for cone cell death, as it has been shown that loss of trophic support makes cones more vulnerable to oxidative and metabolic stress (50). When rods die, accumulation of reactive oxygen species causes loss of cones, which is

worsened by loss of RdCVF expression as it renders cones more vulnerable. Therefore, it is highly challenging, given the genetic complexity of RP and the involved cell death mechanisms, to develop gene therapies on a case-by-case basis.

ii. Current versus emerging ocular gene therapies, and future challenges

1. General principle of gene therapy and advantages of the eye as a target organ

Gene therapy consists in providing a therapeutic DNA to a tissue to reverse disease phenotype. To transfer this gene a vector must be used. I will not focus here on the different vectors used in the field of gene therapy but rather insist on the general principle behind it. Vectorology aspects will be addressed in the third section of the introduction. An example of vector used today in gene therapy is the adeno-associated viral (AAV) vector (Figure 20). So far they are the most frequently used vectors in the context of retinal diseases.

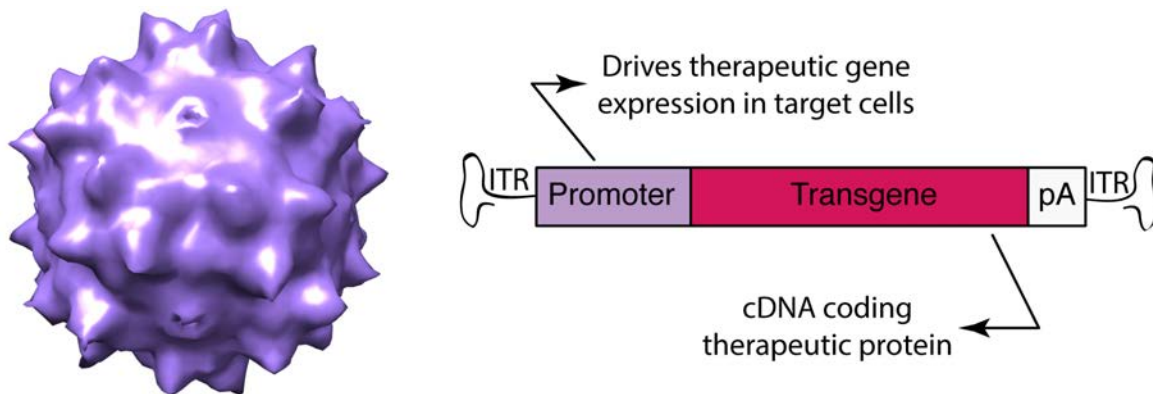


**Figure 19: Principle of vector and DNA combination for gene therapy with the example of adeno-associated viral vectors.** On the left is shown an AAV vector containing the DNA to be transferred. On the right is shown the most important DNA sequences required for expression of the therapeutic gene. ITR : Inverted Terminal Repeats, pA : polyA tail.

The very first gene therapy trial has been developed for immune disorders, in particular for Severe Combined Immune Deficiency (SCID), also known as the ‘bubble baby disease’ (51). SCID is a severe disorder due to genetic mutations causing absence of adaptive immune system. As a result, affected children cannot fight pathogens and death occurs in the first years of life.

These trials were ex vivo gene therapies followed by transplantation of transduced CD34+ cells by retroviral vectors. Sadly, there have been setbacks after a clinical trial as 5 over 20 SCID patients (with  $\gamma$ c mutations, SCID-X1) developed leukemia because of insertional mutagenesis with the gene therapy vector –nevertheless, in another trial for SCID patients with ADA mutations, none of the patients developed any adverse effect. Then, major vector improvements allowed treatment of other patients with success. In spite of these setbacks, treatment of SCID held promise for such serious disorders, but also for other genetic diseases. Since SCID clinical trials, other gene therapies to treat several disorders are in development including ocular disorders, hemophilia (52) or lysosomal storage diseases (53) -and many others (54).

Indeed, in parallel, all of the improvements in identification of genes involved in retinal disorders and better pathophysiological understanding of these diseases, led to focus on the development of gene therapy for retinal dystrophies. The eye is easily accessible for surgical injection, it is an immune privileged compartment and it responds well to local treatments without systemic effects. Moreover, the retina is a post-mitotic tissue where gene transfer can provide long-term production of a therapeutic protein.

## 2. Gene augmentation strategies

There has been fast progress in the field of retinal gene therapy, and groundbreaking proof-of-concept has been obtained in three independent groups of clinical trials in 2008 with the use of AAV vectors for the treatment of type 2 Leber's Congenital Amaurosis (LCA2). LCA2 is a severe, early onset retinal degenerative disorder that affects children and that causes blindness in adulthood. One of the genes involved in LCA is the *RPE65* gene, RPE65 being a crucial enzyme expressed by RPE cells and involved in the visual cycle. There have been independent but simultaneous clinical trials about 10 years ago in the USA and UK (55–57) led by three different groups, and a more recent study published this year about a trial in France by a fourth group. They all reported safety of AAV2-mediated (except for Nantes, which was with AAV4) gene therapy in patients as there were no clinically significant side effects or inflammation -except in one study at higher doses of  $1 \times 10^{12}$  vg (58). The results obtained in these trials were:

- The trial in Univ. of Florida&Pennsylvania, USA first included 3 patients from 21 to 24 years who all had significant improved rod-mediated vision, and cone-mediated improved vision for 2 of the 3 patients, 3 months after injection ( $5.96 \times 10^{10}$  vg in 150 $\mu$ L) (56, 59). One of the patients had foveal thinning (56) which likely is a consequence of direct needle insertion through the fovea to deliver the vector subretinally.

A later study with a larger cohort of 11 patients from 11 to 30 years also showed vision improvement over 1 year which was stable over 3 years with no visual decline,

however retinal degeneration (ONL thinning) continued in spite of this improved retinal sensitivity (60). Importantly, these data support the need for a combinatorial gene therapy to tackle both photoreceptor dysfunction (with AAV-*RPE65*) and retinal degeneration (which was not achieved with AAV-*RPE65*), for example with a neuroprotective strategy (60).

The authors then reported longer-term data at 6 years post-injection for two patients and 4.5 years for a third patient (61). Sadly, they observed an unabated retinal degeneration in all 3 patients, and progressive diminution of visual sensitivity in areas where vision was first improved after 3 years. However, retinal sensitivity still remained higher than baseline in the treated eye.

- The trial in UCL London, UK reported no significant visual acuity (VA) or electroretinogram (ERG) improvements in 3 young adults over 1 year (55) ( $1 \times 10^{11}$  vg in 1mL). However, there was a significantly improved retinal sensitivity and mobility for 1 of the 3 patients, and in mobility.

The longer-term study of UCL on 12 patients (6 to 23 years) over 3 years showed modest vision improvements after 6 months to 1 year in 5 of 8 patients (high dose:  $1 \times 10^{12}$  vg/eye) and 1 of 4 (low dose:  $1 \times 10^{11}$  vg/eye) (58). 5 of the 12 patients reported night vision improvements but only after a substantially extended period of dark adaptation. There were no VA and ERG improvements in any of 12 patients (except 1 patient who had VA increase, but it was observed in the untreated eye as well). However, there was subsequent visual decline during the following years like in the Univ. Florida&Pennsylvania trial. Importantly, 6 of the 10 patients who received subfoveal injections had retinal thinning (ONL thinning and inner segment defects) although there might also be a vector dose-related effect: it was observed in 1/4 patients with  $1 \times 10^{11}$  vg while it was observed in 5/6 patients with  $1 \times 10^{12}$  vg.

- The more recently published results of the clinical trial for LCA in Nantes, France showed a non-significant VA increase over 1 year (9 patients) to 3.5 years (6 patients) of 9 to 42 years old (62) ( $1.22 \times 10^{10}$  to  $4.8 \times 10^{10}$  vg/eye in 200-800 $\mu$ L). That being said, there was no visual decline, except in the only patient who received a subfoveal injection –where retinal thinning was reported during the first year, but no further in years 2 and 3.
- The trial in University of Pennsylvania, USA gave rise to promising results. They first reported vision improvements in 3 patients of 19 to 26 years old ( $1.5 \times 10^{10}$  vg in 150 $\mu$ L), with significant VA and pupillary response improvements, as well as decreased nystagmus –although one of the patient had a macular hole after the surgery (57). Positive outcomes were further confirmed in a total of 12 patients ( $1 \times 10^{10}$  to  $1 \times 10^{11}$  vg in 150-300  $\mu$ L) with improved sensitivity, acuity and mobility in most patients up to 1.5 year (57, 63, 64). They then reported a 3 year follow-up

showing a VA increase and enlargement of visual field in 5 patients that was stable over 3 years with no retinal degeneration (65). Recently, this *RPE65* gene therapy product has been approved and is made available by the company Spark Therapeutics (54).

Re-administration of the vector in contralateral eye of patients already treated in the first eye, did not cause significant immunogenicity, and led to mobility improvement but no significant VA increase ( $1.5 \times 10^{11}$  vg in 300 $\mu$ L) (66).

Since the first results for treatment of LCA published in 2008, about 40 clinical trials are taking place all around the world to tackle other retinal diseases (Table 1) such as choroideremia, X-linked retinoschisis and achromatopsia (67). There are published data for choroideremia (UK) of a six month study (68), and a 3.5 year follow-up (69) with positive outcomes. Six patients aged from 35 to 63 years showed significant vision improvements using REP1 protein with AAV2-CBA-*CHM* injections under the fovea ( $6 \times 10^9$  to  $1 \times 10^{10}$  vg in 100 $\mu$ L). While 2 of 6 patients had significant VA increase at 6 months which persisted at 3.5 years, it was not significant for 3 other patients but they had already good VA at baseline. Only the patient treated with the lower dose had significant decrease of VA and retinal thinning, suggesting again that there might be a side effect resulting from subfoveal injections.

**Table 1. Retinal gene therapy trials (updated on June 7, 2017, from Clinicaltrials.gov)**

Disease	Vector	Number (NCT)	Notes
Achromatopsia	AAV8-hCARp.hCNGB3	03001310	Phase 1/2, recruiting
	AAV2:YF-CNGA3	02935517	Phase 1/2, not yet recruiting
	AAV2:YF-CNGB3	02589922	Phase 1/2, recruiting
	AAV8-hCNGA3	02610582	Phase 1/2, recruiting
Choroideremia	AAV2-hCHM	02341807	Phase 1/2, recruiting
	AAV2-REP1	02407678	Phase 2, recruiting
	AAV2-REP1	02553135	Phase 2, active not recruiting
	AAV2-REP1	01461213	Phase 1/2, active not recruiting
	AAV2-REP1	02077361	Phase 1/2, active not recruiting
	AAV2-REP1	02671539	Phase 2, active not recruiting
Leber congenital amaurosis 2	AAV2-hRPE65v2	01208389	Phase 1/2 (follow-on), active not recruiting
	AAV5-OptiRPE65	02946879	LTRU (Phase 1/2), recruiting
	AAV2-hRPE65v2-301	00989609	Phase 3, active not recruiting
	AAV2-hRPE65v2-101	00516477	Phase 1/2, active not recruiting
	AAV5-OptiRPE65	02781480	Phase 1, recruiting
	AAV2.hRPE65p.hRPE65	00643747	Phase 1/2, completed
	AAV2-hRPE65	00749957	Phase 1/2, active not recruiting
	AAV2-hRPE65	00481546	Phase 1, active not recruiting
	AAV2-hRPE65	00821340	Phase 1, unknown
Leber hereditary optic neuropathy	AAV4-hRPE65	01496040	Phase 1/2, completed
	scAAV2-P1ND4v2	02161380	Phase 1, recruiting
	AAV2-ND4	02652780	Phase 3, active not recruiting
Neovascular/age-related macular degeneration	AAV2-ND4	02652767	Phase 3, recruiting
	AAV2-ND4	03153293	Phase 2/3, recruiting
	AAV2-ND4	01267422	Phase 1/2, completed
	AAV2-ND4	02064569	Phase 1/2, active not recruiting
	AAV.sFlt1	01494805	Phase 2a, unknown
	AAV2-sFLT01	01024998	Phase 1, active not recruiting
Retinitis pigmentosa	AAV8-AntiVEGF	03066258	Phase 1, recruiting
	AAV-CD59	03144999	Phase 1, recruiting
	LV (Retinostat)	01301443	Phase 1, completed
	LV (Retinostat)	01678872	Phase 1 FU, recruiting (by invitation)
	AAV-ChR2	02556736	Phase 1/2, recruiting
Stargardt disease	LV (SAR422459)	01367444	Phase 1/2, recruiting (by invitation)
Usher syndrome type 1B	LV (Ushstat)	01505062	Phase 1/2, recruiting
	LV (Ushstat)	02065011	Phase 1/2, recruiting (by invitation)
X-linked retinitis pigmentosa	AAV-RPGR	03116113	Phase 1/2, recruiting
	AAV2/5-hFK.RPGR	03252847	Phase 1/2, recruiting
X-linked retinoschisis	AAV-RS1	02317887	Phase 1/2, recruiting
	AAV2:YF-hRS1	02416622	Phase 1/2, recruiting

**Table 1: Current retinal gene therapy clinical trials. Adapted from (70).**

Lessons learned from LCA trials are the following. It is important to reduce injected doses to avoid side effects such as inflammatory immune responses (58, 71). Another lesson learned from LCA trials is the possibility to target photoreceptor dysfunction but not degeneration. Indeed there were often first improvements in visual sensitivity for treated eyes while the photoreceptor layer continued to thin, which is indicative of photoreceptor degeneration (60).

The reasons behind the described decrease in efficacy in clinical trials are not fully understood but might be because of multiple causes. We might need therapeutic gene expression all across retina to make the therapy work like suggested in Koch et al. study (72). Another cause might be an inflammation related to the gene therapy product: in the UCL trial, five of the eight patients in the high dose cohort had intraocular inflammation or immune responses, and two of them had VA decline (58). Also, a human *RPE65* promoter was used (55, 58), which is weaker than other promoters such as CBA used by Univ. Pennsylvania/Spark (57, 66), it might be the reason why higher AAV doses were required compared to the Univ. Pennsylvania/Spark trial. Related to optimization of vector genome, in the Univ. Pennsylvania/Spark trial an optimized human Kozak sequence was used to control the expression of RPE65 (57, 66). Besides, it seems important not to inject a high volume subretinally. A longer recovery period of a few days was needed in UCL trial, likely because of the injection method and much higher delivered volume equal to 1mL (55) –this longer recovery period associated to high volumes was also observed for one patient in the Nantes trial (800 $\mu$ L) (62). In contrast, blebs resolved within 14 hours after injection of 150 $\mu$ L in the Univ. Pennsylvania/Spark trial (57). Additionally, in the Univ. Pennsylvania/Spark trial a surfactant was used to prevent AAV agglomeration in the syringe (57). Regarding the production methods, UCL used B50 cells with adenoviruses that can lead to the presence of contaminants in viral preparations (73), while Univ. Pennsylvania/Spark used HEK293 cell-mediated AAV production where a high number of empty capsids can be removed (74). Finally, different immunosuppressive regimens were used in the trials mentioned above. Taken together, all these parameters likely enabled the differences in the therapeutic benefits between the clinical trials.

There is a need to validate more gene-based therapies that can reach the clinic and be used to treat patients with more common retinal diseases. However, important challenges need to be overcome before these proof-of-concept gene therapies can be extended to more common retinal dystrophies such as RP. There are several conditions in order to make a gene therapy like the one used for LCA and choroideremia possible. The causative mutation has to be identified, the disease has to be monogenic and recessive. Moreover, the DNA to be delivered has to be less than 4.7kb –the AAV genome size. There is a published study for RP associated to *MERTK* mutations in 6 patients of 14 to 54 years old (75) ( $5.96 \times 10^{10}$  to  $1.788 \times 10^{11}$ vg in 150-450 $\mu$ L). 3 of the 6 patients had improved VA after injections of AAV2-VMD2-*hMERTK*, which decreased after 2 years in 2 patients.

As stated above, inherited retinal degenerations are particularly heterogeneous. Therefore, it is not possible to develop treatment associated to each mutation in each patient, as it would be highly costly and time consuming. Moreover, there would still be a lack of therapeutic options for patients whose mutation is unknown, i.e. 40% to 50% (Figure 20). What are the alternative therapeutic options?

### 3. Mutation-independent gene therapy approaches

Alternative gene therapy strategies that are more general and applicable to all RP forms are being developed. One promising strategy consists in developing mutation-independent therapies, that do not focus on the underlying mutations but rather on the common phenotype of all RP patients: rod loss followed by progressive cone degeneration.

The first mutation independent approach that was developed was the use of neurotrophic/neuroprotective approach to slow down cell death in RP. Such therapies have been widely studied in the past decade. Following the description of nerve growth factor (NGF), several such growth factors have been shown to promote neuronal survival in the central nervous system, including NGF itself (76), brain-derived neurotrophic factor (BDNF) (77), ciliary neurotrophic factor (CNTF) (78), basic fibroblast growth factor (bFGF) (79) and glial cell line-derived neurotrophic factor (GDNF) (80, 81). This strategy has proven successful in delaying retinal degeneration resulting from gain-of-function or lack of-function mutations (82, 83). Several neurotrophic factors have been shown to delay photoreceptor cell death in animal models of autosomal dominant RP caused by mutations in the rhodopsin gene. AAV vectors carrying the cDNA for GDNF (84), FGF-2, FGF-5, or FGF-18 (85, 86) were evaluated in the S334ter-4 rd line of transgenic rats and showed photoreceptor function preservation.

One factor that is potentially even more relevant in the context of RP is the rod derived-cone viability factor (RdCVF) (45) which has recently been shown to be an efficient neuroprotective factor to delay vision loss when delivered to the retina of rd10 and p23h mice (49). Rod–cone interactions are mediated by secreted proteins and primary loss of rods in RP is one of the causes for secondary loss of cones, because such secreted proteins are lacking after rod cell death. A systematic expression-cloning strategy helped identify one such signaling molecule -RdCVF- encoded by the *Nxn1* gene (45). This gene encodes two proteins: RdCVFL thioredoxin-like enzyme and a truncated form of this enzyme, called RdCVF (45). This trophic factor is specifically expressed by rods and supports cones. RdCVF binds its cell-surface receptor Basigin-1 expressed on the cone



membrane, and promotes aerobic glycolysis (48). AAV vectors carrying RdCVF can efficiently slow down outer segment loss in retinal degeneration for a limited time (46, 49). In slow RP forms RdCVF treatment might keep vision for the rest of the patient's life.

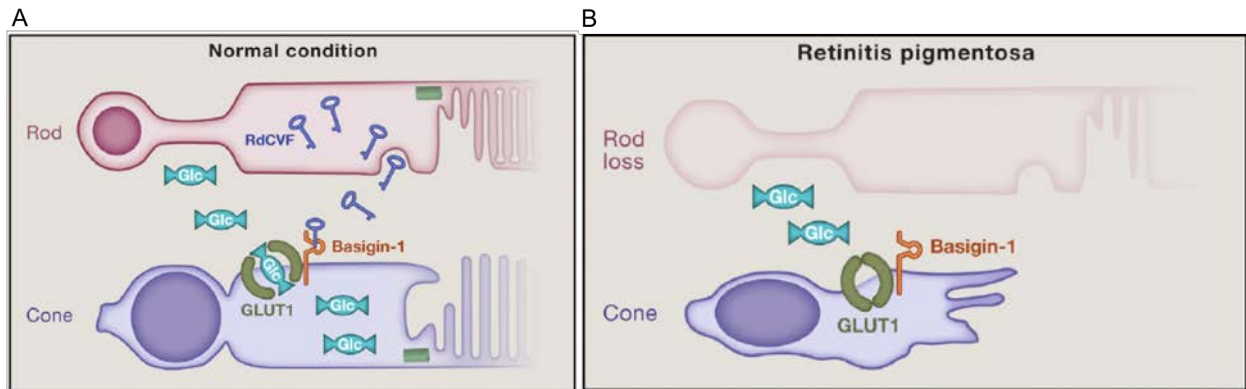


**Figure 20: Rods feed cones to promote their survival through RdCVF secretion. (A)** Under normal conditions, RdCVF is secreted by rods and interacts with its cell surface receptor Basigin-1 expressed by cones, thereby promoting glucose uptake and outer segment renewal. **(B)** As a result of rod cell death, RdCVF expression is lost which leads to outer segment loss and eventually cone cell death. Adapted from (87).

These preventive treatments have been developed for over a decade. A second, restorative approach, emerged more recently. The discovery of light-gated channels (channelrhodopsin (ChR) (Figure 21) or ReachR) and pumps (halorhodopsin (NpHR) or Jaws) enabled to create artificial photoreceptors in the remaining retinal circuits of RP retinas, using AAV-mediated gene therapy. One of the most successful applications of this mode of treatment was by reactivation of cone cell bodies that have lost their outer segments (88, 89) (Figure 22). This strategy used light-sensitive pump halorhodopsin to hyperpolarize cone cell bodies in response to light. Indeed it has been shown that the expression of eNpHR (Figure 21) (88) or its improved version Jaws (89) in remaining photoreceptor cell bodies is able to re-sensitize cones to light after degeneration of their light-receptive outer segments (Figure 22) in vivo in mouse animal models for RP but also in human retinas ex vivo. Dormant cones are relevant cell targets as they are at the source of processing providing closest to natural vision. Until recently there were no evidence of the applicability of this strategy in primates. But in rapid forms of RP, cone cell bodies are eventually lost.

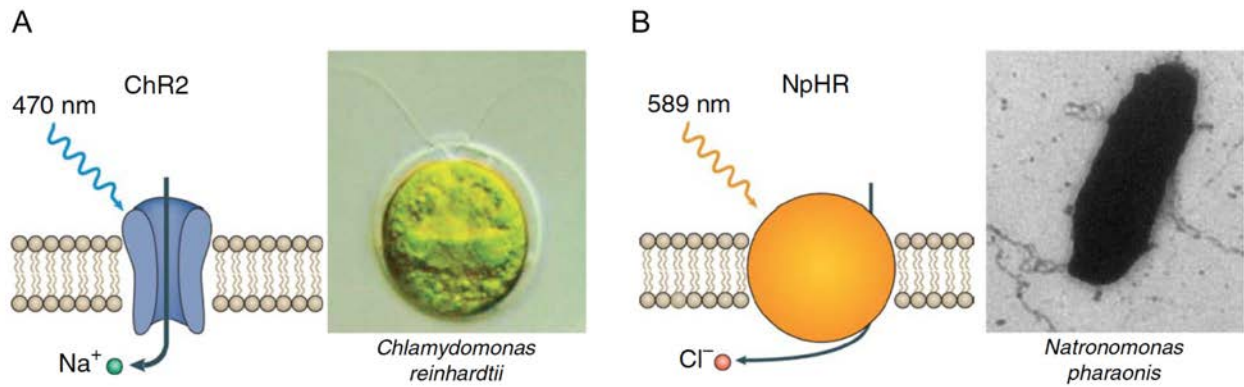


**Figure 21: Optogenetic tools from microbial origin used for vision restoration.** (A) Channelrhodopsin is classically used for neuron depolarization and has been discovered in algae. (B) Halorhodopsin is classically used for neuron hyperpolarization and has been discovered in bacteria. Adapted from (90).

Other strategies have been developed in rodents for activation of more downstream neurons, namely bipolar or ganglion cells with other opsins such as the channelrhodopsin, which are depolarizing opsins (Figure 23). Since then, ganglion cell activation to replace missing photoreceptors has been improved with more efficient opsins in rodents such as ReachR (91) and then translated to primates with Catch (92), and ChrimsonR with a clinical trial planned in RP patients (Gensight Biologics). There are already patients treated using AAV-ChR2 (RetroSense Therapeutics, Table 1), but no published results yet.

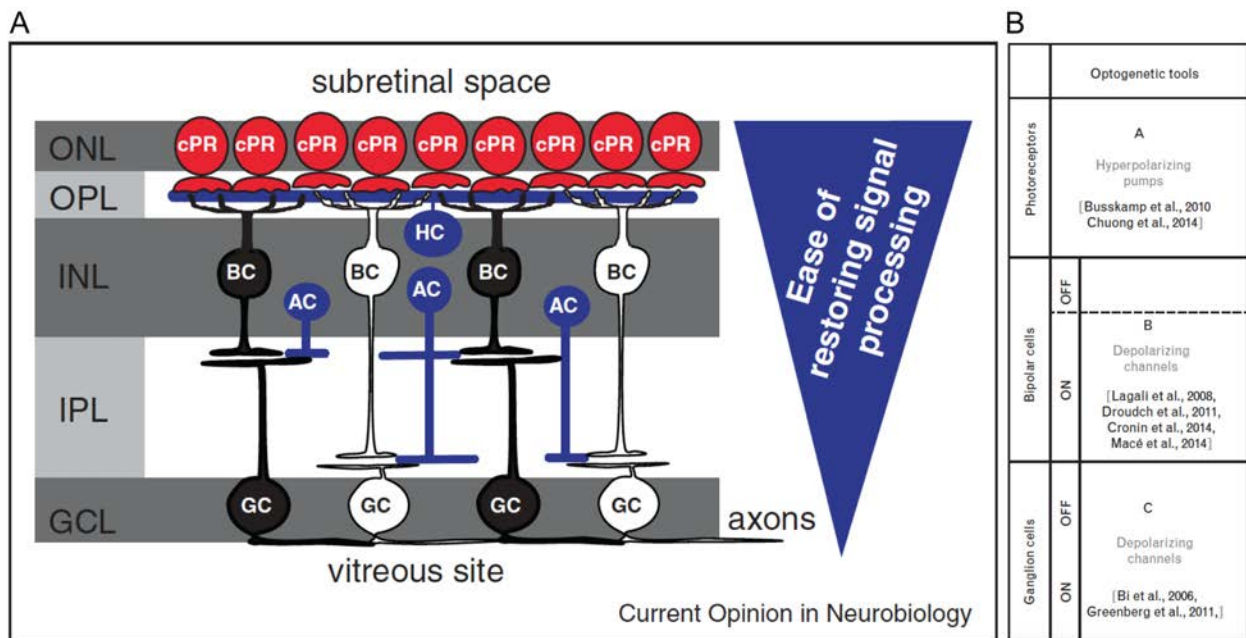


**Figure 22: Optogenetic therapy proof-of-concept studies with different target cells.** (A) The more upstream neurons are targeted, the easier it is to restore signal processing close the normal healthy retina (93). (B) References of studies involving optogenetic vision restoration in animal models. Adapted from (94). cPR : cone photoreceptor ; BC : bipolar cell ; AC : amacrine cell ; HC : horizontal cell ; GC : ganglion cell.

The stimulation of transduced retinal neurons is not possible under ambient light levels as microbial opsins have lower light sensitivity than endogenous opsins. It will however be possible using goggles such as the ones developed by GenSight Biologics (Figure 23). The image will be amplified at the specific, optimal wavelength required for activation of the selected opsin, and then projected to the retina. The device created by GenSight Biologics is composed of a camera and a microarray driven by a microprocessor, to send the visual information signal and light to the macular region.



Figure 23: Goggles compatible with optogenetic reactivation. Adapted from [www.gensight-biologics.com](http://www.gensight-biologics.com)

There is a need for translating promising therapies like optogenetics and RdCVF from mice to patients. In this context, the design of vectors for delivery of therapeutic genes is a critical step. To this aim we must engineer highly efficient vectors with enhanced retinal gene delivery properties and equip them with adequate promoters for targeting specific cell types.

### III. Vectorology: the puzzle of gene therapy

Our general aim is to provide efficient therapeutic options for those who suffer from retinal degenerations. As stated above, gene therapy is today a promising approach to treat patients affected with retinal disease. However, conceiving the gene therapy vector in itself –before even its testing– is an important step with multiple parameters to consider. Careful optimization of the vector is a key condition of gene therapy success in patients, and correct assembly of all of the pieces of the puzzle unlocks the full potential of gene therapy.

In principle, the concept of gene therapy is easy. It consists in inserting a gene into a vector, which is then delivered to target cells to obtain therapeutic effects. But in reality, it is not that simple. There are several objectives to achieve when designing a gene therapy, which have to be taken into account from the beginning at the vector design stage. These objectives are:

- Safe and long-lasting gene transfer
- Specific therapeutic gene expression in target cells
- Efficacious treatment, measured as prevention of vision loss or vision restoration

What are the parameters to take into account to achieve such objectives when designing a vector? Here, I will present the different means to obtain efficient vectors in view of these therapeutic goals with focus on AAV vectors, as they are the most efficient vectors today in the field. Moreover, I will focus mainly on the targeting of cones, as this has been my target cell type for developing gene therapies.

#### i. How to transfer a DNA drug safely to the retina in the long-term?

How can we transfer gene drugs into specific cell types? There are classically non-viral and viral approaches to treat retinal diseases (95). Most frequent vectors include those derived from viruses, namely adeno-associated viruses and lentiviruses. Adenoviruses; or non-viral vectors have also been used to a certain extent (Figure 24).

##### 1. Non-viral vectors

Non-viral approaches include naked DNA or DNA nanoparticles (Figure 25) transferred to the retina via physical methods such as electroporation or iontophoresis. DNA particles and lipoplexes can also be delivered without physical methods. However, in the context of retinal disorders they have generally shown low efficiency (96). Few studies reported vision improvements for 120 days in mouse models (97, 98) and long-term expression, up to 1

year after subretinal injection in mice (99). In particular, CK30PEG (polyethylene glycol-substituted 30-mer lysine peptides) nanoparticles (NPs) were shown to be safe (97, 98) and transduce the retina without inflammatory response (100, 101). An additional and important advantage is their large cargo capacity, up to 14 kb (99). Thanks to this, NPs were used to treat Stargardt disease associated to ABCA4 (ATP binding cassette transporter) mutations, with improved recovery of dark adaptation and reduced lipofuscin accumulation (99). These results will need to be further studied and confirmed in larger animal models. Virus-like but synthetic nucleocapsids also seem promising (102), their testing in vivo remain to be studied.

As non-viral vectors are not efficient enough for now, most pre-clinical studies and clinical trials involve the use of viral vectors.

## 2. Adenoviral and retroviral vectors

Both lentiviral and adenoviral vectors have shown promise in small animal models (103). However, they seem to be immunogenic after subretinal administration in spite of immune privilege. Lentiviral vectors can cause inflammation in NHPs and adenoviral vectors also showed evidence of inflammation or toxicity in preclinical studies (104). Besides their large size (Figure 25) does not allow efficient diffusion of viral particles and hampers their journey within retinal target tissue (95). Another drawback is the possible insertional mutagenesis although attempts to tackle this issue with the creation of self-inactivating or integration-deficient vectors reduced these side effects.

## 3. Adeno-associated vectors

AAV vectors have been used in clinical trials in multiple organs for various diseases to treat muscle, liver, and central nervous system disorders. AAV use is compatible with many strategies namely gene addition (also referred to as gene supplementation or gene replacement), gene correction, gene silencing, and also mutation-independent approaches, such as the use of neuroprotective therapies or optogenetic vision restoration. What makes AAV vectors such a flexible and powerful vector platform?

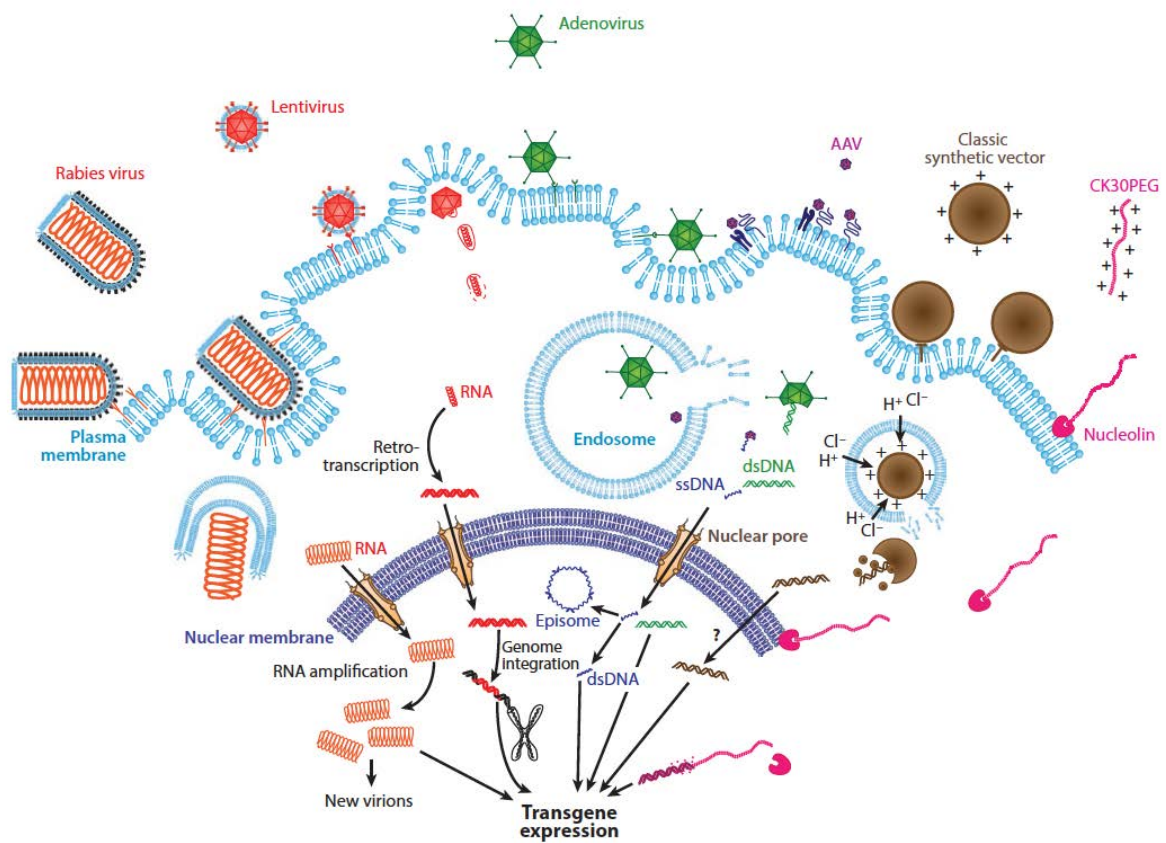


Figure 24: Vectors for gene delivery. Adapted from (105).

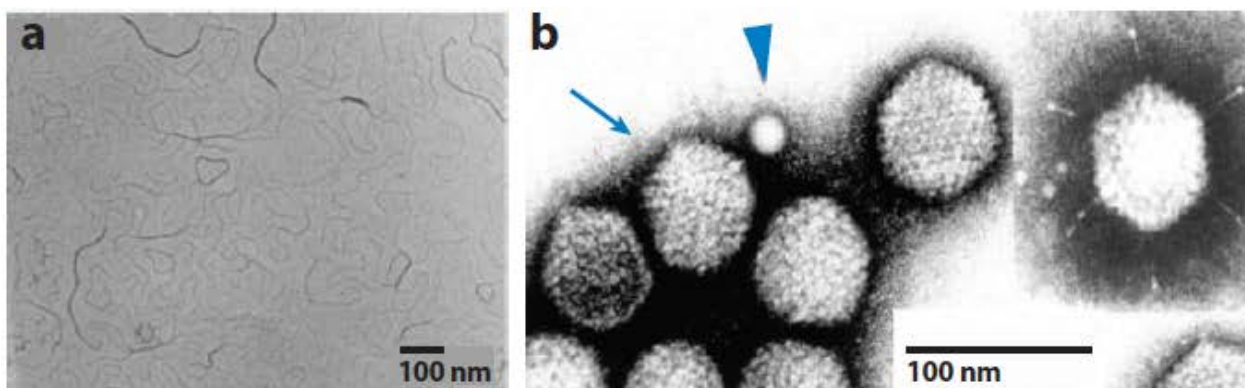


Figure 25: Diversity of gene delivery vector sizes and shapes. (a) Nanoparticles (CK30PEG) with small diameter of 8 to 11 nm. (b) The adeno-associated virus (arrowhead) is smaller than the adenovirus (arrow). Adapted from (105).

## - Wild-type adeno-associated virus

The AAV has been first observed in 1965 as a contaminant in adenoviral preparations (106). AAV owes its name to its incapacity to replicate and form its capsid without the presence of a co-infecting helper virus such as adenovirus, herpesvirus or papillomavirus. AAV is a very small (about 25nm in diameter) non-enveloped virus of icosahedral structure belonging to the dependovirus genus of the parvovirus family. It packages a positive or negative linear single-stranded DNA (ssDNA) of approximately 4.7kb. The viral genome is composed of two open-reading frames (ORFs) of structural (*cap*) and replication (*rep*) genes, like other members of the parvovirus family. The 5'ORF of wild-type AAV generates four functional Rep proteins through the use of two different promoters and alternative splicing. The 3' ORF of wild-type AAV generates three structural Cap proteins (VP1, VP2, and VP3) through alternative mRNA splicing and alternative start codon usage (107). The most unique component of this virus is the presence of Inverted Terminal Repeats (ITRs) flanking the viral genes. ITRs are self-complementary CG-rich sequences of approximately 145 base pairs (bp) in length and form T-shaped structures. ITRs include a terminal resolution site and a Rep binding site, playing a crucial role as both origins of replication and for packaging of viral genome.

About 13 distinct AAV serotypes have been identified (108). The tropism of AAV serotypes (and their variants) is mainly determined by their capsid (Figure 26) that change their interaction with different cell surface receptors for cell entry. Even though our understanding of the AAV has improved, AAV still holds secrets event after multiple years of study and genetic manipulation for creation of AAV vectors.

## - Structure of adeno-associated viral vectors

AAV vectors, or recombinant AAVs, have a different genome than that of wt AAVs. Both rep and cap ORFs are replaced by an expression cassette containing cDNA of interest and a promoter (Figure 21). Each vector, derived from naturally occurring AAV serotypes, have different tropism for cells and tissues. For example, AAV1 and 6 can be chosen to target skeletal muscle while AAV9 can transduce the heart more efficiently. Therefore, the transduction efficiency of a given tissue or cell type can be improved simply by changing the AAV serotype. Over 100 AAV capsid variants have been described (108). However, there is still a need for new viral variants overcoming current challenges, which vary depending on the target tissue and the route of administration.

Several features make AAV a very attractive vector for retinal gene therapy. Contrary to adenoviral vectors, AAV vectors show low immunogenicity. Furthermore, recombinant AAV genomes are non-integrative and persist as episomes in the nucleus unlike many retroviral vectors that can cause insertional mutagenesis by integration in the host genome. Besides

AAV variants are capable of stable transduction leading to efficient, long-term production of a therapeutic gene product in post-mitotic tissues such as the retina. Lastly, their small size allows easy diffusion into neural tissue, providing access to cell types away from the injection site and beyond barriers that stop access to larger viruses or particles.

The use of AAV vectors has two main limitations. Its slow transgene expression onset compared to other vectors –although that is not so problematic as vision loss in retinal diseases usually occurs in long time intervals. Obtaining peak expression several weeks after administration is not a limiting factor. The most problematic issue is its cargo capacity, which is up to about 5kb but there have been attempts to tackle this issue with the creation of dual (109) or even triple (110) AAVs that carry two or three portions of the cDNA, then recombining to allow production of the full-length therapeutic protein.

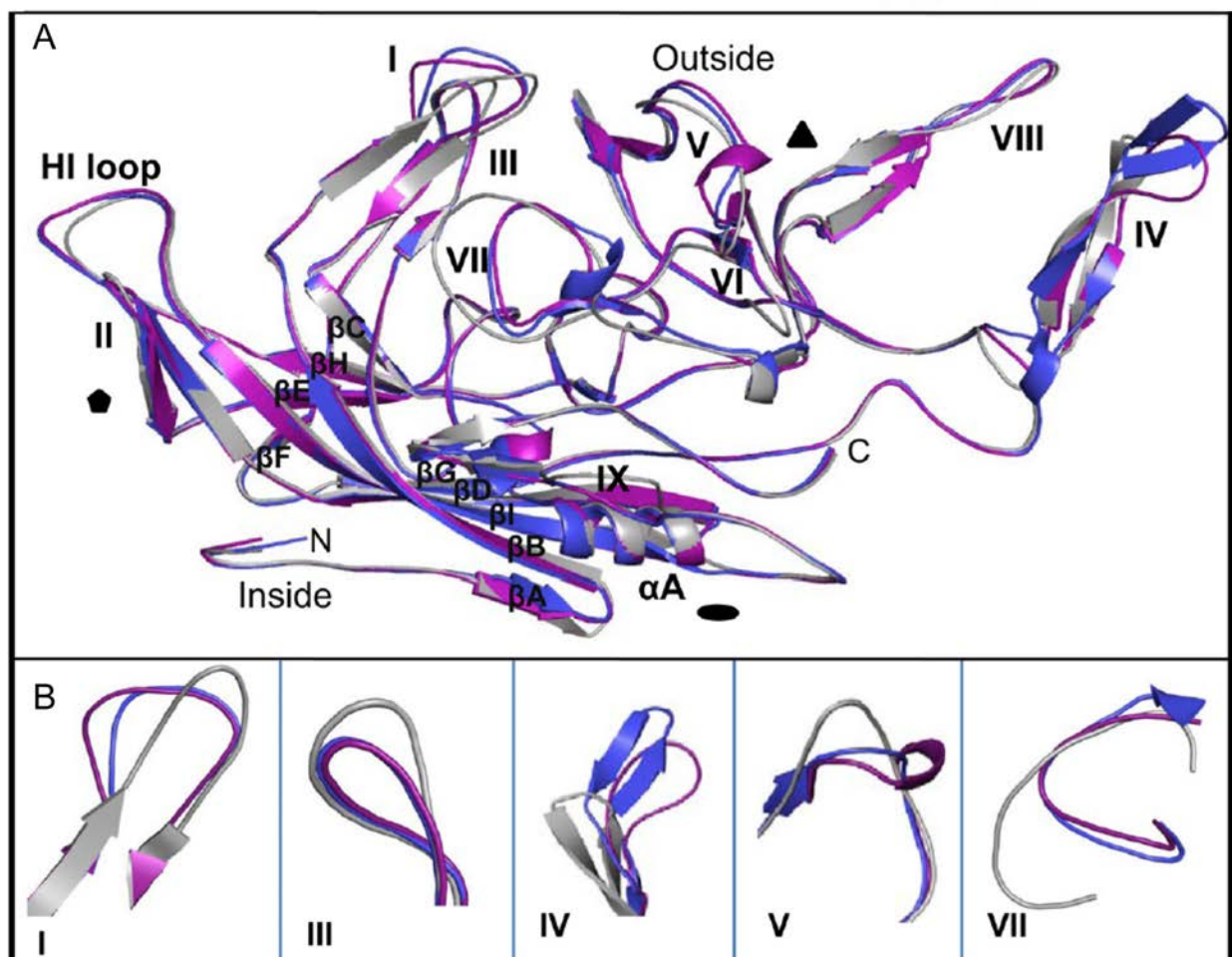


**Figure 26: Structure of AAV capsid proteins.** (A) AAV capsid consist of 60 monomers in (A). There are 9 hypervariable regions that are numbered I to IX. (B) Close-up to hypervariable regions to visualize 3D differences among serotypes. AAV1 is shown in purple, AAV2 in blue and AAV5 in gray. Adapted from (111).



## - Cell attachment and intracellular trafficking of AAVs

The interaction of AAV with its host cell, and attachment to the cell surface occurs via glycans in a serotype-dependant manner. Today, there are 23 known glycan primary or secondary receptors for AAV serotypes (112). For example, galactose is a receptor for AAV9, heparan sulfate proteoglycan (HSPG) for AAV2, AAV3 and AAV6, while sialic acid is a cellular receptor for AAV1, AAV4, AAV5, and AAV6. However, the primary receptors for AAV7, AAV8, AAV9, AAVrh10, AAV11, AAV12, and AAV13 are still unknown. Recently, a multi-serotype proteinaceous receptor has been identified and is referred to as AAVR or KIAA0319L (113). The role of AAVR is still not fully understood and has also been suggested to be not directly involved in virus uptake, but rather in other infection steps during AAV intracellular trafficking –or maybe both functions (114).

Cell entry then occurs through endocytosis with the formation of vesicles that contain AAV particles. AAV escapes the endosomes through the phospholipase domain of its VP1 protein. It is then retrogradely transported from endosomes to the trans-Golgi network via microtubule-dependent pathways, uncoated and imported into the nucleus (115).

## 4. Safety and long-lasting effects of AAV vectors

Are AAV vectors safe? Since the discovery of the wt AAV, rAAVs have been attractive as they are derived from a non-pathogenic virus, which is particularly relevant for its use as a therapeutic vector. There have been only anecdotic reports on AAV toxicity. In vitro reports of toxicity were about transduction of embryonic stem cells (116) or in vivo in the brain, and seem to be due to high-input vector doses (117–119). There are also evidence of side effects in the retina after AAV injections but it is not clear whether it is due to AAV itself or the transgene –often GFP (71, 120). There are evidence that high levels of GFP are neurotoxic (119). This important question remains to be clarified in the context of the retina. It is thus important to carefully select the dose before moving to the clinic, by performing dose-ranging and toxicity studies in small and large animal models to avoid potential dose-related toxic effects (121) or immune responses (122). The persistence of AAV genome as episomes in the nucleus makes it safe (no insertional mutagenesis).

In principle, AAV-mediated gene transfer is long lasting in a post-mitotic tissue as the DNA persists as episomes in the nucleus. There is evidence of long-term expression in large animal models, up to 36 months after administration in retinas of dogs (123). In humans, it is more difficult to assess this, as there is no way to measure transgene expression levels in vivo in retinas of patients. That being said, it appears now from both

pre-clinical and clinical studies that a key condition to maintain transgene expression in the long-term is to avoid any inflammatory immune response. Inflammation is a major concern as it can lead to clearance of transduced cell types (122). As AAV is of low immunogenicity, and the eye benefits from an immune privilege, AAV vectors are today the best therapeutic option to obtain long-term expression, as long as well-tolerated doses are administered and there are no double stranded breaks in the genome.

Today, even if the first ocular trials for LCA and choroideremia are promising, and there was no obvious major side effect ; in certain cases the visual field reduced again after several years in LCA (58, 61). Therefore, there is still a need to optimize gene therapy conditions and AAV vectors to obtain better and longer-lasting effects. The most obvious solution is to increase the vector dose. But as stated above, there are growing evidence that dose increase can be detrimental, and lead to toxicity or immunogenicity (58, 62, 71). Another solution could be to use a stronger, specific promoter to avoid off target therapeutic gene expression obtained with ubiquitous promoters (92). We can also use new capsids that allow dose sparing while increasing transduction efficiency (124).

Modifying these parameters are interesting options, but we also need to better investigate the mechanisms involved in toxicity, immunogenicity after AAV injections; and the potential link with secondary vision loss.

## ii. How to deliver genes specifically to cone photoreceptors?

### 1. Choosing the appropriate administration route

Our target cell type is the cone photoreceptor. How to attain them with AAVs? The classical way to deliver gene therapy vectors to the retina is the subretinal injection, in between the photoreceptor layer and the underlying epithelium, creating a 'bleb' of injected fluid. SR injection creates a retinal detachment that resorbs within 48 hours (125) or even less (57).

This local administration route has been widely used in pre-clinical and clinical studies. SR injection is the preferred injection since the beginning of ocular gene therapy. SR injection has several great advantages such as early-onset and high-level transgene expression in PR and RPE cells.

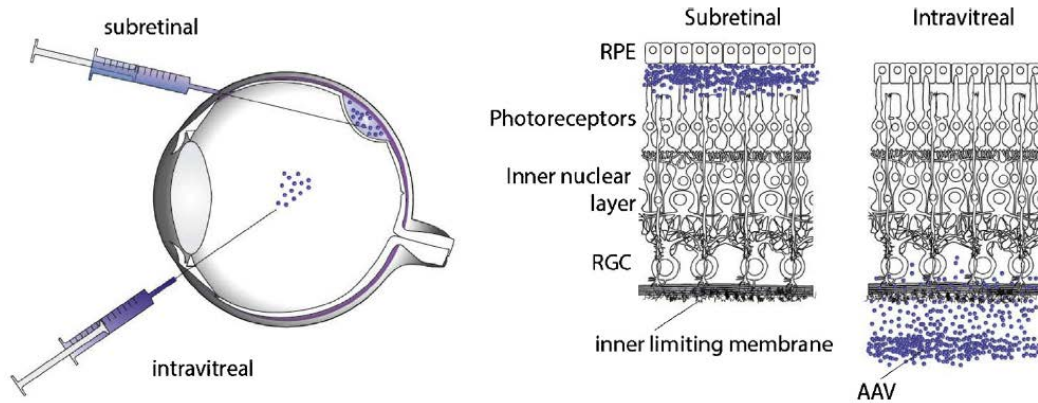


**Figure 27: Delivery of gene therapy drug to the primate retina using subretinal or intravitreal injections.** Adapted from (126).

However, this administration route is challenging and requires important surgical dexterity, especially when the macula/fovea are detached. Also, this administration route gives rise to expression in a limited area of the retina and induces a transitory retinal detachment, thereby increasing the risk of surgical damage –especially when targeting of the fovea is desired. Retinal adhesiveness to RPE is high (127) and is greater in primate than in other vertebrate species (128). Besides the fovea has the highest density of RPE cells, and it is also in the fovea that one RPE cell ensheathes a higher number of photoreceptor tips compared to the periphery (129). The fovea being responsible for high acuity vision, it is particularly important to preserve this region of the retina and not provoke side effects because of surgery that would exacerbate disease state.

Although there are studies suggesting that detaching the macula does not significantly damage cones (68, 130), there is also evidence suggesting the opposite and pointing to the harmful nature of subretinal foveal detachment. Perhaps the clearest examples come from clinical data in LCA trials where there were cases of macular thinning (58, 62, 131) and no visual improvements in the fovea compared to the periphery (131). Also, in the choroideremia trial, one patient treated with the lower dose had a VA decline compared to untreated eye (68, 69). These results support the development of alternative strategies to target the fovea (132).

The intravitreal injection is another local administration route to the eye. It is surgically simpler and non-invasive to the retina, making it a very attractive option for delivering gene drugs. Using this strategy, AAV2 is able to provide pan-retinal (i.e. spanning the entire retina) gene expression and transduce the inner retina (133). However, transduction of deep retinal layers with AAVs from the vitreous has been hampered for many years because of physical and cellular barriers.

- First, AAV vectors injected into the vitreous are highly diluted in the large vitreous volume creating very low local concentrations in proximity of the retina. Moreover, the gel-like structure that fills the eye can trap the vector before it reaches the retina.

- Second, the vector's capsid structure has to be compatible with retinal access. Otherwise, it is 'rejected' at the level of the inner limiting membrane, and cannot go beyond it even to reach superficial retinal layers.

- Third, the retina is a 'crowded', densely packed tissue. It contains dendrites, axons, and cell processes of neurons that compose the retinal tissue. AAV vector has to cross all of these cellular barriers to reach photoreceptors.

- Fourth, when –and if!– AAV reaches photoreceptors; the viral capsid has to be compatible with cell entry. This is achieved thanks to the interaction of AAV with its cell-surface receptors. Efficient cell entry allows therapeutic efficacy.

For all these reasons, efficient delivery of AAV vectors to the fovea from vitreous has been a challenge for many years.

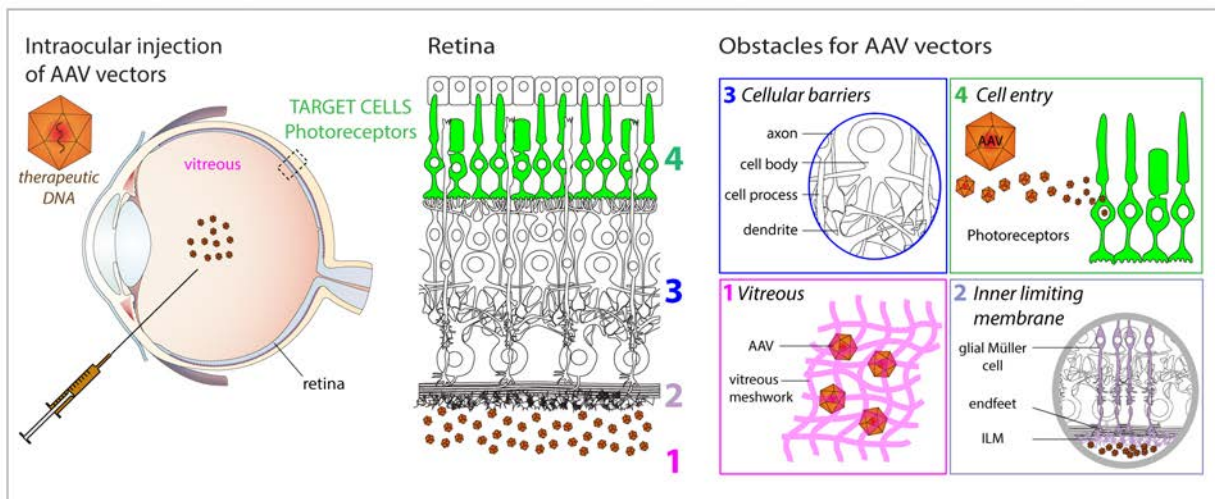


**Figure 28: Barriers to retinal transduction after intravitreal AAV delivery.**

To tackle these issues, i.e. the absence of appropriate vectors compatible with distal subretinal or intravitreal administration to the fovea, new AAV capsids that are able to overcome these obstacles have been developed.

## 2. Choosing the appropriate capsid

### - Limitations of natural capsids and design of new capsids

AAV compatible with SR injections are broadly available and they can target both PRs and the RPE. AAV5, 7, 8 and 9 are able to transduce PRs in mice and monkeys via this mode of injection (134, 135) while AAV2 can transduce mainly RGCs and MGCs from the vitreous in mice and monkeys (133). However, vectors compatible with photoreceptor transduction from the vitreous are limited. How to modify AAV properties to enable outer retinal gene delivery? AAV capsid can be engineered genetically by manipulating the capsid gene. To do so we use molecular biology, namely site directed mutagenesis for rational design and techniques such as DNA shuffling or random mutagenesis to generate combinatorial libraries for screening. By engineering AAV capsid, we can modify its tropism in order to direct it to a tissue or cell type of interest.

### - Design of enhanced capsids through rational design

AAV variants capable of transducing all retinal cell layers after intravitreal injection have been created. The rational mutagenesis strategy manipulates surface residues to increase viral trafficking to the nucleus and has been efficient in increasing efficiency of viral vectors (136). Usually, specific lysines (K), serines (S), threonines (T) or tyrosines (Y) are mutated to improve AAV efficiency by helping avoid ubiquitination of the capsid. An efficient vector is a triple tyrosine to phenylalanine mutant referred to as AAV2-3YF that can transduce photoreceptors when delivered into the vitreous of the mouse retina (136, 137). Another strategy is the insertion of small peptides on the capsid surface to redirect cell tropism of a given AAV. This type of insertion must neither be deleterious for capsid stability nor lead to creation of an immunogenic epitope.

### - Design of enhanced capsids through directed evolution

A major challenge in the field has been to obtain a virus allowing broad retinal transduction from the vitreous in the clinically relevant primate retina. Complex barriers are involved in cell surface attachment and viral distribution in a given tissue, and AAV structure-function relationships are not fully understood. Therefore, combinatorial approaches are more efficient and powerful for making AAVs better suited for a particular application. In this context, directed evolution of AAV has been successfully employed to select for viral capsids with better gene delivery properties. After creation of libraries of millions of AAV capsid variants, an in vivo directed evolution screen has been applied for

isolation of a vector capable of photoreceptor transduction. The variants were created with random mutagenesis, random peptide insertion, or capsid shuffling.

One of these variants developed through directed evolution, AAV2-7m8, outperforms all other AAV variants thus far described for retinal transduction in the mouse and in the NHP retina after vitreal administration (124). This variant is characterized by an insertion of a 10 amino-acid 'LALGETTRPA' peptide, composed of a variable heptamer region (LGETTRP). This '7m8' peptide is inserted into the cap gene of AAV2 at a site corresponding to the 588 residue, and it is exposed 60 times on the AAV capsid. This site has been selected for insertion because previous studies have proven efficacy for AAV2 re-targeting after non-viral sequence insertions at this location which is involved in capsid interaction with its primary receptor, heparan sulfate (138). Altogether these modifications give to AAV2-7m8 new transduction properties that allow better penetration properties, pan-retinal transgene expression and in all retinal layers. AAV2-7m8 was then applied for the treatment of retinal degenerative diseases, namely in the mouse model of X-linked retinoschisis (124), LCA (124), RP (91, 139) and further optimized for gene transfer in non-human primates (92). Recently, an improved version of AAV2-7m8 has been described: AAV2-MAX (140) with four additional Y to F and one T to V substitutions.

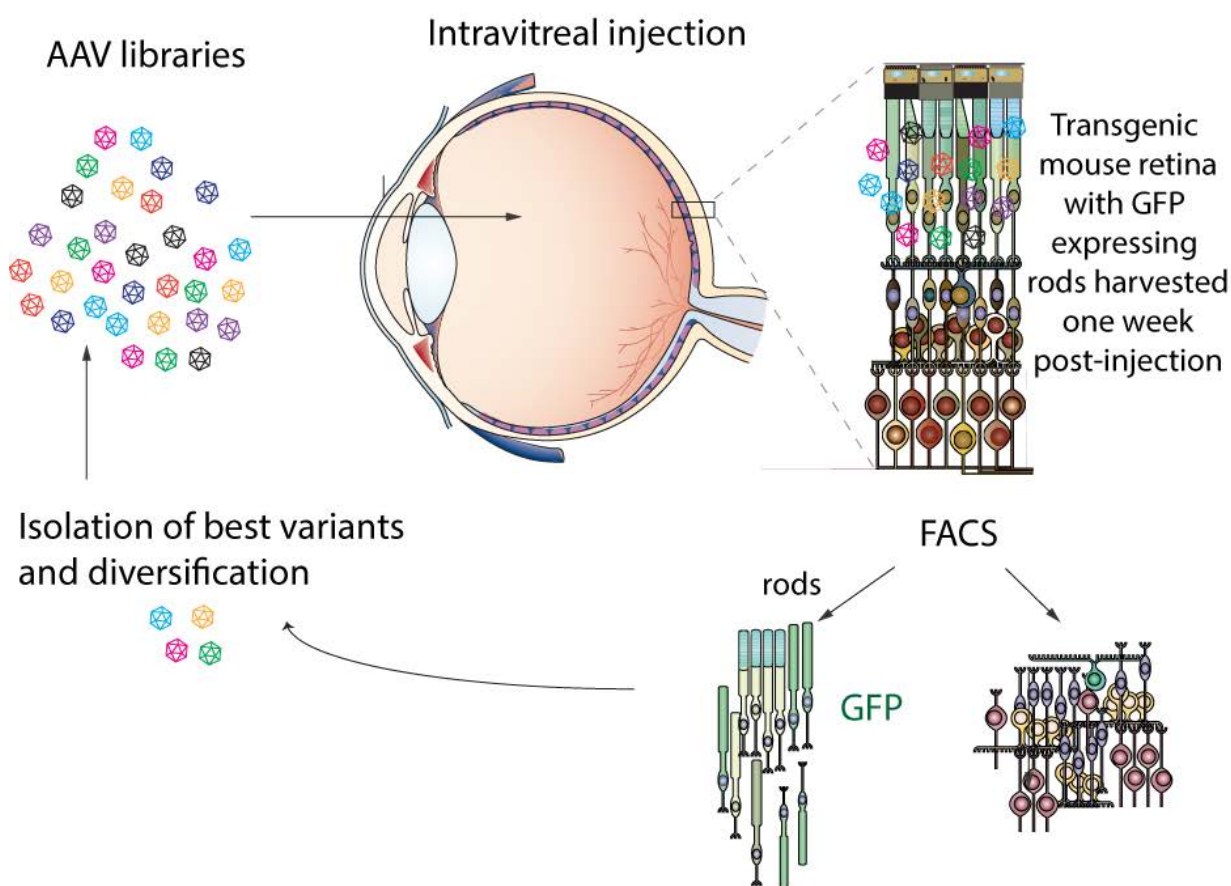


**Figure 29: Directed evolution process to select for best variants to transduce outer retinal layers.** Modified from (124).

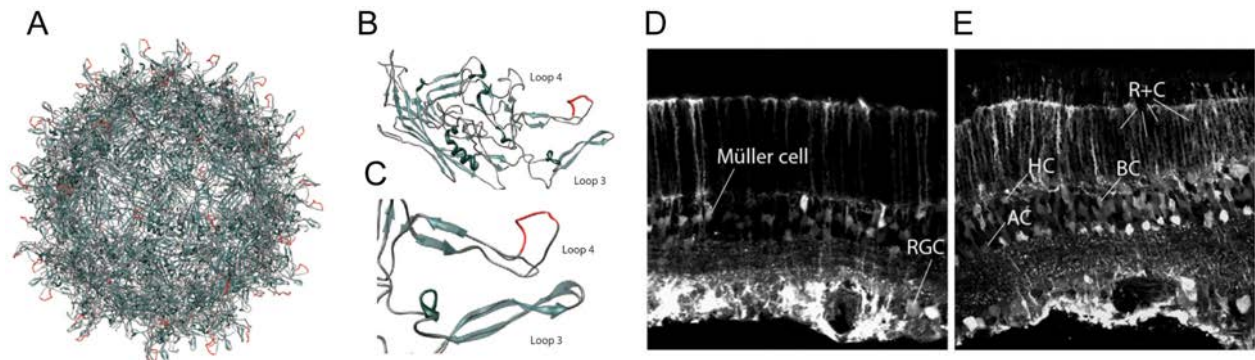


**Figure 30: AAV2-7m8 enhanced retinal gene delivery properties.** (A-C) Structure of AAV2-7m8, with peptide in red. (D-E) Transduction of all layers with AAV2-7m8 (E) but not AAV2 (D). Modified from (124)

All of the parameters evoked above show the importance of combining the right capsid and the appropriate administration route to better target a cell type of interest.

### 3. Selection of cell-type specific promoters

The capsid structure is not the only determinant of transduction efficiency. Modification of AAV genome is also a key parameter of AAV design to improve both the efficiency and kinetics of transduction. Transduction of photoreceptors has been achieved with ubiquitous promoters such as CAG or CMV (141) which mainly transduces both rods and cones as well as RPE cells after SR injection. But specific targeting of photoreceptors can be achieved with hGRK1 promoter (142). Specific targeting of rods has been achieved with rhodopsin promoter (124, 134). Cone-restricted expression has been attempted especially subretinally with mCAR (88), hCAR (but it was leaky in rods) (143), IRBP/GNAT2 chimeric promoter and human red opsin-based promoters, namely PR2.1 and PR1.7 (144–146). Specific targeting of cones from the vitreous has never been achieved in rodent and primates. Although promoter of choice is very important it has to be combined with appropriate capsid and administration route to unlock its potential.

#### iii. How to maximize AAV vector efficiency?

##### 1. Optimizing the expression cassette

To further optimize transduction kinetics there is a strategy that consists in producing self-complementary AAV vectors (scAAV) instead of classical single-stranded AAV (ssAAV). This consists in inserting the transgene in the vector genome so that it will be able

to self-hybridize. Therefore, it will not require a step of second strand DNA synthesis for initiation of transgene expression. This can drive faster expression onset (147). However, because of the double stranded DNA structure, there is a risk that it can activate innate immune responses through the activation of TLR-9 (148), and should most likely be avoided in a therapeutic context in vivo, especially at higher doses.

Other enhancer sequences can be added to help better transcription or to enhance translation. The Kozak consensus sequence plays a major role in the initiation of the translation process and can be modified to enhance translation efficiency (149). Addition of intronic sequences that promote mRNA export can also be used such as SD/SA (splice donor/splice acceptor) splicing sites from simian virus SV40 (146). Stability of transgene expression can be further optimized by codon optimization (150) through the use of codons that are more often used in humans versus other species. The woodchuck hepatitis virus post-transcriptional regulatory element (WPRE) can be added to the expression cassette after the transgene sequence to enhance its expression. WPRE has been recently shown to enhance AAV-mediated gene expression in the mouse retina and in post-mortem human adult retinal explants (151). WPRE sequence is included in Glybera, the first gene therapy drug approved in 2012 in the European Union for the treatment of lipoprotein lipase deficiency (LPLD) (53) and also in the gene therapy product for Parkinson's disease (clinical trial) in the USA (152).

## 2. Other ways of enhancing gene transfer efficiency

The use of exosome-associated AAV (exo-AAV) has been suggested to improve overall AAV efficiency. Exosomes have been shown to cross biological barriers and mediate widespread distribution upon systemic injections applicability in diseases have not been widely studied. When applied to the retina exo-AAV enabled broad retinal targeting following IVT injection (102) but it is unclear if this type of AAV is compatible with clinical use due to a lack of good manufacturing practice (GMP)-compatible production protocol.

This is a non-exhaustive list of ameliorations that can be brought to AAV to enhance its gene delivery efficiency; they are summed up in Figure 31. Although challenging and time-consuming, these steps are necessary to achieve efficient gene therapies. Additional parameters to be taken into account are interspecies differences and retinal disease state, which can dramatically impact transgene expression patterns and efficiency.



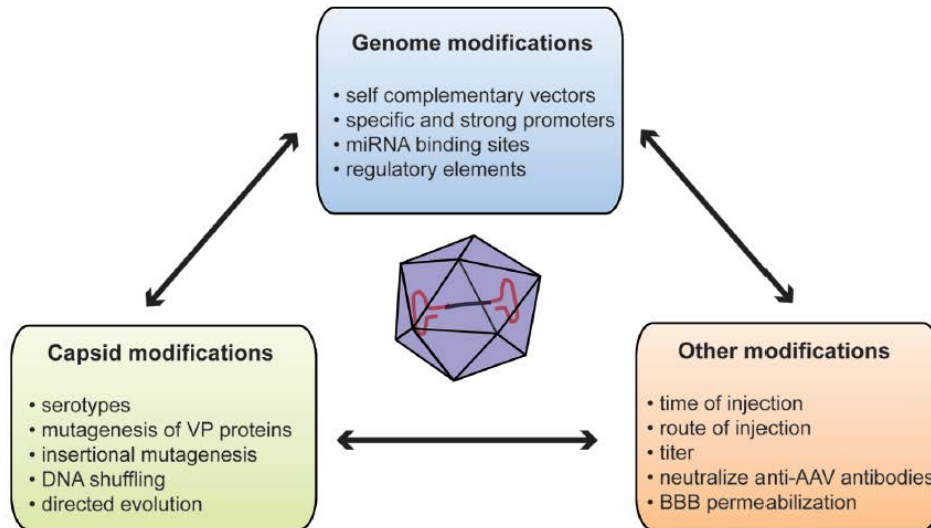


**Figure 31: Summary of methods used to improve gene delivery using AAV vectors.** Adapted from (153).

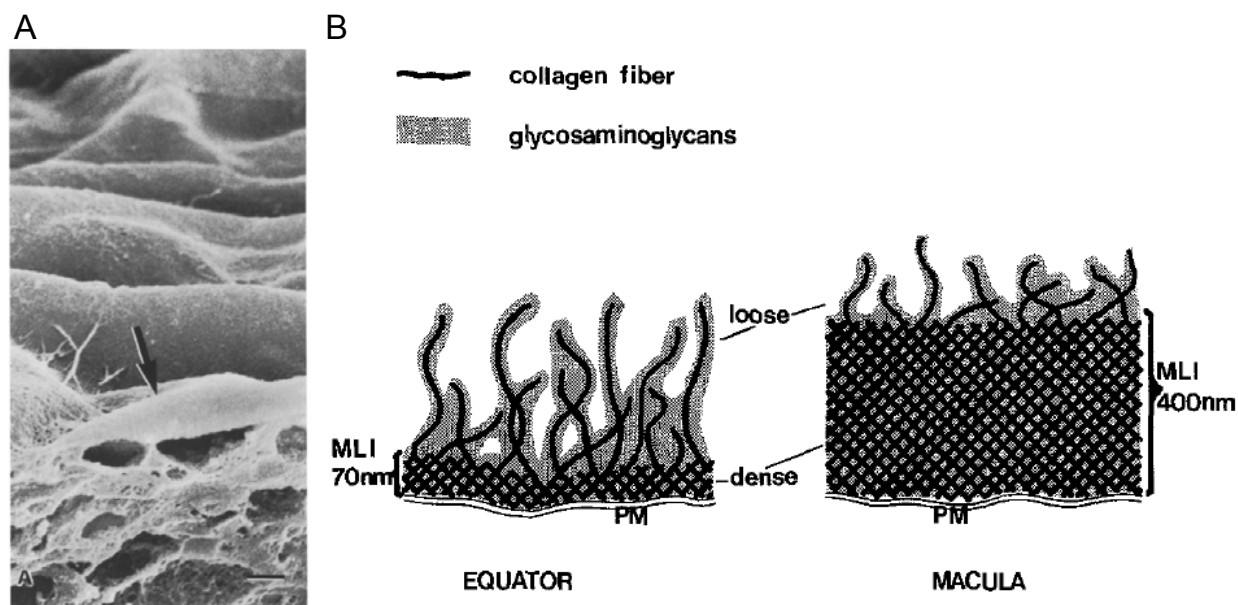
Altogether, vector design and optimization is thus an important step as clever vector design enables best use of the small space (genome) in vectors –which is especially true for AAVs.

#### iv. Translation of gene therapy from rodents to primates

Retinal gene delivery and therapy tools have been extensively developed and optimized in rodents (95). Yet there is a huge gap between results obtained in mouse and their translability to primates and human clinical trials. Indeed, AAV vectors proven to be efficient in mouse retina do not always perform the same way in larger animal models (124, 133, 154). AAV2 has been shown to transduce cones in the canine retina (141) while AAV9 is more efficient for transducing NHP cones (135). The main reason for this being the interspecies difference of retinal structure and the receptors expressed by retinal cell types. This results in interspecies variations of AAV’s behavior because of the structure of the vector, and is also conditioned by physical and cellular barriers. Thus, it is essential to better understand the behavior of AAVs from one species to another, and test gene therapy vectors in multiple animal models before translating these tools to the clinic.

Transduction characteristics also vary with the disease state, as AAV accessibility to retinal layers will depend on retinal health. It has been shown that structural and biochemical characteristics are modified when the retina is damaged, thereby changing AAV diffusion capacities (155, 156). This is due to the ILM, a natural barrier between the

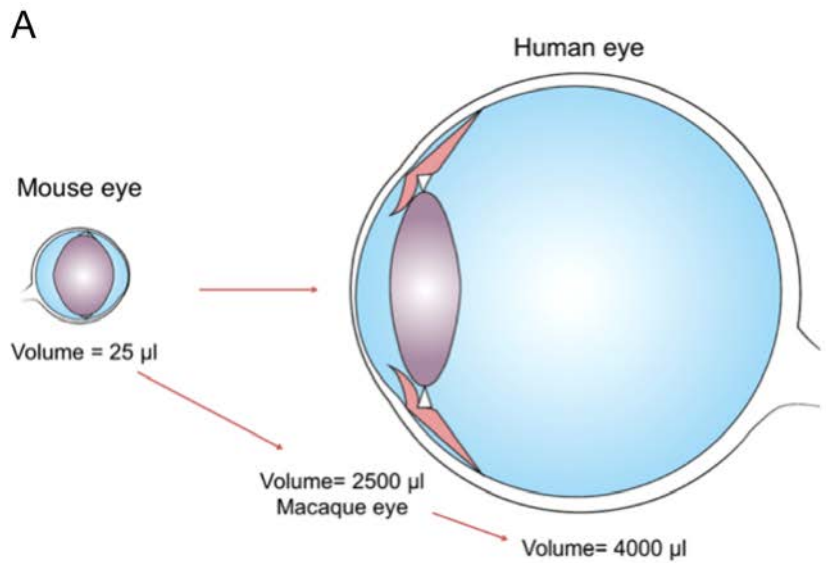
vitreous and the retina. It is constituted by glial Müller cell endfeet and a layer of glycosaminoglycans secreted by Müller cells, responsible for the limitation of passage from the vitreous to the retina. The ILM is disorganized in retinal degeneration, thereby increasing the accessibility for AAV (155, 156).





**Figure 32: Structure and thickness of the inner limiting membrane (ILM), an important barrier to AAV particles and determinant of transduction patterns.** The ILM is thinner in the macula (except in the foveola where it is very thin) compared to the peripheral retina. Adapted from (157).

As already stated the mouse is not always the most appropriate model as the eye structure is different than in humans. Mouse eye volume is about 25 microliters, while the monkey's is 100 times greater and the human vitreous volume is 160 times the volume of mouse vitreous (Figure 33). The proportion of cones versus rods of photoreceptors is different, rodent retinas are rod-dominated and they are nocturnal animals while primates have a much higher number of cones and are diurnal species. Also, the immune system of rodents is different than that of primates.

Nevertheless, mouse models of retinal degenerations are widely used for proof-of-concept gene therapies. There are a large number of mouse models including diseases like achromatopsia (145), and retinitis pigmentosa (158) with spontaneous mutations (referred to as retinal degeneration 1 (rd1) or rd10). The major limitation of NHP however, is the absence of a retinal degeneration model. In the absence of such conditions, experiments are performed in wild-type monkeys. They still allow assessment of AAV efficiency and expression pattern, as well as safety profile.



**B**

Pros	
<ul style="list-style-type: none"> <li>- Many naturally occurring models</li> <li>- Genetic modification</li> <li>- Lots of offspring</li> <li>- Generation time</li> </ul>	<ul style="list-style-type: none"> <li>- Human eye size</li> <li>- Anatomically similar to humans</li> </ul>
 Rat/Mouse	 Macaque
<ul style="list-style-type: none"> <li>- Nocturnal</li> <li>- Photoreceptor anatomy (calyceal processes)</li> </ul>	<ul style="list-style-type: none"> <li>- No IRD model existing</li> <li>- Moderately annotated genome</li> <li>- Ethical restrictions</li> </ul>
Cons	

**Figure 33: Differences between mouse and primate eyes. (A) Comparison of mouse, macaque and human eye volume. (B) Pros and cons of each animal model for gene therapy research (159).**

#### IV. Objectives of the PhD project: gene delivery to cones for mutation independent gene therapy

My main objective is to design efficient gene therapies and vectors to prevent vision loss, and restore vision. In particular, we focus on RP, as it is the most prevalent inherited retinal degeneration, affecting 1.5 million people worldwide with no treatment so far.

##### i. Therapeutic objectives

In particular, I looked for vectors that can target cones for treatment of RP patients using optogenetic strategies. Another aim was to design a combined protective and restorative therapy for longer lasting therapeutic benefits expected than with either therapy alone.

To translate cone reactivation strategy from mice to primates, one important challenge to overcome is to target the fovea non-invasively. Subretinal injection under the central retina is used in most clinical trials to treat the fovea. However it is an invasive technique and can be associated to side effects such as macular holes and VA decrease or retinal thinning (56, 58, 62, 69, 131) and therefore there is a risk to exacerbate disease state by further damaging photoreceptors, especially at advanced disease stages. Given the fragility and importance of the fovea, it is important to develop alternative strategies that can spare the fovea from its detachment when administering the vector. Keeping in mind available data from clinical trials, I found that the gaps in the field to be filled were safer and less invasive foveal cone targeting together with high level therapeutic gene expression.

In this context, during my thesis I focused on the development of viral tools and surgery modalities (Figure 34). To do so I looked for:

- A vector administered subretinally in the peripheral retina, but that is capable of transducing cones of the fovea without detaching it.
- A vector administered into the eye's vitreous without any contact with the retina or the fovea but able to transduce specifically foveal cones.

In parallel, I investigated the safety and toxicity of these vectors. I also optimized and tested combined protective and restorative approaches in the retinal degeneration 10 (rd10) mouse model for RP.

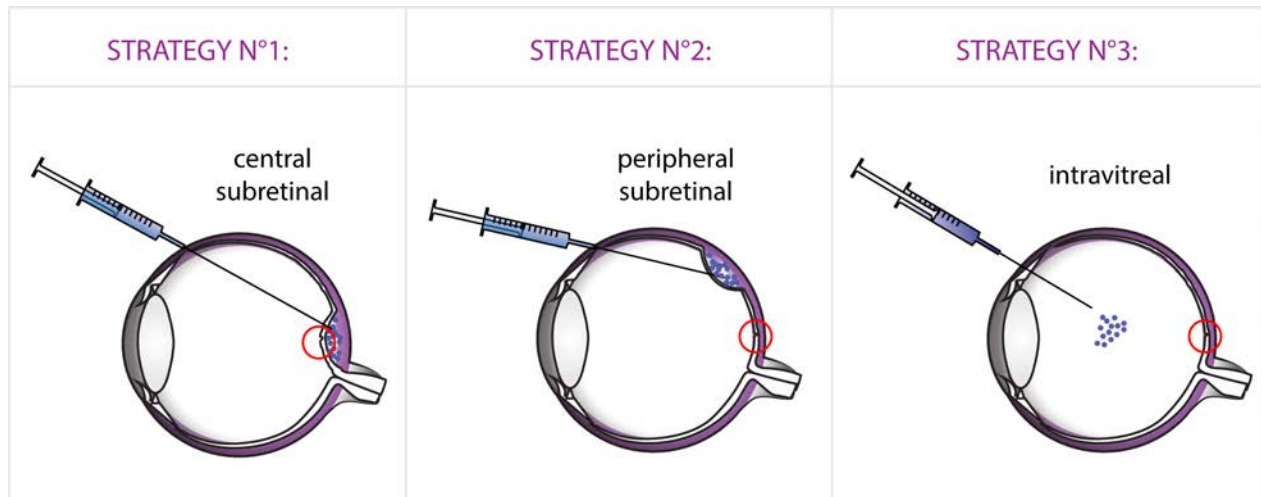


**Figure 34 : Gene therapy strategies to treat the fovea. Strategy n°1: Central subretinal injection. Strategy n°2: Distal bleb without foveal detachment. Strategy n°3: Intravitreal injection. Red circle shows the location of the fovea.**

How to develop vectors adapted to my objectives? I first searched for existing capsids and promoters compatible with cone-specific transgene expression. If not possible, creation of new capsids and promoters is necessary, using for example high-throughput techniques like directed evolution.

There already is a capsid compatible with highly efficient delivery to photoreceptors from the vitreous. This vector was discovered in the Flannery and Schaffer labs (USA), and is referred to as AAV2-7m8 (124). It was combined with a ubiquitous cytomegalovirus (CMV) promoter, thereby transducing all retinal layers. More recently, the company AGTC (USA) characterized and developed new cone-specific promoters. In particular, the promoter PR1.7 is particularly promising in primates (144, 146). I thus decided to combine these for the intravitreal approach. However, the major limitation of intravitreal injections is the pre-existing AAV immunity in the humans, 72% of the general population has pre-existing immunity to AAV2 (107). Neutralizing antibodies block AAV from reaching and entering target cells, thereby preventing transgene expression.

Therefore, I still needed to find another strategy for patients who would have high titer antibodies against AAV2 vectors (160). However, for the development of the distal subretinal approach, AAV2-derived capsids are not the best option as they are not the most efficient for transduction of cones in primates. It has been shown that AAV9 has a better tropism for cones than AAV2 when administered subretinally (135). We thus focused on the development of a new AAV9-derived vector for better transduction of cones from the periphery.

Both strategies had to be compatible with ‘dose sparing’ but still lead to high transgene expression levels, as high-input vector doses can be harmful.

## ii. Specific objectives and steps of my thesis

As previously described, numerous parameters can dramatically affect expression patterns and therapeutic outcomes, namely AAV capsid, expression cassette design involving choice of promoter, enhancer sequences, transgene -not mentioning AAV administration route, organ size and retinal health state.

During my thesis I focused on the following steps for the development and validation of new strategies for foveal gene delivery and combinatorial gene therapy for RP.

- (1) **Dose-ranging and toxicity studies** to determine best parameters for future therapeutic application
- (2) **Development and characterization of AAV capsids** compatible with highly efficient photoreceptor transduction in vivo in the mouse retina
- (3) **Optimization of the expression cassette to obtain cone-specific transduction** in wild-type and retinal degeneration mice

To select best tools for later proof-of-concept in macaques, I screened for best capsids and promoters in the mouse retina. I chose them based on their performance in mouse, macaque and human tissue (88, 89, 124, 144, 145).

- (4) **Translational study**: surgery modalities for foveal transduction in macaques in vivo
- (5) **Validation of gene therapy products in human tissue**

To do so, I focused on two system models:

- a) **Retinal organoids derived from human induced pluripotent stem (iPS) cells**
- b) **Adult human post-mortem retinal explants**

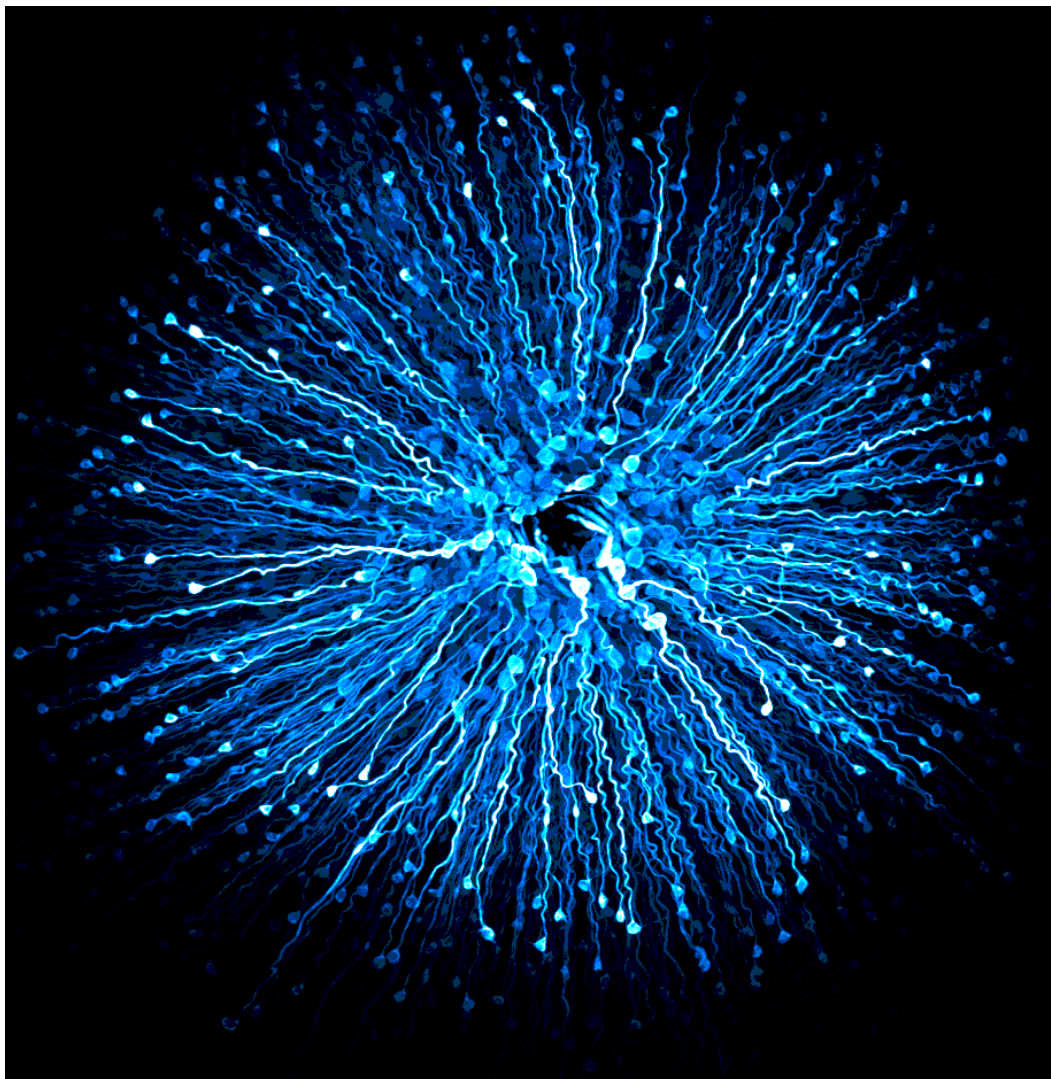
Optimization and validation of a gene-based drug into all of these animal and cellular models, in vitro and in vivo, is challenging, but it eventually provides solid evidence for its potential future application in patients.

- (6) **Test of the combined protective and restorative gene therapy**

An additional aim of my thesis was to design a longer-lasting gene therapy strategy, where expression of neurotrophic factors such as RdCVF would be combined to Jaws expression. In principle, this would enable prolonged cone survival and therefore, prolonged and better efficacy of optogenetic-mediated vision restoration. Although we managed to complete and publish the other works, this part of my work is still ongoing in the lab.



# Results







## I. Toxicity study of AAV vectors at high-input doses

Although AAV is generally admitted to be safe, there are a few reports of neurotoxicity in the brain (117–119) or immunogenicity in the retina (58, 71) when high doses are used (Table 1). Therefore, safety concerns might appear for the very specific conditions of gene therapy where high amounts of vectors are administered locally in a small tissue volume. However, whether these side effects on the retina are due high amounts of capsid or transgene itself remain unclear. Besides, the importance of choosing ubiquitous versus specific promoters is not well characterized. We show here that at high doses, all of these parameters can potentially contribute to inducing side effects, collectively. Moreover, at high doses, we observed apoptosis suggesting cellular toxicity -and not simply inflammation. Therefore, dose sparing is crucial to avoid any side effect in retinal gene therapy, and in gene therapy in general. Dose sparing can be achieved using newly created capsids, and/or more efficient promoters (92). The therapeutic dose of a given protein needs to be determined on a case-by-case basis.

Manuscript in preparation:

**Khabou H.**, Cordeau C., Vendomèle J., Pacot L., Fisson S., and Dalkara D. Deciphering AAV components involved in retinal toxicity at high-input doses.

Additional information including supplementary figures are available in Annex I.

**Table 1: AAV doses and induction of side effects in the retina**

Study	Species	AAVs used	Type of injection	Injected doses	Inflammatory dose	Observations
Barker et al. 2009 (161)	Mouse	AAV2	Subretinal	$5 \times 10^{11}$ vg	None	No inflammation (but variable expression in contralateral eye after AAV re administration)
Vandenbergh et al., 2011 (120)	Nonhuman primate	AAV2, AAV8	subretinal	$10^8, 10^9, 10^{10}, 10^{11}$	$10^{11}$	Retinal defects and inflammation at higher but not lower doses
Dalkara et al. 2013 (124)	Nonhuman primate and mouse	AAV2-7m8	intravitreal	$5 \times 10^{12}$ vg/eye in NHPs; $1 \times 10^{12}$ vg/eye in mice	$5 \times 10^{12}$	Inflammation after injection and 3 months post-injection in NHPs; none in mice.
Ramachandran et al. (162)	Nonhuman primate	AAV2-7m8 and AAV8-BP2	Subretinal and intravitreal	$10^9$ to $10^{12}$	$1 \times 10^{12}$	Glial activation and retinal infiltrates, especially subretinally (at highest dose)
Reichel et al. (71)	Nonhuman primate	AAV8	Subretinal	$10^{11}$ and $10^{12}$	$1 \times 10^{12}$	Inflammation, subretinal and choroidal infiltrates (at higher but not lower doses)
Takahashi et al. (163)	Nonhuman primate	AAV2-3YF	Intravitreal, 1 month after vitrectomy and ILM peeling	$9.5 \times 10^{11}$	$9.5 \times 10^{11}$	No serious side effect
Boye et al. (164)	Nonhuman primate	AAV2	Intravitreal, under the ILM (subILM)	$4.5 \times 10^{10}$	None	No inflammation
Comander et al. 2016 (165)	Nonhuman primate	AAV2 and Anc80	Intravitreal after ILM « peel and puddle »	$1 \times 10^{11}$	$1 \times 10^{11}$	Inflammation related to the surgery or GFP?
Bainbridge et al. 2015 (58)	Human (clinical trial)	AAV2	Subretinal	$10^{11}$ and $10^{12}$	$1 \times 10^{12}$	None of the participant of the low-dose

	number NCT00643 747)					( $1 \times 10^{11}$ vg) cohort had inflammation ; but five of the eight participants from the high-dose group ( $1 \times 10^{12}$ vg) presented intraocular inflammation or immune responses
--	----------------------------	--	--	--	--	--

**Title:**

**AAV vector components involved in retinal toxicity at high-input doses**

**Authors:**

**Hanen Khabou, Chloé Cordeau, Julie Vendomèle, Laure Pacot, Sylvain Fisson  
and Deniz Dalkara**

**Affiliations :**

<sup>1</sup>Sorbonne Universités, UPMC Univ Paris 06, INSERM, CNRS, Institut de la Vision,  
17 rue Moreau, 75012 Paris, France.

<sup>2</sup>Généthon, INSERM U951, Université d'Evry Val d'Essonne.

**Short title: Causes of AAV toxicity in the retina at high doses**

## **Abstract**

Today, there are about 40 recruiting or ongoing ocular clinical trials to treat retinal disorders, globally. Most of them rely on the use of AAV vectors that have an excellent safety profile. Nevertheless there are few reports suggesting neurotoxicity at high-input AAV doses in the brain, and clinical reports about inflammation in treated eyes despite the ocular immune privilege. Whether this is due to high levels of the expressed transgene, the cells in which the protein is expressed or due to the AAV capsid itself remains unclear. Here, we aimed to decipher which components of AAV-mediated gene expression causes side effects at high input doses in wild-type mice. We show that both the capsid and the transgene contribute to toxicity regardless of the nature of the transgene and the cell-type specificity of its expression. We also found that the toxicity leads to cell death by apoptosis, and local inflammation occurs in treated retinas. Nevertheless we did not find significant cellular responses towards AAV or its transgene even at the highest doses. Altogether our data show the importance of reducing input doses while increasing transgene expression levels via the use of more efficient capsids and promoters to avoid side effects in gene therapy.

## Introduction

Over the past twenty years, considerable efforts have been invested in establishing safe and effective gene therapy approaches for a multitude of diseases<sup>1</sup>. Applications in the retina have been particularly successful with positive outcomes and lack of side effects confirming the suitability of the eye as a target organ<sup>2</sup>. Today, more translational studies are being undertaken and there is a noticeable increase in the number of clinical trials being prepared with diverse strategies from gene replacement<sup>3,4</sup> to neuroprotection<sup>5</sup> to optogenetics<sup>6</sup>. The cell targets, the nature and amount of proteins being expressed in these newer applications demand higher level gene expression in more difficult-to-transduce cell types. These studies and others to follow are likely to put higher demands on AAV as a gene delivery vehicle and this might lead to the use of higher input doses. In increasing AAV input doses, several potential obstacles need to be taken into account. These include but are not limited to; 1) phenotoxicity, i.e. problems arising from either overexpression or ectopic expression of the transferred gene; 2) immunotoxicity, i.e. harmful immune responses to either the vector and/or to the transgene product<sup>7,8</sup>.

AAV vectors have been widely adopted as gene delivery vehicles because of their ability to transduce a wide variety of tissues, mediating long-term expression of the transgene after a single in vivo administration. Wild-type AAV is not associated with any disease pathology in humans, and is also naturally replication-defective, requiring a helper virus such as adenovirus to replicate<sup>9</sup>. AAVs are one of the simplest gene therapy vectors, containing only the transgene expression cassette flanked by two non-coding viral inverted terminal repeats (ITRs) enclosed in a capsid composed of three structural proteins, VP1, 2, and 3<sup>10</sup>. The simplicity of AAV vectors, and their low efficiency in transducing professional antigen presenting cells (APCs) (e.g. macrophages or dendritic cells)<sup>11-13</sup> likely contribute to their generally low immunogenicity namely in the eye<sup>14</sup>. Moreover, transferred genomes tend to persist inside the cells mainly in an episomal, non-integrated form, reducing the chances of insertional mutagenesis<sup>15</sup>. All of these favorable properties are accountable for the success of AAV in gene therapy thus far.

Current experience indicates that injection of small doses of AAV vector into immuno-privileged sites are tolerated however the longevity of expression has been debated in recent studies<sup>16,17</sup>. Lack of sufficient expression was put forward as a

potential cause of lack of long term efficacy in these studies<sup>18</sup> but, there is evidence that AAV injections are neurotoxic at high doses in the brain<sup>19-21</sup>, indicating a clear need to adjust the dose of AAV to obtain optimal balance between therapeutic benefit while avoiding toxicity. Thus far there have been a few studies reporting AAV gene delivery related toxicity in the retina, and what elements of AAV mediated gene delivery contribute to toxicity remain unclear. To answer these questions, we tested multiple AAV constructs to determine which parameters of the vector contribute to toxicity at high doses. Here we show that several components of AAVs play a role in causing retinal toxicity and this leads to local inflammation. AAV capsid protein is responsible for some of the toxic effects although non-coding capsids at equal doses cause less toxicity. The nature of the expressed protein as well as the cells in which they are expressed play smaller role in the development of toxicity. These findings collectively support dose sparing to reduce the risk of exacerbating disease state in future therapeutic applications. Importantly, they draw attention to the toxicity of high concentration AAV-GFP vectors frequently used as controls in gene therapy experiments and that can bias the results.



## Results

### High-input AAV doses have deleterious effects on retinal structure and function

Subretinal injections have been the preferred administration route for gene delivery to photoreceptors and the retinal pigmented epithelium (RPE). High input doses are often used to increase therapeutic gene expression in gene therapy settings. To investigate the possible toxicity of vectors as a function of input dose, we used an AAV8 vector, frequently used for targeting the photoreceptors. The vector was produced at high titer and encoded GFP under a ubiquitous CAG promoter. We performed subretinal injections at a dose of  $5 \times 10^{11}$  vg/eye in 1  $\mu$ L volume in  $n=5$  animals, bilaterally. Reporter gene expression was monitored on a weekly basis with fluorescent fundus imaging. Strong GFP expression was visible in all animals two weeks post dosing (Fig. 1A). Interestingly, GFP expression decreased with time as seen on the eye fundus images (Fig. 1A,B). We next injected four lower AAV doses to find the dose at which toxicity starts. To this aim,  $5 \times 10^8$ ,  $5 \times 10^9$ ,  $5 \times 10^{10}$ , and  $5 \times 10^{11}$  viral particles/eye were injected ( $n=8-10$  eyes per condition). Uninjected and PBS-injected animals served as controls ( $n=3-5$  eyes per condition). We measured the electroretinograms (ERGs) five weeks after injections. There was no significant effect of the PBS injection, showing that adverse effects are not due to surgical methods. However, we found a significant dose related decrease in ERG amplitudes (Fig. 1C). To determine whether retinal function alteration was attributable to cell loss we prepared retinal cryosections. We found a correlation between damage to the outer nuclear layer (ONL) and functional effects as a function of injected dose (Fig. 1D). Nearly complete ONL loss was observed at a dose of  $5 \times 10^{11}$  viral particles/eye.

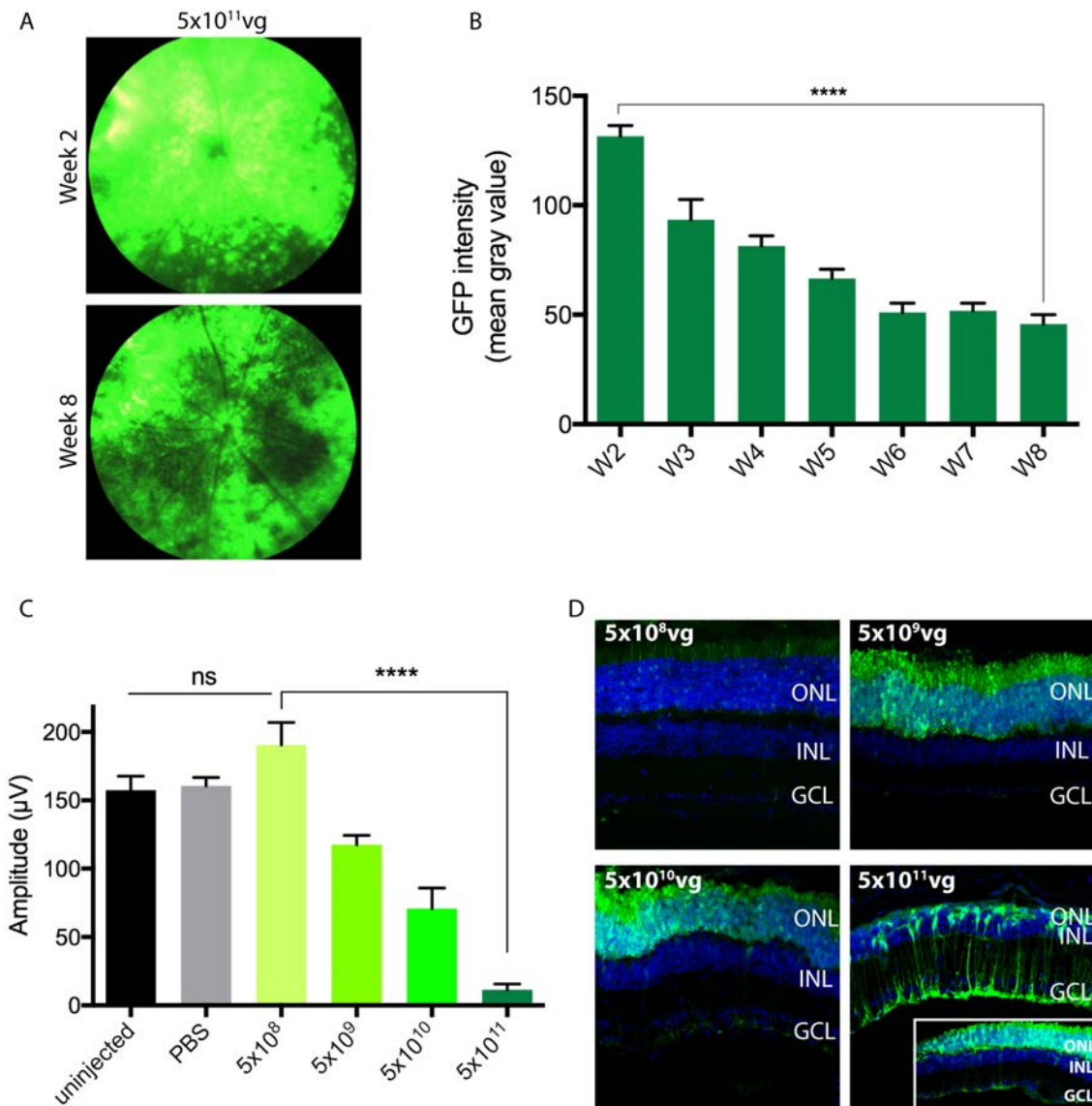


**Figure 1 : Effect of AAV8-GFP injection on retinal structure and function. (A)** Representative eye fundus images showing GFP fluorescence using  $5 \times 10^{11}$  vg/eye at 2 and 8 weeks post-injection. **(B)** GFP expression as a function of time calculated as mean gray value in fluorescent fundus images across n=10 retinas. Errors bars are mean  $\pm$ SEM. Kruskal-Wallis ANOVA test, P value is expressed as the following: P\*\*\*\* :  $P < 0.0001$ . **(C)** Photopic ERG b-wave amplitudes averaged across n=8-10 eyes per dose. Errors bars show mean  $\pm$ SEM. Kruskal-Wallis ANOVA test, P value is expressed as the following: P\*\*\*\* :  $P < 0.0001$  ; ns : non significant. **(D)** Representative cryosections of retinas injected with increasing AAV doses. Green (GFP), blue (DAPI) ; vg : viral genome.

## Cellular and humoral immune responses to high input doses of AAV-GFP

We then asked whether observed defects (Figure 1) were due to cellular immune responses towards the capsid antigens and/or the transgene. To answer this question we first performed unilateral subretinal injections of a control AAV8 where the transgene is oriented in reverse orientation in between loxP sites. This AAV (referred to as AAV8-flox) can only lead to expression in cells expressing Cre recombinase and therefore serves as a non-coding control in our experiments. We extracted viral DNA from spleens of n=4 unilaterally injected animals and n=4 uninjected animals (Figure 2). Viral DNA was detected in spleens suggesting that AAV diffused from the eye to the spleen and/or that AAV genome was detected in the eye and then presented by APCs to splenocytes.

Next, we checked B- and T-cell responses to the vector capsid and to GFP transgene using subretinal unilateral injections of AAV8-GFP, by ELISA and interferon gamma ELISpot assay. We used intramuscular injections of AAV1-GFP as positive controls and PBS-injected mice as negative controls. We first looked at humoral responses using ELISA tests from serum samples 20 to 30 days after injections. Cellular responses from splenocytes were assessed using ELISPOT to detect IFN $\gamma$  producing cells 10 to 30 days after injection. We detected humoral responses against both capsids, although they were stronger in AAV1-injected animals. There was a significant humoral response against GFP with intramuscular but not with subretinal injections. There was a non-significant cellular response against GFP using AAV1 at day 10 or AAV8 at day 20. These results coincided with peak GFP expression for each case. Indeed we observed that muscles were bright green at day 10 (D10) upon necropsy, but there was less GFP expression at D20, suggesting destruction of GFP-expressing cells. Peak GFP expression occurred later in retinas (day 15-20). There was also a significant cellular response towards GFP at D30 using intramuscular injections of AAV1.

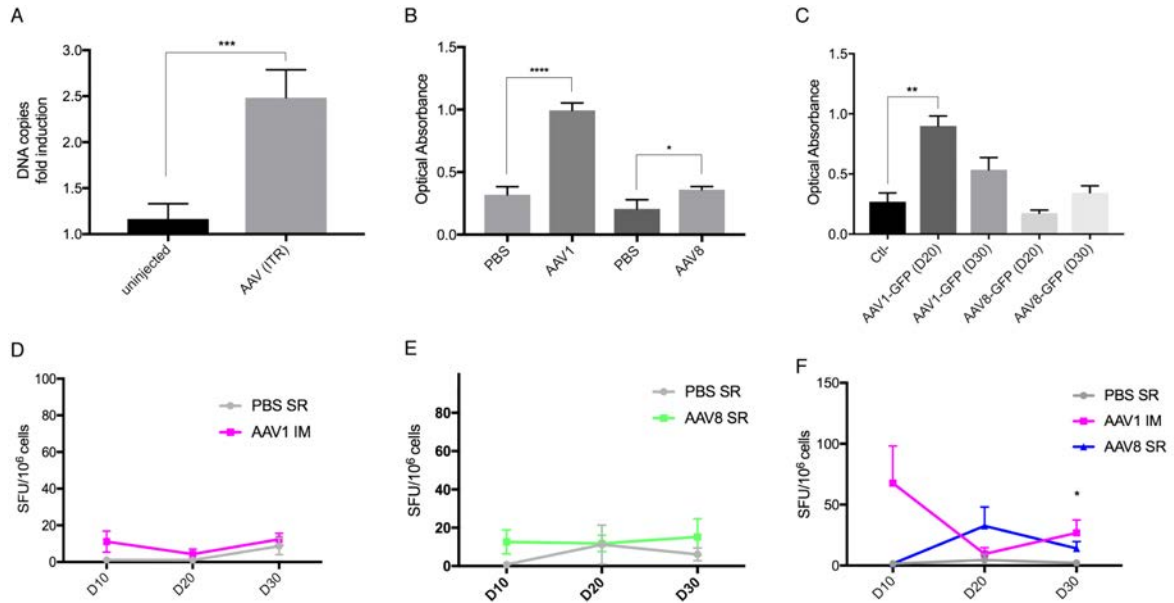


**Figure 2 : High AAV doses delivered subretinally elicit humoral but not cellular immune responses against capsid and transgene. (A)** qPCR for detection of AAV genome after subretinal injection of a non coding-AAV8-flox (n=4) and uninjected animals (n=4). Unpaired Student t-test and P value = 0,0009. **(B)** ELISA test to detect humoral responses against the capsid. Kruskal-Wallis ANOVA test, P value is expressed as the following: P\*\*\*\* : P<0.0001 ; P\* : P<0.0332. **(C)** ELISA test to detect humoral responses against the capsid. Kruskal-Wallis ANOVA test, P value is expressed as the following: P\*\*\*\* : P<0.0001 ; P\* : P<0.0332. **(D)** ELISPOT assay from spleens of AAV1-injected mice to detect cellular response towards AAV1 capsid. There was no significant difference between treated and control groups at any time point, analyzed with an unpaired Student's t-test (P>0,05). **(E)** ELISPOT assay from spleens of AAV8-injected mice to detect cellular response towards AAV8 capsid. There was no significant difference between treated and control groups at each time point. Student's t-test (P>0,05). **(F)** ELISPOT assay from spleens of AAV1- or AAV8-injected mice to detect cellular response towards GFP protein. There was a significant difference between AAV1-GFP and PBS groups at D30 but not between AAV8-GFP and PBS groups (Kruskal-Wallis ANOVA test, P\* : P<0.0332). There were no significant differences at the other timepoints. D10, D20, D30 : Day 10, 20 or 30 post-injection. All error bars are mean  $\pm$ SEM.

We then asked whether local immune responses were elicited within the retina at high doses. Two months after subretinal injections of AAV8-GFP, we prepared retinal cryosections and found positive immunostainings for GFAP, a marker for Müller glial cell activation, and Iba-1, a marker highly expressed by activated microglial cells, in AAV-injected retinas. No labeling was observed with either marker in PBS-treated retinas (Figure 3).

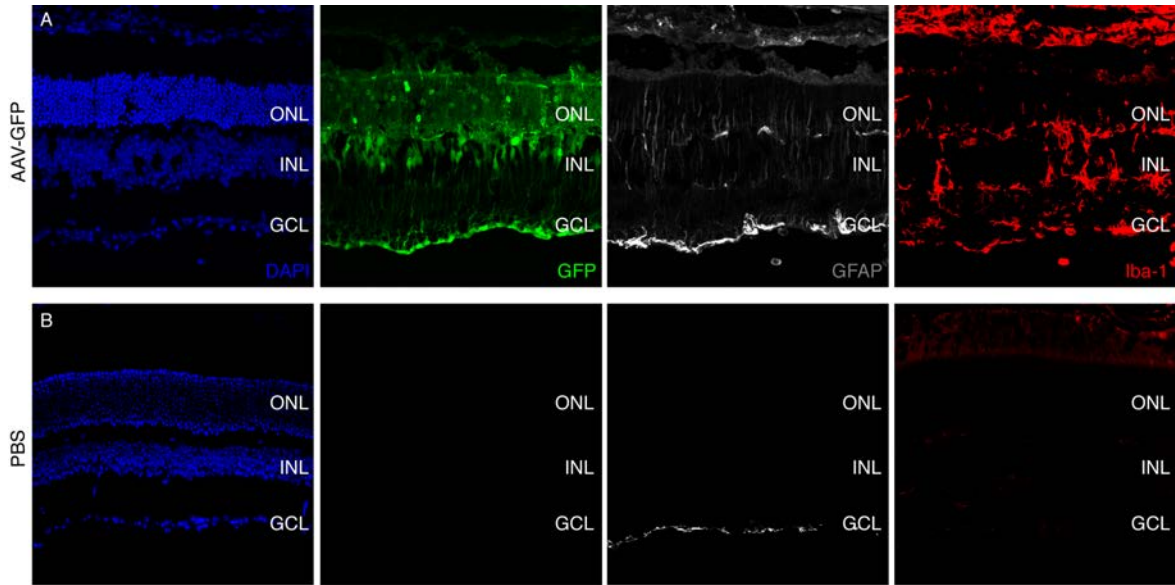


**Figure 3 : Local immune reactions to high AAV doses in retinas.** Representative retinal cryosections showing GFAP and Iba1 immunostainings after subretinal injection of  $5 \times 10^{11}$ vg of **(A)** AAV-GFP or **(B)** PBS.

These findings altogether show that high-dose AAV8-GFP injection leads to humoral responses against the AAV capsid but not the transgene. No significant cellular responses are induced at the peripheral level. However, local inflammation is present at the site of injection.

### **AAV capsid and transgene overexpression together cause apoptosis**

To test whether cell death was due to high levels of GFP protein or high amount of AAV capsids administered locally in a small volume, we performed equal dose injections with AAV8-GFP or AAV8-flox. As indicated by presence of cleaved caspase-3 positive cells, toxicity was observed with both vectors, when the same input dose was injected, suggesting that the capsid alone is responsible for part of the toxicity.

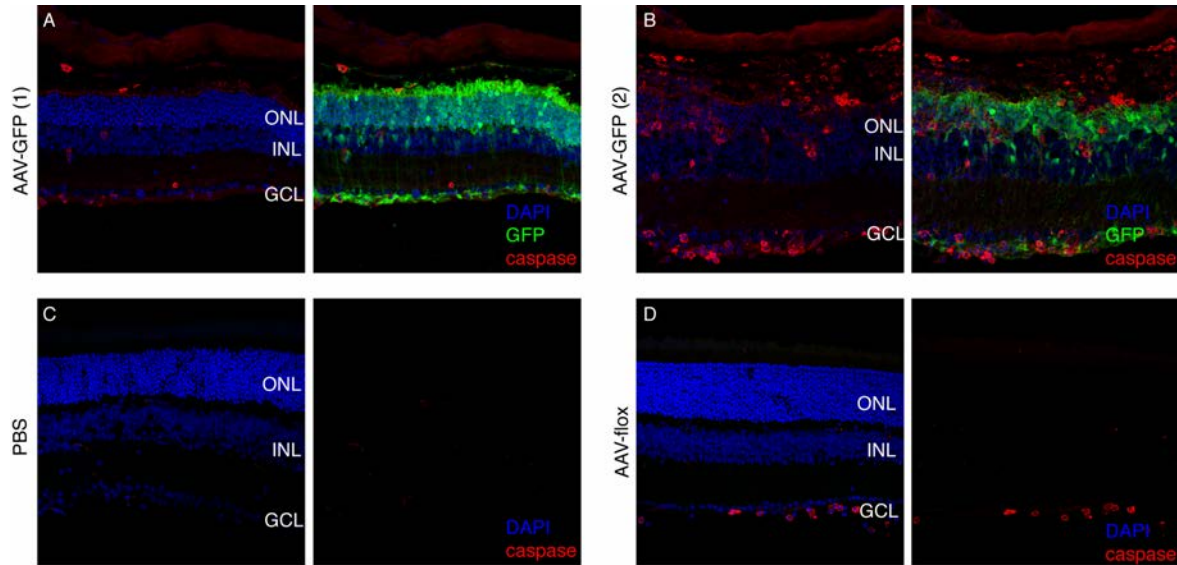


**Figure 4 : High AAV doses induce apoptosis.** Representative retinal cryosections showing activated caspase 3 immunostainings 8 weeks after subretinal injection of  $5 \times 10^{11}$ vg (A) AAV-GFP, ONL still distinguishable, (B) AAV-GFP, ONL damaged, (C) PBS, (D) and floxed AAV construct.

Finally, since GFP is a protein not normally found in the mammalian retina, we asked whether a retinal protein can also induce toxicity at high doses. To address this question, we injected mice with a high dose ( $5 \times 10^{11}$  vg) of AAV8 encoding retinoschisin, a protein already expressed in the retina. We found there was a significant ERG decrease with the retinoschisin (Figure 5). Altogether these data show that AAV capsid and expressed transgenes lead to photoreceptor toxicity and vision loss at high input doses.

### **Contribution of the promoter to cytokine production and ERG reduction**

We assessed the expression of several pro- and anti-inflammatory cytokines using RT-qPCR in retinas treated with non-coding AAVs compared to AAVs encoding GFP. We found expression of IL-6, IL-10 and IL-1B, in AAV-GFP treated retinas (Figure 5). These were lower in AAV-flox treated retinas, suggesting again a synergistic effect of transgene and capsid in inducing toxicity at high doses -as previously seen with apoptosis markers. ERG amplitudes were also reduced in mice treated with non-coding AAV, confirming this result (Figure 5). Interestingly, both cytokine production and ERG reduction were also observed for AAVs encoding GFP under a rod cell specific rhodopsin promoter. GFP expressed under rhodopsin promoter led to less cytokine production and a less dramatic decrease in ERG

compared to GFP expressed under a ubiquitous promoter. This is likely due to restriction of transgene expression to a specific subset of cells rather than the overall expression levels obtained with each promoter (Supplemental Figure 1). Indeed, we see higher expression with rhodopsin promoter although the toxicity is higher with CAG.

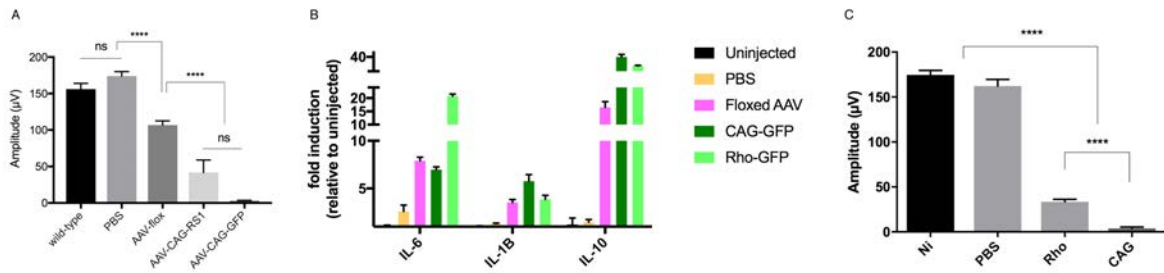


**Figure 5: Effect of different parameters of AAV vectors on the retina at high doses. (A)** Photopic ERG recordings using the highest doses,  $5 \times 10^{11}$ vg/eye subretinally. ANOVA test, P value is expressed as the following: P\*\*\*\* :  $P < 0.0001$  ; ns : non-significant. **(B)** RT-qPCR to measure cytokine expression. **(C)** Photopic ERG recordings using AAV8-CAG-GFP or AAV8-Rho-GFP, with a dose of  $5 \times 10^{11}$ vg/eye subretinally. ANOVA test, P value is expressed as the following: P\*\*\*\* :  $P < 0.0001$ . All error bars are mean  $\pm$ SEM.

## Discussion

Gene therapy holds promise for treating patients with inherited diseases. It is generally admitted that AAVs have an excellent safety profile, are non toxic and display low immunogenicity, nevertheless pre-clinical and clinical experience showed that AAV components can be recognized by the host immune system<sup>22</sup>. The extent of the impact of potential toxicity or inflammation on therapeutic efficiency remains poorly understood. In this context it is important to investigate what aspects of AAV vectors can induce toxic effects, in order to control them in gene therapy protocols. Indeed, there are now a few reports supporting acute toxicity from AAV at high-input doses, such as injections in the brain<sup>19,20</sup> or systemic injections to treat liver disorders<sup>23</sup>, but also when transducing embryonic stem cells in vitro, likely through disruption of DNA damage pathways<sup>24</sup>. Mechanism of AAV induced toxicity is likely distinct for each scenario.

We showed here that AAV can be toxic to the retina, at high input doses. High levels of both retinal and foreign reporter proteins expressed via AAV8 were neurotoxic to photoreceptors leading to ERG decrease. Both the capsid and the transgene played a role in toxicity suggesting that GFP encoding vectors should be carefully dosed when used as controls in gene therapy experiments. Indeed, high-level GFP expression in control retinas can give rise to false positive data by increasing the difference between control and treated groups. Importantly, high amounts of AAV capsids without any transgene expression, also led to retinal defects suggesting that the AAV capsid by itself accounts for part of the toxicity.

There are reports suggesting that the immune system plays a role in the toxic side effects observed at higher doses<sup>26</sup>. This can potentially affect therapeutic benefits by causing immune clearance of the transduced cells<sup>22</sup>. Even if efficient transgene expression and vision restoration are obtained at early timepoints, high-input doses can compromise long-term benefits by causing neurotoxicity and inflammation. We did not detect significant anti-AAV cellular responses using ELISpot assays. There is often no cellular response to AAVs after administration in the eye<sup>14</sup>, but it occurs with other administration routes<sup>27</sup>. On the other hand, we detected increased but non-significant anti-GFP cellular response after subretinal injections. This can be attributed to the fact that GFP is minimally immunogenic in C57BL6J mice<sup>28</sup>. Therefore, a very small number of T cells are likely to respond to



GFP, falling beneath the sensitivity of our ELISPOT assay. We detected local inflammation measured by inflammatory cytokine expression together with GFAP and Iba-1 overexpression in eyes treated with AAV-GFP or AAV-flox indicating immunogenicity at the local level.

Several studies suggest dosing thresholds to maintain safety<sup>26,29</sup>. However since there are numerous parameters that play a role on the efficacy of transduction and transgene expression –such as the promoter, the capsid and other cis regulatory elements– it is difficult to define one single dose for all retinal gene therapy settings. The threshold dose needs to be determined for each vector and target tissue, as a function of the administration route and animal model used. It has been shown in NHP studies, that intravitreal injections of  $1 \times 10^{12}$  vg/eye or more is harmful and inflammatory when associated to GFP and ubiquitous promoters<sup>32,33</sup>. Subretinally the threshold seems to be lower and around to  $1 \times 10^{11}$  vg/eye in NHPs<sup>3,29,33</sup> as higher doses were associated to inflammation<sup>26</sup>, also in patients<sup>16</sup>, likely because the vector is directly in contact with target cells. In mice the dose range is usually between  $1 \times 10^8$  and  $1 \times 10^{10}$ <sup>3,34,35</sup>.

Dose sparing using enhanced AAVs that allow to use low particle numbers while maintaining satisfying expression levels is an attractive strategy to alleviate AAV related toxicity issues<sup>6</sup>. Engineered capsids can be combined with cell-type-specific promoters that restrict transgene expression to target cells without the need to increase the dose<sup>6,36</sup>.

## **Material and Methods**

### **AAV production**

AAV vectors were produced as previously described using the co-transfection method and purified by iodixanol gradient ultracentrifugation<sup>37</sup>. AAV vector stocks were titered by quantitative PCR<sup>38</sup> using SYBR Green (Thermo Fischer Scientific).

### **Animals and intraocular injections**

Wild-type C57BL6/j mice (Janvier Labs) were used for this study. For ocular injections, mice were anesthetized by isoflurane inhalation. Pupils were dilated and a 33-gauge needle was inserted into the eye to deliver 1  $\mu$ L of AAV vector solution subretinally. Ophthalmic ointment (Fradexam) was applied after surgery. Eyes with extensive subretinal hemorrhage were excluded from the analysis. GFP expression was visualized using Micron III ophthalmoscope after dilation of the pupils and under isoflurane anesthesia.

### **ELISpot assays**

Spleens from injected mice were harvested and pulverized on cell strainers. Cellular content was collected in RPMI Medium (ThermoFischer Scientific) and red blood cells were lysed. Splenocytes were isolated after centrifugation at 4°C (350g for 5 minutes) by harvesting the cell pellet, which was resuspended in 2mL of RPMI medium. Cell concentration was determined using a 1:10 dilution in trypan blue to exclude dead cells. ELISpot plates were coated with anti-IFN $\gamma$  capture antibody (AN-18, eBioscience, 1mg/mL). Fifty microlitres of capture antibody (dilution 1/200) was added to each well in PBS and plates were incubated overnight at 4°C. The following day, plates were washed with PBS and blocked with 150 $\mu$ l per well of RPMI medium with 10% serum for 3 hours at 37°C. Plates were then washed again three times with PBS. Cells from splenocytes were diluted to 1x10<sup>6</sup> cells/well transferred to ELISpot plates in triplicate. For stimulation, medium contained either AAV8, AAV1 or GFP immunodominant peptide<sup>39</sup>, and a positive stimulation control with Concavalin A was included. ELISpot plates were then incubated at 37°C for 24 hours. After this time,

plates were emptied by flicking and wells were washed five times with 150  $\mu$ l of PBS with 0.05% Tween-20 (Sigma). Anti-IFN $\gamma$ -biotin detection antibody (XMG1.2, BD Pharmingen, 0,5mg/mL) was diluted (1/500) in PBS with 0.1% BSA and 50  $\mu$ l added to each well. Plates were then incubated at 4°C overnight. Plates were washed in PBS/Tween0.05% and 50  $\mu$ l per well of streptavidin (Boehringer-Manheim, 1089161) in PBS/BSA0.1% was added to each well. Plates were again incubated at room temperature for 1 hour. After final washes of 3x PBS/Tween0.05% and 3x PBS, plates were developed for up to 30 minutes with BCIP/NBT. Reactions were stopped by washing with tap water after which plates were allowed to dry before spot counting.

### **ERG recordings**

Mice were dark adapted overnight and then anesthetized. Pupils were dilated and mice were placed on a 37°C heated pad. Electrodes with contact lenses were positioned on the cornea of both eyes. A reference electrode was inserted into the forehead and a ground electrode into the back. ERGs were first recorded under scotopic conditions (Espion ERG System, Diagnosys) on a dark background. For recording of photopic ERGs, mice were initially exposed to a rod-saturating background for 10 minutes. Stimuli ranged were 1, 10 and 30  $\text{cd}\times\text{s}/\text{m}^2$  and were presented 60 times on a lighted background. Flicker ERGs were recorded following presentation of a 10-Hz stimulus on a rod-saturating background. Data were analyzed with Espion ERG, and then with GraphPad Prism.

### **RT-qPCR**

Animals were euthanized by CO<sub>2</sub> inhalation and cervical dislocation. Retinas were collected from each experimental condition (n = 3-4 retinas). Total RNA was harvested using a RNA-extraction kit (NucleoSpin RNA, Macherey-Nagel) and subjected to DNase digestion with Turbo DNase (ThermoFischer Scientific). Reverse transcription was performed with Superscript Reverse Transcriptase III (ThermoFischer Scientific) with oligodT primers (ThermoFischer Scientific). For qPCR, no-RT controls were used to confirm the absence of genomic DNA. The following primers were used: B-Actin: forward, 5'-GCTCTTTTCCAGCCTTCCTT-3' and

reverse, 5'-CTTCTGCATCCTGTCAGCAA-3'; IL-6: forward, 5'-  
AGGATACCACTCCCAACAGACCT-3' and reverse, 5'-  
CAAGTGCATCATCGTTGTTTCATAC-3'; IL-10: forward, 5'-  
ATTTGAATTCCTGGGTGAGAAG-3' and reverse, 5'-  
CACAGGGGAGAAATCGATGACA-3'; IL-1B: forward, 5'-  
ATGGCAACTGTTCTGAACTCAACT-3' and reverse, 5'-  
CAGGACAGGTATAGATTCTTTCCTTT-3'. cDNA levels were determined with  
relative cDNA quantification and are expressed as the fold induction compared to  
control groups (uninjected or PBS-injected animals). Samples were run in triplicates.

### **Histology, immunohistochemistry and microscopy**

Mouse eyes were enucleated and immediately fixed in 10% formalin – 4% formaldehyde for 2 hours for cryosections. After multiple washes and anterior parts removal, eyecups were immersed in PBS-30% sucrose overnight at 4°C. Afterwards they were embedded in OCT medium and frozen in liquid nitrogen. 10 µm-thick vertical sections were cut with a Microm cryostat. After incubation in the blocking buffer, sections were incubated with primary antibodies overnight at 4°C : Iba-1 antibody (019-19741, Wako); GFAP antibody (G3893, Sigma), Cleaved caspase 3 (9661S, Ozyme). After multiple washes of the sections, the secondary antibodies (Alexa Fluor 488, 594 or 647, Thermo Fischer Scientific) were added for 2 hours at room temperature, followed by several washes. Retinal flatmounts or cryosections were mounted in Vectashield mounting medium (Vector Laboratories) for fluorescence microscopy and retinal sections were visualized using an Olympus confocal microscope.

## **Acknowledgements**

This study was supported by Marie Curie CIG (334130, RETINAL GENE THERAPY), INSERM, Labex-Lifesenses (ANR-10-LABX-65), the Agence Nationale pour la Recherche - Recherche Hospitalo-Universitaire en santé (RHU) (Light4Deaf), Fondation NRJ. HK was supported by a PhD fellowship from the AFM-Téléthon. We thank Céline Winckler and Camille Robert for assistance with the production of plasmids and AAV vectors.

## **Author contributions**

HK and DD designed the study. HK performed surgery in mice. CC, LP and HK performed eye fundus imaging and ERG recordings. JV and HK performed ELISPOT assays. LP and HK performed ELISA tests. HK and CC performed immunohistochemistry. JV and SF helped design and execute experiments regarding analysis of immune responses, and gave feedback on the manuscript. HK, CC and JV analyzed the data. HK prepared the figures. HK and DD wrote the manuscript.

## References

1. Dunbar, CE, High, KA, Joung, JK, Kohn, DB, Ozawa, K and Sadelain, M (2018). Gene therapy comes of age. *Science* (80-. ). **359**: eaan4672.
2. Bennett, J (2017). Taking Stock of Retinal Gene Therapy: Looking Back and Moving Forward. *Mol. Ther.* **25**: 1076–1094.
3. Ye, G, Budzynski, E, Sonnentag, P, Nork, TM, Sheibani, N, Gurel, Z, *et al.* (2016). Cone-Specific Promoters for Gene Therapy of Achromatopsia and Other Retinal Diseases. *Hum. Gene Ther.* **27**: 72–82.
4. Scalabrino, ML, Boye, SL, Fransen, KMH, Noel, JM, Dyka, FM, Min, SH, *et al.* (2015). Intravitreal delivery of a novel AAV vector targets ON bipolar cells and restores visual function in a mouse model of complete Congenital Stationary Night Blindness. *Hum. Mol. Genet.* **9342**: 1–32.
5. Byrne, LC, Dalkara, D, Luna, G, Fisher, SK, Clérin, E, Sahel, JA, *et al.* (2015). Viral-mediated RdCVF and RdCVFL expression protects cone and rod photoreceptors in retinal degeneration. *J. Clin. Invest.* **125**: 105–116.
6. Khabou, H, Garita-Hernandez, M, Chaffiol, A, Reichman, S, Jaillard, C, Brazhnikova, E, *et al.* (2018). Noninvasive gene delivery to foveal cones for vision restoration. *J. Clin. Investig. Insight* **3**: e96029.
7. Manno, CS, Pierce, GF, Arruda, VR, Glader, B, Ragni, M, Rasko, JJ, *et al.* (2006). Successful transduction of liver in hemophilia by AAV-Factor IX and limitations imposed by the host immune response. *Nat. Med.* **12**: 342–7.
8. Mingozi, F, Maus, M V, Hui, DJ, Sabatino, DE, Murphy, SL, Rasko, JEJ, *et al.* (2007). CD8+ T-cell responses to adeno-associated virus capsid in humans. *Nat. Med.* **13**: 419–422.
9. Mouw, MB and Pintel, DJ (2000). Adeno-associated virus RNAs appear in a temporal order and their splicing is stimulated during coinfection with adenovirus. *J. Virol.* **74**: 9878–88.
10. Samulski, RJ, Berns, KI, Tan, M and Muzyczka, N (1982). Cloning of adeno-associated virus into pBR322: rescue of intact virus from the recombinant plasmid in human cells. *Proc. Natl. Acad. Sci. U. S. A.* **79**: 2077–81.
11. Jooss, K, Yang, Y, Fisher, KJ and Wilson, JM (1998). Transduction of dendritic cells by DNA viral vectors directs the immune response to transgene products in muscle fibers. *J. Virol.* **72**: 4212–23.

12. Zaiss, A-K, Son, S and Chang, L-J (2002). RNA 3' readthrough of oncoretrovirus and lentivirus: implications for vector safety and efficacy. *J. Virol.* **76**: 7209–19.
13. VANDENDRIESSCHE, T, THORREZ, L, ACOSTA-SANCHEZ, A, PETRUS, I, WANG, L, MA, L, *et al.* (2007). Efficacy and safety of adeno-associated viral vectors based on serotype 8 and 9 vs. lentiviral vectors for hemophilia B gene therapy. *J. Thromb. Haemost.* **5**: 16–24.
14. Bennett, J (2003). Immune response following intraocular delivery of recombinant viral vectors. *Gene Ther.* **10**: 977–982.
15. Duan, D, Sharma, P, Yang, J, Yue, Y, Dudus, L, Zhang, Y, *et al.* (1998). Circular intermediates of recombinant adeno-associated virus have defined structural characteristics responsible for long-term episomal persistence in muscle tissue. *J. Virol.* **72**: 8568–77.
16. Bainbridge, JWBJWB, Mehat, MSMS, Sundaram, V, Robbie, SJSJ, Barker, SESE, Ripamonti, C, *et al.* (2015). Long-Term Effect of Gene Therapy on Leber's Congenital Amaurosis. *N. Engl. J. Med.* **372**: 150504083137004.
17. Jacobson, SG, Cideciyan, A V., Roman, AJ, Sumaroka, A, Schwartz, SB, Heon, E, *et al.* (2015). Improvement and Decline in Vision with Gene Therapy in Childhood Blindness. *N. Engl. J. Med.*: 150503141523009doi:10.1056/NEJMoa1412965.
18. Koch, SF, Tsai, YT, Duong, JK, Wu, WHWPW, Hsu, CW, Wu, WHWPW, *et al.* (2015). Halting progressive neurodegeneration in advanced retinitis pigmentosa. *J. Clin. Invest.* **125**: 9–11.
19. Klein, RL, Dayton, RD, Leidenheimer, NJ, Jansen, K, Golde, TE and Zweig, RM (2006). Efficient Neuronal Gene Transfer with AAV8 Leads to Neurotoxic Levels of Tau or Green Fluorescent Proteins **13**: 0–10.
20. Cearley, CN and Wolfe, JH (2006). Transduction characteristics of adeno-associated virus vectors expressing cap serotypes 7, 8, 9, and Rh10 in the mouse brain. *Mol. Ther.* **13**: 528–37.
21. Ulusoy, A, Sahin, G, Björklund, T, Aebischer, P and Kirik, D (2009). Dose Optimization for Long-term rAAV-mediated RNA Interference in the Nigrostriatal Projection Neurons **17**: 1574–1584.
22. Mingozzi, F and High, KA (2017). Overcoming the Host Immune Response to Adeno-Associated Virus Gene Delivery Vectors: The Race Between

Clearance, Tolerance, Neutralization, and Escapeddoi:10.1146/annurev-virology.

23. Hinderer, C, Katz, N, Buza, EL, Dyer, C, Goode, T, Bell, P, *et al.* (2018). Severe toxicity in nonhuman primates and piglets following high-dose intravenous administration of an AAV vector expressing human SMN. *Hum. Gene Ther.*: in pressdoi:10.1089/hum.2018.015.
24. Hirsch, ML, Fagan, BM, Dumitru, R, Bower, JJ, Yadav, S, Porteus, MH, *et al.* (2011). Viral Single-Strand DNA Induces p53-Dependent Apoptosis in Human Embryonic Stem Cells. *PLoS One* **6**: 1–13.
25. Chan, F, Bradley, A, Wensel, TG and Wilson, JH (2004). Knock-in human rhodopsin – GFP fusions as mouse models for human disease and targets for gene therapy. *Proc. Natl. Acad. Sci. U. S. A.* **101**: 9109–9114.
26. Reichel, FF, Dauletbekov, DL, Klein, R, Peters, T, Ochakovski, GA, Seitz, IP, *et al.* (2017). AAV8 Can Induce Innate and Adaptive Immune Response in the Primate Eye. *Mol. Ther.* **25**: 1–13.
27. Vandenberghe, LH, Wang, L, Somanathan, S, Zhi, Y, Figueredo, J, Calcedo, R, *et al.* (2006). Heparin binding directs activation of T cells against adeno-associated virus serotype 2 capsid. *Nat. Med.* **12**: 967–971.
28. Skelton, D, Satake, N and Kohn, DB (2001). The enhanced green fluorescent protein (eGFP) is minimally immunogenic in C57BL/6 mice. *Gene Ther* **8**: 1813–1814.
29. Vandenberghe, LH, Bell, P, Maguire, AM, Cearley, CN, Xiao, R, Calcedo, R, *et al.* (2011). Dosage Thresholds for AAV2 and AAV8 Photoreceptor Gene Therapy in Monkey **3**.
30. Maclaren, RE, Groppe, M, Barnard, AR, Cottrill, CL, Tolmachova, T, Seymour, L, *et al.* (2014). Retinal gene therapy in patients with choroideremia: Initial findings from a phase 1/2 clinical trial. *Lancet* **383**: 1129–1137.
31. Khabou, H, Desrosiers, M, Winckler, C, Fouquet, S, Auregan, G, Bemelmans, AP, *et al.* (2016). Insight into the mechanisms of enhanced retinal transduction by the engineered AAV2 capsid variant -7m8. *Biotechnol. Bioeng.* **113**: 2712–2724.
32. Dalkara, D, Byrne, LLC, Klimczak, RR, Visel, M, Yin, L, Merigan, WH, *et al.* (2013). In vivo-directed evolution of a new adeno-associated virus for therapeutic outer retinal gene delivery from the vitreous. *Sci. Transl. Med.* **5**:



189ra76.

33. Ramachandran, P, Lee, V, Wei, Z, Song, JY, Casal, G, Cronin, T, *et al.* (2016). *Evaluation of dose and safety of AAV7m8 and AAV8BP2 in the non-human primate retina. Hum. Gene Ther.*, 1-40ppdoi:10.1089/hum.2016.111.
34. Allocca, M, Mussolino, C, Garcia-Hoyos, M, Sanges, D, Iodice, C, Petrillo, M, *et al.* (2007). Novel adeno-associated virus serotypes efficiently transduce murine photoreceptors. *J. Virol.* **81**: 11372–11380.
35. Allocca, M, Manfredi, A, Iodice, C and Vicino, U Di (2011). AAV-Mediated Gene Replacement , Either Alone or in Combination with Physical and Pharmacological Agents , Results in Partial and Transient Protection from Photoreceptor Degeneration Associated with <sup>n</sup>. PDE Deficiency. *IOVS* **52**.
36. Chaffiol, A, Caplette, R, Jaillard, C, Brazhnikova, E, Desrosiers, M, Dubus, E, *et al.* (2017). A New Promoter Allows Optogenetic Vision Restoration with Enhanced Sensitivity in Macaque Retina. *Mol. Ther.*doi:10.1016/j.ymthe.2017.07.011.
37. Choi, VW, Asokan, A, Haberman, R a and Samulski, RJ (2007). Production of recombinant adeno-associated viral vectors. *Curr. Protoc. Hum. Genet.*  
**Chapter 12**: Unit 12.9.
38. Aurnhammer, C, Haase, M, Muether, N, Hausl, M, Rauschhuber, C, Huber, I, *et al.* (2012). Universal Real-Time PCR for the Detection and Quantification of Adeno-Associated Virus Serotype 2-Derived Inverted Terminal Repeat Sequences. *Hum. Gene Ther. Methods* **23**: 18–28.
39. Han, W, Unger, W and Wauben, M (2008). Identification of the immunodominant CTL epitope of EGFP in C57BL/6 mice. *Gene Ther.* **15**: 700–701.
40. Barker, SE, Broderick, C, Robbie, SJ, Duran, Y, Natkunarajah, M, Buch, P, *et al.* (2009). Subretinal delivery of adeno-associated virus serotype 2 results in minimal immune responses that allow repeat vector administration in immunocompetent mice. *J. Gene Med.* **11**: 486–497.
41. Takahashi, K, Igarashi, T, Miyake, K, Kobayashi, M, Yaguchi, C, Iijima, O, *et al.* (2017). Improved Intravitreal AAV-Mediated Inner Retinal Gene Transduction after Surgical Internal Limiting Membrane Peeling in Cynomolgus Monkeys. *Mol. Ther.* **25**: 296–302.
42. Boye, SE, Alexander, JJ, Witherspoon, CD, Boye, SL, Peterson, JJ, Clark, ME,

*et al.* (2016). Highly Efficient Delivery of Adeno-Associated Viral Vectors to the Primate Retina. *Hum. Gene Ther.* **27**: 580–597.

43. Comander, J, Carvalho, L, Wassmer, S, Xiao, R, Plovie, E, Langsdorf, A, *et al.* (2016). Novel Surgical Method for Intravitreal AAV Administration Overcomes Transduction Barriers in Non-Human Primates. *Mol. Ther.* **24**: S13–S14.



## II. Design and characterization of enhanced capsids for photoreceptor transduction

AAV2-7m8 is an AAV2-derived vector that outperforms all other AAVs so far described for gene delivery to photoreceptors in the mouse and primate retina (124). However, the effect of 7m8 peptide insertion onto AAV2 capsid remained unclear. To better understand the effect of 7m8 peptide insertion, we asked whether it is responsible for better infectivity or diffusion properties. We also asked if 7m8 insertion could enhance properties of other AAV serotypes as it did for AAV2. We therefore inserted 7m8 onto AAV5, 8 and 9, chosen because they had better performance for transduction of photoreceptors compared to AAV2 in mice and large animal models. In this work, we showed that AAV2-7m8 has significantly enhanced infectivity compared to AAV2. Moreover, we showed that only AAV9 -but not AAV5 and AAV8- benefited from 7m8 insertion, enabling a 30-fold increase in infectivity. This newly described AAV9-7m8 vector has great potential in the primate retina as AAV9, its parental serotype, is better than other serotypes at transducing cones in monkeys when delivered subretinally (135). This set the foundation for our follow up work in non-human primates to transduce foveal cones.

These results have been published as a research article, highlighted on the Journal Cover.

**Khabou, H.**, Desrosiers, M., Winckler, C., Fouquet S., Auregan, G., Bemelmans, AP., Sahel, JA., Dalkara, D. Insight into the mechanisms of enhanced retinal transduction by the engineered AAV2 capsid variant - 7m8. *Biotechnology and Bioengineering*. 2016;12: 2712–2724.



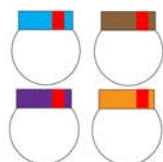
Additional information including supplementary figures and movies are available here, and in Annex II:

<http://onlinelibrary.wiley.com/doi/10.1002/bit.26031/abstract>

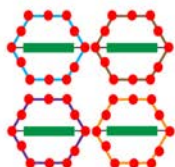
Graphical abstract

**1) Insertion of 7m8 peptide onto other AAV capsids**

Creation of AAV2, 5, 8, 9 -7m8 capsid genomes

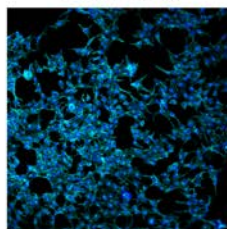


Production of the 7m8-modified vectors expressing GFP

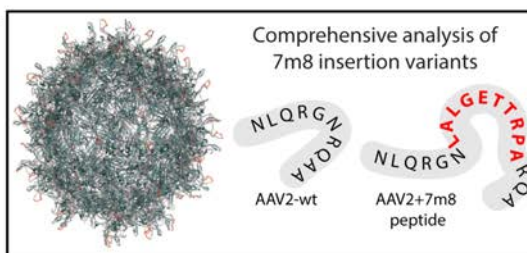
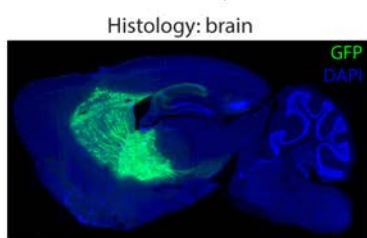


**2) In vitro analysis of viral infectivity and cell entry**

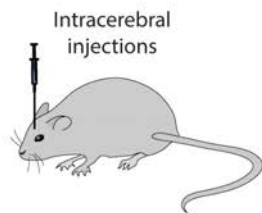
Cell infection



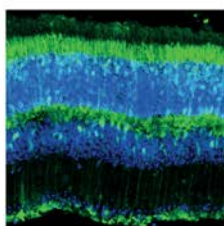
Visualization of AAV particles within single cells  
cytoplasmic/nuclear AAV particles



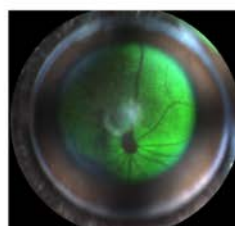
Intraocular injections



Histology: retina



Eye fundus imaging



**3) In vivo analysis of transduction efficiency**

# Insight Into the Mechanisms of Enhanced Retinal Transduction by the Engineered AAV2 Capsid Variant -7m8

Hanen Khabou,<sup>1</sup> MéliSSa Desrosiers,<sup>1</sup> Céline Winckler,<sup>1</sup> Stéphane Fouquet,<sup>1</sup> Gwenaëlle Auregan,<sup>2,3</sup> Alexis-Pierre Bemelmans,<sup>2,3</sup> José-Alain Sahel,<sup>1,4</sup> Deniz Dalkara<sup>1</sup>

<sup>1</sup>Sorbonne Universités, UPMC Univ Paris 06, INSERM, CNRS, Institut de la Vision, 17 rue Moreau, Paris 75012, France; telephone: +33 1 53 46 25 32;

fax: +33 1 40 02 14 99; e-mail: deniz.dalkara@gmail.com

<sup>2</sup>Commissariat à l'Énergie Atomique et aux Énergies Alternatives (CEA), Département des Sciences du Vivant (DSV), Institut d'Imagerie Biomédicale (I2BM), Molecular Imaging Research Center (MIRCen), F-92260 Fontenay-aux-Roses, France

<sup>3</sup>Centre National de la Recherche Scientifique (CNRS), Université Paris-Sud, Université Paris-Saclay, UMR 9199, Neurodegenerative Diseases Laboratory, F-92260 Fontenay-aux-Roses, France

<sup>4</sup>CHNO des Quinze-Vingts, DHU Sight Restore, INSERM-DHOS CIC, 28 rue de Charenton, Paris, France

**ABSTRACT:** Recently, we described a modified AAV2 vector—AAV2-7m8—having a capsid-displayed peptide insertion of 10 amino acids with enhanced retinal transduction properties. The insertion of the peptide referred to as 7m8 is responsible for high-level gene delivery into deep layers of the retina when virus is delivered into the eye's vitreous. Here, we further characterize AAV2-7m8 mediated gene delivery to neural tissue and investigate the mechanisms by which the inserted peptide provides better transduction away from the injection site. First, in order to understand if the peptide exerts its effect on its own or in conjunction with the neighboring amino acids, we inserted the 7m8 peptide at equivalent positions on three other AAV capsids, AAV5, AAV8, and AAV9, and evaluated its effect on their infectivity. Intravitreal delivery of these peptide insertion vectors revealed that only AAV9 benefited from 7m8 insertion in the context of the retina. We then investigated AAV2-7m8 and AAV9-7m8 properties in the brain, to better evaluate the spread and efficacy of viral transduction in view of the peptide insertion. While 7m8 insertion led to higher intensity gene expression, the spread of gene expression remained unchanged compared to the parental serotypes. Our results indicate that the 7m8 peptide insertion acts by increasing efficacy of cellular entry, with little effect on the spread of viral particles in neural tissue. The effects of peptide insertion are capsid and tissue

dependent, highlighting the importance of the microenvironment in gene delivery using AAV.

Biotechnol. Bioeng. 2016;9999: 1–13.

© 2016 Wiley Periodicals, Inc.

**KEYWORDS:** gene delivery; gene therapy; AAV; directed evolution; retina

## Introduction

Adeno-associated viruses (AAVs) are small (25 nm in diameter) non-enveloped viruses of icosahedral structure belonging to the *Dependovirus* genus of the *Parvoviridae* family. They are single-stranded DNA viruses with ~4.7 kilobases carrying capacity and their infectious life cycle depends on helper viruses such as adeno-, herpes- or papillomaviruses. Recombinant AAV vectors have a low immunogenicity and an excellent safety profile, providing long-term therapeutic gene expression, important for clinical application in gene therapy. Not surprisingly, AAVs are currently the vectors of choice and have been used successfully in the treatment of hemophilia (Nathwani et al., 2011, 2014) and in retinal degeneration (Bainbridge et al., 2008; Cideciyan et al., 2008; Maguire et al., 2008). Retinal gene therapy has been successful in the treatment of Leber congenital amaurosis (LCA) (Bainbridge et al., 2008; Cideciyan et al., 2008; Maguire et al., 2008) and choroideremia (MacLaren et al., 2014)—although for LCA the benefits were limited in time (Bainbridge et al., 2015; Jacobson et al., 2015). However, first generation vector technology used in these clinical trials needs improvements, for better

Correspondence to: D. Dalkara

Contract grant sponsor: AFM-Téléthon

Contract grant sponsor: Marie Curie CIG

Contract grant sponsor: INSERM

Contract grant sponsor: Labex-Lifesenses

Received 7 January 2016; Revision received 26 May 2016; Accepted 29 May 2016

Accepted manuscript online xx Month 2016;

Article first published online in Wiley Online Library

(wileyonlinelibrary.com).

DOI 10.1002/bit.26031

efficacy and for widespread gene delivery to the neural retina. Vector engineers have thus been working on improving AAV for future applications in the neural retina over the past 10 years (Vandenbergh and Auricchio, 2012).

The efficacy of AAV-mediated gene delivery to retinal cells is an intricate equation involving viral dose, administration route, disease state, animal model and viral capsid. These aforementioned parameters determine the ability of AAV to transduce various retinal cell types—the key cell targets in inherited retinal degeneration being the photoreceptors and the retinal pigmented epithelium (RPE) cells. Local ocular administration routes include subretinal and intravitreal delivery. Subretinal injections are most commonly used to access the outer retina, where vector is injected between photoreceptor and RPE cells. These cause a reversible retinal detachment and lead to high-level transduction in adjacent cells. One of the benefits of this administration route is the immune privilege in this compartment. AAV2, -5, -7, -8, -9 have been successful in gene transfer to photoreceptors when delivered into the subretinal space (Allocca et al., 2007; Auricchio et al., 2001; Mowat et al., 2014; Natkunarajah et al., 2008). However, retinal detachment can be associated with mechanical damage, especially in the fragile degenerating retina (Jacobson et al., 2012). The second administration route is intravitreal delivery, which deposits the vector dose in the vitreous—the gel-filled cavity of the eye. Intravitreal delivery is surgically simpler and can deliver genes pan-retinally in the rodent retina without surgical damage. However, natural AAVs cannot reach deep retinal layers when delivered into the vitreous, which usually prevents the use of this delivery route for outer retinal gene therapy. Naturally occurring AAV2 is highly efficient for pan-retinal transduction of the inner retina (Dalkara et al., 2013), directly exposed to the viral particles. But the photoreceptors and the RPE are not efficiently targeted by natural AAVs as they are buried under inner retinal neurons. Furthermore, the inner limiting membrane (ILM)—rich in AAV binding sites and composed of polysaccharides—acts as a strong physical diffusive barrier that limits AAV particles' access to the retina, thereby hampering retinal transduction efficiency from the vitreous (Dalkara et al., 2009). It has been shown that the vitreoretinal junction is a serotype-specific obstacle for AAV, and the abundance of AAV receptors on the ILM is potentially a factor that controls diffusion across this barrier (Dalkara et al., 2009).

To overcome these issues, various AAV engineering approaches have been used to create vectors capable of transducing the entire retina through intravitreal injections (Cronin et al., 2014; Dalkara et al., 2013; Petrs-Silva et al., 2009, 2011). One photoreceptor permissive variant was obtained using an *in vivo* directed evolution approach (Dalkara et al., 2013). In this study, a large library of laboratory-generated capsid variants was subjected to selective pressure for their ability to penetrate into the photoreceptor layer of the mouse retina when injected into the vitreous. The successful variant isolated from this screen, called AAV2-7m8, is characterized by a 10-amino acid peptide “LALGETTRPA,” referred to as “7m8,” inserted at position 588 of the AAV2 capsid protein sequence. The insertion is composed of a variable heptamer (LGETTRP) region and three amino acids used as linkers for creating the library from which the variant was chosen. This new vector, AAV2-7m8, was recently used for therapeutic inner and outer retinal gene delivery

in various animal models of retinal disease leading to successful proof-of-concept gene therapies (Byrne et al., 2014, 2015; Dalkara et al., 2013; Macé et al., 2014).

Directed evolution does not require understanding of AAV's structure-function biology, as it uses an unbiased selection approach. However, it is worth studying the viral variants resulting from such screens to obtain further information on their mechanisms of enhanced transduction. The heptamer peptide (LGETTRP), inserted into the loop IV of AAV2, is responsible for the enhanced retinal transduction properties of AAV2-7m8 over its parental serotype AAV2. In this study, we set out to decipher the mechanisms by which 7m8 provides increased retinal transduction. We asked whether the peptide exerts an effect on its own or does it synergize with its surrounding amino-acid environment? To address this question, we generated AAV5, -8, and -9 (AAV9/Hu.14) vectors displaying the 7m8 peptide at the residues corresponding to AAV2's 588 residue (in loop IV) on their respective capsids. We found that 7m8 insertion improved retinal transduction properties of AAV9 when virus is administered into the vitreous, as previously observed with AAV2-7m8 compared to AAV2. Peptide insertion had no positive effect on the retinal transduction properties of AAV5 or -8 after intravitreal injection. Subsequent intracerebral administration allowed an unbiased comparison of AAV2-7m8's diffusion versus increased infectivity, which could not be fully addressed in the retina because of the limited thickness of the tissue and the presence of the ILM as an additional diffusive barrier. This data together with data obtained *in vitro*, indicate that 7m8 improves the vectors' infectivity rather than tissue diffusion. Altogether, our results suggest that 7m8 peptide exerts its effects in synergy with surrounding amino acids, and effects of such insertions on various capsids are dependent on tissue and cellular environment.

## Results

### Molecular Modeling of AAV2 and AAV2-7m8

AAV2-7m8 is characterized by the insertion of a 10 amino-acid peptide “LALGETTRPA” referred to as “7m8” (Fig. 1A–D) composed of a heptamer (LGETTRP) and three amino acids as linkers, all inserted in the loop IV. The arginines R585 and R588 interact with each other and are involved in binding to the heparan sulfate proteoglycan (HSPG) (Fig. 1D) (Kern et al., 2003; Opie et al., 2003). The 7m8 peptide insertion in position 588 impedes this interaction (Fig. 1D) thus reducing interactions between the virus and HSPG. Since HSPG is abundant on the inner limiting membrane (ILM)—the dense network of glycosaminoglycans between the vitreous and the retina—we hypothesized that AAV2's strong interaction with the HSPG of the ILM limits its diffusion into the retina. Accordingly, AAV2-7m8's reduced affinity for HSPG might increase passage through the ILM, partially accounting for increased retinal penetration. Alternatively, the 7m8 peptide can exert an effect on its own, by interacting with another cell-surface glycan. To tease apart the effect of 7m8 insertion from the properties of AAV2 capsid (such as HSPG binding), we decided to insert this peptide onto other AAV capsids and evaluate how the behavior of vectors change in view of the peptide insertion.

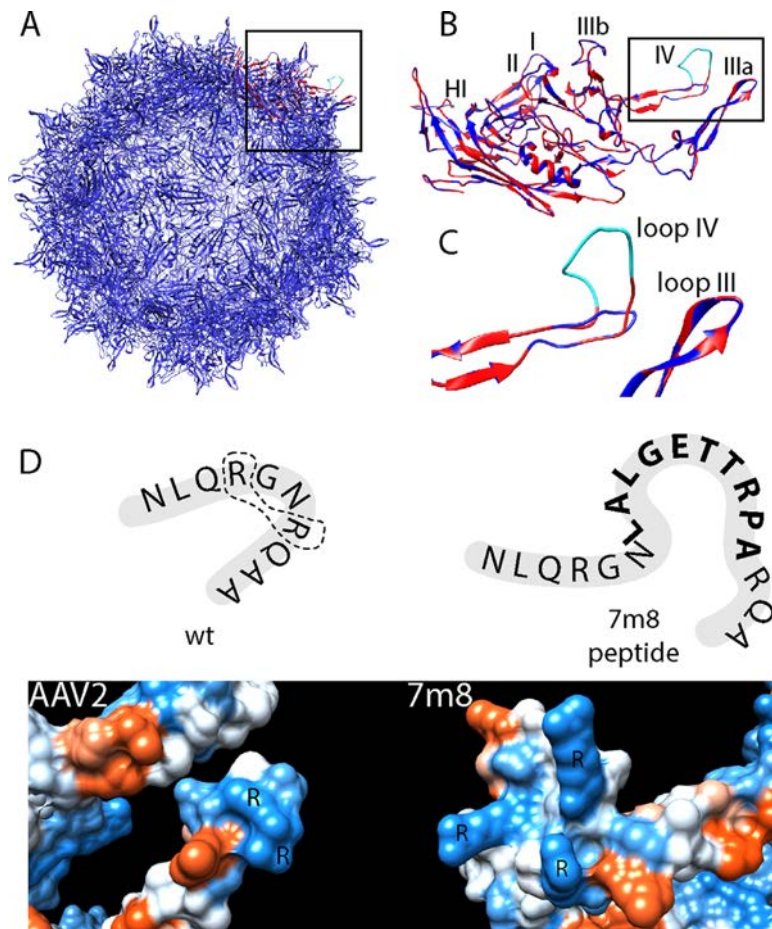


**Figure 1.** Structural model of AAV2-7m8 capsid and proposed mechanism for the influence of 7m8 peptide insertion on HSPG binding. (A) Superposition of the 60 monomers forming AAV2 capsid (dark blue) and one monomer of AAV2-7m8 (red) containing the insertion LALGETTRPA (shown in cyan). (B) Superposition of AAV2 and AAV2-7m8 capsid monomers. (C) Zoom onto the 7m8 insertion (cyan) in loop IV. (D) Model for the effect of 7m8 insertion on HSPG binding. Schematic for AAV2 or AAV2-7m8 loop IV (top) and three-dimensional atomic structure of the 587 region with focus on the interaction between the arginines (R). In the AAV2 capsid, the two arginines (R585 and R588 indicated as R) interact with each other and are part of the heparin-binding motif. In the AAV2-7m8 variant, 7m8 disrupts the HSPG-binding motif, taking the arginines apart. Molecular models were generated using UCSF Chimera (Pettersen et al., 2004).

### Generation of 7m8 Inserted AAV Serotypes 5, 8, and 9

To better investigate the effects of 7m8 insertion, we incorporated 7m8 onto the capsid of three other AAVs (Fig. 2A). We used previously reported potential capsid regions amenable for the insertion of the 7m8 peptide that may re-direct the natural viral tropism (Fig. 2B–E) (Boerner et al., [307] Rational Development of 12 Different AAV Serotypes as Scaffolds for Peptide Display. At: Annual meeting of Am. Soc. Gene and Cell Ther. New Orleans, 2015) (Koerber et al., 2007; Michelfelder et al., 2011). We hypothesized that the 7m8 peptide may improve transduction on its own or in conjunction with its surrounding amino acids. AAV2, –5, –8, and –9 vectors displaying the 7m8 peptide “LALGETTRPA” were generated and molecular models of the capsid monomers were generated using the Robetta prediction software. The molecular models show the 3D changes of each AAV monomer (Fig. 2A–E) after 7m8 insertion, which mainly affects the structure of loops III

and IV. The RepCap plasmids generated after DNA sequence synthesis and cloning were then used for AAV production. In parallel, we produced control AAVs of each serotype with no peptide insertion and another scrambled peptide insertion variant where random 10 amino acids are inserted at the identical location as 7m8 peptide on the AAV2 capsid (Table S1). All AAVs generated encoded for GFP under the control of a ubiquitous CAG promoter. Genomic titers were comparable between the parental serotypes and their 7m8 modified variants (Table S1), suggesting that 7m8 peptide insertion did not significantly impair genome packaging and capsid stability.

### Infectivity of 7m8 Modified Vectors In Vitro

We aimed to test the infectivity and receptor binding properties of the newly generated peptide insertion vectors compared to their parental serotypes on relevant cell types, in vitro. In vitro



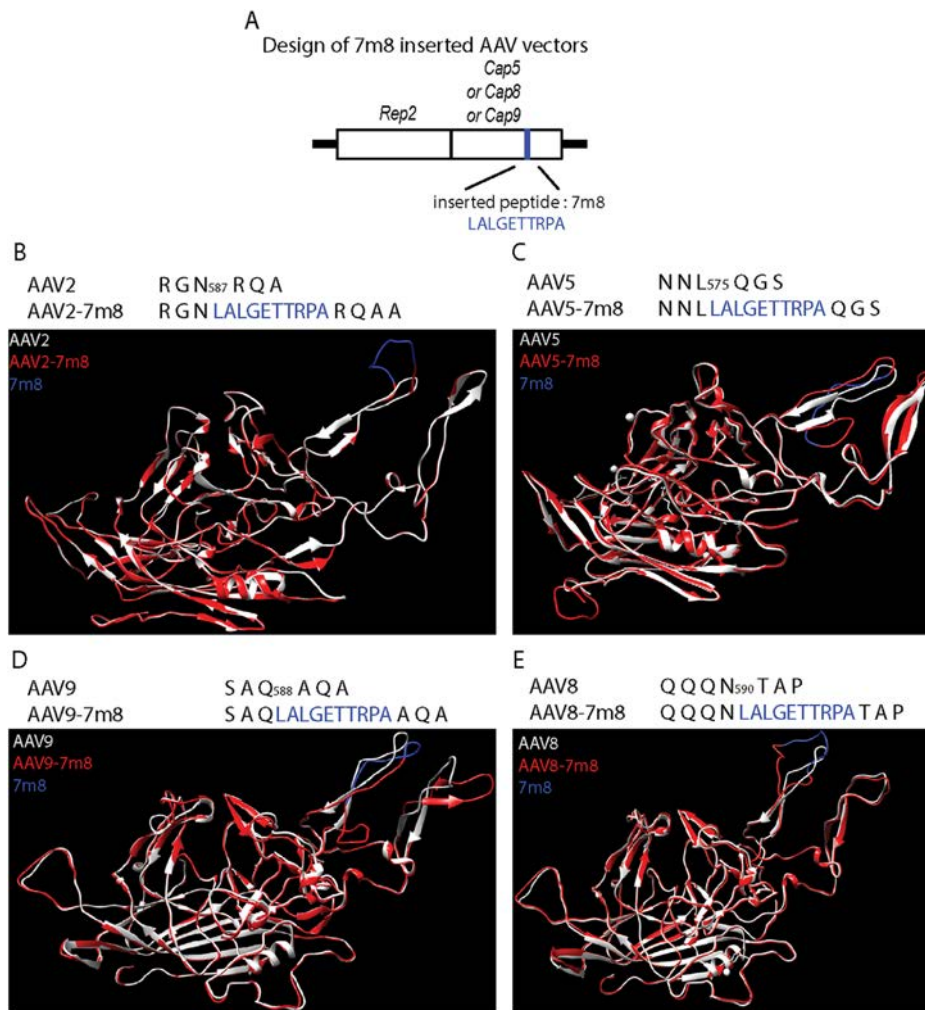


**Figure 2.** Sequence and structural representation of AAV2, 5, 8, and 9 after 7m8 insertion. **(A)** Schematic representation of the AAV packaging plasmids with the peptide insertion sites indicated in blue. **(B–E)** The wild-type AAV monomers of AAV2 **(B)**, AAV5 **(C)**, AAV8 **(D)**, and AAV9 **(E)** are represented in white, and their corresponding 7m8 variants in red. The 7m8 peptide is shown in blue for each capsid. Molecular models were generated using UCSF Chimera (Pettersen et al., 2004). Rep, replication; Cap, capsid.

transduction assays allow us to study the efficiency of the vectors in overcoming cellular barriers (cell entry and nuclear localization) in absence of more complex extracellular barriers, present in vivo. To this aim, HEK293T cells were infected at a MOI of 5,000 with each vector and viral DNA was extracted 22 h after infection. Viral genomes extracted from each condition were quantified using qPCR (Fig. 3). We detected higher amounts of viral DNA within the infected cells for AAV2-7m8—concurring with our previous observations (Dalkara et al., 2013)—and for AAV9-7m8 compared to their respective parental vectors, whereas less infection was observed for AAV5-7m8 compared to AAV5. The infectivity was similar between AAV8 and AAV8-7m8.

As the amount of genomes present inside the cells does not directly reflect if the peptide insertion improves cell entry, or intracellular trafficking; we conducted a follow-up microscopy study for AAV2 versus its 7m8 variant to gain further insight into how the 7m8 peptide influences infectivity. We used a commercially

available antibody (A20) to detect AAV capsids in HEK cells. HEK cells were infected with either AAV2 or AAV2-7m8 and viral particles were tracked by microscopy essentially as described by Bartlett and coworkers (Bartlett et al., 2000). Negative controls without viral particles were used to calibrate images and remove background. Confocal images of individual cells infected with the vectors were then processed to visualize the amount of viral particles present inside the cells versus in the nucleus (Fig. 3 and Supplemental Movies S1 and S2).

Lastly, to better understand whether the insertion site of the peptide is critical in the resulting capsid's properties, we next generated alanine substitution mutants of each serotype where the residues responsible for receptor binding are mutated (Schmidt et al., 2008). Since each of the serotypes we tested bind different primary receptors via different capsid regions, we blocked the regions responsible for cell binding for each serotype to mimic the theoretical mechanism of AAV2 HSPG-ablation. This was done for

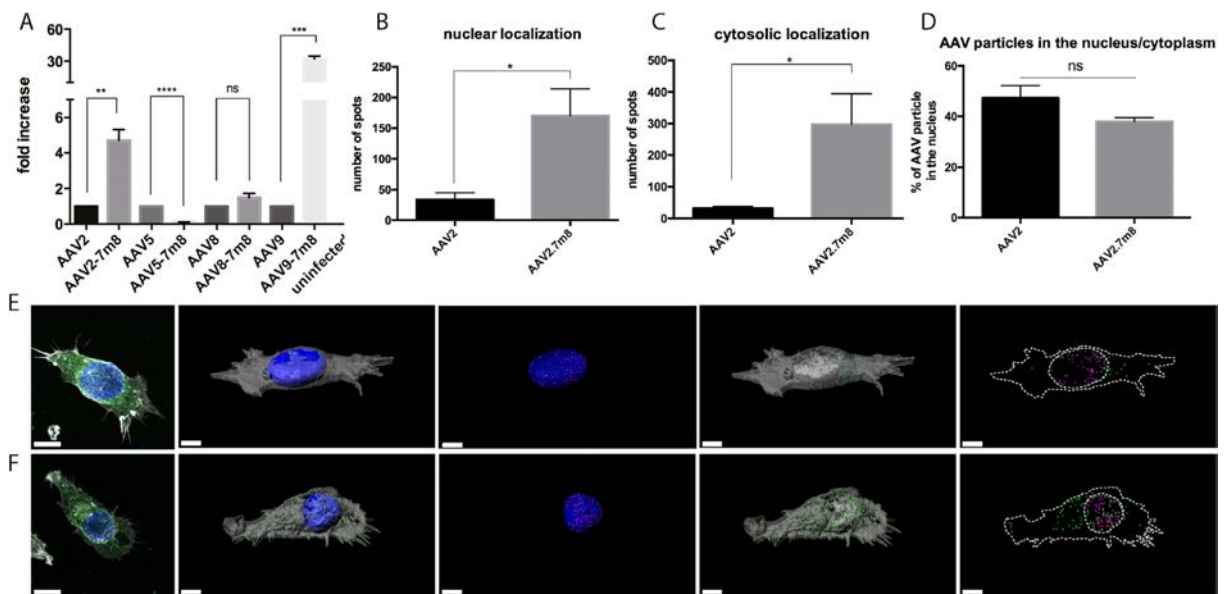


**Figure 3.** Effect of 7m8 insertion on transduction efficiency. **(A)** Fold increase in intracellular DNA levels with 7m8 modified AAV2, 5, 8 and 9- vectors with respect to unmodified serotypes. DNA was extracted from HEK cells infected with MOI of 5,000 for each vector encoding GFP 22 h post infection. Infections were performed in triplicates. After qPCR, the relative quantitation method was used to calculate fold differences in GFP expression by 7m8 modified vectors normalized against each parental serotype. **(B)** Nuclear, **(C)** Cytosolic and **(D)** Intracellular localization of AAV2 and AAV2-7m8 particles calculated as number of spots from  $n = 4$  cells for AAV2 and  $n = 5$  cells for AAV2-7m8 analyzed by Imaris after 3D reconstructions shown in E and F. Image stacks were acquired with confocal microscopy using the same acquisition parameters, calibrated to control images. A representative z-projection of a stack is shown for each vector in the first columns of E and F. Localization of the spots with respect to cellular compartments represented in 3D are shown for each cell in columns 2–5. Scale bars are 5  $\mu\text{m}$ .

each serotype except for AAV8 whose primary receptor is currently unknown. These alanine substitution mutants are described in Table S1. The resulting vectors were tested for their infectious properties in vitro on HEK (for AAV2), 661 W (for AAV5) or CHO Lec2 (for AAV9) cell lines permissive for each serotype vector (Supplemental Fig. S1). We found that mutating the receptor binding sites abolished the infectivity of the vectors (with the exception of AAV2 which retained some infectivity). For AAV5, the mutated residues were also those surrounding the peptide insertion, suggesting that disrupting the receptor binding site by peptide insertion or mutagenesis both impede viral infection. For AAV9, we have shown through galactose competition transduction assay that the peptide insertion does not impede galactose binding (See Supplemental Fig. S2). AAV9-7m8 retains AAV9's ability to bind galactose while displaying significantly increased transduction on both CHO Lec2 and HEK cell lines (Supplemental Fig. S1 and Fig. 3).

### Retinal Transduction Efficiency of AAV2, 5, 8 and 9, Compared to Their 7m8 Insertion Variants

Next, we questioned whether the LALGETTRPA sequence is responsible for the increased uptake of AAV2-7m8 or if having any peptide insertion at the same location results in similar transduction behavior in vitro and in vivo. A scrambled 10 amino acid sequence (AAKKTIEENRA) was inserted at the same site on AAV2 capsid as the 7m8. Insertion of this scrambled sequence

had no beneficial effect on the AAV2 capsid's transduction efficiency in vivo or in vitro on HEK cells (Fig. 4). To assess retinal transduction efficiency of the AAV variants described above, we analyzed GFP expression after intravitreal injections by eye fundus examination (Figs. 4A and 5). For in vivo experiments, six eyes of C57BL/6J mice were injected bilaterally with  $10^{10}$  vg per eye of each vector encoding GFP under the ubiquitous CAG promoter. Six weeks after injection eye fundus exams were conducted to evaluate the extent of GFP expression in treated retinas. Each peptide insertion variant was compared to its parental serotype. In agreement with the in vitro results (Fig. 3A), insertion of 7m8 did not seem to modify retinal transduction by AAV8, while it had a positive influence when inserted into the AAV2 and AAV9 capsids. 7m8 insertion weakened retinal transduction of AAV5 (Fig. 5).

We then focused our analysis on the variants with improved transduction patterns in the retina: AAV2-7m8, AAV9-7m8, and their parental capsids for further in vivo studies. Specifically, we investigated the capacity of AAV9-7m8 to transduce deep retinal layers. We wondered if AAV9-7m8 was also capable of reaching deep retinal layers as observed with AAV2-7m8. Using the CAG promoter, the expression in Müller glial cells often convolutes the interpretation of results concerning viral penetration as Müller cells span the entire retina making it difficult to distinguish infected cell types. We therefore evaluated potential photoreceptor transduction with AAV9 and its 7m8 variant under a rhodopsin promoter (Allocca et al., 2007) (Fig. 6). In this experiment, GFP

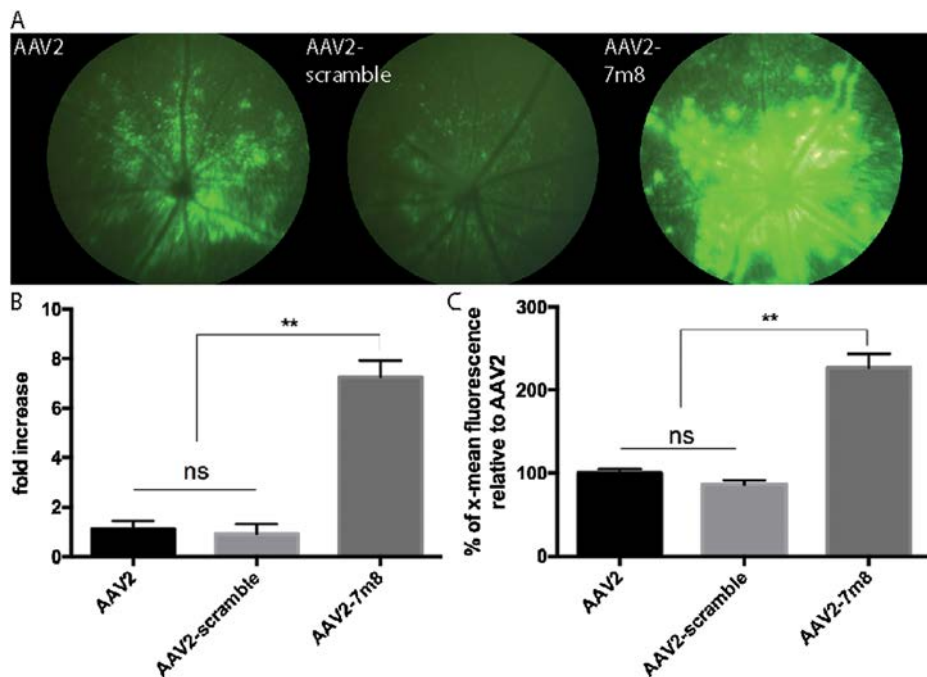


**Figure 4.** The effect of 7m8 peptide insertion on AAV2 capsid compared to a random scrambled peptide insertion at identical position. (A) Eye fundus imaging at equal settings 3 weeks after intravitreal injection of AAV2 ( $n=3$ ), AAV2-scramble (AAKTIENR) ( $n=3$ ) or AAV2-7m8 (LALGETTRPA) ( $n=3$ ). (B) GFP cDNA was extracted from retinas at 4 weeks after injection. Relative cDNA from each sample was measured by qRT-PCR and expressed as fold-increase relative to AAV2. (C) Transduction efficiency of AAV2, AAV2-scramble and AAV2-7m8 on HEK cells measured by flow cytometry. GFP fluorescence is shown in percentage relative to the x-mean fluorescence of the AAV2 condition (adjusted to 100%).

expression was observed in photoreceptors using the AAV9-7m8. AAV9 did not transduce the photoreceptors in the central and peripheral areas. 7m8 thus improves both AAV2 and AAV9 transduction from the vitreous.

Lastly, the same vectors were tested for their ability to transduce the retina when injected subretinally (Supplemental Fig. S4). This comparison revealed results mostly in line with the previous in vitro and in vivo results except for AAV8-7m8 that was more efficient than its parental serotype when delivered subretinally. This disparate result might be due to the variable nature of subretinal injections. The cell types transduced by the new vectors did not seem to be modified with respect to their parental serotypes (Supplemental Fig. S4).

### Cerebral Transduction Patterns of AAV2 and 9, Compared to Their 7m8 Insertion Variants

One of our initial questions was whether 7m8 improved the tissue diffusion properties and/or infectivity of AAV2. To test this we performed stereotactic injections in another neural tissue—the brain parenchyma—to better evaluate spreading of the different vectors from the site of injection. We performed bilateral intra-atrial injections of  $5 \times 10^{10}$  vg for each vector into brains of C57BL/6J mice ( $n=5$  mice were injected for each vector). Mice were sacrificed 6 weeks after injections and sagittal cryosections were prepared for examination with Nanozoomer technology at

$20\times$  resolution. Our results show that the spread of viral particles was not altered between the peptide insertion vector AAV2-7m8 and its parental serotype as indicated by area of GFP expression (Fig. 7B). AAV2 and AAV2-7m8 lead to GFP expression in a relatively small zone around the injection site (Fig. 7A and B), whereas both AAV9 and AAV9-7m8 lead to GFP expression in a broader zone (Fig. 7A and B). Regarding expression intensity, AAV2-7m8 resulted in significantly higher intensity GFP compared to its parental serotype AAV2. Interestingly, intensity of gene expression calculated as mean gray value was reduced with AAV9-7m8 compared to AAV9. Our results collectively suggest that the effects of 7m8 insertion depend on the viral capsid on which it is inserted and for AAV2-7m8, the peptide insertion provides better infectivity rather than better spread in neural tissue.

There were discrepancies between the cerebral versus in vitro as well as retinal versus cerebral expression levels with AAV9-7m8. The discrepancy between the cerebral versus in vitro and retinal expression with AAV9-7m8 is possibly due to the saturation of the extent of expression using AAV9 in this brain region (Cearley and Wolfe, 2006). Indeed, AAV9 already performs very well in brain transduction, thereby making it difficult to show increase in intensity under the experimental conditions we used. Furthermore, the number of particles we used in our study might lead to toxic GFP expression levels with the more infectious AAV9-7m8 variant compared to AAV9-GFP (Klein et al., 2006; Vandenberghe et al., 2011) leading to a reduction in expression.

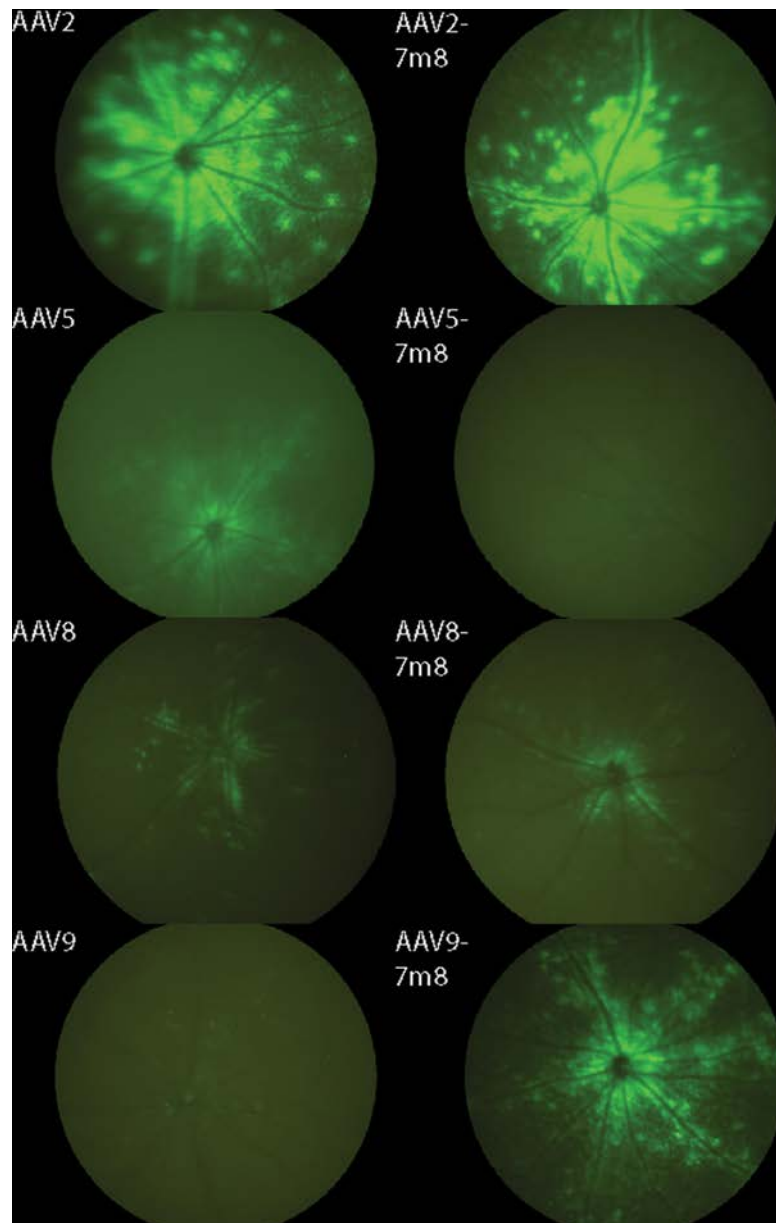


**Figure 5.** Effect of 7m8 insertion on retinal transduction efficiency of AAV2-, AAV5-, AAV8- and AAV9-CAG-GFP vectors. In vivo eye fundus imaging showing GFP fluorescence 6 weeks after intravitreal injection with the different AAV vectors. Note that the only variants that benefit from 7m8 insertion are AAV2 and AAV9. All images were acquired using the same acquisition parameters.

## Discussion

Subretinal delivery is the most common administration route to target deep retinal layers involved in inherited retinal degenerations, but intravitreal injections can be preferable because they are less invasive, provide broader coverage and are surgically simpler. AAV vectors that are capable of efficient retinal transduction from the vitreous have been designed only recently, using rational design (Boyd et al., 2015; Boye et al., 2016; Kay et al., 2013; Petrs-Silva et al., 2011) or in vivo directed evolution (Cronin et al., 2014; Dalkara

et al., 2013). In the latter study, we used directed evolution of random peptide libraries displayed on AAV2 capsid for selection of capsid variants that overcome the natural AAV transduction barriers of retinal tissue from the vitreous.

Here we wanted to understand the mechanisms by which 7m8 peptide insertion enhances gene delivery to deeper layers of retinal tissue. Thanks to this peptide insertion, AAV2-7m8 outperforms other AAV variants thus far described for retinal transduction from the vitreous in the mouse and in the non-human primate retina (Dalkara et al., 2013) but it was not clear whether this performance

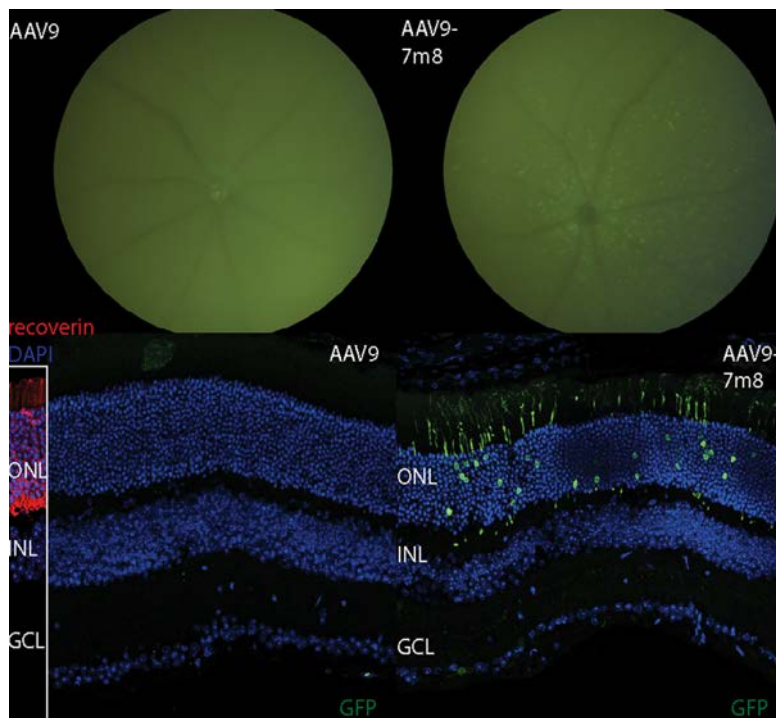


**Figure 6.** Analysis transduction patterns by AAV9 and AAV9-7m8 vectors encoding GFP under the rhodopsin promoter. (Top) Representative eye fundus images acquired at equal settings showing GFP fluorescence 6 weeks after intravitreal injection (Bottom) Transverse sections of representative retinas treated with the same vectors. Endogenous GFP (green), DAPI (blue), Recoverin (red).

was the result of better diffusion across extracellular barriers (i.e., ILM and extracellular matrix) and/or better cellular/nuclear entry (Fig. 8). Moreover, it was not clear whether the peptide itself was responsible for these properties and if it exerted its effects in conjunction with its amino-acid microenvironment. The first aim of this study was thus to investigate whether the 7m8 peptide could change AAV5, -8, and -9 properties when inserted at equivalent sites within these capsids. Second, we aimed to better understand the effects of 7m8 insertion on the two AAV capsids for which transduction was increased: was this increase due to better spread of viral particles and/or better infectivity?

First, we confirmed that the 7m8 peptide sequence was responsible for the increased transduction properties of AAV2-7m8, as a scrambled peptide sequence inserted at the same location did not provide a similar increase in transduction. We found that 7m8 insertion was compatible with capsid assembly of all AAV serotypes studied with no significant reduction in viral titers upon production by transient transfection of 293T cells. However, 7m8 insertion had different effects on each of the viral capsids. These results suggest that 7m8 exerts its effects in conjunction with its amino-acid environment, working well with some amino acids and not with others. The insertion improved AAV2 and AAV9's transduction properties in the retina. The other vectors did not benefit from 7m8 insertion. These findings are consistent with previous studies that demonstrate that peptide functionality is largely determined by the capsid scaffold, thus preventing a direct transfer of lead sequences from AAV2 onto other capsids and rather requiring a firsthand

selection for each new serotype (Grimm et al., 2008; Michelfelder et al., 2011; Varadi et al., 2012; Ying et al., 2010).

The increase in infectivity of AAV2-7m8 and AAV9-7m8 were observed both *in vivo*, in the retina and *in vitro* on HEK cells and CHO Lec2 cells. AAV9-7m8 gave better results than its parental serotype AAV9 in the retina but was nevertheless less efficient in providing photoreceptor transduction compared to AAV2-7m8. One factor that could explain the performance of AAV2-7m8 in the retina is its interactions with HSPG and therefore the ILM and ganglion cell layer (GCL). It is well established that peptide insertion at the position 587–588 of AAV2 capsid sequence induces a reduced HSPG binding phenotype (Dalkara et al., 2013; Lochrie et al., 2006; Opie et al., 2003; Wu et al., 2000), which is also the case for AAV2-7m8 mutant (Dalkara et al., 2013). It is thus possible that 7m8 improved AAV2's access to the deeper retinal layers by reducing interactions with HSPG, which is abundant in the ILM and GCL (Clark et al., 2011) (Fig. 7). Several previous studies established that reduced HSPG binding leads to increased transduction volumes in the CNS (Arnett et al., 2013; Nguyen et al., 2001). It remains unclear why reduced HSPG binding did not allow increased transduction volume for AAV2-7m8 when vector was delivered into the striatum. Unlike mutants deficient in HSPG binding, AAV2-7m8 has other new properties arising from the insertion of the peptide. We think these other properties (which might include binding to a currently unidentified cell-surface glycan) might counter-balance diffusion that would have been afforded by reduced HSPG binding.

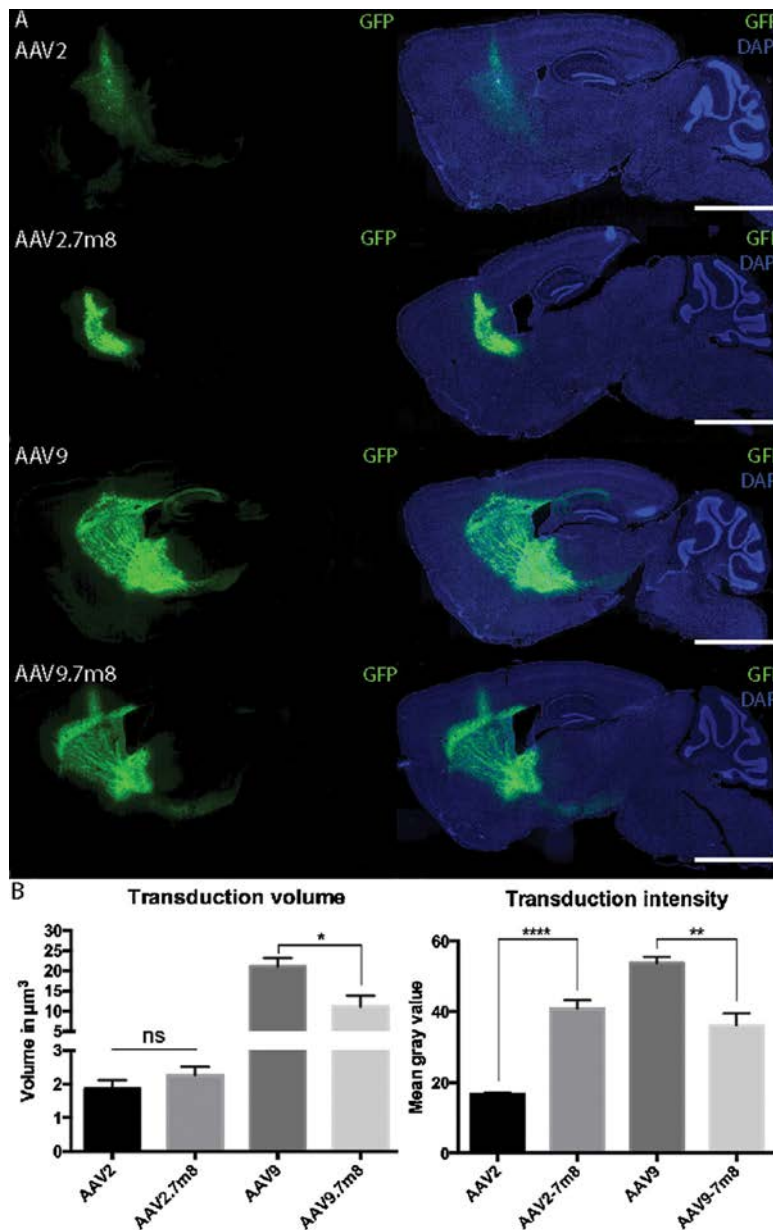


**Figure 7.** Expression patterns resulting from intrastriatal injections of AAV2, 9, and their 7m8 insertion variants. **(A)** Sagittal brain sections showing extent and intensity of GFP expression across a representative brain section (at equal settings). **(B)** Transduction volumes in  $\mu\text{m}^3$  based on transduced surface areas across one series of sections multiplied by total thickness of the sections ( $n = 5$  mouse brains for each vector) (left). Mean transduction intensity expressed as mean gray value across the section for each vector measured in ImageJ in series of sections of 5 mouse brains (right). Error bars represent SEM between different mice.

AAV2 binds HSPG through its interaction with the amino acids R585 and R588 (required for binding), in addition to R475, R484, and K532. In a large number of studies the 587/588 position was chosen for insertional mutagenesis to redirect AAV2 tropism mainly leading to a reduced-HSPG binding phenotype (Boye et al., 2016; Dalkara et al., 2013; Perabo et al., 2006). For AAV9, the amino acids N470, D271, N272, Y446, and W503 form a pocket required for galactose binding (Bell et al., 2012). In addition, the  $^{512}\text{NGR}^{514}$  sequence has been described as an integrin recognition motif (Shen

et al., 2014). The insertion site for 7m8 in our study was the 588/589 position, which according to the previous studies is not necessary for galactose binding. Thus, we can suppose that 7m8 insertion did not affect galactose binding but improved viral cell entry/nuclear trafficking through another mechanism- although the cerebral transduction efficiency results with AAV9-7m8 remain discordant and do not support improved viral trafficking. AAV9 has remarkable properties for brain transduction compared to AAV2 and lack of HSPG binding likely facilitates its larger spread in neural

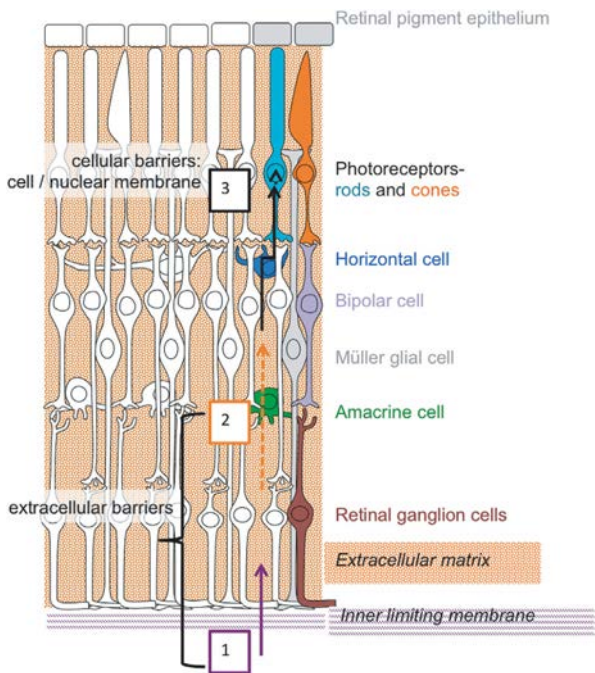


**Figure 8.** Retinal barriers to AAV transduction. Illustration representing the three main physical barriers to retinal transduction by AAVs injected into the vitreous. The vectors first diffuse in the vitreous and reach the first barrier—the inner limiting membrane (ILM), which is composed of a dense network of polysaccharides secreted via Müller glial cell endfeet. The second barrier is the extracellular matrix of retinal cells which impedes diffusion and cell entry. Lastly AAV particles are faced with the third barrier for entry inside the nucleus: the cell and nuclear membrane.

tissue (Boye et al., 2016; Zhang et al., 2011). Although AAV9-7m8 did not outperform AAV2-7m8 for transduction of the mouse retina, it could be interesting to compare the vectors' efficiency in the non-human primate retina since AAV9 has higher cone photoreceptor tropism than AAV2 and this cell type is of interest for gene therapy applications (Vandenberghe et al., 2013). Indeed the cone-rich fovea is a region that is accessible through intravitreal injections and AAV9-7m8 can display favorable properties at this site. Sialic acid is required for AAV5 binding and infection (Walters et al., 2004). Afione and collaborators have recently identified AAV5 sialic acid binding region (Afione et al., 2015), showing that mutation of amino acids 569 and 585 or 587 results in alteration of sialic acid-dependent transduction. In our study 7m8 was made at the 575 position, which likely hampered sialic acid binding region and was detrimental to the vectors performance both in vivo and in vitro. On the other hand, AAV8's primary receptor is unknown. The 37-67-kDa laminin receptor (lamR) has been identified as its co-receptor and AAV8 binding to lamR is mediated by the amino acids 491–547 and 593–623 (Akache et al., 2006). Moreover, peptide insertions on AAV8 capsid at position 590 allow modification of its tropism (Michelfelder et al., 2011; Raupp et al., 2012) but amino acids 588–592 are not necessary for AAV8 binding and uptake. This region is thus involved in but not necessary for interaction with cellular receptors (Raupp et al., 2012). In our study the 7m8 peptide

was inserted around this region and we observed no significant improvement in AAV8's infectivity.

Lastly, our study sheds light onto the consequences of 7m8 insertion on AAV2's gene transfer efficiency. Our data suggest that 7m8 "LALGETRPA" peptide strongly improves AAV2 infectivity by increasing its efficacy in overcoming cellular barriers (mainly cell entry). The different effects of 7m8 insertion on various serotypes' capsids can be explained by the complexity of capsid structure relationships of AAVs. The capsid structures of all the AAVs used in this study have been resolved by X-ray crystallography (AAV5, PDB id 3NTT; AAV8 (Nam et al., 2007), PDB id 2QA0; and AAV9 (DiMattia et al., 2012), PDB id 3UX1). Resolution of the different AAVs' capsid structures, identification of their primary or co-receptors, and mutational analyses of their receptor binding regions all deepen our understanding of this important vector's structure-function relationships. This knowledge is further enriched by the discovery of artificial serotypes through combinatorial screens and the mechanistic study of their properties.

## Experimental Procedures

### AAV Vector Production

Recombinant AAVs were produced as previously described using the co-transfection method and purified by iodixanol gradient ultracentrifugation (Choi et al., 2007). Concentration and buffer exchange was performed against PBS containing 0.001% Pluronic. AAV vector stocks titers were then determined based on real-time quantitative PCR titration method (Aurnhammer et al., 2011) using SYBR Green (Life Technologies, France).

### Structure Analysis

VP3 monomers of 7m8 insertion vectors were generated using the Robetta modeling server (Chivian et al., 2003; Kim et al., 2004) and superimposed to their parental serotypes using UCSF Chimera (Pettersen et al., 2004).

### AAV Cell Entry and Trafficking Assays

The protocol from Bartlett et al (Bartlett et al., 2000) was used with the following modifications: cells were incubated with an MOI of 250,000 of each vector. After 2 h, cells were fixed and anti-AAV2 capsid antibody (A20 from American Research Products, Waltham, MA) was used according to manufacturers instructions to reveal AAV particles. Cells were additionally labeled with phalloidin and DAPI. Confocal images were acquired using Olympus FV1000 Inverted confocal microscope at equal settings. To identify cellular localization of AAV particles, confocal images were processed with Imapris software (Bitplane). Several masks were created to isolate cellular compartments: DAPI counterstaining was used to define the nuclear zone. Phalloidin staining of the cell membrane allowed us to define the cytosolic compartment by subtraction of the nuclear zone from the membrane. Each mask was used to segment AAV immunostaining and spot detection was performed to quantify the amount of particles in different cellular compartments.

## Animals

The experiments were realized in accordance with the National Institutes of Health Guide for Care and Use of Laboratory Animals and approved by local ethics committees.

For all experiments AAV vector stocks were titer adjusted by dilution in PBS containing 0.001% Pluronic. For eye injections, mice were anesthetized by isoflurane inhalation. Pupils were dilated and 33-gauge needle was inserted into the eye to deliver 2  $\mu$ L of AAV vector solution ( $10^{10}$  vg) into the vitreous or 1  $\mu$ L subretinally. GFP expression was visualized using Micron III ophthalmoscope after dilation of the pupils and under isoflurane anesthesia. For intrastriatal injections, mice were anesthetized by intraperitoneal injection of ketamine (100 mg/kg) and xylazine (10 mg/kg) and placed on a stereotaxic frame (Köpf Apparatus). After skin incision, the skull was exposed to position injection cannulae at +1 mm anteroposterior and  $\pm$ 2 mm lateral relative to bregma. After drilling of the skull, the cannulae were lowered to 2.5 mm relative to the dura and 2  $\mu$ L of viral solution ( $5 \times 10^{10}$  vg) was injected in 8 min. The skin was sutured and mice monitored until complete awakening.

## Histology and Microscopy

Eyes were enucleated and immediately fixed in 4% paraformaldehyde (PFA) at 4°C, for 20 min for flatmounts or for 2 h for cryosections. For brain histology, mice were deeply anesthetized for trans-cardiac perfusion with ice-cold PBS followed by 4% PFA in PBS. Brains were then removed and post-fixed for 4 h in the same fixative. For cryosections, eye-cups and brains were immersed in PBS-30% sucrose overnight at 4°C. They were embedded in OCT medium and frozen in liquid nitrogen. Vertical sections were cut with a Microm cryostat and mounted in Vectashield mounting medium for fluorescence microscopy. Brain section images were acquired with Nanozoomer technology (Hamamatsu) and retinal sections were visualized using an Olympus IX81 and Olympus FV1000 Inverted confocal microscopes.

## Quantification of AAV Vector Internalization In Vitro Using Quantitative PCR

HEK 293 cells were plated onto 24-well plates coated with poly-L-lysine and cells were infected with various AAV vectors at 5,000 MOI. After 22 h of incubation at 37°C, cells were washed three times in PBS and viral DNA was harvested using a DNA-extraction kit (NucleoSpin Tissue, Macherey-Nagel). Relative genome quantification was performed through qPCR, using primers targeted against the GFP transgene and actin as the housekeeping gene.

## Quantification of AAV Transduction Using Flow Cytometry

Cells were plated in 24 well plates at a concentration of 40,000 cells/well for Lec2 or 661W and 100,000 cells/well for HEK293s. The following day, they were infected with AAV vectors or a mix of AAV vector and PNA lectin (Life Technologies). One day post infection, cells were dissociated with trypsin and fixed. Ten thousand cells per sample were counted and analyzed using a CytomicsFC500 flow

cytometer (Beckman Coulter, France). Uninfected control cells were also counted and analyzed to establish transduction efficiency baselines. Data were obtained from 3 to 4 technical replicates for each vector with the exception of AAV9-7m8 alanine mutant where two technical replicates were used due to low viral titer.

## Statistical Tests

Data were analyzed using a Student *t*-test in Graphpad Prism. Error bars on the graphs show the Standard Error of the Mean (SEM). *P* values are expressed as the following \**P* < 0.05, \*\**P* < 0.01, \*\*\**P* < 0.001.

## Authors' Contributions

M.D. and H.K. created and produced the 7m8 vectors. H.K. and G.W. conducted the in vivo experiments. M.D. and H.K. conducted and analyzed the in vitro experiments. C.W. created all of the alanine mutants and scrambled peptide insertion variant. S.F. designed and performed image analysis for subcellular localization of AAV. A-P.B. helped design and execute experiments in the striatum, and gave feedback on the manuscript. J-A.S. gave feedback on the manuscript and provided scientific input. D.D. designed and supervised the experiments. D.D. and H.K. wrote the manuscript.

We thank Giulia Spampinato and Anna Bochicchio for helpful discussions and advice. We also thank the Flow cytometry, Imaging and Animal facilities of the Institut de la Vision. We thank Arthur Planul for providing plasmids, Camille Robert, and Peggy Barbe for technical assistance. This study was supported by AFM-Téléthon, Marie Curie CIG (334130, RETINAL GENE THERAPY), INSERM, and Labex-Lifesenses.

## References

- Afione S, DiMattia MA, Halder S, Di Pasquale G, Agbandje-McKenna M, Chiorini JA. 2015. Identification and mutagenesis of the adeno-associated virus 5 sialic acid binding region. *J Virol* 89:1660–1672.
- Akache B, Grimm D, Pandey K, Yant SR, Xu H, Kay MA. 2006. The 37/67-kilodalton laminin receptor is a receptor for adeno-associated virus serotypes 8, 2, 3, and 9. *J Virol* 80:9831–9836.
- Allocca M, Mussolino C, Garcia-Hoyos M, Sanges D, Iodice C, Petrillo M, Vandenberghe LH, Wilson JM, Marigo V, Surace EM, Auricchio A. 2007. Novel adeno-associated virus serotypes efficiently transduce murine photoreceptors. *J Virol* 81:11372–11380.
- Arnett ALH, Beutler LR, Quintana A, Allen J, Finn E, Palmiter RD, Chamberlain JS. 2013. Heparin-binding correlates with increased efficiency of AAV1- and AAV6-mediated transduction of striated muscle, but negatively impacts CNS transduction. *Gene Ther* 20:497–503.
- Auricchio A, Kobinger G, Anand V, Hildinger M, O'Connor E, Maguire AM, Wilson JM, Bennett J. 2001. Exchange of surface proteins impacts on viral vector cellular specificity and transduction characteristics: The retina as a model. *Hum Mol Genet* 10:3075–3081.
- Aurnhammer C, Haase M, Muether N, Hausl M, Rauschhuber C, Huber I, Nitschko H, Busch U, Sing A, Ehrhardt A, Baiker A. 2011. Universal real-time PCR for the detection and quantification of adeno-associated virus serotype 2-derived inverted terminal repeat sequences. *Hum Gene Ther* 23:18–28.
- Bainbridge JWB, Smith AJ, Barker SS, Robbie S, Henderson R, Balaggan K, Viswanathan A, Holder GE, Stockman A, Tyler N, Petersen-Jones S, Bhattacharya SS, Thrasher AJ, Fitzke FW, Carter BJ, Rubin GS, Moore AT, Ali RR. 2008. Effect of gene therapy on visual function in Leber's congenital amaurosis. *N Engl J Med* 358:2231–2239.



- Bainbridge JWB, Mehat MS, Sundaram V, Robbie SJ, Barker SE, Ripamonti C, Georgiadis A, Mowat FM, Beattie SG, Gardner PJ, Feathers KL, Luong VA, Yzer S, Balaggan K, Viswanathan A, de Ravel TJJ, Casteels I, Holder GE, Tyler N, Fitzke FW, Weleber RG, Nardini M, Moore AT, Thompson DA, Petersen-Jones SM, Michaelides M, van den Born LI, Stockman A, Smith AJ, Rubin G, Ali RR. 2015. Long-term effect of gene therapy on leber's congenital amaurosis. *N Engl J Med* 372:1887–1897.
- Bartlett JS, Wilcher R, Samulski RJ. 2000. Infectious entry pathway of adeno-associated virus and adeno-associated virus vectors. *J Virol* 74:2777–2785.
- Bell CL, Gurda BL, Van Vliet K, Agbandje-McKenna M, Wilson JM. 2012. Identification of the galactose binding domain of the adeno-associated virus serotype 9 capsid. *J Virol* 86:7326–7333.
- Boyd RF, Sledge DG, Boye SL, Boye SE, Hauswirth WW, Komáromy AM, Petersen-Jones SM, Bartoe JT. 2015. Photoreceptor-targeted gene delivery using intravitreally administered AAV vectors in dogs. *Gene Ther* 23:400.
- Boye SL, Bennett A, Scalabrino ML, Mccullough KT, Van Vliet K, Choudhury S, Ruan Q, Peterson J, Agbandje-mckenna M, Boye E. 2016. Impact of heparan sulfate binding on transduction of retina by recombinant adeno-associated virus vectors. *J Virol* 90:4215–4231.
- Byrne LC, Öztürk BE, Lee T, Fortuny C, Visel M, Dalkara D, Schaffer DV, Flannery JG. 2014. Retinoschisin gene therapy in photoreceptors, Müller glia or all retinal cells in the Rslh-/- mouse. *Gene Ther* 21:585–592.
- Byrne LC, Dalkara D, Luna G, Fisher SK, Clérin E, Sahel J, Léveillard T, Flannery JG. 2015. Viral-mediated RdCVF and RdCVFL expression protects cone and rod photoreceptors in retinal degeneration. *J Clin Invest* 125:105–116.
- Cearley CN, Wolfe JH. 2006. Transduction characteristics of adeno-associated virus vectors expressing cap serotypes 7, 8, 9, and Rh10 in the mouse brain. *Mol Ther* 13:528–537.
- Cideciyan AV, Aleman TS, Boye SL, Schwartz SB, Kaushal S, Roman AJ, Pang JJ, Sumaroka A, Windsor EA, Wilson JM, Flotte TR, Fishman GA, Heon E, Stone EM, Byrne BJ, Jacobson SG, Hauswirth WW. 2008. Human gene therapy for RPE65 isomerase deficiency activates the retinoid cycle of vision but with slow rod kinetics. *Proc Natl Acad Sci USA* 105(39):15112–15117.
- Chivian D, Kim DE, Malmström L, Bradley P, Robertson T, Murphy P, Strauss CEM, Bonneau R, Rohl C a, Baker D. 2003. Automated prediction of CASP-5 structures using the rosetta server. *Proteins* 53:524–533.
- Choi VW, Asokan A, Haberman RA, Samulski RJ. 2007. Production of recombinant adeno-associated viral vectors. *Curr Protoc Hum Genet* 53:12.9:12.9.1–12.9.21.
- Clark SJ, Keenan TDL, Fielder HL, Collinson LJ, Holley RJ, Merry CLR, van Kuppevelt TH, Day AJ, Bishop PN. 2011. Mapping the differential distribution of glycosaminoglycans in the adult human retina, choroid, and sclera. *Invest Ophthalmol Vis Sci* 52:6511.
- Cronin T, Vandenberghe LH, Hantz P, Juttner J, Reimann A, Kacsó A-E, Huckfeldt RM, Busskamp V, Kohler H, Lagali PS, Roska B, Bennett J. 2014. Efficient transduction and optogenetic stimulation of retinal bipolar cells by a synthetic adeno-associated virus capsid and promoter. *EMBO Mol Med* 6:1–16.
- Dalkara D, Byrne LLC, Klimczak RR, Visel M, Yin L, Merigan WH, Flannery JG, Schaffer DV. 2013. In vivo-directed evolution of a new adeno-associated virus for therapeutic outer retinal gene delivery from the vitreous. *Sci Transl Med* 5:189ra76.
- Dalkara D, Kolstad KD, Caporale N, Visel M, Klimczak RR, Schaffer DV, Flannery JG. 2009. Inner limiting membrane barriers to AAV-mediated retinal transduction from the vitreous. *Mol Ther* 17:2096–2102.
- DiMattia a. M, Nam H-J, Van Vliet K, Mitchell M, Bennett a., Gurda BL, McKenna R, Olson NH, Sinkovits RS, Potter M, Byrne BJ, Aslanidi G, Zolotukhin S, Muzyczka N, Baker TS, Agbandje-McKenna M. 2012. Structural insight into the unique properties of adeno-associated virus serotype 9. *J Virol* 86:6947–6958.
- Grimm D, Lee JS, Wang L, Desai T, Akache B, Storm TA, Kay MA. 2008. In vitro and in vivo gene therapy evolution via multispecies interbreeding and retargeting of adeno-associated viruses. *J Virol* 82:5887–5911.
- Jacobson SG, Cideciyan AV, Ratnakaram R, Heon E, Schwartz SB, Roman AJ, Peden MC, Aleman TS, Boye SL, Sumaroka A, Conlon TJ, Calcedo R, Pang J, Erger KE. 2012. Gene therapy for leber congenital amaurosis caused by RPE65 mutations: Safety and efficacy in fifteen children and adults followed up to three years. *Arch Ophthalmol* 130:9–24.
- Jacobson SG, Cideciyan AV, Roman AJ, Sumaroka A, Schwartz SB, Heon E, Hauswirth WW. 2015. Improvement and decline in vision with gene therapy in childhood blindness. *N Engl J Med* 372:1920–1926.
- Kay CN, Ryals RC, Aslanidi GV, Min SH, Ruan Q, Sun J, Dyka FM, Kasuga D, Ayala AE, Van Vliet K, Agbandje-McKenna M, Hauswirth WW, Boye SL, Boye SE. 2013. Targeting photoreceptors via intravitreal delivery using novel, capsid-mutated AAV vectors. *PLoS ONE* 8:e62097.
- Kern A, Schmidt K, Leder C, Müller OJ, Wobus CE, Lieth CW, Von Der, King JA, Mu OJ, Bettinger K. 2003. Identification of a heparin-binding motif on adeno-associated virus type 2 capsids identification of a heparin-binding motif on adeno-associated virus type 2 capsids. *J Virol* 77:11072–11081.
- Kim DE, Chivian D, Baker D. 2004. Protein structure prediction and analysis using the Robetta server. *Nucleic Acids Res* 32:526–531.
- Klein RL, Dayton RD, Leidenheimer NJ, Jansen K, Golde TE, Zweig RM. 2006. Efficient neuronal gene transfer with AAV8 leads to neurotoxic levels of tau or green fluorescent proteins. *Mol Ther* 13:517–527.
- Koerber JT, Jang J-H, Yu JH, Kane RS, Schaffer DV. 2007. Engineering adeno-associated virus for one-step purification via immobilized maffinity chromatography. *Hum Gene Ther* 18:367–378.
- Lochrie M a, Tatsuno GP, Christie B, McDonnell JW, Zhou S, Pierce GF, Colosi P, Surosky R. 2006. Mutations on the external surfaces of adeno-associated virus type 2 capsids that affect transduction and neutralization mutations on the external surfaces of adeno-associated virus type 2 capsids that affect transduction and neutralization. *J Virol* 80:821–834.
- Macé E, Caplette R, Marre O, Sengupta A, Chaffiol A, Barbe P, Desrosiers M, Bamberg E, Sahel J-A, Picaud S, Duebel J, Dalkara D. 2014. Targeting channelrhodopsin-2 to ON-bipolar cells with vitreally administered AAV restores ON and OFF visual responses in blind mice. *Mol Ther* 23:7–16.
- MacLaren RE, Groppe M, Barnard AR, Cottrill CL, Tolmachova T, Seymour L, Clark KR, During MJ, Cremers FPM, Black GCM, Lotery AJ, Downes SM, Webster AR, Seabra MC. 2014. Retinal gene therapy in patients with choroideremia: Initial findings from a phase 1/2 clinical trial. *Lancet* 383:1129–1137.
- Maguire AM, Simonelli F, Pierce EA, Pugh EN, Mingozzi F, Bennicelli J, Banfi S, Marshall KA, Testa F, Surace EM, Rossi S, Lyubarsky A, Arruda VR, Konkle B, Stone E, Sun J, Jacobs J, Dell'Osso L, Hertle R, Ma J, Redmond TM, Zhu X, Hauck B, Zelenia O, Shindler KS, Maguire MG, Wright JE, Volpe NJ, McDonnell JW, Auricchio A, High KA, Bennett J. 2008. Safety and efficacy of gene transfer for Leber's congenital amaurosis. *New Engl J Med* 358:2240–2248.
- Michelfelder S, Varadi K, Raupp C, Hunger A, Körbelin J, Pahrman C, Schrepfer S, Müller OJ, Kleinschmidt a. J, Trepel M. 2011. Peptide ligands incorporated into the threefold spike capsid domain to re-direct gene transduction of AAV8 and AAV9 in vivo. *PLoS ONE* 6:e23101.
- Mowat FM, Gornik KR, Dinculescu A, Boye SL, Hauswirth WW, Petersen-Jones SM, Bartoe JT. 2014. Tyrosine capsid-mutant AAV vectors for gene delivery to the canine retina from a subretinal or intravitreal approach. *Gene Ther* 21:96–105.
- Nam H-J, Lane MD, Padron E, Gurda B, McKenna R, Kohlbrenner E, Aslanidi G, Byrne B, Muzyczka N, Zolotukhin S, Agbandje-McKenna M. 2007. Structure of adeno-associated virus serotype 8, a gene therapy vector. *J Virol* 81:12260–12271.
- Nathwani AC, Rosales C, McIntosh J, Rastegarlar G, Nathwani D, Raj D, Nawathe S, Waddington SN, Bronson R, Jackson S, Donahue RE, High KA, Mingozzi F, Ng CYC, Zhou J, Spence Y, McCarville MB, Valentine M, Allay J, Coleman J, Sleep S, Gray JT, Nienhuis AW, Davidoff AM. 2011. Long-term safety and efficacy following systemic administration of a self-complementary AAV vector encoding human FIX pseudotyped with serotype 5 and 8 capsid proteins. *Mol Ther* 19:876–885.
- Nathwani AC, Reiss UM, Tuddenham EGD, Rosales C, Chowdhary P, McIntosh J, Della Peruta M, Lheriteau E, Patel N, Raj D, Riddell A, Pie J, Rangarajan S, Bevan D, Recht M, Shen Y-M, Halka KG, Basner-Tschakarjan E, Mingozzi F, High KA, Allay J, Kay MA, Ng CYC, Zhou J, Cancio M, Morton CL, Gray JT, Srivastava D, Nienhuis AW, Davidoff AM. 2014. Long-term safety and efficacy of factor IX gene therapy in hemophilia B. *N Engl J Med* 371:1994–2004.
- Natkunarajah M, Trittibach P, McIntosh J, Duran Y, Barker SE, Smith a J, Nathwani a C, Ali RR. 2008. Assessment of ocular transduction using single-stranded and self-complementary recombinant adeno-associated virus serotype 2/8. *Gene Ther* 15:463–467.
- Nguyen JB, Sanchez-Pernaute R, Cunningham J, Bankiewicz KS. 2001. Convection-enhanced delivery of AAV-2 combined with heparin increases TK gene transfer in the rat brain. *Neuroreport* 12:1961–1964.
- Opie SR, Warrington KH, Agbandje-McKenna M, Zolotukhin S, Muzyczka N. 2003. Identification of amino acid residues in the capsid proteins of adeno-associated virus type 2 that contribute to heparan sulfate proteoglycan binding. *J Virol* 77:6995–7006.

- Perabo L, Goldnau D, White K, Endell J, Boucas J, Humme S, Work LM, Janicki H, Hallek M, Baker AH, Büning H. 2006. Heparan sulfate proteoglycan binding properties of adeno-associated virus retargeting mutants and consequences for their in vivo tropism. *J Virol* 80:7265–7269.
- Petrs-silva H, Dinculescu A, Li Q, Deng W, Pang J, Min S, Chiodo V, Neeley AW, Govindasamy L, Bennett A, Agbandje-McKenna M, Zhong L, Li B, Jayandharan GR, Srivastava A, Lewin AS, Hauswirth WW. 2011. Novel properties of tyrosine-mutant AAV2 vectors in the mouse retina. *Mol Ther* 19:293–301.
- Petrs-Silva H, Dinculescu A, Li Q, Min S-H, Chiodo V, Pang J-J, Zhong L, Zolotukhin S, Srivastava A, Lewin AS, Hauswirth WW. 2009. High-efficiency transduction of the mouse retina by tyrosine-mutant AAV serotype vectors. *Mol Ther* 17:463–471.
- Pettersen EF, Goddard TD, Huang CC, Couch GS, Greenblatt DM, Meng EC, Ferrin TE. 2004. UCSF chimera—A visualization system for exploratory research and analysis. *J Comput Chem* 25:1605–1612.
- Raup C, Naumer M, Muller OJ, Gurda BL, Agbandje-McKenna M, Kleinschmidt J a. 2012. The threefold protrusions of adeno-associated virus type 8 are involved in cell surface targeting as well as postattachment processing. *J Virol* 86:9396–9408.
- Schmidt M, Govindasamy L, Afione S, Kaludov N, Agbandje-McKenna M, Chiorini JA. 2008. Molecular characterization of the heparin-dependent transduction domain on the capsid of a novel adeno-associated virus isolate, AAV(VR-942). *J Virol* 82:8911–8916.
- Shen S, Berry GE, Castellanos Rivera RM, Cheung RY, Troupes AN, Brown SM, Kafri T, Asokan A. 2014. Functional analysis of the putative integrin recognition motif on adeno-associated virus 9. *J Biol Chem* 290:1496–1504.
- Vandenberghe LH, Auricchio A. 2012. Novel adeno-associated viral vectors for retinal gene therapy. *Gene Ther* 19:162–168.
- Vandenberghe LH, Bell P, Maguire AM, Cearley CN, Xiao R, Calcedo R, Wang L, Castle MJ, Maguire AC, Grant R, Wolfe JH, Wilson JM, Bennett J. 2011. Dosage thresholds for AAV2 and AAV8 photoreceptor gene therapy in monkey. *Sci Transl Med* 3:88ra54.
- Vandenberghe LH, Bell P, Maguire AM, Xiao R, Hopkins TB, Grant R, Bennett J, Wilson JM. 2013. AAV9 targets cone photoreceptors in the nonhuman primate retina. *PLoS ONE* 8:e53463.
- Varadi K, Michelfelder S, Korff T, Hecker M, Trepel M, Katus a H, Kleinschmidt a J, Müller OJ. 2012. Novel random peptide libraries displayed on AAV serotype 9 for selection of endothelial cell-directed gene transfer vectors. *Gene Ther* 19:800–809.
- Walters RW, Agbandje-mckenna M, Valorie D, Moninger TO, Olson NH, Chiorini JA, Baker TS, Bowman VD, Seiler M, Zabner J. 2004. Structure of adeno-associated virus structure of adeno-associated virus serotype 5. *J Virol* 78:3361–3371.
- Wu P, Xiao W, Conlon T, Hughes J, Agbandje-McKenna M, Ferkol T, Flotte T, Muzyczka N. 2000. Mutational analysis of the adeno-associated virus type 2 (AAV2) capsid gene and construction of AAV2 vectors with altered tropism. *J Virol* 74:8635–8647.
- Ying Y, Müller OJ, Goehring C, Leuchs B, Trepel M, Katus a H, Kleinschmidt a J. 2010. Heart-targeted adeno-associated viral vectors selected by in vivo biopanning of a random viral display peptide library. *Gene Ther* 17:980–990.
- Zhang H, Yang B, Mu X, Ahmed SS, Su Q, He R, Wang H, Mueller C, Sena-Esteves M, Brown R, Xu Z, Gao G. 2011. Several rAAV vectors efficiently cross the blood-brain barrier and transduce neurons and astrocytes in the neonatal mouse central nervous system. *Mol Ther* 19:1440–1448.

## Supporting Information

Additional supporting information may be found in the online version of this article at the publisher's web-site.



### III. Translational aspects: noninvasive foveal targeting and efficient vision restoration

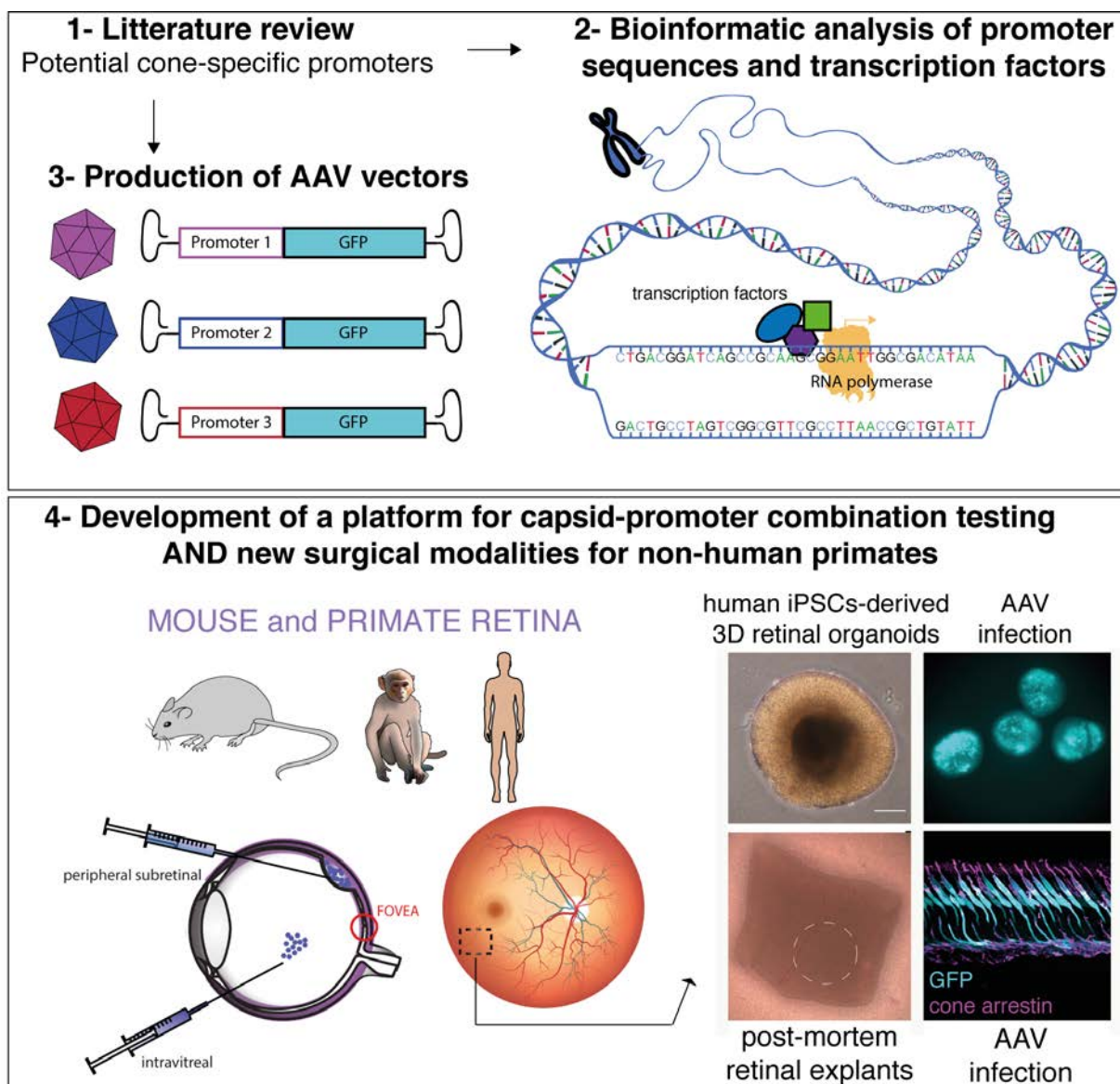
A gap in the field is the possibility to target foveal cones specifically and non-invasively, in particular without sub-foveal vector administration. We sought to develop new vectors to achieve this objective, in particular in the context of RP. After characterization of AAV2-7m8 and AAV9-7m8 in my previous paper (166), I selected these vectors for translational application in primates based on the following facts. AAV2-7m8 is the best vector so far described for intravitreal delivery in primates (124). Therefore, it is the most relevant vector to develop new modalities for foveal cone targeting from the vitreous. On the other hand, AAV9 is the most efficient capsid to target cones using a subretinal delivery approach in monkeys (135). AAV9-7m8 has a 30-fold increase of infectivity compared to AAV9 (166) so it is a promising vector for enhanced gene delivery to cones subretinally when delivered away from the fovea. When combined with the strong cell-type specific promoter PR1.7, both modalities provided highly efficient delivery to cones. We first proved the efficiency of these different tools in the mouse retina. But in a translational context, and since mice do not have a fovea, we deemed it necessary to validate these tools in vivo in macaques as well as in human tissue. Macaque foveal cones were rendered light sensitive via the expression of a highly efficient opsin referred to as Jaws showing the usefulness of our vector for optogenetic vision restoration. Collectively, our data provide evidence for therapeutic potential of our vectors in the treatment of retinal pathologies associated to cone dysfunction such as RP, or achromatopsia.

These results have been published this year as a research article, highlighted on the Journal Cover of the month issue: <https://insight.jci.org/posts/58>. It is also one of the Editors Picks: <https://insight.jci.org/this-month/2018/2>.

**Khabou H.**, Garita-Hernandez M., Chaffiol A., Reichman S., Jaillard C., Brazhnikova E., Bertin S., Forster V., Desrosiers M., Winckler C., Goureau O., Picaud S., Duebel J., Sahel JA., Dalkara D. Noninvasive gene delivery to foveal cones for vision restoration. *JCI Insight*. 2018; 3(2):e96029.

Additional information including supplemental figures and movie are available here and in Annex III: <https://doi.org/10.1172/jci.insight.96029DS1>

# Graphical Abstract



# Noninvasive gene delivery to foveal cones for vision restoration

Hanen Khabou,<sup>1</sup> Marcela Garita-Hernandez,<sup>1</sup> Antoine Chaffiol,<sup>1</sup> Sacha Reichman,<sup>1</sup> Céline Jaillard,<sup>1</sup> Elena Brazhnikova,<sup>1</sup> Stéphane Bertin,<sup>1,2</sup> Valérie Forster,<sup>1</sup> Mélissa Desrosiers,<sup>1</sup> Céline Winckler,<sup>1</sup> Olivier Goureau,<sup>1</sup> Serge Picaud,<sup>1</sup> Jens Duebel,<sup>1</sup> José-Alain Sahel,<sup>1,2,3,4</sup> and Deniz Dalkara<sup>1</sup>

<sup>1</sup>Sorbonne Universités, UPMC Univ Paris 06, INSERM, CNRS, Institut de la Vision, Paris, France. <sup>2</sup>CHNO des Quinze-Vingts, DHU Sight Restore, INSERM-DGOS CIC 1423, Paris, France. <sup>3</sup>Fondation Ophtalmologique Rothschild, Paris, France.

<sup>4</sup>Department of Ophthalmology, The University of Pittsburgh School of Medicine, Pittsburgh, Pennsylvania, USA.

Intraocular injection of adeno-associated viral (AAV) vectors has been an evident route for delivering gene drugs into the retina. However, gaps in our understanding of AAV transduction patterns within the anatomically unique environments of the subretinal and intravitreal space of the primate eye impeded the establishment of noninvasive and efficient gene delivery to foveal cones in the clinic. Here, we establish new vector-promoter combinations to overcome the limitations associated with AAV-mediated cone transduction in the fovea with supporting studies in mouse models, human induced pluripotent stem cell-derived organoids, postmortem human retinal explants, and living macaques. We show that an AAV9 variant provides efficient foveal cone transduction when injected into the subretinal space several millimeters away from the fovea, without detaching this delicate region. An engineered AAV2 variant provides gene delivery to foveal cones with a well-tolerated dose administered intravitreally. Both delivery modalities rely on a cone-specific promoter and result in high-level transgene expression compatible with optogenetic vision restoration. The model systems described here provide insight into the behavior of AAV vectors across species to obtain safety and efficacy needed for gene therapy in neurodegenerative disorders.

**Conflict of interest:** HK, DD, JD, and JAS are inventors on pending patent applications on noninvasive methods to target cone photoreceptors (EP17306429.6 and EP17306430.4). MGH, AC, DD, JD, and JAS are inventors on a pending patent on the use of iPSC to treat retinal degeneration (EP16306225). DD is an inventor on a patent of adeno-associated virus virions with variant capsid and methods of use thereof with royalties paid to Avalanche Biotech (WO2012145601 A2). SR, OG, and JAS are inventors on a patent on iPSC retinal differentiation (WO 2014174492 A1). JAS is a founder and consultant for Pixium Vision and GenSight Biologics and is a consultant for Sanofi-Fovea, Genesignal, and Vision Medicines. SP is a founder of GenSight Biologics and a consultant for Pixium Vision. DD and JD are consultants for GenSight Biologics.

**Submitted:** July 5, 2017

**Accepted:** December 12, 2017

**Published:** January 25, 2018

**Reference information:**

*JCI Insight.* 2018;3(2): e96029.  
<https://doi.org/10.1172/jci.insight.96029>.

## Introduction

The fovea — located at the center of the macula — is a specialized region of the retina that dominates the visual perception of primates by providing high-acuity color vision (1). The highest density of cones is found at the center of the fovea (<0.3 mm from the foveal center), devoid of rod photoreceptors (2). Cone density decreases by up to 100-fold with distance from the fovea (3). Cone cells in the fovea are the primary targets of gene therapies aiming to treat inherited retinal diseases like midstage retinitis pigmentosa (4, 5) and achromatopsia (6). Currently, viral vectors encoding therapeutic proteins need to be injected into the subretinal space between the photoreceptors and the retinal pigment epithelium (RPE) cells in order to provide gene delivery to cones. In this approach, gene delivery is limited to cells that contact the local bleb of injected fluid. Furthermore, retinal detachment that occurs during subretinal injections is a concern in eyes with retinal degeneration. The earliest clinical trials using subretinal delivery of adeno-associated virus (AAV) to deliver a healthy retinal pigment epithelium-specific 65 kilodalton protein (*RPE65*) gene in Leber's congenital amaurosis patients (7–9) led to some improvements in vision, despite the detachment of the macula to deliver the viral vector (10, 11). However, the treatment was, in certain cases, complicated by macular holes and increased macular thinning in the case of subfoveal injections (11). Furthermore, contrary to the surrounding regions, there were no treatment benefits in the fovea (12). Gene therapy using AAV has also been studied for patients with choroideremia in which the macula was the target for gene delivery (13). The 6-month follow-up results from this latter study thus far suggest that subfoveal retinal detachment does not cause vision reduction in this region, but one of the patients in this trial had visual acuity loss in the treated eye compared with his untreated eye (13). With more gene therapies reaching clinical stages of application, there is a growing need to find new methods for delivering gene therapy to the fovea without detaching this brittle region (14). This can be achieved by engineering the viral vectors to permit gene delivery away from the injection site. AAV capsids that can provide gene delivery to foveal cones

after injection into the vitreous cavity are one possible option. Another option would be through subretinal injections in the periphery using vectors that spread laterally to reach the foveal region.

To minimize the risks associated with foveal detachments, we developed vector-promoter combinations that can successfully deliver genes into foveal cones without detaching them from their underlying epithelium. As a key element to gene therapy, we first searched for promoters that are able to afford high-level transgene expression in cones without leading to off-target expression in neighboring cells. We then combined this promoter with 2 potent AAV capsid variants that are able to provide gene delivery to cone photoreceptors when injected intravitreally or via distal subretinal injections outside the fovea. We validated the utility of these gene delivery strategies in the context of cone-directed optogenetic therapy (15) using electrophysiology, histology, *in vivo*, and *ex vivo* imaging techniques in mouse, macaque, and human retinal tissue. Our results highlight the importance of viral vector development in overcoming surgical delivery challenges, as gene therapy to restore vision becomes a potentially attainable goal for those who treat inherited retinal degenerations in the clinic.

## Results

*Selection of a strong and specific cone cell-specific promoter in murine models.* In order to find vector-promoter combinations suitable for strong and specific cone targeting away from the injection site, we compared several AAVs after intravitreal and subretinal delivery in mouse retinas. To enable efficient cone photoreceptor targeting, we used an engineered AAV variant called AAV2-7m8, which has been shown to target photoreceptors efficiently via both administration routes (16, 17). Specific targeting of cone cells has never been attempted using vitreally administered AAV. In order to find suitable promoter sequences for restricted gene expression in cones applicable in the clinic, we focused on promoters that have previously been validated in either nonhuman primate (NHP) (18) or human tissue (4). We generated AAV2-7m8 vectors encoding GFP under the control of mouse cone arrestin (mCAR), PR2.1 and PR1.7 promoters (synthetic promoters based on the human red opsin gene enhancer and promoter sequences — their size is equal to 2.1 and 1.7 kilobases, respectively) and injected them at equal titers into eyes of 6-week-old WT mice. Three weeks after subretinal injections, retinal cross-sections were stained with cone arrestin, and GFP expression was examined (Figure 1, A–C). We found GFP expression in both rod and cone photoreceptors with mCAR promoter, while PR2.1 and PR1.7 led to strong expression mostly in cones, as reported previously (18, 19). Using the same vectors, we obtained strikingly different expression patterns after intravitreal delivery (Figure 1, D–F). The mCAR promoter led to GFP expression in some cones but was leaky toward rods as well as cells of the inner nuclear layer (INL) and ganglion cell layer (GCL) (Figure 1D). Both PR2.1 and PR1.7 promoters led to more cone labeling than the mCAR promoter (Figure 1, D–F, and Supplemental Figure 1; supplemental material available online with this article; <https://doi.org/10.1172/jci.insight.96029DS1>). PR2.1 transduced more cones than PR1.7, but it also produced nonspecific GFP expression in the INL and GCL. Only the PR1.7 promoter showed GFP expression in cones with minimal expression in rods and was not leaky toward the inner retina (Figure 1F). Finally, as retinal disease state can influence AAV-mediated gene delivery and transgene expression patterns (20, 21), we validated AAV2-7m8-PR1.7 vector-promoter combination in a mouse model of retinal degeneration. We injected AAV2-7m8-PR1.7-GFP intravitreally in the retinal degeneration 10 (rd10) mouse model of retinitis pigmentosa. Two months after injection, GFP expression was restricted to cones (Figure 1G and Supplemental Figure 2). Based on these results, we decided to test it in the primate retina.

*Bioinformatic analysis of mCAR, PR1.7, and PR2.1 promoter sequences.* Before moving on to further studies in other species, we aimed to better understand the reasons behind the divergent expression patterns obtained with the 3 promoters. To do so, we analyzed transcription factor (TF) binding sites within each promoter sequence using bioinformatics (Supplemental Tables 1 and 2). The present analysis aimed to answer the following questions: (i) why is PR1.7 more efficient than PR2.1 in cones (18), and (ii) why do PR2.1 and mCAR promoters lead to off-target expression after intravitreal administration? We hypothesized that the differential expression patterns observed between PR1.7 and PR2.1 are due to additional TF binding sites found in the 337-bp sequence located in the 5' region of the PR2.1 promoter but not in the PR1.7 promoter (Figure 2, A and B). Interestingly, we found a chicken ovalbumin upstream promoter-transcription factor I (COUP-TFI) binding site within this 337-bp sequence (Supplemental Table 1). COUP-TFI has been shown to suppress green opsin gene (*Opn1mw*) expression in the mouse retina (22) and might thus be accountable for lower expression with the PR2.1 promoter in macaque cones when AAV is delivered subretinally as previously shown (18). Within the same specific 337-bp region, we also found

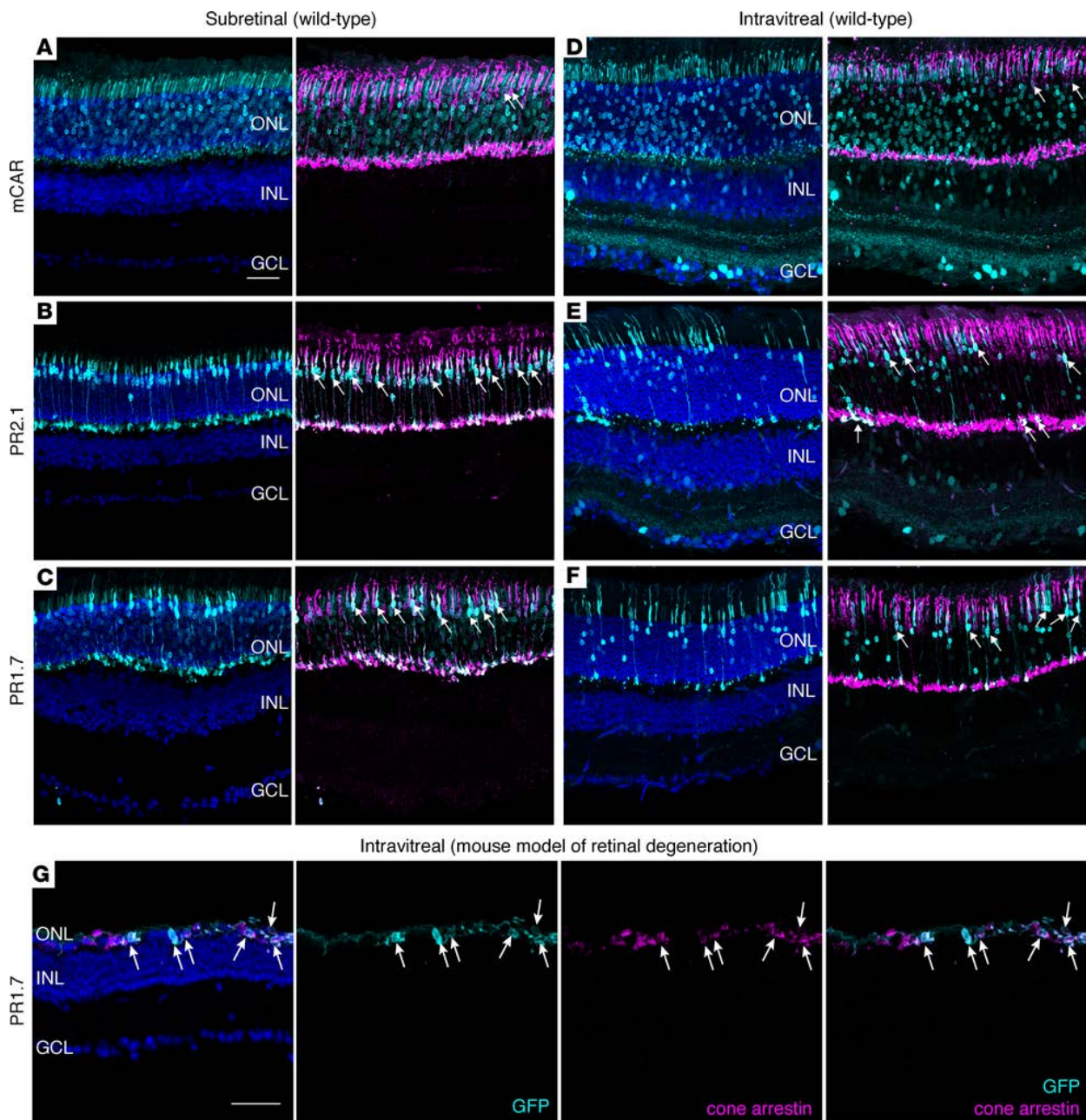


**Figure 1. Adeno-associated viral (AAV) vector administration route defines retinal transduction patterns with mCAR, PR2.1, and PR1.7 promoters.** (A–C) Representative retinal cross sections of WT mouse retinas ( $n = 6$  eyes per condition) 3 weeks after subretinal injection of AAV2-7m8-mCAR-GFP (A), AAV2-7m8-PR2.1-GFP (B), and AAV2-7m8-PR1.7-GFP (C). (D–F) Representative retinal cross sections 2 months after intravitreal injection ( $n = 6$  eyes per condition) of AAV2-7m8-mCAR-GFP (D), AAV2-7m8-PR2.1-GFP (E), and AAV2-7m8-PR1.7-GFP (F). Scale bar: 50  $\mu\text{m}$  in A–F. (G) GFP expression in rd10 retina ( $n = 4$  eyes) 2 months after intravitreal injection of AAV2-7m8-PR1.7-GFP. Transduced cone cell bodies remaining after degeneration express GFP (cyan). Cone arrestin is shown in magenta, and DAPI is shown in blue. Native GFP expression is shown in cyan, and arrows indicate cells where cone arrestin is colocalized with GFP. Scale bar is 50  $\mu\text{m}$  in G. mCAR, mouse cone arrestin promoter; PR1.7 and PR2.1, promoters of 1.7 and 2.1 kilobases in length, respectively, based on the human red opsin gene enhancer and promoter sequences.

multiple binding sites for generic, ubiquitous activator TFs (Figure 2B and Supplemental Table 1), such as CCAAT/enhancer binding protein  $\beta$  (CEBPB) and general transcription factor II-I (GTF2I). These additional binding sites of TFs that enhance binding and basal transcriptional machinery assembly and that are not specifically expressed in cones might be responsible for some of the off-target expression observed with PR2.1 compared with PR1.7 (Figure 2). We also analyzed TF binding sites in the genomic mouse *Arr3* promoter sequence to explain the lack of specificity using the short version of this promoter (referred to as



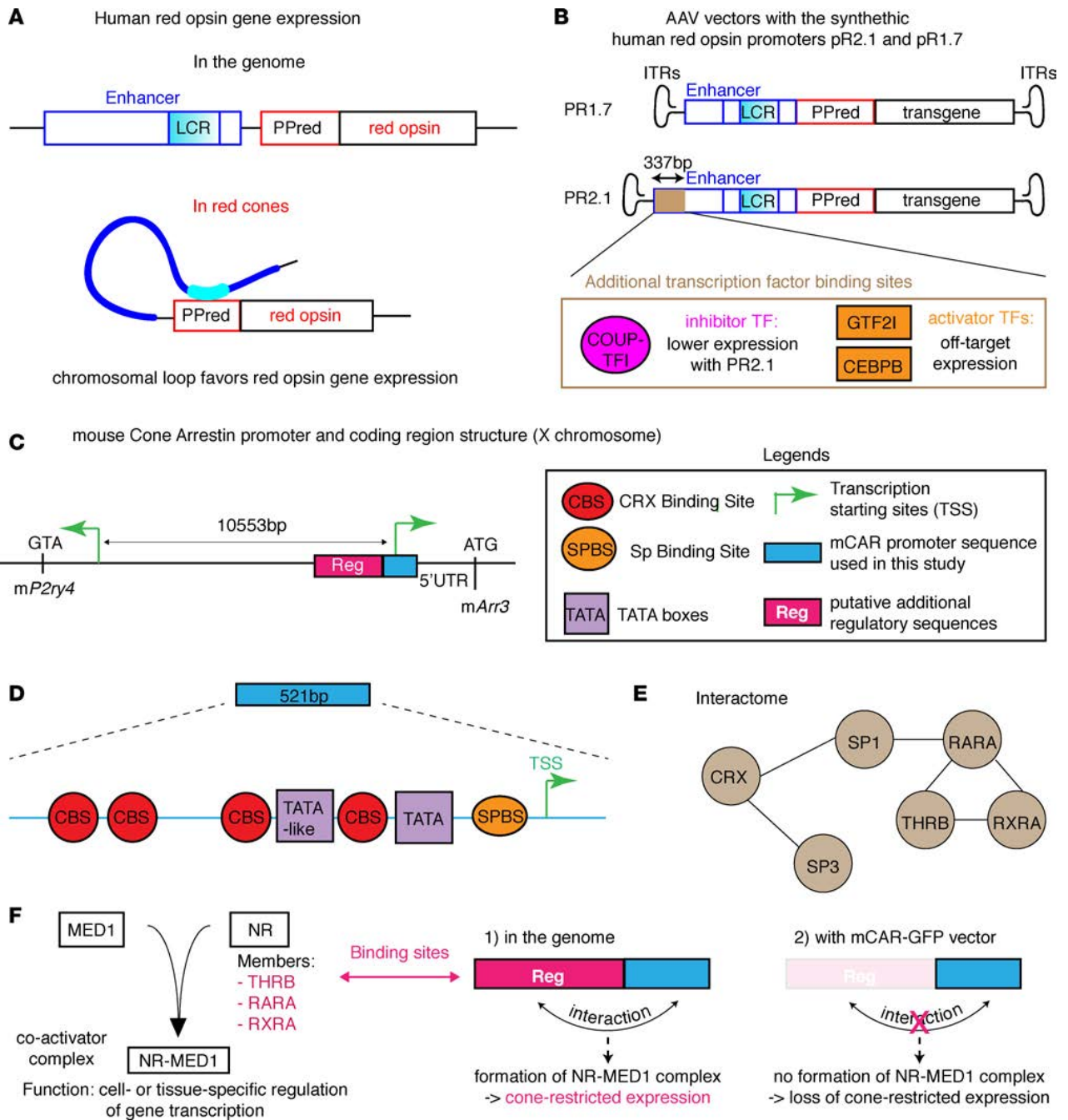


**Figure 2. Model for the regulation of transgene expression under the control of PR2.1 and PR1.7 synthetic promoters and mouse cone arrestin (mCAR) promoter.** (A) Red opsin gene is located on the X chromosome. It has its own proximal promoter and shares its enhancer sequence with green opsin gene. Chromosomal loops between the enhancer and the red opsin proximal promoter provide cell-type specificity of gene expression. PPred, proximal promoter of red opsin gene; LCR, locus control region. (B) Schematic representation of PR2.1 and PR1.7 promoter constructs. Interaction with inhibitory transcription factors such as COUP-TFI (chicken ovalbumin upstream promoter-transcription factor), that binds the 337bp region specific to PR2.1 might explain low expression levels obtained with PR2.1 compared with PR1.7 in macaque cones subretinally (18). On the other hand, activator TFs such as CEBPB (CCAAT/enhancer binding protein  $\beta$ ) and GTF2I (general transcription factor II-1) that are not specific to cones likely lead to off-target expression in other retinal cells when injected into the vitreous. ITRs, inverted terminal repeats. (C) Structure of cone arrestin 3 genomic locus region. Transcription starting sites (TSS) of mouse arrestin 3 (mArr3) gene and mouse pyrimidergic receptor P2Y4 (mP2ry4) gene are separated by 10.5 kilobases. The short 521-bp mCAR promoter used in this study is shown in blue and the supposed regulatory region referred to as “Reg” in magenta. (D) Structure of the 521-bp mCAR promoter portion used in this study. This sequence contains CRX-binding sites (CBS) and SP (Specificity Protein) binding sites. It also contains 1 TATA and 1 TATA-like box. (E) Interactome network of several transcription factors that bind cone arrestin genomic promoter analyzed using the STRING tool. CRX (cone-rod homeobox protein), SP, RARA (retinoic acid receptor  $\alpha$ ), RXRA (retinoid X receptor  $\alpha$ ), and THR $\beta$  (thyroid hormone receptor  $\beta$  2). (F) NR-MED1 transcription regulator complex confers gene expression specificity. MED1 (mediator complex subunit 1) is a transcription activator when associated to nuclear receptors (NRs). RARA, RXRA, and THR $\beta$  are NRs. Several NR binding sites for RARA, RXRA, and THR $\beta$  were found in the Reg region. AAV, adeno-associated virus; mCAR, mouse cone arrestin promoter; PR1.7 and PR2.1, promoters of 1.7 and 2.1 kilobases in length, respectively, based on the human red opsin gene enhancer and promoter sequences.

**Table 1. Summary of injections in nonhuman primates**

Animal	Age (years)	Weight (kg)	Sex	Injection type; eye	AAV capsid	Transgene	Dose (vg/eye)	Volume ( $\mu$ l)
NHP 1	7	8.65	M	intravitreal; LE	AAV2-7m8	PR1.7-GFP	$1 \times 10^{11}$ vg	100
NHP 2	8	11.81	M	intravitreal; LE	AAV2-7m8	CMV-GFP	$1 \times 10^{11}$ vg	100
NHP 3	13	12.93	M	intravitreal; LE	AAV2-7m8	PR1.7-GFP	$1 \times 10^{11}$ vg	100
				intravitreal; RE	AAV2-7m8	CMV-GFP	$1 \times 10^{11}$ vg	
NHP 4	4	5.03	M	intravitreal; RE	AAV2-7m8	PR1.7-Jaws-GFP	$1 \times 10^{11}$ vg	100
NHP 5	4	6.26	M	subretinal, sup; RE	AAV9-7m8	PR1.7-Jaws-GFP	$1 \times 10^{10}$ vg	50
				intravitreal; LE	AAV2-7m8	PR1.7-Jaws-GFP	$1 \times 10^{10}$ vg	
NHP 6	5	6.83	M	subretinal, sup; RE	AAV9-7m8	PR1.7-Jaws-GFP	$5 \times 10^{10}$ vg	50
NHP 7	3	3	M	subretinal, inf; RE	AAV9-7m8	PR1.7-Jaws-GFP	$5 \times 10^9$ vg	50
NHP 8	3	3.23	M	subretinal, inf; RE	AAV9-7m8	PR1.7-Jaws-GFP	$5 \times 10^9$ vg	50

NHP, nonhuman primate; kg, kilograms; M, male; sup, superior bleb; inf, inferior bleb; LE, left eye; RE, right eye; AAV, adeno-associated virus; CMV, cytomegalovirus promoter; PR1.7, Promoter 1.7 kilobases, based on human red opsin gene enhancer and promoter sequences; vg, viral genome.

mCAR) used in the AAV constructs. The short sequence consists of a 521-bp portion of the genomic proximal CAR promoter (Figure 2, C and D) and presents a TATA-box, a TATA-like box, as well as binding sites for cone-rod homeobox protein (CRX) and specificity protein (SP) TFs (23) (Figure 2D). However, the “Reg” sequence (Figure 2C) modulating *Arr3* promoter activity (23) located directly upstream of the 521-bp region is excluded from the short mCAR sequence (Figure 2C). Based on the interactome of the TFs binding mCAR promoter obtained from the STRING database (24), CRX and SP TFs interact with each other and with retinoic acid receptor  $\alpha$  (RARA), retinoid X receptor  $\alpha$  (RXRA), and thyroid hormone receptor  $\beta$  (THR $\beta$ ) TFs (Figure 2E). These 3 nuclear receptors (NRs) are involved in cell type-specific regulation of gene expression via mediator complex subunit 1 (MED1) (25) by forming a cell-specific transcription coactivator complex (26, 27) (Figure 2F). CRX and SP binding sites are located on the 521-bp region, while RXRA, RARA, and THR $\beta$  binding sites are positioned on the Reg region (Figure 2F). Moreover, the Reg region contains 5 binding sites for THR $\beta$ 2, an important NR expressed in cones (28) (Supplemental Table 2). For all of these reasons, removal of the Reg region is likely responsible for the off-target expression observed with the short mCAR promoter (Figure 2F).

*Safe gene delivery to macaque foveal cones via intravitreal administration of AAV.* We and others have shown transduction of macaque cones using AAV variants with ubiquitous promoters (16, 29–32), but achieving cone transduction by vitreally administered AAV has only been possible at high doses, leading to inflammation (16, 29). We reasoned that foveal cone targeting could be achieved if we use a strong cone-specific promoter at lower intravitreally injected AAV doses compatible with safety (29, 33). To test if such “dose sparing” is possible, we injected 2 macaque eyes with AAV2-7m8-PR1.7-GFP and 2 other macaque eyes were injected with AAV2-7m8-GFP under the control of the cytomegalovirus (CMV) promoter at a dose of  $1 \times 10^{11}$  viral genomes (vg) per eye (Table 1). Using in vivo eye fundus imaging, we observed GFP expression as early as 2 weeks after injection with CMV and increased until 2 months after injection (Figure 3, A and B, and Supplemental Figure 3). GFP fluorescence was predominantly in the periphery and in the parafoveal region. GFP expression with PR1.7 became detectable 4–6 weeks after administration and was restricted to the fovea (Figure 3, C and D). There was no detectable damage to the fovea as assessed by optical coherence tomography (OCT) (Figure 4). We then examined flatmounts of the maculas and cryosections of the fovea using confocal microscopy, with equal acquisition settings for each eye (Figure 3). These images corroborated the in vivo findings showing specific and robust foveal cone transduction from the vitreous (Supplemental Video 1), at a dose of  $1 \times 10^{11}$  particles, using AAV2-7m8-PR1.7. About 58% of the hCAR<sup>+</sup> cells were found to express detectable levels of GFP in the foveola. The CMV promoter did not provide detectable transgene expression in cones at an identical dose.

*Therapeutic gene delivery to foveal cones for vision restoration using optogenetics.* We next aimed to evaluate the possibility of using this promoter for therapeutic gene delivery. There is no existing blind macaque or primate model of retinal degeneration to test functional outcomes after gene replacement (e.g., *CNGB3* for treatment of achromatopsia). However, it is possible to evaluate vision restoration in WT macaques using optogenetic strategies, since we can distinguish between optogenetic-mediated light responses versus endog-

enous cone opsin-mediated responses (4). We evaluated the potential of optogenetic vision restoration by expression of Jaws, a hyperpolarizing microbial opsin (15), in foveal cones. We injected 1 macaque eye with  $1 \times 10^{11}$  vg of AAV2-7m8-PR1.7-Jaws-GFP in the vitreous to evaluate its therapeutic potential for reactivation of dormant cones in midstage retinitis pigmentosa as described previously in mice (4, 15). We found high-level Jaws-GFP expression restricted to the foveal cones in the injected eye (Figure 5, A–C) similar to GFP expression alone (Figure 3). The animal was then sacrificed 2 months after injection, and half of the retina was processed for histology. Retinal flat-mounts showed typical anatomy of cones in the foveola (Figure 5, D and E), the region of the fovea that contains densely packed cones responsible for our high-acuity vision. Immunostaining for hCAR was used to quantify transduced cones (Supplemental Figure 4). About 50% of the hCAR<sup>+</sup> cells were found to express detectable levels of Jaws-GFP in this foveola.

The other half of the retina was conserved as explants (34) for characterization of optogenetic light responses arising from the hyperpolarizing pump Jaws (Figure 5, F–K). Electrophysiological recordings were performed on transduced cones expressing Jaws and in control cones without Jaws expression (Figure 5, F and G). Whole-cell patch-clamp recordings in GFP<sup>+</sup> Jaws cones exhibited robust light responses to orange light flashes ( $n = 4$ ) (Figure 5, H and I). Action spectrum of recorded cells showed that highest light responses were obtained using orange light between 575 nm and 600 nm (Figure 5J) as previously shown for Jaws (15). Jaws-expressing cones recorded in current-clamp configuration displayed light-elicited hyperpolarizations followed by short depolarizations ( $n = 4$  cells), while control cones did not respond to the same light stimuli ( $n = 3$  cells) (Figure 5K).

Finally, we injected intravitreally another macaque eye with  $1 \times 10^{10}$  particles of AAV2-7m8-PR1.7-Jaws-GFP to evaluate feasibility of foveal transduction at even lower doses. We obtained detectable foveal Jaws expression even with this lower dose, although expression levels were lower than with  $1 \times 10^{11}$  particles (Supplemental Figure 5, A and B). Altogether, all 4 macaque eyes injected with AAV2-7m8-PR1.7-GFP ( $n = 2$ ) or Jaws-GFP ( $n = 2$ ) show reproducibility and strength of the intravitreal approach compatible with optogenetic reactivation of cones.

*Enhanced optogenetic responses in foveal cones via distal subretinal administration of AAV9-7m8-Jaws.* Transduction of foveal cones via intravitreal injection of AAV2-7m8 with a strong cone promoter is likely an ideal approach to treat cones in fragile retinas of retinitis pigmentosa patients with dormant cones present mainly in the foveola. However, for achromatopsia patients, as well as the subset of retinitis pigmentosa patients with strong neutralizing antibody titers against AAV2 (33), a subretinal approach might be advantageous. Previous studies have shown that subretinal injection of AAV9 leads to efficient transgene expression in cones both centrally and peripherally at low doses, likely due to the abundance of galactosylated glycans, the primary receptor for AAV9, on cone photoreceptors (30, 35). Based on this, we reasoned that an enhanced AAV9 variant might afford efficient transduction of foveal cones from a distal bleb. We previously described a variant called AAV9-7m8, which provides a 30-fold increase in infectivity over AAV9 (17). To promote foveal cone gene delivery through a distal subretinal injection site, we used an AAV9-7m8 variant. We injected 1 animal subretinally with  $5 \times 10^{10}$  particles of this vector encoding Jaws-GFP into the peripheral retina (Figure 6, A and B) without detaching the fovea. As early as 2 weeks after injection, we observed strong Jaws-GFP fluorescence in the bleb (delimited by the dashed cyan line) and also in the foveola (Figure 6C). Fluorescence intensity was higher in the foveola compared with intravitreally treated retinas. We observed the same result in a second eye injected with  $1 \times 10^{10}$  vg of the same vector (Supplemental Figure 5C). To further confirm that the superior peripheral blebs did not descend toward the fovea once the animal was in upright position and to see if further dose reduction was possible, we injected 2 other eyes with a dose of  $5 \times 10^9$  vg, this time inferior to the fovea (Table 1). Using OCT, we observed that the fovea was not detached after surgery (Supplemental Figure 6). The same expression pattern, extending to the foveal cones, was obtained in these retinas (Supplemental Figure 5D). These results collectively show the reproducibility of this approach and its compatibility with low viral doses.

Flatmounts were then prepared, and fovea was processed for histology and showed strong Jaws-GFP expression in a large population of cones (Figure 6D) in the region between the injection site and inside the fovea (Figure 6, D–F). Cell counting of GFP and CAR<sup>+</sup> cells showed about 95% of cones were labeled using this subretinal approach (Figure 6, E and F) compared with about 50% obtained with intravitreal injection (Supplemental Figure 4). The amplitude of photocurrents were 5 times higher in Jaws cones after subretinal delivery compared with those in Jaws cones after intravitreal delivery, with similarly shaped light sensitivity curves (Figure 5H and Figure 6, G and H). This is likely due to

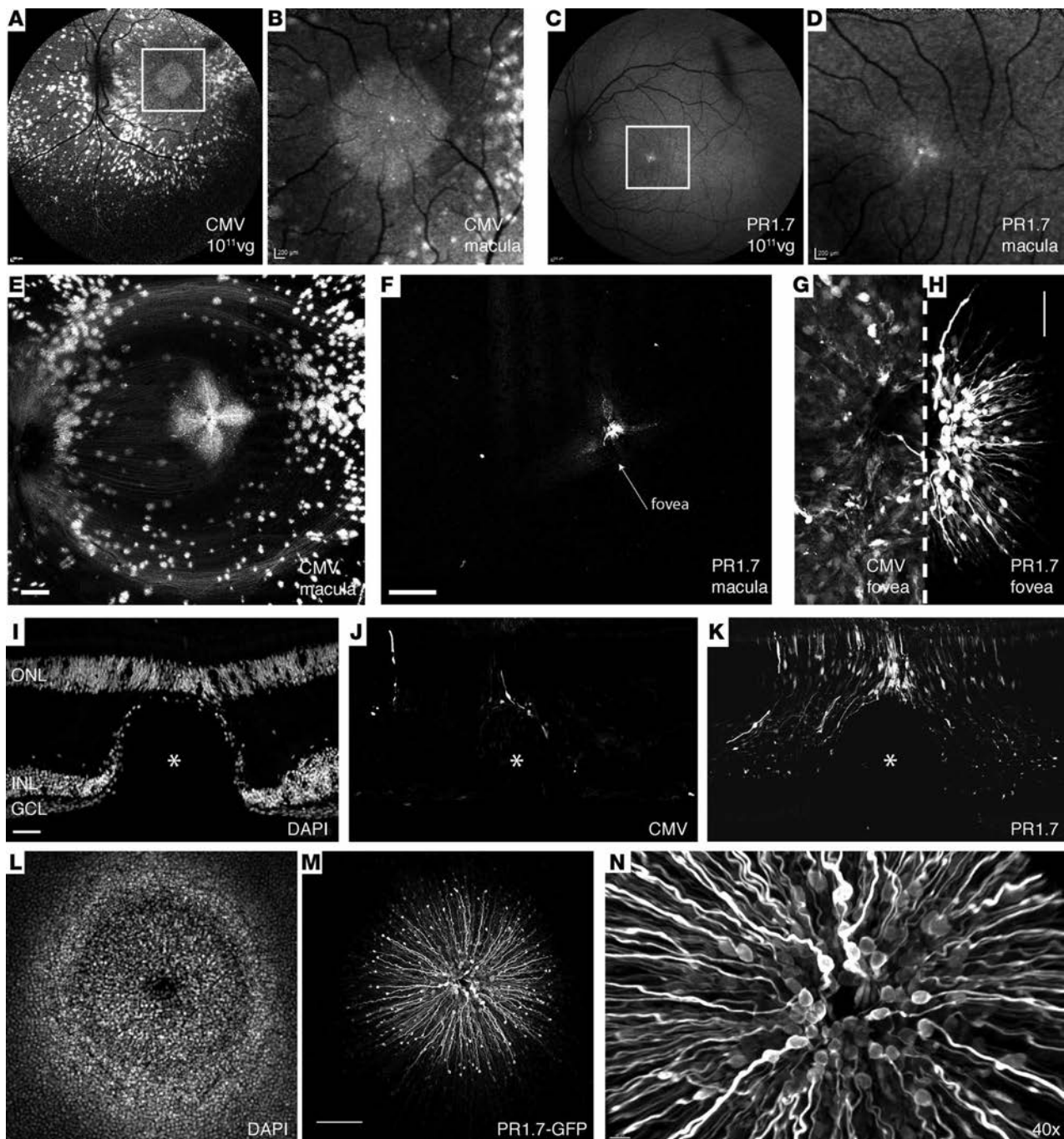


**Figure 3. Foveal cone transduction with PR1.7 promoter versus cytomegalovirus (CMV) promoter 2-3 months after intravitreal delivery of AAV2-7m8 in nonhuman primates.** Representative eye fundus images after intravitreal injection of AAV2-7m8-CMV-GFP ( $n = 2$  eyes) (A and B) or AAV2-7m8-PR1.7-GFP ( $n = 2$  eyes) (C and D) at  $1 \times 10^{11}$  viral particles per eye. B and D are inset of images shown in A and C. Scale bars: 200  $\mu\text{m}$ . Confocal images of the maculas mounted with the ganglion cell layer facing upward using CMV (E) and PR1.7 (F) promoters. Scale bars: 500  $\mu\text{m}$ . (G and H) Zoomed images of the fovea with CMV (G) and with PR1.7 (H). Scale bars: 100  $\mu\text{m}$  in G and H. (I-K) Retinal cryosections at the level of the fovea. (I) DAPI staining at the level of the fovea. Asterisk represents foveal pit. GFP expression under the control of CMV (J) or PR1.7 (K) promoters. Scale bar: 50  $\mu\text{m}$  in I, J, and K. (L-N) Confocal image projection of the whole foveal flatmount showing nuclei (L) and GFP expression in cones (M). Scale bar: 100  $\mu\text{m}$ . (N) Zoom into 3-D-reconstructed fovea seen in M with close-up to the cell bodies (facing upward). Scale bar: 10  $\mu\text{m}$ . AAV, adeno-associated virus; PR1.7, a promoter of 1.7 kilobases in length, based on the human red opsin gene enhancer and promoter sequences.

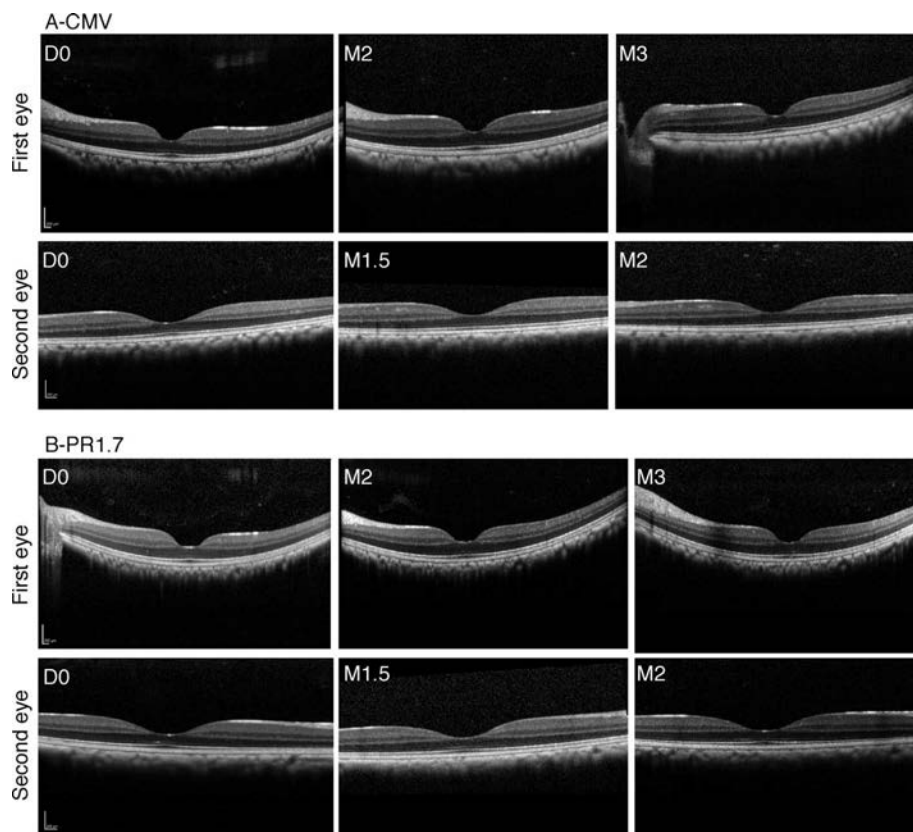


**Figure 4. Optical coherence tomography (OCT) follow-up of AAV2-7m8-CMV-GFP- and PR1.7-GFP-treated eyes.** (A) Foveal OCT images of CMV-treated eyes ( $n = 2$ ). (B) Foveal OCT images of PR1.7-treated eyes ( $n = 2$ ). D0, day of injection, predose; M1.5, -2, -3, month 1.5, 2, or 3 after dose; AAV, adeno-associated virus; CMV, cytomegalovirus promoter; PR1.7, promoter of 1.7 kilobases in length, based on the human red opsin gene enhancer and promoter sequences.

higher Jaws expression in cones transduced subretinally compared with cones transduced intravitreally. Temporal analysis using flicker stimulation at different frequencies showed very fast and robust photocurrent responses from 2 Hz up to 30 Hz at  $8 \times 10^{16}$  photons  $\text{cm}^{-2}\cdot\text{s}^{-1}$  (Figure 6L). In both cases, the light intensity response threshold was observed at around  $1 \times 10^{15}$  photons  $\text{cm}^{-2}\cdot\text{s}^{-1}$ . While recording cones in current-clamp configuration in current zero mode enables the experimenter to record the actual resting membrane potential of the cells, we observed light-elicited hyperpolarization (Figure 6, I and J), followed by short depolarization, that was more visible with subretinally injected retinas, correlating with higher expression levels of Jaws-GFP than in intravitreally injected retinas. Jaws-induced photocurrents varied in amplitude as a function of stimulation wavelength peaking at 575 nm, as expected (Figure 6K). Application of increasing stimulation frequencies showed that reliable photocurrents could be obtained with a return to baseline at up to 30 Hz, at  $8 \times 10^{16}$  photons  $\text{cm}^{-2}\cdot\text{s}^{-1}$  (Figure 6L).

*PR1.7 promoter drives strong and highly specific gene expression in human cones.* Altogether, our data in NHPs show for the first time to our knowledge noninvasive, specific, and high-level primate foveal cone transduction compatible with optogenetic applications for vision restoration. However, as promoter activity shows important variations across species (16, 29, 36), we deemed it necessary to validate PR1.7 in human cells and tissues. Due to the lack of a good human photoreceptor cell line or other model that could be used to test efficiency of cone promoter activity, we used 3-D retinal organoids derived from human induced pluripotent stem cells (iPSCs) (37). We generated photoreceptor-enriched retinal organoids and infected them with AAV2-7m8 vectors encoding GFP under the control of the PR1.7 promoter (Figure 7, A–C). GFP expression was observed as early as 5 days after infection and continued to increase until the experiment was terminated for analysis on day 43. GFP expression in these organoids colocalized with human CAR (hCAR) immunostaining (Figure 7, D–F). Lastly, as human retinal organoids do not represent all features of mature human retina, we validated the efficacy and specificity of the PR1.7 promoter in postmortem

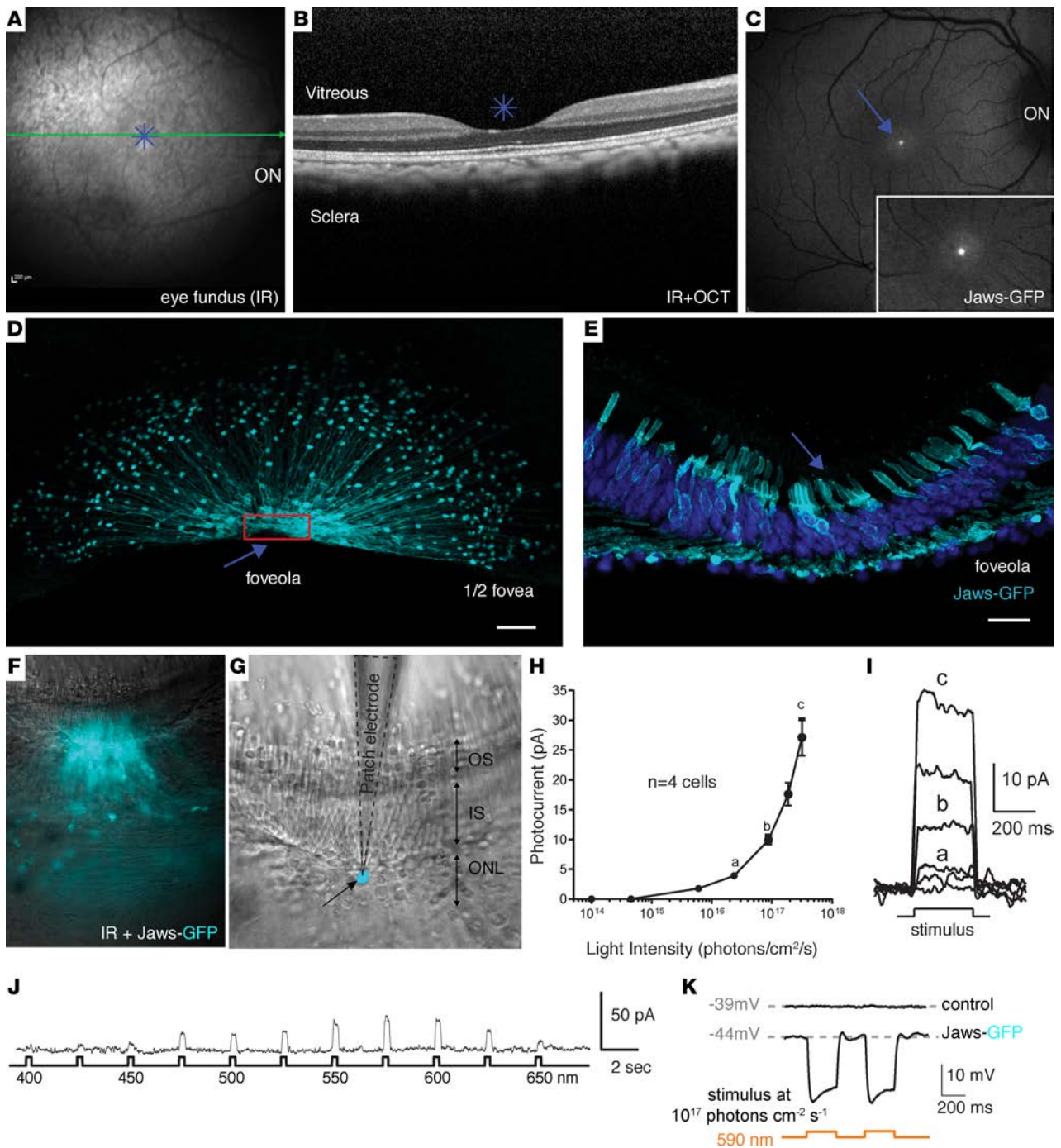


**Figure 5. Optogenetic activation of foveal cones using AAV2-7m8-PR1.7-Jaws-GFP.** (A) Infrared eye fundus image and (B) optical coherence tomography (OCT) image of the eye injected intravitreally with AAV2-7m8-PR1.7-Jaws-GFP ( $n = 1, 1 \times 10^{11}$  vg and  $n = 1, 1 \times 10^{10}$  vg). (C) Eye fundus fluorescence image 2 months after injection shows Jaws-GFP expression in the fovea. Inset magnification (B and C):  $\times 1.5$ . (D) Half foveal flatmount showing efficient and specific foveal transduction using AAV2-7m8-PR1.7-Jaws-GFP. Scale bar:  $50 \mu\text{m}$ . Arrow, foveola; red rectangle, close-up to the foveola shown in retinal sections in E; scale bar:  $20 \mu\text{m}$ . (E–K) Characteristics of the cone photoreceptor light responses triggered by optogenetic stimulation of Jaws in living macaque retinas ( $n = 4$  cells). (F) Superimposed infrared and epifluorescence images showing strong Jaws-GFP fluorescence in the foveal cones of patched explants. (G) Infrared image of the same tissue. Patch electrode (black dotted line) is shown in contact with a Jaws-GFP<sup>+</sup> cone cell body highlighted in cyan. ONL, outer nuclear layer; IS, inner segments; OS, outer segments. (H and I) Whole-cell patch clamp recordings of Jaws-GFP-expressing macaque cones. Jaws-induced photocurrents as a function of light intensity. Orange light stimulation ranged from  $1 \times 10^{14}$  to  $3 \times 10^{17}$  photons  $\text{cm}^{-2} \cdot \text{s}^{-1}$ . (J) Jaws-induced photocurrents as a function of stimulation wavelength in intravitreally injected macaque eye. Stimuli were applied from 400–650 nm, separated by 25-nm steps, at an intensity equal to  $8 \times 10^{16}$  photons  $\text{cm}^{-2} \cdot \text{s}^{-1}$ . Maximal responses were obtained at 575 nm. (K) Jaws-GFP-expressing cones recorded in current-clamp configuration in current zero mode (with their resting membrane potential indicated in gray), displaying light-elicited hyperpolarizations followed by short depolarizations. AAV, adeno-associated virus; PR1.7, promoter of 1.7 kilobases in length, based on the human red opsin gene enhancer and promoter sequences.

human retinal explants. Human retinal explants were cultured as described previously (38) and infected with a single drop of  $1 \times 10^{10}$  particles of AAV2-7m8-PR1.7-GFP (Figure 7). Fifteen days after infection, GFP expression was analyzed on cryosections. The expression was restricted to the ONL (Figure 7I) and colocalized with M/L-opsin, a cone cell marker (Figure 7J). These data collectively point toward high efficiency and specificity of PR1.7 in leading to restricted gene expression in human cones.

## Discussion

The fovea accounts for less than 1% of the retinal surface area in primates, yet it provides the input to about 50% of the cells in the primary visual cortex (1). The high concentration of cones in the fovea, the thinnest and most delicate part of the retina, allows for high-acuity vision, and it is of utmost importance to preserve the unique functions (39) and architecture (40) of the cones in this area during therapeutic interventions. Foveal cones can be targeted via different administration routes, using either subretinal or intravitreal injections (12, 16), but detaching the fovea might lead to mechanical damage, especially in the degenerating retina (12). For all of these reasons, ways to deliver therapeutics to the fovea, without detaching this region, are needed. Intravitreal injections are surgically simple ways to deliver therapeutics without retinal detachment. Gene therapy vectors can target the outer retina via intravitreal injections in rodents without damage to the photoreceptors (16, 17). However, safe and efficient gene delivery to primate cones via intravitreal injection had not been achieved so far, likely due to the substantial dilution of the vector in the vitreous and resulting loss of efficacy. The use of cell type-specific promoters that provide high-level gene expression with a lower local concentration is critical to overcome this challenge (29, 41).

In this study, we sought to first achieve strong and exclusive transduction of cones via noninvasive, intravitreal injection using various promoters in combination with AAV2-7m8 capsid. We selected 3 previously described promoters in view of their utility in driving gene expression in cones (4, 18, 19, 42, 43) and tested them for specificity and strength of cone transduction side by side. All promoters tested *in vivo* in mouse retinas led to transgene expression in the photoreceptor layer when delivered subretinally. The mCAR promoter led to expression in rods and cones. Surprisingly, after intravitreal delivery, only PR1.7 maintained its specificity toward cones, while PR2.1 and mCAR gave rise to nonspecific gene expression in inner retinal neurons. mCAR and PR2.1 gave rise to nonspecific expression in inner retinal cells, making them unsuitable for optogenetic applications where any expression in downstream neurons would cancel out the response from the photoreceptors. Subsequent *in silico* analysis of TF binding sites within each promoter sequence proposed a basis for more specific transduction with PR1.7 and the observed lack of specificity with the mCAR promoter. Next, to study the ability of AAV2-7m8 equipped with the PR1.7 promoter to transduce foveal cones, we conducted gene delivery studies in macaque eyes. Complete restriction of gene expression to primate cones was achieved using AAV2-7m8-PR1.7 in the fovea via intravitreal administration.

One shortcoming with the intravitreal injection route is the higher susceptibility of AAVs administered into this compartment to interactions with the immune system compared with subretinal administration (33). It has been shown that antibody neutralization poses a barrier to intravitreal AAV vector-mediated gene delivery in NHPs, and this will likely pose a challenge for human application. We thus aimed to develop another gene delivery approach for patients who have neutralizing antibodies toward AAV2. To this aim, we tested gene delivery to foveal cones by subretinal administration of AAV9-7m8 at a distal site (Figure 8 and Table 2). We demonstrated that robust light responses could be obtained with this new delivery approach, thanks to the vector's ability to diffuse laterally and mediate expression outside of the bleb. Using the same optogenetic cone reactivation strategy, we showed that this approach also affords robust light responses mediated by Jaws but in a higher percentage of cones compared with a intravitreal route. AAV9-7m8's behavior is similar to a previously described AAV2-derived mutant that exhibits enhanced lateral spread after subretinal injections in mouse retina (44). However, in the macaque retina, we believe that the transduction beyond the bleb with AAV9-7m8 is correlated with its increased infectivity compared with its parental serotype (17) rather than with altered binding to its primary receptor.

Our *in vivo* findings collectively point to 3 important considerations in retinal gene delivery. First, enhanced AAV vectors, whether obtained via directed evolution (AAV2-7m8; ref. 16) or rational design (AAV9-7m8; ref. 17), can achieve therapeutic objectives where parental serotypes fail to provide sufficient gene delivery. Indeed, AAV2 and AAV9 cannot perform efficient noninvasive foveal targeting

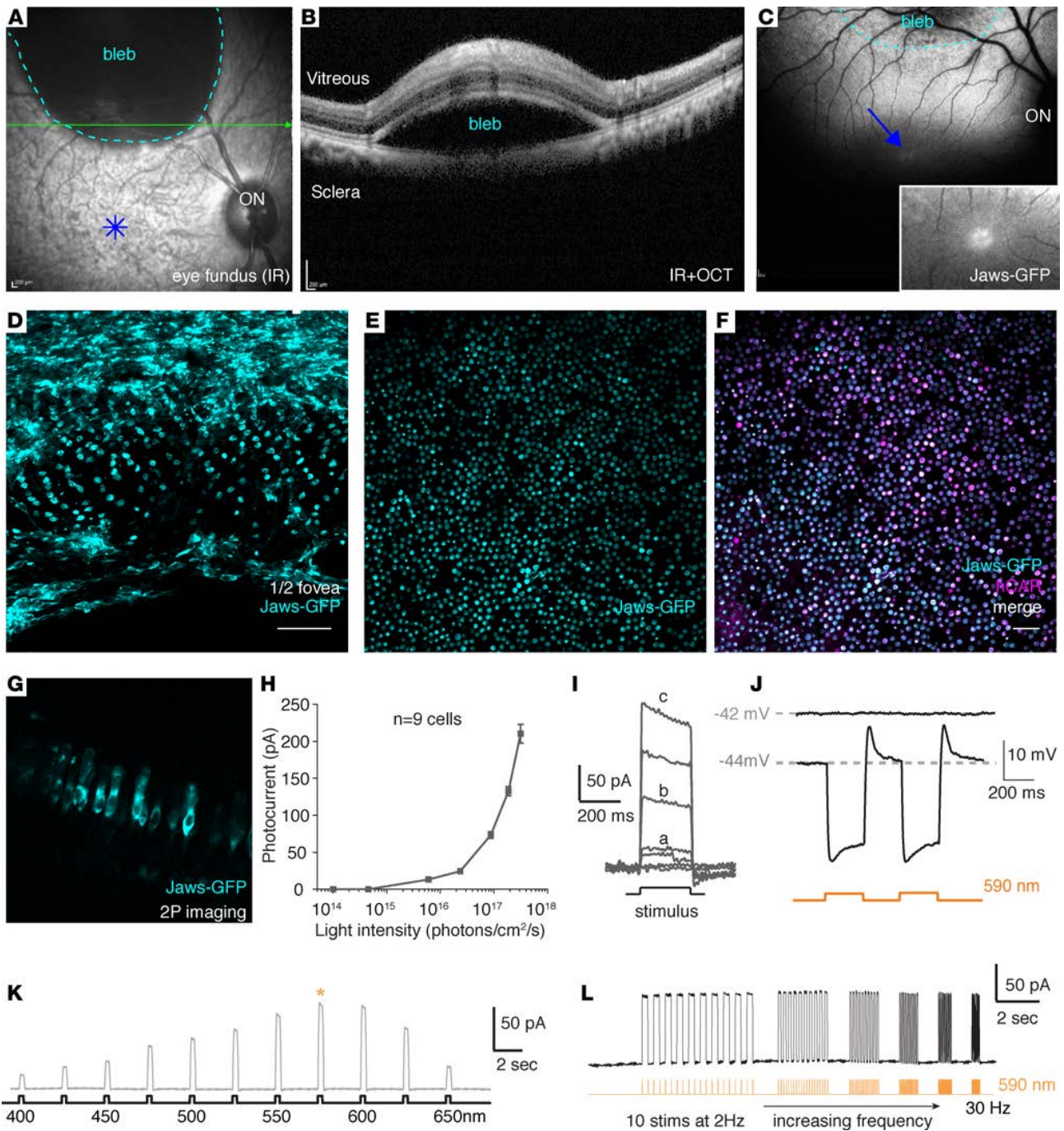


**Figure 6. AAV9-7m8 transduces the fovea via delivery in a distal bleb and provides robust optogenetic light responses with PR1.7-Jaws.** (A) Eye fundus infrared image and (B) optical coherence tomography (OCT) image immediately after subretinal delivery of AAV9-7m8 in peripheral retina. (C) Eye fundus fluorescence image 1 month after injection shows strong Jaws-GFP expression within the subretinal bleb and away from the injection site, including the fovea. Inset magnification:  $\times 1.5$ . (D–F) Foveal flatmount shows highly efficient and specific foveal transduction using subretinal AAV9-7m8-PR1.7-Jaws-GFP. Scale bar: 50  $\mu\text{m}$ . (G–L) Characteristics of the light responses triggered by optogenetic stimulation of Jaws. (G) Lateral view of Jaws-expressing cones in living tissue using 2-photon imaging. (H and I) Whole-cell patch clamp recordings of Jaws-GFP<sup>+</sup> macaque cones. Jaws-induced photocurrents as a function of light intensity. Stimuli were applied from  $1 \times 10^{14}$  to  $3 \times 10^{17}$  photons  $\text{cm}^{-2} \text{s}^{-1}$  ( $n = 9$  cells from 2 retinas of 2 animals). (J) Jaws-GFP<sup>+</sup> cones recorded in current-clamp configuration in current zero mode (with resting membrane potential indicated in gray), displaying light-elicited hyperpolarizations followed by short depolarizations. (K) Jaws-induced photocurrents as a function of stimulation wavelength in subretinally injected macaque eye. Stimuli were applied from 400–650 nm, separated by 25-nm steps, at an intensity equal to  $8 \times 10^{16}$  photons  $\text{cm}^{-2} \text{s}^{-1}$ . Maximal responses were obtained at 575 nm (asterisk). (L) Characterization of temporal properties. Modulation of Jaws-induced membrane photocurrents at increasing stimulation frequencies in Jaws-expressing macaque cones, from 2–30 Hz, at  $8 \times 10^{16}$  photons  $\text{cm}^{-2} \text{s}^{-1}$ . AAV, adeno-associated virus; PR1.7, promoter of 1.7 kilobases in length, based on the human red opsin gene enhancer and promoter sequences. IR, infrared.



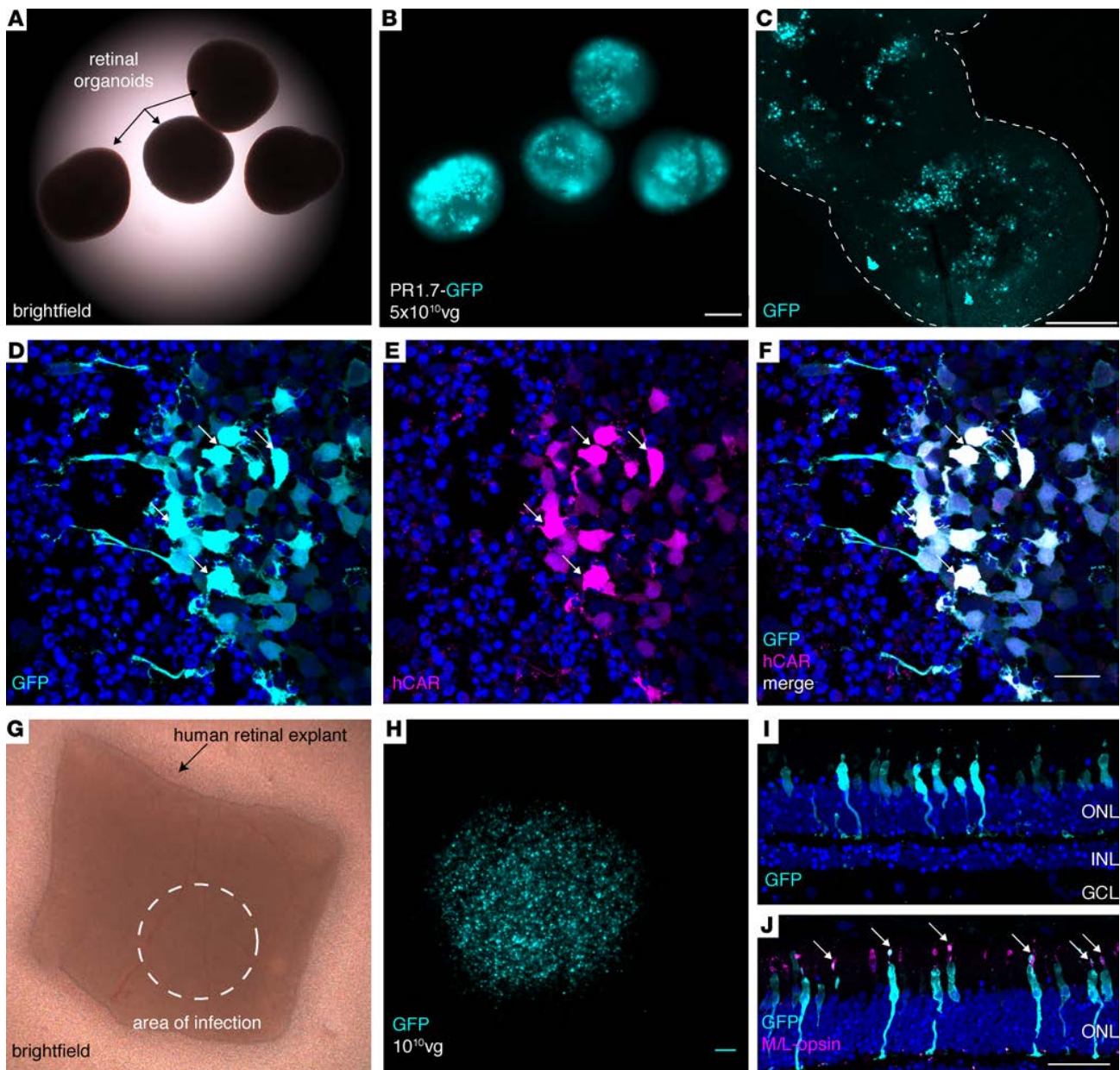


**Figure 7. Performance of AAV2-7m8-PR1.7 vector-promoter combination in human cones.** (A–C) GFP expression in human induced pluripotent stem cell-derived (iPSC-derived) retinal organoids ( $n = 10$  organoids) infected with AAV2-7m8-PR1.7-GFP. (A) Brightfield, (B) epifluorescence, and (C) confocal images of 43-day-old whole mount organoids infected with AAV2.7m8-PR1.7-GFP at day 28 with a dose of  $5 \times 10^{10}$  vg/organoid. Scale bar: 200  $\mu$ m in A and B, and 250  $\mu$ m in C. Outline in C represents the edges of the organoids (D–F) Retinal organoid cryosections for visualization of GFP expression (cyan). Transduced cones are visualized by superimposition of GFP (cyan) and human cone arrestin (hCAR) immunostaining (magenta). Scale bar: 20  $\mu$ m in D–F. Arrows represent colocalization of GFP and hCAR stainings. (G–I) Efficient and specific transduction of human cones in postmortem retinal explants. (G) Postmortem human retinal explant placed in culture. Dashed circle shows the approximate area where  $1 \times 10^{10}$  viral particles were deposited onto the explant ( $n = 2$  explants from 2 eyes of a single donor). (H) Close-up of the transduced area showing high-level GFP fluorescence in region of the explant in contact with the vector. Scale bar: 100  $\mu$ m. (I) GFP expression (cyan) is restricted to the photoreceptor layer as shown by DAPI (blue) staining. (J) GFP is expressed in cones as shown by colocalization of GFP staining of cone markers, namely M/L opsin. Scale bar: 50  $\mu$ m in I–J. Arrows represent colocalization of GFP and M/L opsin stainings. AAV, adeno-associated virus; vg, viral genome; PR1.7, promoter of 1.7 kilobases in length, based on the human red opsin gene enhancer and promoter sequences.

(30, 31) while 7m8 modified vectors bridge this gap. Second, strong cell type-specific promoters allow dose sparing (Table 3) important for the safety of gene therapy (i.e., avoiding immune response). Third, our study shows the nonnegligible impact of the vector administration route on transgene expression patterns. Finally, to complement our in vivo results in animals, we performed a battery of ex vivo tests

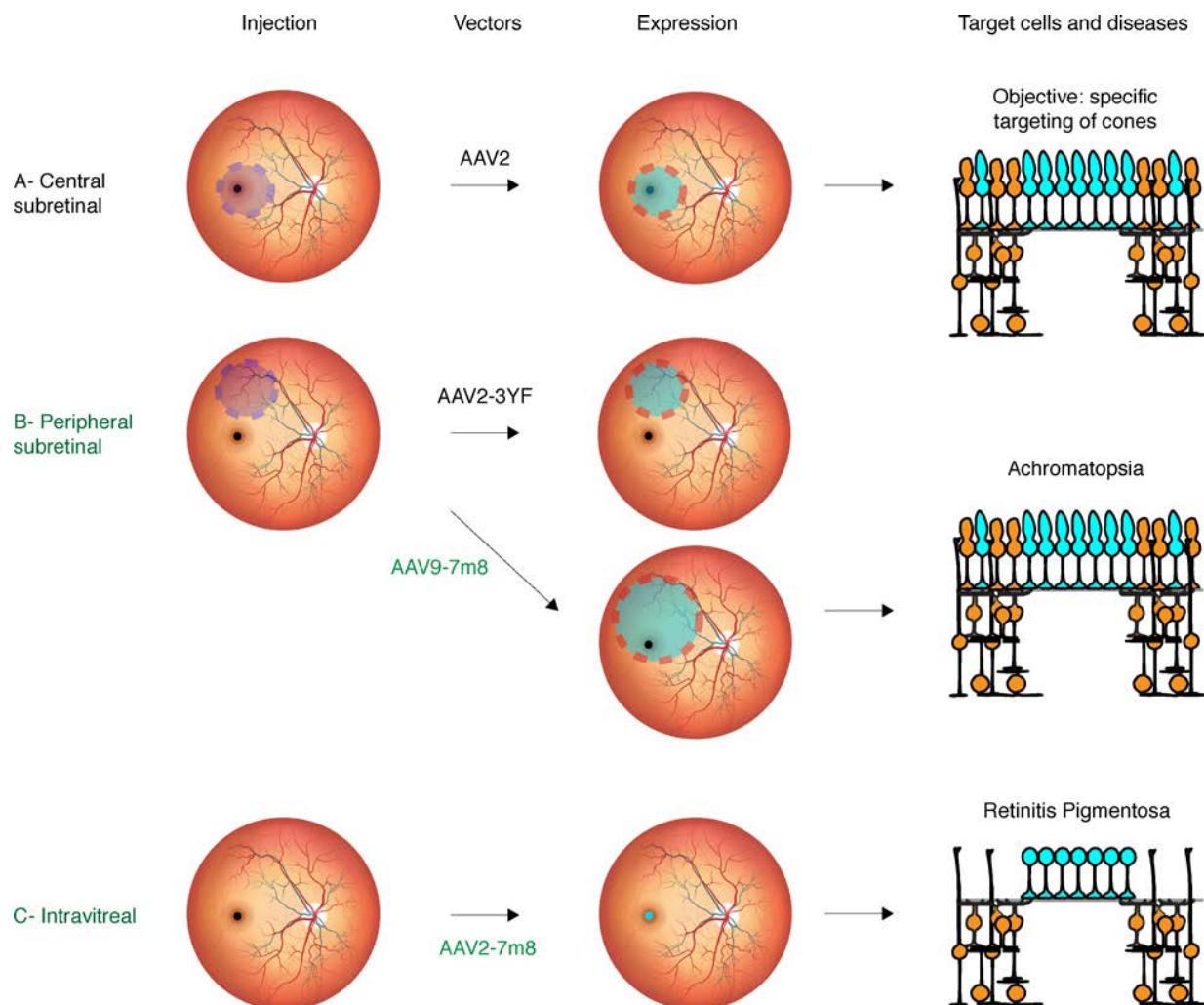


**Figure 8. Vector delivery strategies to meet therapeutic gene expression requirements.** (A) Central subretinal injection is the most risky and can be associated to adverse effects in the macula. (B) Peripheral subretinal injection using classical vectors does not reach the fovea; however, use of AAV9-7m8 is a promising strategy for achromatopsia patients. (C) Intravitreal injection is surgically simpler and the safest administration route to transduce cones of the foveola, the region responsible for high-acuity vision. It is a preferred delivery approach for retinitis pigmentosa patients to benefit from optogenetic therapy. AAV, adeno-associated virus.

in human tissues that, in combination with in vivo experiments, constitute a versatile platform for validating gene therapy for clinical application. The vector-promoter combinations described here will find utility in all retinal diseases where cone targeting is desired. Each administration route and vector can be considered based on the serological state of the patient and natural history of the targeted disease (Table 2). The combination of PR1.7 and AAV2-7m8 is ideal for therapeutic gene expression in human foveal cones when delivered into the vitreous (Figure 8) and can be an ideal way to reanimate remaining dormant cones with optogenetics in retinitis pigmentosa (4). Since cones subsist in both the center and the periphery in achromatopsia, gene delivery in the periphery using AAV9-7m8-PR1.7 can be more efficacious, as it would deliver the therapeutic gene into both the foveal and peripheral cones (Figure 8).

## Methods

**AAV production.** AAV vectors were produced as previously described using the cotransfection method and purified by iodixanol gradient ultracentrifugation (45). AAV vector stocks were titered by quantitative PCR (qPCR) (46) using SYBR Green (Thermo Fischer Scientific).

**Animals and intraocular injections.** WT C57BL6/j mice (Janvier Labs) or rd10 mice (bred and raised in the animal facility of the Vision Institute) were used for this study. For eye injections ( $n = 6$  eyes/condition),

**Table 2. Adeno-associated viral (AAV) vector administration strategies for cone-directed gene therapy in primates**

Injection route	Peripheral subretinal	Central subretinal	Peripheral subretinal (near macula)	Intravitreal
<b>Therapeutic gene expression</b>	Peripheral	Central (macula-fovea)	Peripheral and central	Central
<b>Potential capsids</b>	AAV2-3YF (18, 43) AAV9 (18, 30, 43)	AAV2 in clinical trials (7–9)	AAV9-7m8 as used in this study	AAV2 and its tyrosine mutants (7, 32) AAV2-7m8 as used in this study
<b>Advantages</b>	Immune privilege High-level therapeutic gene expression	Immune privilege High-level therapeutic gene expression Foveal transduction High-acuity vision	Immune privilege High-level therapeutic gene expression Larger expression area that includes the fovea High-acuity vision Not invasive to the fovea	Noninvasive Potential high-acuity vision Controlled area of expression pattern
<b>Disadvantages</b>	Invasive No foveal transduction Low-acuity vision	Invasive, risk of adverse effects such as macular thinning (11)		Presence of NABs in the vitreous (use of glucocorticoids could prevent antivector immune response if patient is seropositive for AAV2; ref. 50) Lower gene expression than subretinal
<b>Potential target diseases and applications</b>	Retinitis pigmentosa: optogenetic vision restoration (Jaws) (4, 15) Achromatopsia: CNGA3 or CNGB3 (43)			

NABs, neutralizing antibodies; CNGA3, cyclic nucleotide gated channel  $\alpha$  3; CNGB3: cyclic nucleotide gated channel  $\beta$  3.

6-week-old female mice were anesthetized by isoflurane inhalation. Pupils were dilated, and a 33-gauge needle was inserted into the eye to deliver 2  $\mu$ l of AAV vector solution intravitreally or 1  $\mu$ l subretinally.

Cynomolgus macaques (Noveprim, Mauritius) were first selected based on the absence of neutralizing antibody titers against AAV. Prior to surgery, they were anesthetized with an intramuscular injection of Ketamine, 10mg/kg (Imalgene 1000, Merial) and Xylazine 0.5mg/kg (Rompun 2%, Bayer). Anesthesia was maintained with an intravenous injection of propofol, 1ml/kg/h (PropoVet Multidose 10mg/ml, Zoetis). Then, their pupils were dilated and their eyelids were kept open using eyelid speculum. A 1-ml syringe equipped with a 32-mm, 27-gauge needle was used for intravitreal injections. The needle was inserted into the sclera approximately 2 mm posterior to the limbus to deliver 100  $\mu$ l of the viral vector solution. Finally, the needle was slowly removed. Animals did not receive local corticosteroid injections.

For subretinal AAV injections, two 25-gauge vitrectomy ports were set approximately 2 mm posterior to the limbus, one for the endo-illumination probe and the other for the subretinal cannula. A 1-ml Hamilton syringe equipped with a 25-gauge subretinal cannula with a 41-gauge tip was used for the injection. The endoillumination probe and cannula were introduced into the eye. The viral vector solution (50  $\mu$ l) was

**Table 3. Summary of studies involving intravitreal injections with the objective of targeting photoreceptors in primates**

AAV and expression cassette	Dose (vg/eye)	Results	References
AAV2-7m8-CMV-GFP	$5 \times 10^{12}$ vg	Transduction of photoreceptors	16
AAV2-7m8-CMV/CBA-GFP	$1 \times 10^{12}$ vg	Transduction of photoreceptors	29
AAV2-CBA-GFP	$4.5 \times 10^{10}$ vg	Transduction of photoreceptors in the injected area. AAV injections were under the ILM (referred to as subILM injections).	32
AAV2-3YF-CBA-GFP	$9.5 \times 10^{11}$ vg	Transduction of PRs in the ILM peeled area, following vitrectomy and surgical ILM peeling. AAV injections were done 1 month after surgery.	51
AAV2-7m8-PR1.7-GFP	$1 \times 10^{11}$ vg and $1 \times 10^{10}$ vg	Specific transduction of cone photoreceptors	Present study

AAV, adeno-associated virus; CMV, cytomegalovirus promoter; CBA, chicken  $\beta$ -actin promoter; CMV/CBA, hybrid promoter composed of CMV enhancer and CBA promoter; PR1.7, Promoter 1.7 kilobases based on human red opsin gene enhancer and promoter sequences; ILM, inner limiting membrane; vg, viral genome; PRs: photoreceptors.

injected subretinally to create a bleb either below or above the fovea. The instruments were then withdrawn. Eyes received corticosteroid treatment (47) that consisted of a laterobulbar injection of 12 mg of Kenacort (Bristol-Myers Squibb) except right eye of NHP5.

After subretinal or intravitreal vector administration, ophthalmic steroid and antibiotic ointments (Fradexam, TVM) were applied to the corneas after injections.

*In vivo macaque eye imaging.* After pupil dilation, a Spectralis HRA+OCT system (Heidelberg Engineering) was used to acquire OCT images and fluorescent images of GFP using the Fundus Autofluorescence mode (excitation wavelength of 488 nm and barrier filter of 500 nm).

*Two-photon imaging and ex vivo electrophysiological recordings of macaque retinas.* A 2-photon microscope equipped with a 40× water immersion objective (LUMPLFLN40×/W/0.80, Olympus) with a pulsed femto-second laser (InSight DeepSee, Newport Corporation) was used for imaging GFP<sup>+</sup> retinal cells from whole-mount retinas (with photoreceptor cell side up) or retina slices (vertical sections). AAV-treated macaque retinas were isolated and later imaged in oxygenized (95% O<sub>2</sub>, 5% CO<sub>2</sub>) Ames medium (MilliporeSigma). For live 2-photon imaging, retinas were placed in the recording chamber of the microscope, and Z-stacks were acquired using the excitation laser at a wavelength of 930 nm. Images were processed offline using ImageJ (NIH). For whole-cell patch-clamp recordings, an Axon Multiclamp 700B amplifier was used. Electrodes were made from borosilicate glass (BF100-50-10, Sutter Instruments) and pulled to 6–9 MΩ. Pipettes were filled with 115 mM K gluconate, 10 mM KCl, 1 mM MgCl<sub>2</sub>, 0.5 mM CaCl<sub>2</sub>, 1.5 mM EGTA, 10 mM HEPES, and 4 mM ATP-Na<sub>2</sub> (pH 7.2). Cells were clamped at a potential of –40 mV in voltage-clamp configuration or recorded in current-clamp (current 0) configuration. Retinas were dark-adapted at least 30 minutes in the recording chamber prior to recordings.

*Human iPSC cultures.* We have generated retinal organoids from human iPSCs based on a previously published protocol (37). Clone hiPSC-2 was expanded and differentiated on fibroblast feeders from postnatal human foreskins (ATCC CRL 2429) in proneural medium, as already described (37). Starting from highly confluent adherent iPSC cultures and in the absence of fibroblast growth factor 2 (FGF2), self-forming retinal organoids can be identified after 2 weeks. At this point, the organoids were mechanically isolated and cultured in 3-D conditions for up to 43 days. FGF2 was supplemented to the medium in 3 conditions for 7 days after the mechanical isolation of the organoids to promote their growth. The retinal organoids were infected at day 28 of differentiation at a dose of  $5 \times 10^{10}$  vg/organoid with AAV2-7m8 vectors carrying the GFP gene under the control of the PR1.7 promoter. DAPT (10 μM; Selleck) was added to the medium for a week from day 28 on to promote cell cycle arrest of the existent cell populations. Fluorescence intensity was observed for the first time 5 days after infection and continued to increase up to day 43.

*Human postmortem retinal explants.* Human retinal explants were prepared using a previously described protocol (38). Briefly, eyes were dissected in CO<sub>2</sub> independent medium (Thermo Fischer Scientific). The anterior parts were removed, and retina was isolated and cut into small pieces. These explants were placed photoreceptor side-up on a Transwell cell culture insert (Corning), and 2 ml of neurobasal medium (Thermo Fischer Scientific) supplemented with B27 (Thermo Fischer Scientific) were added to each well below each explant. The following day, each explant was infected with a single 0.5-μl drop of AAV2-7m8-PR1.7-GFP containing  $1 \times 10^{10}$  viral particles. Vector-infected explants were incubated for 10–15 days to allow GFP expression, which was checked using an epifluorescence microscope.

*Histology, IHC, and microscopy.* Mouse eyes were enucleated and immediately fixed in 10% formalin and 4% formaldehyde (Sigma) for 2 hours for cryosections. Macaque retinas were fixed after dissection in 4% formaldehyde (Sigma) for 3 hours. Retinal organoids and human retinal explants were rinsed in PBS at the end of their culture periods and fixed in 4% paraformaldehyde for 10 minutes. For cryosections, mouse and macaque retinas, retinal organoids, and human retinal explants were immersed in PBS-30% sucrose (Sigma) overnight at 4°C. Mouse eye cups, human retinal explants, and macaque retinas were embedded optimal cutting temperature compound (Microm Microtech France) compound and frozen in liquid nitrogen, while retinal organoids were embedded in 7.5% gelatin (Sigma) and 10% sucrose (Sigma) in PBS and frozen in dry ice-cold isopentane (Merck Millipore). Vertical sections (10 μm-thick) were cut with a Microm cryostat. After incubation in the blocking buffer, sections were incubated with primary antibodies overnight at 4°C: hCAR antibody (gift from Cheryl Craft, University of Southern California, Los Angeles, USA), M/L opsin antibody (Merck Millipore, AB5405), and mouse cone arrestin antibody (Merck Millipore, AB15282). After multiple washes of the sections, the secondary antibody Alexa Fluor 594 (A10040, Thermo Fischer Scientific)

ic) and DAPI were added, followed by several washes. Retinal flatmounts or cryosections were mounted in Vectashield mounting medium (Vector Laboratories) for fluorescence microscopy, and retinal sections were visualized using an Olympus Upright confocal microscope and then analyzed with Fiji software. Three-dimensional projections of the fovea were created with Imaris software (Bitplane).

*In silico identification of potential regulatory elements and transcriptomic analysis.* TF binding site analysis was performed on red opsin gene promoter sequence — PR2.1 and PR1.7 sequences — and the cone arrestin 3 genomic region. The TRANSFAC database 8.3 (<http://alggen.lsi.upc.es/>) was used for TF binding site prediction. Each TF from the predicted list was analyzed using the Knowledge Base for Sensory System (KBaSS, <http://kbass.institut-vision.org/KBaSS/transcriptomics/index.php>) to select those expressed in human retina using the transcriptomic experiment RNG209 (48). A filter was used to retain TFs with a signal intensity value superior to 40 units in the sample prepared from the experiment RNG209 after normalization by robust multi-array average (RMA) as previously described (49). In this experiment, human retinal specimens used as controls were postmortem specimens collected within 12 hours following death of patients with no past medical history of eye disease or diabetes. Nineteen samples were collected from 19 eyes, representing 17 patients. Sex ratio was 12 men/7 women with a mean age of 61 years (range 25–78 years).

*Statistics.* Data were analyzed using ANOVA test in Graphpad Prism (multiple comparison, Tukey correction). Error bars on the graphs show the  $\pm$  SEM.  $P < 0.033$  was considered significant.

*Study approval.* For animals, the experiments were realized in accordance with the NIH *Guide for Care and Use of Laboratory Animals* (National Academies Press, 2011). The protocols were approved by the Local Animal Ethics Committees and conducted in accordance with Directive 2010/63/EU of the European Parliament.

Postmortem human ocular globes from donors were acquired from the School of Surgery (Ecole de Chirurgie, Assistance Publique Hôpitaux de Paris, Paris, France). The protocol was approved by the IRBs of the School of Surgery and the Quinze-Vingts National Ophthalmology Hospital (Paris, France). All experiments on postmortem human retinal explants were performed according to the local regulations, as well as the guidelines of the Declaration of Helsinki.

### Author contributions

HK, MGH, and DD designed experiments. HK, CW, and MD generated plasmid constructs used in the study. HK performed all surgical procedures on mice. MD optimized neutralizing antibody detection protocol. SB performed surgical procedures on macaques. CJ and EB performed macaque eye imaging and ophthalmic examinations. MGH prepared human iPSC-derived retinal organoids and optimized their AAV-mediated infection and characterization. AC performed patch-clamp recordings in macaque retinal explants. SR analyzed promoter sequences and provided lists of TF binding sites. HK, SR, and MGH analyzed these data. HK and VF prepared postmortem macaque and human retinal explants. HK performed histology and imaging on mouse, macaque, and human tissue. HK and DD designed the study and wrote the manuscript. HK prepared the figures and tables. OG, SP, JD, and JAS provided scientific input and gave feedback on the manuscript.

### Acknowledgments

This study was supported by The Foundation Fighting Blindness (Wynn-Gund translational research award), AFM-Téléthon (Young Researcher PhD Fellowship to HK), Marie Curie CIG (334130, RETINAL GENE THERAPY), INSERM, Labex-Lifesenses (ANR-10-LABX-65), the Agence Nationale pour la Recherche - Recherche Hospitalo-Universitaire en santé (RHU) (Light4Deaf), Fondation NRJ and ERC StGs (OPTOGENRET and REGENETHER). We thank Emilie kéomani and Camille Robert for assistance with the production of AAV vectors, Amélie Slembrouck and Laure Guibbal for assistance on hiPSC maintenance, Estelle Dias and Marie-Laure Niepon (Histology Platform) for assistance on retinal cryosections. We also thank Claire-Maëlle Fovet and Joanna Demilly for technical assistance on the MIRCEN NHP platform, Stéphane Fouquet for technical assistance on the Imaging Platform of the Vision Institute and Laure Pacot for help with cell counting on confocal images. We are thankful to Thierry Léveillard for access to the human retinal transcriptomics data in the KBaSS.

Address correspondence to: Deniz Dalkara, Vision Institute, 17 rue Moreau, Paris, 75012, France. Phone: 33153462532; Email: [deniz.dalkara@gmail.com](mailto:deniz.dalkara@gmail.com).

1. Wässle H, Grünert U, Röhrenbeck J, Boycott BB. Cortical magnification factor and the ganglion cell density of the primate retina. *Nature*. 1989;341(6243):643–646.
2. Kolb H, Zhang L, Dekorver L, Cuenca N. A new look at calretinin-immunoreactive amacrine cell types in the monkey retina. *J Comp Neurol*. 2002;453(2):168–184.
3. Wikler KC, Williams RW, Rakic P. Photoreceptor mosaic: number and distribution of rods and cones in the rhesus monkey retina. *J Comp Neurol*. 1990;297(4):499–508.
4. Busskamp V, et al. Genetic reactivation of cone photoreceptors restores visual responses in retinitis pigmentosa. *Science*. 2010;329(5990):413–417.
5. Byrne LC, et al. Viral-mediated RdCVF and RdCVFL expression protects cone and rod photoreceptors in retinal degeneration. *J Clin Invest*. 2015;125(1):105–116.
6. Komáromy AM, et al. Gene therapy rescues cone function in congenital achromatopsia. *Hum Mol Genet*. 2010;19(13):2581–2593.
7. Maguire AM, et al. Safety and efficacy of gene transfer for Leber's congenital amaurosis. *N Engl J Med*. 2008;358(21):2240–2248.
8. Bainbridge JW, et al. Effect of gene therapy on visual function in Leber's congenital amaurosis. *N Engl J Med*. 2008;358(21):2231–2239.
9. Cideciyan AV, et al. Human gene therapy for RPE65 isomerase deficiency activates the retinoid cycle of vision but with slow rod kinetics. *Proc Natl Acad Sci USA*. 2008;105(39):15112–15117.
10. Bainbridge JW, et al. Long-term effect of gene therapy on Leber's congenital amaurosis. *N Engl J Med*. 2015;372(20):1887–1897.
11. Jacobson SG, et al. Improvement and decline in vision with gene therapy in childhood blindness. *N Engl J Med*. 2015;372(20):1920–1926.
12. Jacobson SG, et al. Gene therapy for leber congenital amaurosis caused by RPE65 mutations: safety and efficacy in 15 children and adults followed up to 3 years. *Arch Ophthalmol*. 2012;130(1):9–24.
13. MacLaren RE, et al. Retinal gene therapy in patients with choroideremia: initial findings from a phase 1/2 clinical trial. *Lancet*. 2014;383(9923):1129–1137.
14. Duncan JL. Visual Consequences of Delivering Therapies to the Subretinal Space. *JAMA Ophthalmol*. 2017;135(3):242–243.
15. Chuong AS, et al. Noninvasive optical inhibition with a red-shifted microbial rhodopsin. *Nat Neurosci*. 2014;17(8):1123–1129.
16. Dalkara D, et al. In vivo-directed evolution of a new adeno-associated virus for therapeutic outer retinal gene delivery from the vitreous. *Sci Transl Med*. 2013;5(189):189ra76.
17. Khabou H, et al. Insight into the mechanisms of enhanced retinal transduction by the engineered AAV2 capsid variant -7m8. *Biotechnol Bioeng*. 2016;113(12):2712–2724.
18. Ye GJ, et al. Cone-Specific Promoters for Gene Therapy of Achromatopsia and Other Retinal Diseases. *Hum Gene Ther*. 2016;27(1):72–82.
19. Ye GJ, et al. Safety and Biodistribution Evaluation in CNGB3-Deficient Mice of rAAV2tYF-PR1.7-hCNGB3, a Recombinant AAV Vector for Treatment of Achromatopsia. *Hum Gene Ther Clin Dev*. 2016;27(1):27–36.
20. Kolstad KD, et al. Changes in adeno-associated virus-mediated gene delivery in retinal degeneration. *Hum Gene Ther*. 2010;21(5):571–578.
21. Vacca O, et al. AAV-mediated gene delivery in Dp71-null mouse model with compromised barriers. *Glia*. 2014;62(3):468–476.
22. Satoh S, et al. The spatial patterning of mouse cone opsin expression is regulated by bone morphogenetic protein signaling through downstream effector COUP-TF nuclear receptors. *J Neurosci*. 2009;29(40):12401–12411.
23. Pickrell SW, Zhu X, Wang X, Craft CM. Deciphering the contribution of known cis-elements in the mouse cone arrestin gene to its cone-specific expression. *Invest Ophthalmol Vis Sci*. 2004;45(11):3877–3884.
24. von Mering C, et al. STRING 7—recent developments in the integration and prediction of protein interactions. *Nucleic Acids Res*. 2007;35(Database issue):D358–D362.
25. Blazek E, Mittler G, Meisterernst M. The mediator of RNA polymerase II. *Chromosoma*. 2005;113(8):399–408.
26. Bourbon HM, et al. A unified nomenclature for protein subunits of mediator complexes linking transcriptional regulators to RNA polymerase II. *Mol Cell*. 2004;14(5):553–557.
27. Yuan CX, Ito M, Fondell JD, Fu ZY, Roeder RG. The TRAP220 component of a thyroid hormone receptor-associated protein (TRAP) coactivator complex interacts directly with nuclear receptors in a ligand-dependent fashion. *Proc Natl Acad Sci USA*. 1998;95(14):7939–7944.
28. Viets K, Eldred K, Johnston RJ. Mechanisms of Photoreceptor Patterning in Vertebrates and Invertebrates. *Trends Genet*. 2016;32(10):638–659.
29. Ramachandran PS, et al. Evaluation of Dose and Safety of AAV7m8 and AAV8BP2 in the Non-Human Primate Retina. *Hum Gene Ther*. 2017;28(2):154–167.
30. Vandenberghe LH, et al. AAV9 targets cone photoreceptors in the nonhuman primate retina. *PLoS ONE*. 2013;8(1):e53463.
31. Vandenberghe LH, et al. Dosage thresholds for AAV2 and AAV8 photoreceptor gene therapy in monkey. *Sci Transl Med*. 2011;3(88):88ra54.
32. Boye SE, et al. Highly Efficient Delivery of Adeno-Associated Viral Vectors to the Primate Retina. *Hum Gene Ther*. 2016;27(8):580–597.
33. Kotterman MA, Yin L, Strazzeri JM, Flannery JG, Merigan WH, Schaffer DV. Antibody neutralization poses a barrier to intravitreal adeno-associated viral vector gene delivery to non-human primates. *Gene Ther*. 2015;22(2):116–126.
34. Sengupta A, et al. Red-shifted channelrhodopsin stimulation restores light responses in blind mice, macaque retina, and human retina. *EMBO Mol Med*. 2016;8(11):1248–1264.
35. Bell CL, Gurda BL, Van Vliet K, Agbandje-McKenna M, Wilson JM. Identification of the galactose binding domain of the adeno-associated virus serotype 9 capsid. *J Virol*. 2012;86(13):7326–7333.
36. Yin L, et al. Intravitreal injection of AAV2 transduces macaque inner retina. *Invest Ophthalmol Vis Sci*. 2011;52(5):2775–2783.
37. Reichman S, et al. From confluent human iPSCs to self-forming neural retina and retinal pigmented epithelium. *Proc Natl Acad Sci USA*. 2014;111(23):8518–8523.
38. Fradot M, et al. Gene therapy in ophthalmology: validation on cultured retinal cells and explants from postmortem human eyes. *Hum Gene Ther*. 2011;22(5):587–593.

39. Sinha R, Hoon M, Baudin J, Okawa H, Wong RO, Rieke F. Cellular and Circuit Mechanisms Shaping the Perceptual Properties of the Primate Fovea. *Cell*. 2017;168(3):413–426.e12.
40. Anderson DH, Fisher SK. The relationship of primate foveal cones to the pigment epithelium. *J Ultrastruct Res*. 1979;67(1):23–32.
41. Tenenbaum L, Lehtonen E, Monahan PE. Evaluation of risks related to the use of adeno-associated virus-based vectors. *Curr Gene Ther*. 2003;3(6):545–565.
42. Boyd RF, et al. Photoreceptor-targeted gene delivery using intravitreally administered AAV vectors in dogs. *Gene Ther*. 2016;23(2):223–230.
43. Ye GJ, et al. Safety and Biodistribution Evaluation in Cynomolgus Macaques of rAAV2tYF-PR1.7-hCNGB3, a Recombinant AAV Vector for Treatment of Achromatopsia. *Hum Gene Ther Clin Dev*. 2016;27(1):37–48.
44. Boye SL, et al. Impact of Heparan Sulfate Binding on Transduction of Retina by Recombinant Adeno-Associated Virus Vectors. *J Virol*. 2016;90(8):4215–4231.
45. Choi VW, Asokan A, Haberman RA, Samulski RJ. Production of recombinant adeno-associated viral vectors. *Curr Protoc Hum Genet*. 2007;Chapter 12:Unit 12.9.
46. Aurnhammer C, et al. Universal real-time PCR for the detection and quantification of adeno-associated virus serotype 2-derived inverted terminal repeat sequences. *Hum Gene Ther Methods*. 2012;23(1):18–28.
47. Reichel FF, et al. AAV8 Can Induce Innate and Adaptive Immune Response in the Primate Eye. *Mol Ther*. 2017;25(12):2648–2660.
48. Delyfer MN, et al. Transcriptomic analysis of human retinal detachment reveals both inflammatory response and photoreceptor death. *PLoS One*. 2011;6(12):e28791.
49. Reichman S, et al. The homeobox gene CHX10/VSX2 regulates RdCVF promoter activity in the inner retina. *Hum Mol Genet*. 2010;19(2):250–261.
50. Gernoux G, Wilson JM, Mueller C. Regulatory and Exhausted T Cell Responses to AAV Capsid. *Hum Gene Ther*. 2017;28(4):338–349.
51. Takahashi K, et al. Improved Intravitreal AAV-Mediated Inner Retinal Gene Transduction after Surgical Internal Limiting Membrane Peeling in Cynomolgus Monkeys. *Mol Ther*. 2017;25(1):296–302.





## IV. Combined gene therapies for longer lasting vision restoration

Today, one objective of retinal gene therapy is to obtain and enhance treatment longevity (60), to give patients sight as long as possible. In a similar way, it is primordial for sight restoration to be effective over the life-span of the patients. Here we build on the past work done on optogenetic reanimation of foveal cones using microbial opsins but wish to synergize this therapy with the addition of a survival factor in hopes of restoring and maintaining vision in future clinical applications.

### iii. Aims and methodology

The ultimate goal of my PhD project is to design a long-lasting gene therapy for rod-cone dystrophies such as RP. Indeed, we have evidence from the literature (167) and a preliminary clinical study done at our CIC suggesting that 17% of RP patients have dormant cones remaining in their fovea (168). This significant proportion of RP patients could be treated with the gene therapy strategy presented in the previous chapter, using Jaws to restore vision in dormant cones and we have optimized all parameters to enable this (see previous chapter). Combining it with a neuroprotective treatment would increase its longevity helping maintain cone cell bodies. Indeed, without survival factors it is uncertain how long the reanimated cones can be maintained in degenerating retinas. The aim of this work was to prove that optogenetics and survival factors could be co-expressed and help get longer-term vision restoration than either treatment alone in RP.

Among different trophic factors that can provide neuroprotection and thereby increase photoreceptor survival, RdCVF is the most relevant for the particular preservation of cones (47). RdCVF slows down the loss of cones after rod cell death when administered as a protein (46), or using AAV-mediated gene delivery in mice (49). Although therapeutic outcomes have been achieved using both the optogenetic vision restoration and RdCVF secretion, the combination of both treatments has not been attempted so far. In my thesis I explored the possibility of combining these mutation independent gene therapies, which turned out to be very challenging. I faced several technical issues, in addition to the difficulties related to proving vision restoration at late disease stages. These technical issues gave rise to interesting research axes that I decided to investigate, although during my PhD I could not complete the work on the combination approach using RdCVF and optogenetics. Nevertheless, I summarize the results I was able to obtain in going towards this goal over the course of several years.

The first aim was to co-express RdCVF and Jaws in the rd10 mouse model of RP. This mouse model is characterized by milder retinal degeneration than the rd1, thereby allowing neuroprotection studies. I first asked how to simultaneously deliver two gene products to the mouse retina and which AAVs should be used?

The first possibility was to combine an early systemic injection of AAV9.2YF-CAG-RdCVF (49), and a later subretinal injection of AAV8-mCAR-Jaws (89, 169), as previously used. As the subretinal injection can lead to complications such as PR damage or subretinal blood (120) –which would decrease benefits from RdCVF, I first focused on the intravitreal injection.

AAV2-7m8– in combination with either a ubiquitous CAG promoter to secrete RdCVF in the retina or a cone-specific promoter to express Jaws in cones could be used. I chose this approach as AAV2-7m8 is compatible with a noninvasive administration route, and is therefore clinically relevant. However, intravitreal injection is not relevant for RdCVF expression in light-reared rd10 mice as the degeneration occurs too quickly to obtain a therapeutic effect. Indeed, it requires 8 weeks to obtain peak transgene expression in all retinal layers with lower expression levels than with SR injection. Given that the rd10 retina degenerates rapidly and the peak cone degeneration occurs at 8 weeks of age, RdCVF expression would not be optimal when using this vector. This is why RdCVF was delivered intravitreally in dark-reared rd10 mice (49) as it has been shown to delay vision loss, and I could not obtain vision improvements in the light-reared rd10 mice. I went back to systemic delivery of AAV-RdCVF.

However, AAV2-7m8 is still potentially compatible with Jaws expression. I first combined it with mCAR promoter as it has been used in previous restorative approach papers, subretinally with AAV8, the best capsid for mouse cone targeting (88, 89). Surprisingly, AAV2-7m8 vector combined with mCAR promoter and an intravitreal injection, led to high-level expression in rods, and we also obtained undesired expression in ganglion cells and other inner retinal neurons using this leaky promoter. This is problematic for vision restoration, because many off-target cells can be activated (hyperpolarization of rods) or inhibited (depolarization of ganglion cells) at the same time upon light stimulation of Jaws, and cancel out retinal output. As a consequence, I went back to the subretinal injection with AAV8 combined with the mCAR promoter. But at the same time, I kept looking for a promoter compatible with cone-specific expression. PR1.7 promoter was described some time later allowing us to target specifically cones. This gave rise to my paper published in JCI Insight and presented in the Chapter 3 of the Results section. I am now using this promoter to express Jaws in cones via an intravitreal injection in blind rd10 mice.

Under mCAR promoter and AAV8 combined conditions, Jaws expression was high and only in photoreceptors, but the subretinal injection of a control vector encoding GFP induced a strong deleterious ERG amplitude decrease. I first hypothesized that my observations were due to unsuccessful subretinal injections leading to damaging retinal detachments. To test this, I compared uninjected wt animals with PBS-injected wt mice (to

eliminate any effect due to disease and study the effect of the vectors themselves) and found no differences in ERG amplitudes between the two conditions, thereby excluding this hypothesis. My second hypothesis was that GFP expression was too high, leading to toxicity to retinal cells. I showed later indeed an unwanted death of retinal neurons in treated retinas because of high-injected doses. I thus optimized my gene therapy conditions by reducing injected doses and looked for the reasons underlying this toxicity, resulting in the manuscript presented in the Chapter I of the Results section.

The results I obtained towards combined RdCVF and Jaws expression after fixing these conditions are described below.

#### iv. Evaluation of the therapeutic benefits of RdCVF *in vivo*

It has been previously shown that RdCVF delays cone-mediated vision loss, by preserving cone photoreceptors (46). This result was supported by ERG measurements (49) as well as cone cell counting in different mouse models, but no behavioral tests had been done to support this result so far. The mechanisms by which this occurs, likely is maintenance of overall cone health and outer segment metabolism and renewal (48).

Therefore, I first evaluated the therapeutic benefits of RdCVF using the optokinetics reflex of treated and control rd10 mice in photopic conditions at one month of age. This test allows measurement of the visual acuity and is a highly relevant way to assess the extent of cone-mediated vision restoration. I showed here strongly significant vision improvements with RdCVF in rd10 mice (Figure 35), confirming previous ERG data (49), after delivery of AAV9-2YF-CAG-RdCVF using intracardiac injections (48).

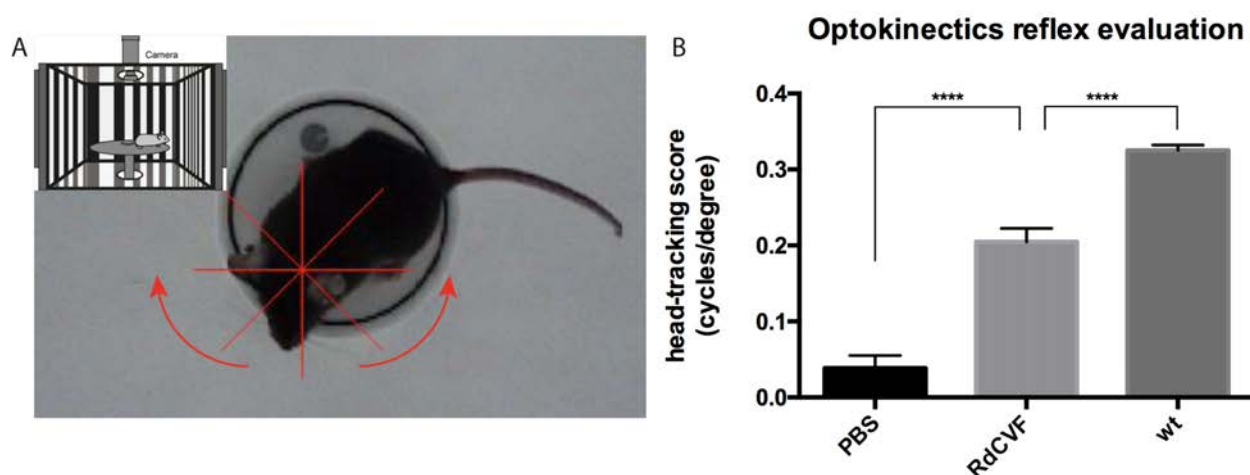


**Figure 35: Optokinetics reflex is improved after early AAV-RdCVF administration in rd10 pups. (A)** Schematic representation of the setup used for analysis of the optokinetic reflex. **(B)** Quantification of the visual improvements at one month of age after systemic injection of AAV9-2YF-scCAG-RdCVF. Data were analyzed using a Student *t*-test. *p* values are expressed as the following \*\*\*\**P*<0.0001. Errors bars show mean ±SEM. A total number of 23 animals was analyzed: *n*=10 for AAV-scCAG-RdCVF injected animals, *n*=8 for PBS condition and *n*=5 for wt C57BL6/J mice.

Then I counted the number of cones 1 year after injection on n=4 animals (8 retinas/condition) per condition. Although these data need to be confirmed on a larger number of animals given the variability between animals, they show no significant difference between RdCVF and control groups (Figure 36), i.e. no benefits on cone cell body preservation in the long-term.

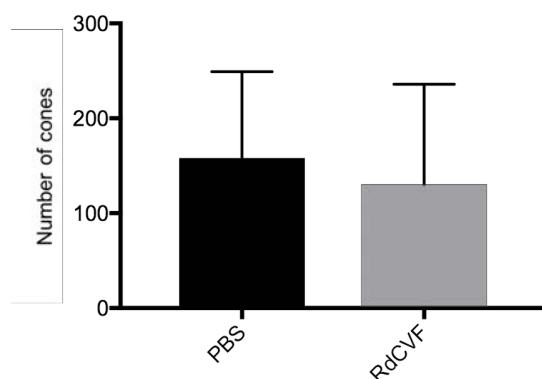


**Figure 36: Effect of RdCVF on cones in the long-term.** Retinas from animals treated with PBS or AAV9-2YF-CAG-RdCVF were harvested 1 year after injections. The number of cones (cone arrestin-positive cells) were quantified using high-resolution confocal images acquired with a 40x confocal microscope, in areas of  $0.1 \text{ mm}^2$ . Error bars show SD.

Thus, these preliminary data suggest that RdCVF does not have a significant effect on the number of cone cell bodies after 1 year. An important point that emerged during the last years, is the role of RdCVFL. It has been shown that AAV-mediated RdCVFL expression can preserve vision, but with less efficiency than with RdCVF (49), as RdCVF promotes cone survival through aerobic glycolysis (48). This work suggests that RdCVFL had not a strong direct effect on cones, but rather that it protects rod function through its thioloxydoreductase activity (49). For this reason, I did not focus on RdCVFL at first.

However, more recent evidence revealed that cones are more vulnerable to oxidative stress when trophic support is reduced (50) –which occurs during retinal degeneration. This work showed that RdCVFL protects cones in rd10 mice after subretinal injection. Therapeutic benefits were measured using ERG recordings and cone counting (170).

Therefore, it appears now that the co-expression of RdCVF and RdCVFL might be better suited than RdCVF alone (170) to be combined with Jaws in providing long term vision restoration.

#### v. Restorative optogenetic therapy using Jaws in blind mice

Here, I faced several difficulties related to recording functional benefits in vivo using optogenetic tools, namely Jaws.

First, I could not use our regular optokinetic setup to evaluate optogenetic vision restoration and combined protective/restorative treatment because of insufficient light intensities that are required to activate Jaws. Indeed, Jaws activation requires above  $10^{16}$

photons/cm<sup>2</sup>/s light intensity. The same was true with all other tests we typically use to assess visual improvements such as ERGs. As a consequence, I used another behavioral test measuring light perception, and ex-vivo multi-electrode array (MEA) recordings to investigate the efficacy of optogenetic cone reactivation using Jaws.

I performed the light/dark box experiment (Figure 37A) using orange light (3x10<sup>16</sup> photons/cm<sup>2</sup>/s) compatible with optogenetic activation on control versus Jaws-injected rd10 animals. I first validated the setup and light intensity with a positive control that consists of subretinal injections of AAV-Jaws (n=11 mice) compared to untreated animals (n=3) as it has previously shown that it is possible to restore vision using this strategy (88, 89). There was a significant difference between the control and SR-Jaws groups (Figure 37B).

In the meantime I optimized specific cone delivery from the vitreous (171). We cloned both PR1.7-GFP and PR1.7-Jaws-GFP plasmids, produced AAV2-7m8 vectors and then I injected them in rd10 mice. There was a significant difference between uninjected (n=3) and IVT-Jaws (n=17) groups, but not between the others, including GFP-IVT (n=3) and Jaws-IVT (n=17) groups (Figure 37C). I now need to increase the number of animals for control groups in this experiment, as there is consequent variability between animals.

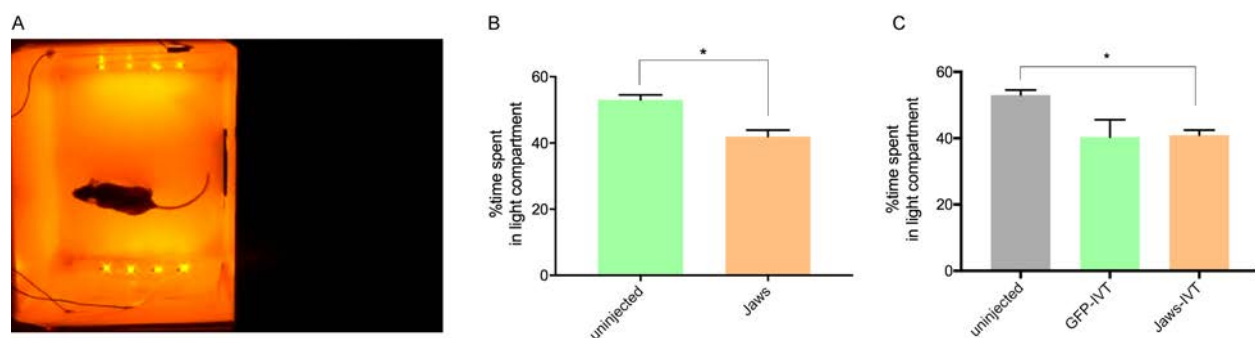


**Figure 37: Evaluation of vision restoration in Jaws injected animals.** (A) Setup of the light/dark box setup with orange light illumination on the left compartment, and a dark compartment (right), to measure light perception. (B-C) Time (in %) spent in light compartment. A total number of 34 animals were analyzed: n=3 for uninjected mice, n=3 for GFP-IVT, n=11 for Jaws mice injected subretinally and n=17 for mice injected intravitreally.

In parallel, I used ex vivo electrophysiology –multi-electrode array recordings (MEA)– to assess the effect of Jaws on blind retinas, and confirm whether RGC reactivation occurs in IVT Jaws-retinas. This is a more precise way of quantifying vision restoration as it can give us the number of ganglion cells responding to light under Jaws treatment condition, which is proportional to the number of cones that are being reactivated.

Jaws-IVT treated retinas showed light responses upon repeated stimulation, which were not observed in GFP control retinas (Figure 38). These MEA results show for the first time that optogenetic reactivation of dormant cones can be achieved with a gene therapy vector delivered intravitreally in blind mice.

With this method, we now aim to demonstrate that an efficient combined neuroprotective and optogenetic treatment is longer-lasting than each treatment alone. For each experimental group, we need to wait for 3 months for the animals to be completely blind—meaning that OS are lost and no detection of cone residual activity— at the time of MEA experiments. These experiments are challenging, mainly because of the variability of retinal degeneration in rd10 mice between each animal, together with the variability associated to injections, resulting percentage of transduced cones and expression levels of Jaws. On top of that, there is also variability with MEA experiments, and it is difficult to obtain spikes from the exact region of interest placed on the microarray.

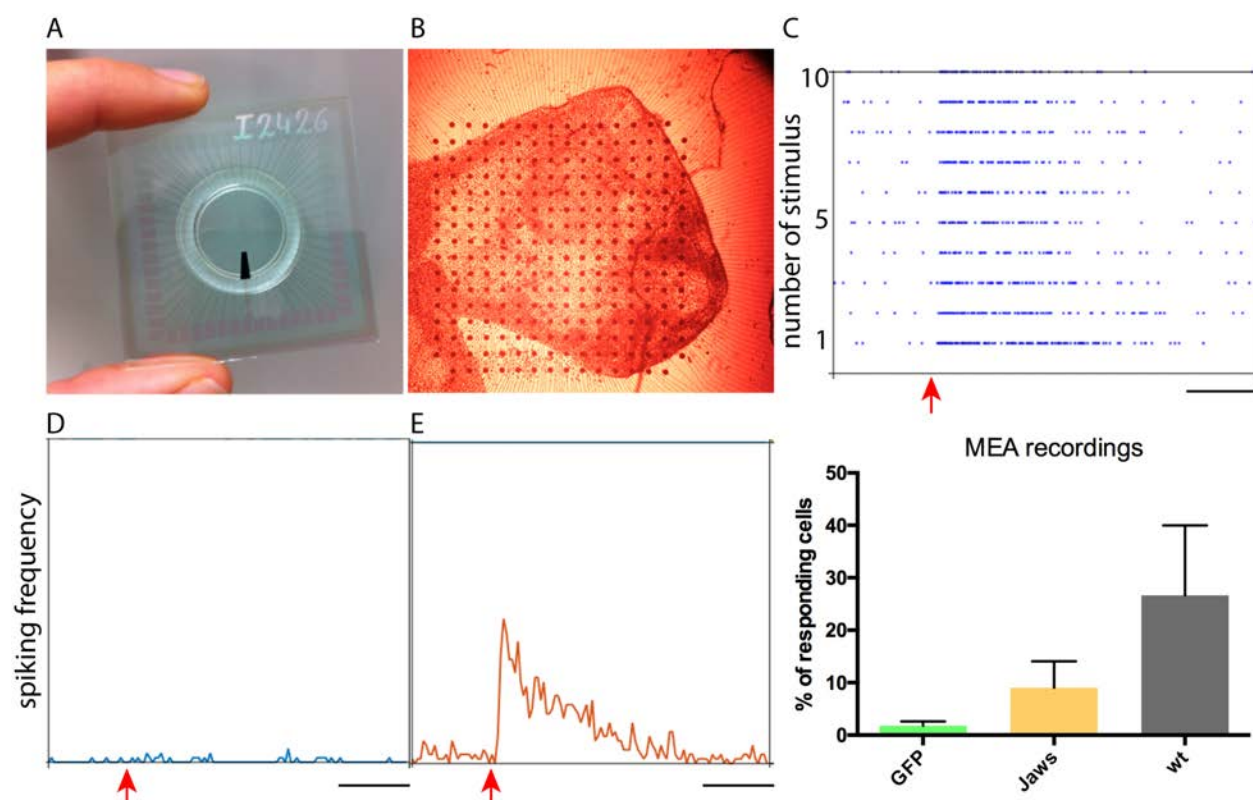
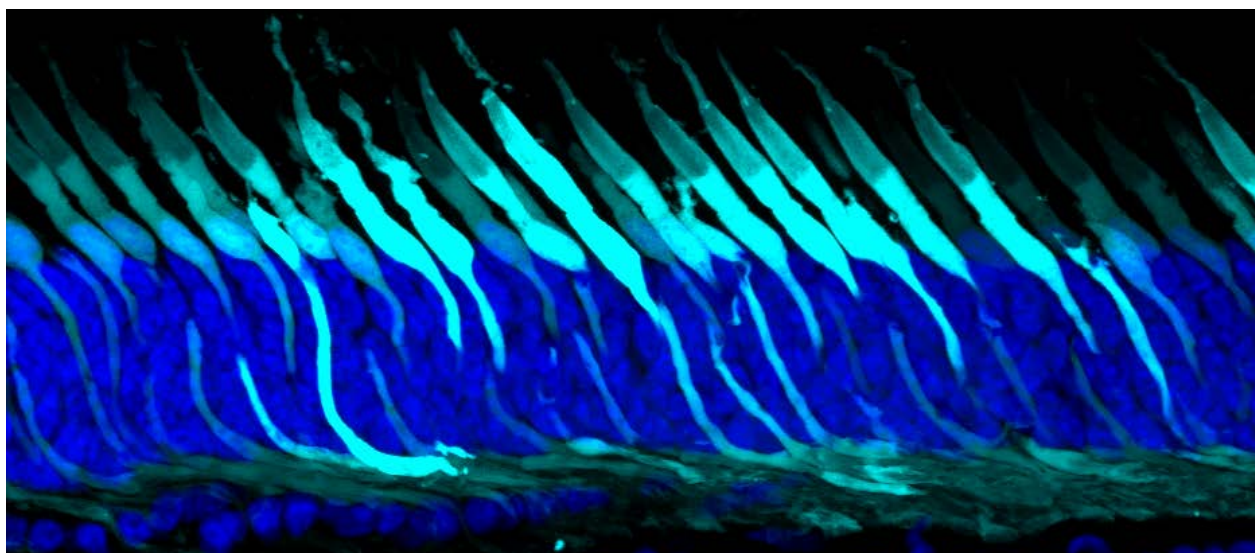


**Figure 38: Ex-vivo recordings of retinal activity after injection with Jaws or GFP. (A)** A multi-electrode array with 254 electrodes. The retina is flat-mounted and placed on top of the electrodes in the center of the array. **(B)** A portion of retina is showed in contact with the electrodes (black dots), ganglion cells facing the array. **(C-E)** Scale bar is 0.5 seconds. **(C)** An example of a cell in a Jaws-transduced retina that was illuminated with orange light. A series of 10 light flashes were applied. Each dot corresponds to a spike and each line to a stimulus (a light flash). Note the increase of the number of spikes after the light stimulus (red arrow): the spiking frequency is increased. **(D)** An example of a cell that does not react to light stimuli: the spike frequency is not modified upon light stimulation (red arrow). **(E)** An example of a cell that reacted to the light flash: the spike frequency is increased upon light stimulation (red arrow). **(F)** Quantification of the number of cells that respond to light upon light stimulus (average of 10 stimulations, n=3 retinas for each condition).

vi. Progress made towards the initial aim and next steps

I performed in vivo and ex vivo experiments that allowed me to improve gene delivery to cones without side effects and to study the efficacy of each treatment using various tests. I eliminated the reason that caused retinal toxicity in my first Jaws-GFP subretinal injection groups and optimized safe and efficient gene delivery to the cones from the vitreous, thereby facilitating analysis of cone reactivation with MEA recordings. We will now test the efficacy of the combined neuroprotective and restorative treatments to obtain maximal therapeutic effects using MEA recordings.

# Discussion & Perspectives





During my thesis I developed viral tools for mutation independent gene therapy strategies to treat rod-cone dystrophies. A certain number of questions were addressed in mice, showing importance of dose sparing and promoter choice for safety. We went further by developing new surgical modalities for efficient gene transfer to cones in non-human primates, with the focus on the fovea for our vision restoration strategy. AAV2-7m8- and AAV9-7m8-PR1.7 capsid-promoter combinations with Jaws provided restoration of light sensitivity in foveal cones. Finally, as our ultimate goal is to reach the clinic to restore sight and maintain it in patients, we are currently attempting to implement a neuroprotective strategy to stave off the loss of optogenetically engineered cones. Altogether my PhD work points to several important considerations in the field:

### **(1) Vector design is a key factor in gene therapy success**

Transduction of target cells is not always feasible with natural capsids. Through the combination of directed evolution and rational design, we have been able to create two new AAVs that answer our therapeutic needs, namely efficient transduction of photoreceptors both intravitreally and subretinally in mice with AAV2-7m8 and AAV9-7m8 (Khabou et al., Biotech Bioeng, 2016) while parental capsids AAV2 and AAV9 are less efficient (subretinally) or not efficient at all (intravitreally).

### **(2) Dose sparing allows preservation of target cells**

There are some evidence that the use of higher vector doses can cause side effects, even if the eye is an immune privileged site (71, 120). In this context we showed that high input AAV dose in the retina can also cause apoptosis, not simply inflammation (Khabou et al., in preparation). Reducing the injected dose can prevent this. The design of highly efficient AAVs and promoters is an essential step to avoid any risk of exacerbating disease state in patients.

Even with enhanced capsids dose sparing is not always possible. It is necessary to have a strong promoter to unlock full capsid potential. The use of ubiquitous promoters can be an option, but is not always relevant in a therapeutic context. For example AAV2-7m8 used at too high doses combined with ubiquitous promoters can cause significant inflammation (124, 162) while when combined with stronger cell type specific promoters and lower doses it is safe (92) and (Khabou et al., JCI Insight, 2018). Also, ubiquitous promoters can potentially lead to transgene expression in antigen presenting cells and therefore compromise long-term therapeutic effects.

### **(3) Translational considerations**

One major argument in favor of the use of the gene therapy tools developed during my thesis is their performance in all tested system models, including mice (in vivo), macaques

(in vivo) and human tissue (in vitro, retinal organoids derived from human iPSCs and post-mortem adult retinal explants). Validation of the use of AAV2-7m8- or AAV9-7m8-PR1.7 capsid-promoter combination in cones of these three species (Khabou et al., JCI Insight, 2018) supports the use of our gene therapy products for clinical applications.

The combination of efficient capsids and strong, cell specific promoters also allowed the development of new surgical modalities to target the fovea in primates, which has been classically possible only with sub-foveal injections. Transduction of foveal cones is compatible with an intravitreal injection of AAV2-7m8-PR1.7 while a distal subretinal delivery of AAV9-7m8-PR1.7 provides expression in both peripheral and central cones through lateral spread of the vector (Khabou et al., JCI Insight, 2018). These new vector-promoter combinations and surgical modalities provide new therapeutic opportunities for treatment of patients affected with RP and achromatopsia.

By taking all of the above-mentioned parameters into account, we can hopefully expand longevity and efficiency of current retinal gene therapies. There are several further developments and applications that can follow up from the work described in this thesis:

### **(1) Development of a Jaws DNA construct without GFP protein**

The paper that originally described the highly efficient hyperpolarizing opsin Jaws, reported a version of the protein that is fused to the GFP (89) and we used the same fusion protein between Jaws and GFP for our studies. In going towards translation, it will be important to design Jaws without GFP as fluorescent proteins should be avoided in clinical application. Correct Jaws expression can be checked with an anti-Jaws antibody. Its functional effect can be tested as well with patch-clamp recordings though it is very challenging without GFP because we cannot easily locate Jaws-cells through fluorescence microscopy. This can be circumvented by another DNA construct that contains both Jaws and GFP but non-fused, separated for example by 2A peptide or IRES sequences.

### **(2) Analysis of immune responses against non-self proteins in mice and primates**

When transferred in patients for gene therapy, Jaws –and other optogenetic constructs in general– is a non-self protein from microbial origin. Its expression in patients has to be safe, not leading to toxicity or immunogenicity in the long term. Although optogenetic vision restoration transferred to patients without any adverse effects thus far (i.e. ChR2 (RetroSense Therapeutics)), it will be important to characterize if any immune responses towards this type of proteins is observed in large animal models at higher doses—even if the eye is an immune privileged site. Whether it happens in the long-term and not only in the short-term is also an important point to investigate.

### **(3) Application of newly described vector tools with other therapeutic proteins or to other retinal dystrophies**

We proved here cone reactivation in macaques with Jaws for treatment of late stage RP patients. However, the tools we developed can also be used for other applications-

Some examples include transfer of *CNGA3* or *CNGB3*, which could potentially restore vision in achromatopsia patients. Expression of these therapeutic proteins has already been done before using peripheral or central subretinal injections in NHPs (71, 144), but not distal ones that transduce the fovea, or intravitreal injections.

AAV2-7m8-PR1.7 provides specific expression of the therapeutic protein in the foveola. Although it is a very relevant expression pattern for late stage RP patients, since only cones of the fovea are preserved at those stages, it would be preferable to extend expression to the periphery for other diseases. In achromatopsia, both peripheral and central cones are preserved and their targeting would allow vision restoration in a larger visual field. Extension has been achieved in the past with subILM injections (164) or after vitrectomy and ILM peeling (163) -although these are more invasive strategies.

AAV9-7m8-PR1.7 is a relevant vector for treatment of achromatopsia and RP since a distal delivery transduces both peripheral and central cones. As it is able to spread laterally and transduce larger areas outside of the bleb, it also allows injection of low volumes (50 $\mu$ L in our study). Finally, this vector has a good tropism for cones and is 30 more infectious than AAV9, thereby allowing dose sparing.

### **(4) Design of long-lasting gene therapies**

- Combination of neuroprotection and optogenetics for RP treatment

The ectopic expression of *Nxn1* gene products, RdCVF or RdCVFL through AAV vectors can slow down vision loss in mice (49, 170), while halorhodopsin (88) or Jaws (89) expression restores light-sensitivity of dormant cones from mice and to primates to humans. We hypothesize that a combination therapy with a neurotrophic strategy and optogenetic protein will be longer lasting than either therapy alone. This would allow us to develop a long-term mutation independent treatment applicable to all forms of RP, while restoring high acuity, close to natural vision.

The precise characterization of RdCVF and RdCVFL during the last years (48–50, 170) suggest that cone death occurs because of RdCVF loss, but also that cones later are nonfunctional –loss of OS– and die because of RdCVFL expression decrease, which leads to oxidative damage in cones. Thus, it appears now that RdCVFL expression could be more

relevant than RdCVF in maintaining dormant cones –i.e. end-stage RP, while RdCVF can be better suited for earlier RP stages. We could thus design an expression cassette containing both RdCVFL and Jaws separated by 2A peptide and under the control of PR1.7 promoter to drive the expression of both therapeutic genes in cones and test vision restoration using this combination.

Also, it has been suggested that the expression of both RdCVF and RdCVFL might be combined to obtain even better therapeutic effects on cones in RP (170). In mice, the strategy to do the proof of concept could be a systemic injection of AAV9-2YF-CAG-RdCVF-2A-RdCVFL, and later an intravitreal injection of AAV2-7m8-Jaws. In NHPs (and potentially in RP patients), a co-injection of AAV2-7m8-CAG-RdCVF and AAV2-7m8-PR1.7-Jaws-2A-RdCVFL could be envisioned.

- Combination of neuroprotection and gene addition

The combination of trophic factor secretion with gene replacement could benefit other retinal disorders: For example combining RPE65 gene addition and RdCVF-RdCVFL mediated neuroprotection may prolong retinal function in LCA (60).



# Bibliography

1. Marshel JH, Garrett ME, Nauhaus I, Callaway EM. Functional specialization of seven mouse visual cortical areas. *Neuron* 2011;72(6):1040–1054.
2. Mustafi D, Engel AH, Palczewski K. Structure of cone photoreceptors. *Prog. Retin. Eye Res.* 2009;28(4):289–302.
3. Euler T, Haverkamp S, Schubert T, Baden T. Retinal bipolar cells: Elementary building blocks of vision. *Nat. Rev. Neurosci.* 2014;15(8):507–519.
4. Masland RH. The Neuronal Organization of the Retina. *Neuron* 2012;76(2):266–280.
5. Chapot CA, Euler T, Schubert T. How do horizontal cells “talk” to cone photoreceptors? Different levels of complexity at the cone–horizontal cell synapse. *J. Physiol.* 2017;595(16):5495–5506.
6. Ferrington D, Sinha D, Kaarniranta K. Defects in Retinal Pigment Epithelial Cell Proteolysis and the Pathology Associated with Age-related Macular Degeneration Deborah. *Prog. Retin. Eye Res.* 2016;51:69–89.
7. Reichenbach A, Bringmann A. New functions of müller cells. *Glia* 2013;61(5):651–678.
8. Franze K et al. Muller cells are living optical fibers in the vertebrate retina. *Proc. Natl. Acad. Sci.* 2007;104(20):8287–8292.
9. Distler C, Dreher Z. Glia cells of the monkey Retina-II. Muller cells. *Vision Res.* 1996;36(16):2381–2394.
10. Nickla DL, Wallman J. The multifunctional choroid. *Prog. Retin. Eye Res.* 2010;29(2):144–168.
11. Kur J, Newman EA, Chan-Ling T. Cellular and physiological mechanisms underlying blood flow regulation in the retina and choroid in health and disease. *Prog. Retin. Eye Res.* 2012;31(5):377–406.
12. Lemke G, Rothlin C V. Immunobiology of the TAM receptors. *Nat. Rev. Immunol.* 2008;8(5):327–336.
13. Tinsley JN et al. Direct detection of a single photon by humans. *Nat. Commun.* 2016;7(1813):1–17.
14. Rieke F. Single photon detection by rod cells of the retina. *Rev. Mod. Phys* 1998;70(3):1027.
15. Tikidji-hamburyan A et al. Rods progressively escape saturation to drive visual responses in daylight conditions. *Nat. Commun.* 2017;8(1813):1–17.
16. Jeon CJ, Strettoi E, Masland RH. The major cell populations of the mouse retina. *J Neurosci* 1998;18(21):8936–8946.
17. Pang JJ et al. Achromatopsia as a Potential Candidate for Gene Therapy. *Adv Exp Med Biol* 2010;664:639–646.
18. Viets K, Eldred KC, Johnston RJ. Mechanisms of Photoreceptor Patterning in Vertebrates and Invertebrates. *Trends Genet.* 2016;32(10):638–659.

19. Baden T et al. A tale of two retinal domains: Near-Optimal sampling of achromatic contrasts in natural scenes through asymmetric photoreceptor distribution. *Neuron* 2013;80(5):1206–1217.
20. El-Amraoui A, Petit C. The retinal phenotype of Usher syndrome: Pathophysiological insights from animal models. *Comptes Rendus - Biol.* 2014;337(3):167–177.
21. M B. Through the eyes of a mouse. *Nature* 2013;502:156–158.
22. Larsson T a, Larhammar D, Nordstro K, Nordström K, Larsson T a. Evolution of vertebrate rod and cone phototransduction genes. *Philos. Trans. R. Soc. London* 2009;364(1531):2867–2880.
23. Wang JS, Kefalov VJ. The Cone-specific visual cycle. *Prog. Retin. Eye Res.* 2012;30(2):115–128.
24. Ingram NT, Sampath AP, Fain GL. Why are rods more sensitive than cones ?. *J. Physiol.* 2016;19:5415–5426.
25. Wässle H, Grünert U, Röhrenbeck J, Boycott BB. Cortical magnification factor and the ganglion cell density of the primate retina. *Nature* 1989;341:643–646.
26. Provis JM, Dubis AM, Maddess T, Carroll J. Adaptation of the central retina for high acuity vision: Cones, the fovea and the avascular zone. *Prog. Retin. Eye Res.* 2013;35:63–81.
27. Snodderly DM, Weinhaus RS, Choi JC. Neural-Vascular Relationships Monkeys (Macaca fascicularis) in Central Retina of Macaque. *J. Neurosci.* 1992;12(4):1169–1193.
28. John D, Kuriakose T, Devasahayam S, Braganza A. Dimensions of the foveal avascular zone using the Heidelberg retinal angiogram-2 in normal eyes. *Indian J. Ophthalmol.* 2011;59(1):9–11.
29. Mitchell JF, Leopold DA. The marmoset monkey as a model for visual neuroscience. *Neurosci. Res.* 2015;93:20–46.
30. Rossi EA, Roorda A. The relationship between visual resolution and cone spacing in the human fovea. *Nat. Neurosci.* 2009;13(2):156–157.
31. Curcio CA, Sloan KR, Kalina RE, Hendrickson AE. Human Photoreceptor Topography. *J. Comp. Neurol.* 1990;292:497–523.
32. Baden T, Euler T. Early vision: Where (Some of) the magic happens. *Curr. Biol.* 2013;23(24):R1096–R1098.
33. Sinha R et al. Cellular and Circuit Mechanisms Shaping the Perceptual Properties of the Primate Fovea [Internet]. *Cell* 2017;168(3):413–426.e12.
34. Ban N, Siegfried CJ, Apte RS. Monitoring Neurodegeneration in Glaucoma: Therapeutic Implications. *Trends Mol. Med.* 2017;xx:1–11.
35. Kingman S. Glaucoma is second leading cause of blindness globally. *Bull. World Health Organ.* 2004;82(11):887–888.
36. Wright AF et al. Photoreceptor degeneration: Genetic and mechanistic dissection of a complex trait. *Nat. Rev. Genet.* 2010;11(4):273–284.
37. Guillonneau X et al. On phagocytes and macular degeneration. *Prog. Retin. Eye Res.* 2017;61:98–128.
38. Bennett J. Taking Stock of Retinal Gene Therapy: Looking Back and Moving Forward. *Mol. Ther.* 2017;25(5):1076–1094.

39. Buch H et al. Prevalence and Causes of Visual Impairment and Blindness among 9980 Scandinavian Adults: The Copenhagen City Eye Study. *Ophthalmology* 2004;111(1):53–61.
40. Hamel C. Retinitis pigmentosa. *Orphanet J. Rare Dis.* 2006;1(1):1–12.
41. Luo YHL, da Cruz L. The Argus® II Retinal Prosthesis System. *Prog. Retin. Eye Res.* 2016;50:89–107.
42. Dias MF et al. Molecular genetics and emerging therapies for retinitis pigmentosa: Basic research and clinical perspectives. *Prog. Retin. Eye Res.* 2017;(October):1–25.
43. Dalkara D, Goureau O, Marazova K, Sahel J-A. Let There Be Light: Gene and Cell Therapy for Blindness. *Hum. Gene Ther.* 2016;27(2):134–147.
44. Campochiaro PA, Mir TA. The mechanism of cone cell death in Retinitis Pigmentosa. *Prog. Retin. Eye Res.* 2017;62:24–37.
45. Léveillard T et al. Identification and characterization of rod-derived cone viability factor. *Nat. Genet.* 2004;36(7):755–759.
46. Yang Y et al. Functional Cone Rescue by RdCVF Protein in a Dominant Model of Retinitis Pigmentosa. *Mol. Ther.* 2009;17(5):787–795.
47. Léveillard T, Sahel JA. Rod-derived cone viability factor for treating blinding diseases: From clinic to redox signaling. *Sci. Transl. Med.* 2010;2(26):1–6.
48. Aït-Ali N et al. Rod-derived cone viability factor promotes cone survival by stimulating aerobic glycolysis. *Cell* 2015;161(4):817–832.
49. Byrne LC et al. Viral-mediated RdCVF and RdCVFL expression protects cone and rod photoreceptors in retinal degeneration. *J. Clin. Invest.* 2015;125(1):105–116.
50. Elachouri G et al. Thioredoxin rod-derived cone viability factor protects against photooxidative retinal damage. *Free Radic. Biol. Med.* 2015;81:22–29.
51. Fischer A, Hacein-Bey-Abina S, Cavazzana-Calvo M. 20 years of gene therapy for SCID. *Nat. Immunol.* 2010;11(6):457–460.
52. Nathwani AC et al. Long-Term Safety and Efficacy of Factor IX Gene Therapy in Hemophilia B. *N. Engl. J. Med.* 2014;371(21):1994–2004.
53. Ylä-Herttuala S. Endgame: Glybera finally recommended for approval as the first gene therapy drug in the European union. *Mol. Ther.* 2012;20(10):1831–1832.
54. Morrison C. Landmark gene therapy poised for US approval. *Nat. Rev. Drug Discov.* 2017;16(11):739–741.
55. Bainbridge JWB et al. Effect of gene therapy on visual function in Leber's congenital amaurosis. *N. Engl. J. Med.* 2008;358(21):2231–2239.
56. Hauswirth WW et al. Treatment of leber congenital amaurosis due to RPE65 mutations by ocular subretinal injection of adeno-associated virus gene vector: short-term results of a phase I trial. *Hum. Gene Ther.* 2008;19(10):979–990.
57. Maguire AM et al. Safety and efficacy of gene transfer for Leber's congenital amaurosis. *N. Engl. J. Med.* 2008;358(21):2240–2248.
58. Bainbridge JWB et al. Long-Term Effect of Gene Therapy on Leber's Congenital Amaurosis. *N. Engl. J. Med.* 2015;372(20):150504083137004.
59. Cideciyan A V et al. Human gene therapy for RPE65 isomerase deficiency activates the retinoid cycle of vision but with slow rod kinetics. *Proc. Natl. Acad. Sci. U. S. A.* 2008;105(39):15112–7.



60. Cideciyan A V et al. Human retinal gene therapy for Leber congenital amaurosis shows advancing retinal degeneration despite enduring visual improvement. *Proc. Natl. Acad. Sci. U. S. A.* 2013;517–525.
61. Jacobson SG et al. Improvement and Decline in Vision with Gene Therapy in Childhood Blindness. *N. Engl. J. Med.* 2015;150503141523009.
62. Le Meur G et al. Safety and Long-Term Efficacy of AAV4 Gene Therapy in Patients with RPE65 Leber Congenital Amaurosis. *Mol. Ther.* 2017;26(1):256–268.
63. Simonelli F et al. Gene therapy for leber's congenital amaurosis is safe and effective through 1.5 years after vector administration. *Mol. Ther.* 2009;18(3):643–650.
64. Maguire AM et al. Age-dependent effects of RPE65 gene therapy for Leber's congenital amaurosis: a phase 1 dose-escalation trial. *Lancet* 2015;374(9701):1597–1605.
65. Testa F et al. Three-year follow-up after unilateral subretinal delivery of adeno-associated virus in patients with leber congenital amaurosis type 2. *Ophthalmology* 2013;120(6):1283–1291.
66. Bennett J et al. Safety and durability of effect of contralateral-eye administration of AAV2 gene therapy in patients with childhood-onset blindness caused by RPE65 mutations: a follow-on phase 1 trial. *Lancet* 2016;388(10045):661–672.
67. Moore NA, Morral N, Ciulla TA, Bracha P. Gene therapy for inherited retinal and optic nerve degenerations. *Expert Opin. Biol. Ther.* 2017;18(1):1–13.
68. Maclaren RE et al. Retinal gene therapy in patients with choroideremia: Initial findings from a phase 1/2 clinical trial. *Lancet* 2014;383(9923):1129–1137.
69. Edwards TL et al. Visual Acuity after Retinal Gene Therapy for Choroideremia [Internet]. *N. Engl. J. Med.* 2016;374(20):1996–1998.
70. Auricchio A, Smith AJ, Ali RR. The future looks brighter after 25 years of retinal gene therapy. *Hum. Gene Ther.* 2017;28(11):982–987.
71. Reichel FF et al. AAV8 Can Induce Innate and Adaptive Immune Response in the Primate Eye. *Mol. Ther.* 2017;25(12):1–13.
72. Koch SF et al. Halting progressive neurodegeneration in advanced retinitis pigmentosa. *J. Clin. Invest.* 2015;125(9):9–11.
73. Grieger J, Samulski R. Adeno-associated Virus as a Gene Therapy Vector: Vector Development, Production and Clinical Applications. In: *Adv Biochem Engin/Biotech.* 2005:119–145
74. Lock M et al. Rapid, Simple, and Versatile Manufacturing of Recombinant Adeno-Associated Viral Vectors at Scale. *Hum. Gene Ther.* 2010;21(10):1259–1271.
75. Ghazi NG et al. Treatment of retinitis pigmentosa due to MERTK mutations by ocular subretinal injection of adeno-associated virus gene vector: results of a phase I trial. *Hum. Genet.* 2016;135(3):327–343.
76. Hamburger V. Neuronal death in the spinal ganglia of the chick embryo and its reduction by nerve growth factor. *J. Neurosci.* 1981;1(1):60–71.
77. Hofer MM, Barde YA. Brain-derived neurotrophic factor prevents neuronal death in vivo. *Nature* 1988;331:261–262.
78. Sendtner M, Kreutzberg GW, Thoenen H. Ciliary neurotrophic factor prevents the degeneration of motor neurons after axotomy. *Nature* 1990;345:440–441.
79. Faktorovich EG, Steinberg RH, Yasumura D, Matthes MT, LaVail MM.

Photoreceptor degeneration in inherited retinal dystrophy delayed by basic fibroblast growth factor. *Nature* 1990;347(6288):83–86.

80. Henderson C et al. GDNF: a potent survival factor for motoneurons present in peripheral nerve and muscle. *Science* (80-. ). 1994;266(5187):1062–1064.

81. Dalkara D et al. AAV mediated GDNF secretion from retinal glia slows down retinal degeneration in a rat model of retinitis pigmentosa. *Mol. Ther.* 2011;19(9):1602–1608.

82. Liang FQ et al. Long-term protection of retinal structure but not function using rAAV.CNTF in animal models of retinitis pigmentosa. *Mol. Ther.* 2001;4(5):461–472.

83. Bok D et al. Effects of adeno-associated virus-vectored ciliary neurotrophic factor on retinal structure and function in mice with a P216L rds/peripherin mutation. *Exp. Eye Res.* 2002;74(6):719–735.

84. Sanftner LHM, Abel H, Hauswirth WW, Flannery JG. Glial Cell Line Derived Neurotrophic Factor Delays Photoreceptor Degeneration in a Transgenic Rat Model of Retinitis Pigmentosa. *Mol. Ther.* 2001;4(6):622–629.

85. Lau D et al. Retinal degeneration is slowed in transgenic rats by AAV-mediated delivery of FGF-2. *Investig. Ophthalmol. Vis. Sci.* 2000;41(11):3622–3633.

86. Green ES et al. Two animal models of retinal degeneration are rescued by recombinant adeno-associated virus-mediated production of FGF-5 and FGF-18. *Mol. Ther.* 2001;3(4):507–515.

87. Krol J, Roska B. Rods feed cones to keep them alive. *Cell* 2015;161(4):706–708.

88. Buskamp V et al. Genetic reactivation of cone photoreceptors restore visual responses in Retinitis pigmentosa. *Science* (80-. ). 2010;329:413–417.

89. Chuong AS et al. Noninvasive optical inhibition with a red-shifted microbial rhodopsin. *Nat. Neurosci.* 2014;17(8):1123–1129.

90. Zhang F et al. Optogenetic interrogation of neural circuits: Technology for probing mammalian brain structures. *Nat. Protoc.* 2010;5(3):439–456.

91. Sengupta A et al. Red-shifted channelrhodopsin stimulation restores light responses in blind mice, macaque retina, and human retina. *EMBO Mol. Med.* 2016;8(11):1248–1264.

92. Chaffiol A et al. A New Promoter Allows Optogenetic Vision Restoration with Enhanced Sensitivity in Macaque Retina. *Mol. Ther.* 2017;25(11):2546–2560.

93. Buskamp V, Roska B. Optogenetic approaches to restoring visual function in retinitis pigmentosa. *Curr. Opin. Neurobiol.* 2011;21(6):942–946.

94. Dalkara D, Duebel J, Sahel JA. Gene therapy for the eye focus on mutation-independent approaches. *Curr. Opin. Neurol.* 2015;28(1):51–60.

95. Trapani I, Puppo A, Auricchio A. Vector platforms for gene therapy of inherited retinopathies. *Prog. Retin. Eye Res.* 2014;43:108–128.

96. Souied EH et al. Non-invasive gene transfer by iontophoresis for therapy of an inherited retinal degeneration. *Exp. Eye Res.* 2008;87(3):168–175.

97. Cai X et al. Gene delivery to mitotic and postmitotic photoreceptors via compacted DNA nanoparticles results in improved phenotype in a mouse model of retinitis pigmentosa. *FASEB J.* 2010;24(4):1178–1191.

98. Cai X et al. A partial structural and functional rescue of a retinitis pigmentosa

model with compacted DNA nanoparticles. *PLoS One* 2009;4(4):e5290.

99. Han Z et al. Comparative Analysis of DNA Nanoparticles and AAVs for Ocular Gene Delivery. *PLoS One* 2012;7(12):1–11.

100. Farjo R, Skaggs J, Quiambao AB, Cooper MJ, Naash MI. Efficient Non-Viral Ocular Gene Transfer with Compacted DNA Nanoparticles. *PLoS One* 2006;(1):e38.

101. Ding X et al. Ocular Delivery of Compacted DNA-Nanoparticles Does Not Elicit Toxicity in the Mouse Retina. *PLoS One* 2009;4(10):e7410.

102. Butterfield GL et al. Evolution of a designed protein assembly encapsulating its own RNA genome. *Nature* 2017;552(7685):415–420.

103. Bemelmans A et al. Lentiviral Gene Transfer of Rpe65 Rescues Survival and Function of Cones in a Mouse Model of Leber Congenital Amaurosis. *Plos Med.* 2006;3(10):e347.

104. Matet A et al. Evaluation of tolerance to lentiviral LV-RPE65 gene therapy vector after subretinal delivery in non-human primates. *Transl. Res.* 2017;188:40–57.e4.

105. Planul A, Dalkara D. Vectors and Gene Delivery to the Retina. *Annu. Rev. Vis. Sci.* 2017;3(1):121–140.

106. Melnick JL, Mayor HD, Smith KO, Rapp F. Association of 20-Millimicron Particles with Adenoviruses. *J. Bacteriol.* 1965;90(1):271–274.

107. Kotterman MA, Schaffer D V. Engineering adeno-associated viruses for clinical gene therapy. *Nat. Rev. Genet.* 2014;15(7):445–451.

108. Leberherz C, Maguire A, Tang W, Bennett J, Wilson JM. Novel AAV serotypes for improved ocular gene transfer. *J. Gene Med.* 2010;10(4):375–382.

109. Trapani I et al. Effective delivery of large genes to the retina by dual AAV vectors. *EMBO Mol. Med.* 2014;6(2):194–211.

110. Maddalena A et al. Triple vectors expand AAV transfer capacity in the retina. *Mol. Ther.* 2018;26(2):1–18.

111. Gurda BL et al. Capsid Antibodies to Different Adeno-Associated Virus Serotypes Bind Common Regions. *J. Virol.* 2013;87(16):9111–9124.

112. Srivastava A. In vivo tissue-tropism of adeno-associated viral vectors. *Curr. Opin. Virol.* 2016;21:75–80.

113. Pillay S et al. An essential receptor for adeno-associated virus infection. *Nature* 2016;530(7588):108–112.

114. Summerford C, Samulski RJ. AAVR: A multi-serotype receptor for AAV. *Mol. Ther.* 2016;24(4):663–666.

115. Büning H, Perabo L, Coutelle O, Quadts-Humme S, Hallek M. Recent developments in adeno-associated virus vector technology. *J. Gene Med.* 2008;10:717–733.

116. Hirsch ML et al. Viral Single-Strand DNA Induces p53-Dependent Apoptosis in Human Embryonic Stem Cells. *PLoS One* 2011;6(11):1–13.

117. Ulusoy A, Sahin G, Björklund T, Aebischer P, Kirik D. Dose Optimization for Long-term rAAV-mediated RNA Interference in the Nigrostriatal Projection Neurons. *Mol. Ther.* 2009;17(9):1574–1584.

118. Cearley CN, Wolfe JH. Transduction characteristics of adeno-associated virus vectors expressing cap serotypes 7, 8, 9, and Rh10 in the mouse brain. *Mol. Ther.*

2006;13(3):528–37.

119. Klein RL et al. Efficient Neuronal Gene Transfer with AAV8 Leads to Neurotoxic Levels of Tau or Green Fluorescent Proteins. *Mol. Ther.* 2006;13(3):517–527.

120. Vandenberghe LH et al. Dosage Thresholds for AAV2 and AAV8 Photoreceptor Gene Therapy in Monkey. *Sci. Transl. Med.* 2011;3(88):88ra54.

121. Berns KI, Muzyczka N. AAV: An Overview of Unanswered Questions. *Hum. Gene Ther.* 2017;28(4):308–313.

122. Mingozi F, High KA. Overcoming the Host Immune Response to Adeno-Associated Virus Gene Delivery Vectors: The Race Between Clearance, Tolerance, Neutralization, and Escape. *Annu. Rev. Virol.* 2017;4:511–534.

123. Le Meur G et al. Postsurgical assessment and long-term safety of recombinant adeno-associated virus-mediated gene transfer into the retinas of dogs and primates. *Arch. Ophthalmol.* 2005;123(4):500–506.

124. Dalkara D et al. In vivo-directed evolution of a new adeno-associated virus for therapeutic outer retinal gene delivery from the vitreous. *Sci. Transl. Med.* 2013;5(189):189ra76.

125. Nork TM et al. Functional and Anatomic Consequences of Subretinal Dosing in the Cynomolgus Macaque. *Arch. Ophthalmol.* 2013;130(1):65–75.

126. Dalkara D, Sahel JA. Gene therapy for inherited retinal degenerations. *Comptes Rendus - Biol.* 2014;337(3):185–192.

127. Anderson DH, Fisher SK. The relationship of primate foveal cones to the pigment epithelium. *J. Ultrastructure Res.* 1979;67(1):23–32.

128. Kita M, Marmor MF. Retinal Adhesive Force in Living Rabbit, Cat, and Monkey Eyes Normative Data and Enhancement by Mannitol and Acetazolamide. *Invest. Ophthalmol. Vis. Sci.* 1992;33(6):1879–1882.

129. Snodderly DM, Sandstrom MM, Leung IY, Zucker CL, Neuringer M. Retinal Pigment Epithelial Cell Distribution in Central Retina of Rhesus Monkeys. *Investig. Ophthalmology Vis. Sci.* 2002;43(9):2815–2818.

130. Ochakovski GA et al. Subretinal injection for gene therapy does not cause clinically significant outer nuclear layer thinning in normal primate foveae. *Investig. Ophthalmol. Vis. Sci.* 2017;58(10):4155–4160.

131. Jacobson SG et al. Gene Therapy for Leber Congenital Amaurosis caused by RPE65 mutations: Safety and Efficacy in Fifteen Children and Adults Followed up to Three Years. *Arch. Ophthalmol.* 2012;130(1):9–24.

132. Duncan JL. Visual Consequences of Delivering Therapies to the Subretinal Space. *JAMA Ophthalmol.* 2017;135(3):242–243.

133. Yin L et al. Intravitreal injection of AAV2 transduces macaque inner retina. *Investig. Ophthalmol. Vis. Sci.* 2011;52(5):2775–2783.

134. Allocca M et al. Novel adeno-associated virus serotypes efficiently transduce murine photoreceptors. *J. Virol.* 2007;81(20):11372–11380.

135. Vandenberghe LH et al. AAV9 Targets Cone Photoreceptors in the Nonhuman Primate Retina. *PLoS One* 2013;8(1):e53463.

136. Petrs-Silva H et al. Novel properties of tyrosine-mutant AAV2 vectors in the mouse retina. *Mol. Ther.* 2011;19(2):293–301.

137. Petrs-Silva H et al. High-efficiency transduction of the mouse retina by tyrosine-mutant AAV serotype vectors. *Mol. Ther.* 2009;17(3):463–471.
138. Summerford C, Samulski RJ. Membrane-associated heparan sulfate proteoglycan is a receptor for adeno-associated virus type 2 virions. *J. Virol.* 1998;72(2):1438–1445.
139. Macé E et al. Targeting channelrhodopsin-2 to ON-bipolar cells with vitreally administered AAV restores ON and OFF visual responses in blind mice. *Mol. Ther.* 2014;23:7–16.
140. Reid CA, Ertel KJ, Lipinski DM. Improvement of Photoreceptor Targeting via Intravitreal Delivery in Mouse and Human Retina Using Combinatory rAAV2 Capsid Mutant Vectors. *Investig. Ophthalmology Vis. Sci.* 2017;58(14):6429.
141. Bainbridge JWB et al. Stable rAAV-mediated transduction of rod and cone photoreceptors in the canine retina. *Gene Ther.* 2003;10:1336–1344.
142. Boye SE et al. The Human Rhodopsin Kinase Promoter in an AAV5 Vector Confers Rod- and Cone-Specific Expression in the Primate Retina. *Hum. Gene Ther.* 2012;23(10):1101–1115.
143. Dyka FM et al. Cone Specific Promoter for Use in Gene Therapy of Retinal Degenerative Diseases. *Adv Exp Med Biol* 2014;801:695–701.
144. Ye G et al. Safety and Biodistribution Evaluation in Cynomolgus Macaques of rAAV2tYF-PR1.7-hCNGB3, a Recombinant AAV Vector for Treatment of Achromatopsia. *Hum. Gene Ther.* 2016;27(1):37–48.
145. Ye G et al. Safety and Biodistribution Evaluation in CNGB3-Deficient Mice of rAAV2tYF-PR1.7-hCNGB3, a Recombinant AAV Vector for Treatment of Achromatopsia. *Hum. Gene Ther.* 2016;27(1):27–37.
146. Ye G et al. Cone-Specific Promoters for Gene Therapy of Achromatopsia and Other Retinal Diseases. *Hum. Gene Ther.* 2016;27(1):72–82.
147. Goncalves MAF V et al. Transfer of the Full-Length Dystrophin-Coding Sequence into Muscle Cells by a Dual High-Capacity Hybrid Viral Vector with Site-Specific Integration Ability. *J. Virol.* 2005;79(5):3146–3162.
148. Martino AT et al. The genome of self-complementary adeno-associated viral vectors increases Toll-like receptor 9 – dependent innate immune responses in the liver. *Blood* 2011;117(24):6459–6468.
149. Bennicelli J et al. Reversal of blindness in animal models of leber congenital amaurosis using optimized AAV2-mediated gene transfer. *Mol. Ther.* 2008;16(3):458–465.
150. Fischer MD et al. Codon-Optimized RPGR Improves Stability and Efficacy of AAV8 Gene Therapy in Two Mouse Models of X-Linked Retinitis Pigmentosa. *Mol. Ther.* 2017;25(8):1854–1865.
151. Patrício MI, Barnard AR, Orlans HO, McClements ME, MacLaren RE. Inclusion of the Woodchuck Hepatitis Virus Posttranscriptional Regulatory Element Enhances AAV2-Driven Transduction of Mouse and Human Retina. *Mol. Ther. - Nucleic Acids* 2017;6:198–208.
152. Kaplitt MG et al. Safety and tolerability of gene therapy with an adeno-associated virus (AAV) borne. *Lancet* 2007;369:2097–2105.
153. Bourdenx M, Dutheil N, Bezard E, Dehay B. Systemic gene delivery to the

central nervous system using Adeno-associated virus. *Front. Mol. Neurosci.* 2014;7(50):1–8.

154. Dalkara D et al. Inner limiting membrane barriers to AAV-mediated retinal transduction from the vitreous. *Mol. Ther.* 2009;17(12):2096–2102.

155. Kolstad KD et al. Changes in Adeno-Associated Virus-Mediated Gene Delivery in Retinal Degeneration 2010;578:571–578.

156. Vacca O et al. AAV-mediated gene delivery in Dp71-null mouse model with compromised barriers. *Glia* 2014;62(3):468–476.

157. Heegaard S, Jensen OA, Prause JU. Structure and composition of the inner limiting membrane of the retina. *Graefe's Arch. Clin. Exp. Ophthalmol.* 1986;224(4):355–360.

158. Barhoum R et al. Functional and structural modifications during retinal degeneration in the rd10 mouse. *Neuroscience* 2008;155(3):698–713.

159. Slijkerman RWN et al. The pros and cons of vertebrate animal models for functional and therapeutic research on inherited retinal dystrophies. *Prog. Retin. Eye Res.* 2015;48:137–159.

160. Kotterman M a et al. Antibody neutralization poses a barrier to intravitreal adeno-associated viral vector gene delivery to non-human primates. *Gene Ther.* 2014;1–11.

161. Barker SE et al. Subretinal delivery of adeno-associated virus serotype 2 results in minimal immune responses that allow repeat vector administration in immunocompetent mice. *J. Gene Med.* 2009;11:486–497.

162. Ramachandran P et al. Evaluation of dose and safety of AAV7m8 and AAV8BP2 in the non-human primate retina. *Hum. Gene Ther.* 2016;1–40.

163. Takahashi K et al. Improved Intravitreal AAV-Mediated Inner Retinal Gene Transduction after Surgical Internal Limiting Membrane Peeling in Cynomolgus Monkeys. *Mol. Ther.* 2017;25(1):296–302.

164. Boye SE et al. Highly Efficient Delivery of Adeno-Associated Viral Vectors to the Primate Retina. *Hum. Gene Ther.* 2016;27(8):580–597.

165. Comander J et al. Novel Surgical Method for Intravitreal AAV Administration Overcomes Transduction Barriers in Non-Human Primates. *Mol. Ther.* 2016;24:S13–S14.

166. Khabou H et al. Insight into the mechanisms of enhanced retinal transduction by the engineered AAV2 capsid variant -7m8. *Biotechnol. Bioeng.* 2016;113(12):2712–2724.

167. Li ZY, Kljavin IJ, Milam AH. Rod photoreceptor neurite sprouting in retinitis pigmentosa. *J. Neurosci.* 1995;15(8):5429–38.

168. Azoulay-Sebban L. Study of the anatomical and functional correlations for Retinitis Pigmentosa: Identification of predictive markers and validation of new biomarkers. 2015;

169. Fradot M, Buskamp V, Bennett J. Gene Therapy in Ophthalmology : Validation on Cultured. *Hum. Gene Ther.* 2011;593(May):587–593.

170. Mei X et al. The Thioredoxin Encoded by the Rod-Derived Cone Viability Factor Gene Protects Cone Photoreceptors Against Oxidative Stress. *Antioxidants Redox Signal.* 2016;24(16):909–923.

171. Khabou H et al. Noninvasive gene delivery to foveal cones for vision restoration. *JCI Insight* 2018;3(2):e96029.



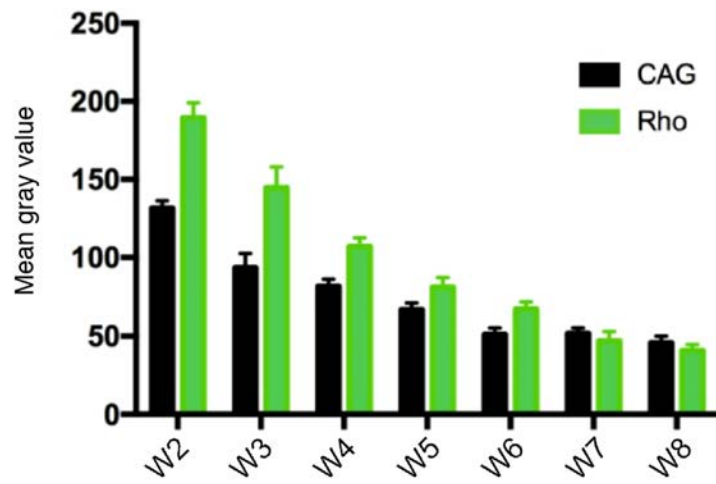
# Annexes



## I. **Supplementary results of Chapter I**

## Supplementary results

### Supplementary Figure 1



**Supplementary figure 1 :** GFP expression follow-up using eye fundus imaging after subretinal injections of AAV8-CAG-GFP and AAV8-Rho-GFP. A dose of  $5 \times 10^{11}$  vg was administered.

## II. Supplementary results of Chapter II

**Table S1:** AAV vectors used in this study. Genomic titers of AAV-CAG-GFP vector stocks were determined by quantitative real-time PCR.

GFP vector	Genomic titers (vector genomes vg/mL)
AAV2	$6 \times 10^{12}$
AAV2-7m8	$3 \times 10^{12}$
AAV2-scramble (AAKKTIENTRA)	$3 \times 10^{12}$
AAV2-Ala	$8 \times 10^{11}$
AAV2-7m8.Ala	$2 \times 10^{11}$
AAV5	$2 \times 10^{13}$
AAV5-7m8	$1 \times 10^{14}$
AAV5-Ala	$6.91 \times 10^{12}$
AAV5-7m8.Ala	$4.91 \times 10^{11}$
AAV9	$2 \times 10^{13}$
AAV9-7m8	$6 \times 10^{12}$
AAV9-Ala	$2.34 \times 10^{12}$
AAV9-7m8.Ala	$1.42 \times 10^{11}$
AAV8	$7.5 \times 10^{13}$
AAV8-7m8	$9 \times 10^{13}$

**Figure S1.** In vitro transduction efficiency of AAV2, 5, 9 and their mutated versions analyzed by flow cytometry.

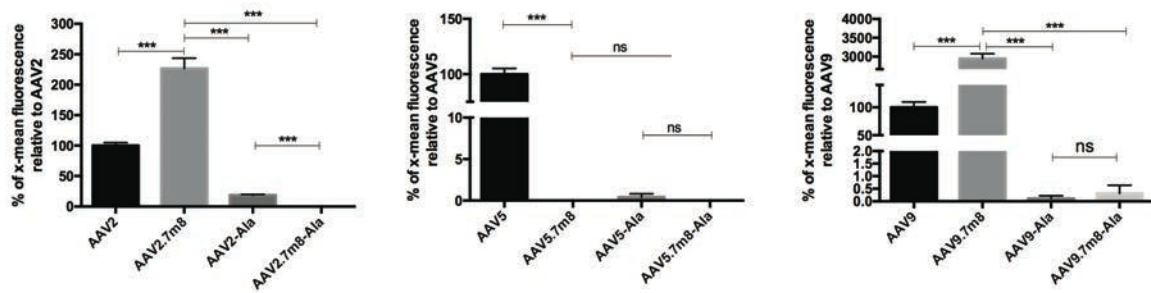
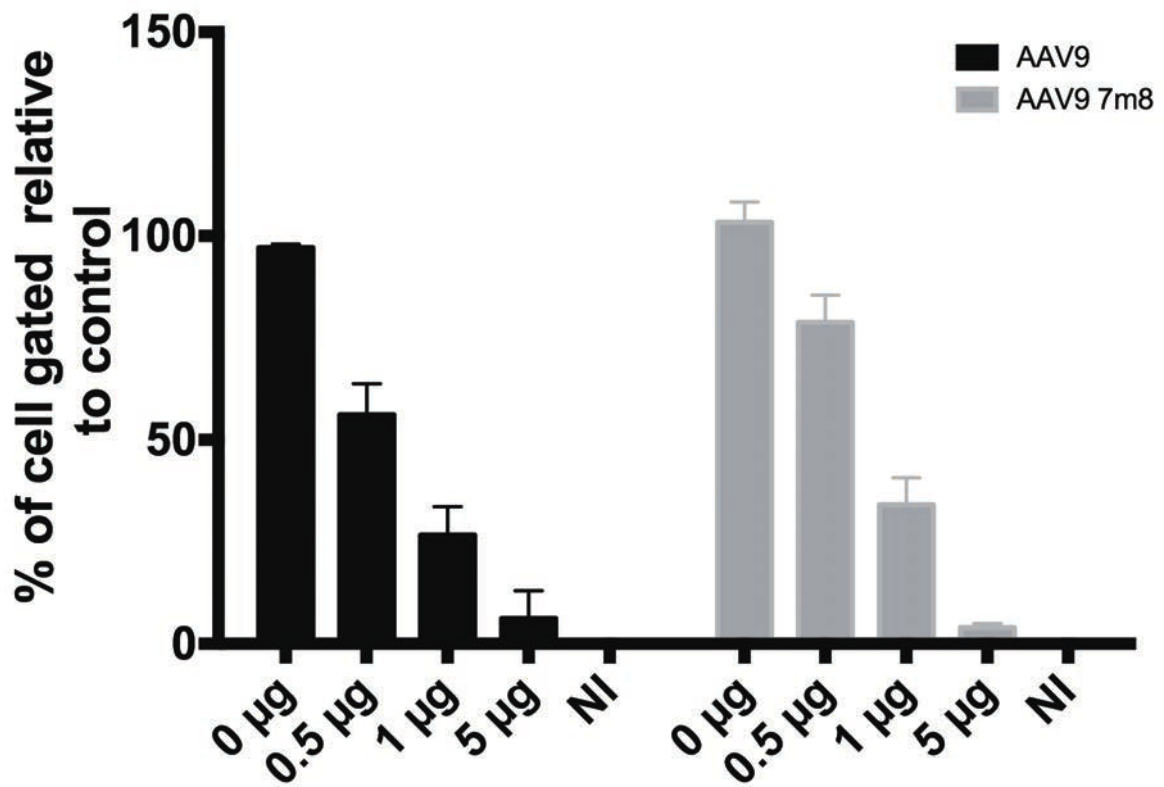
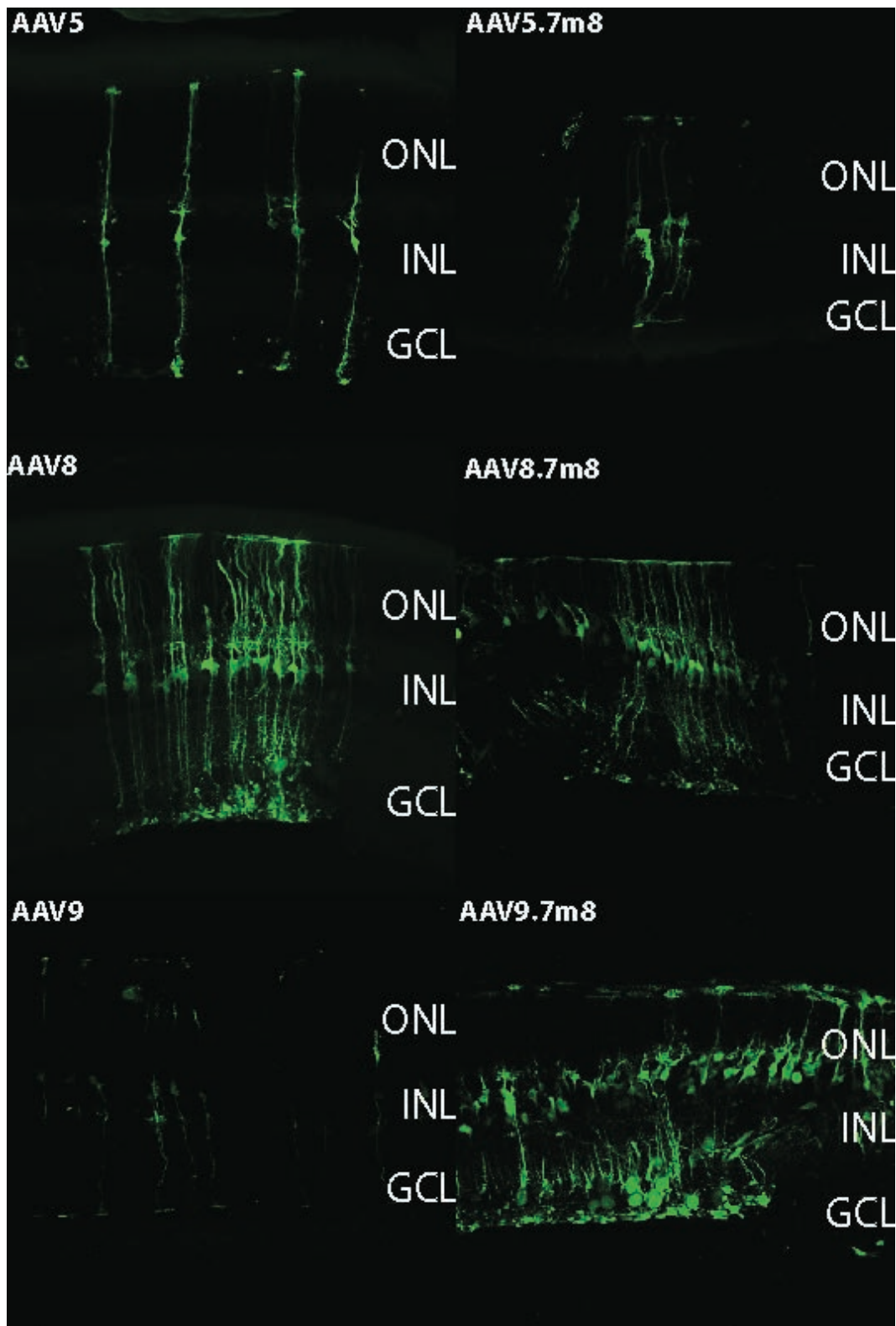


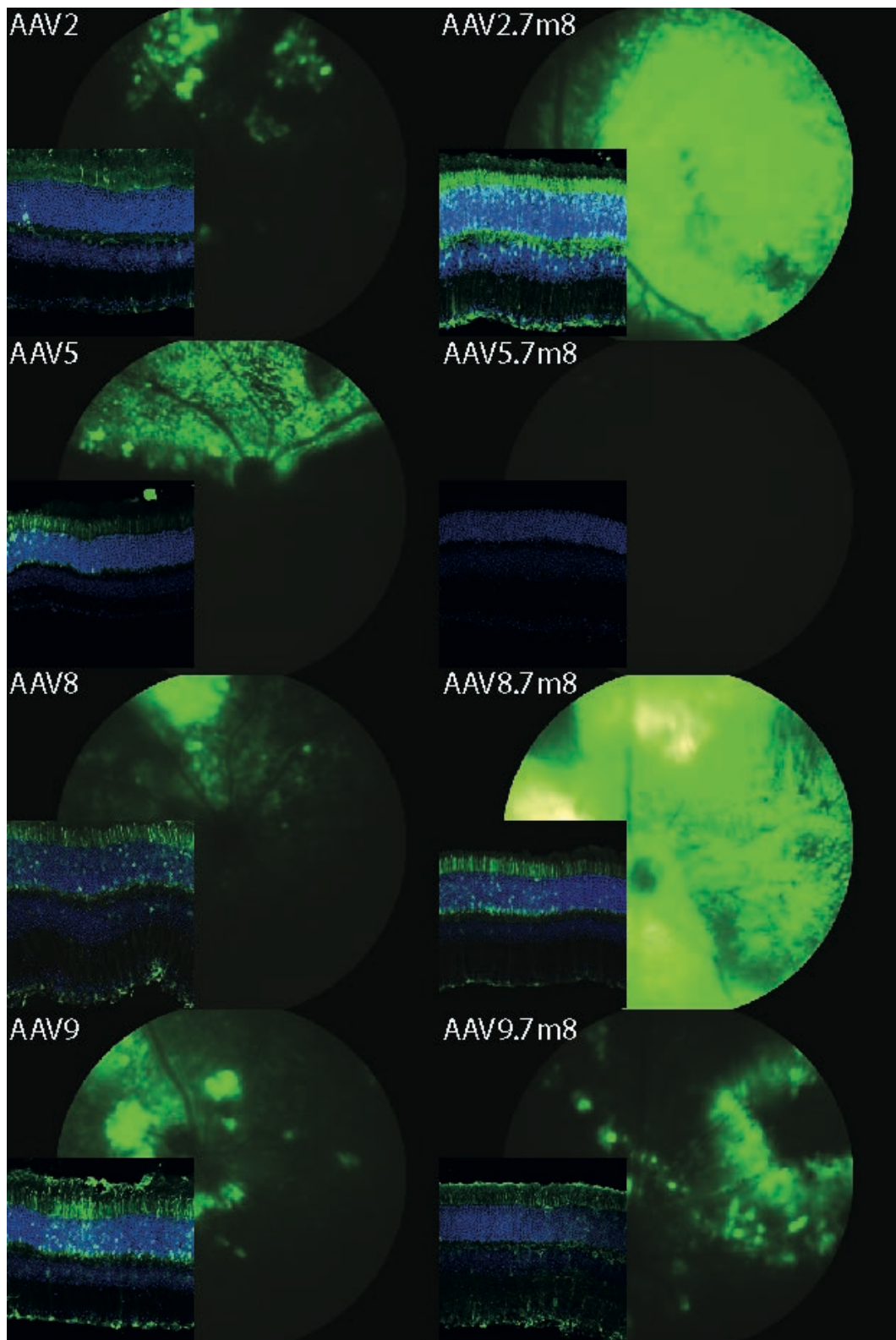
Figure S2. Receptor binding properties of AAV9 and AAV9-7m8.



**Figure S3.** Effect of 7m8 insertion on the retinal tropism of AAV5-, AAV8- and AAV9-CAG-GFP vectors after intravitreal injections.



**Figure S4.** Retinal transduction efficiency of AAV2, 5, 8, 9, and their peptide insertion variants after subretinal injection.

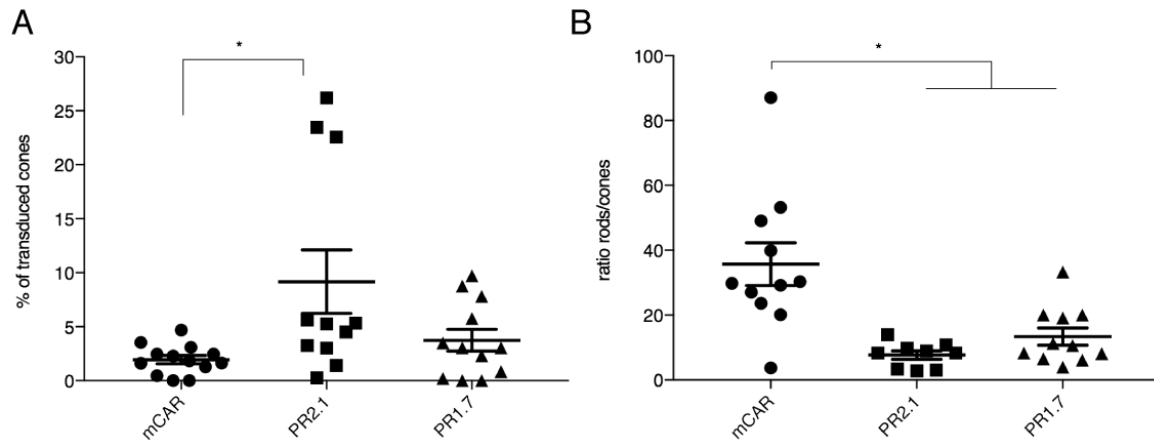




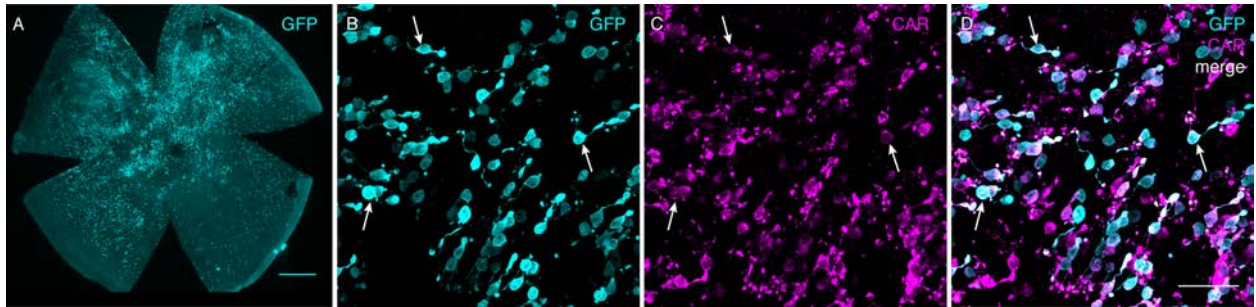
### III. Supplementary results of Chapter III

## Supplemental data

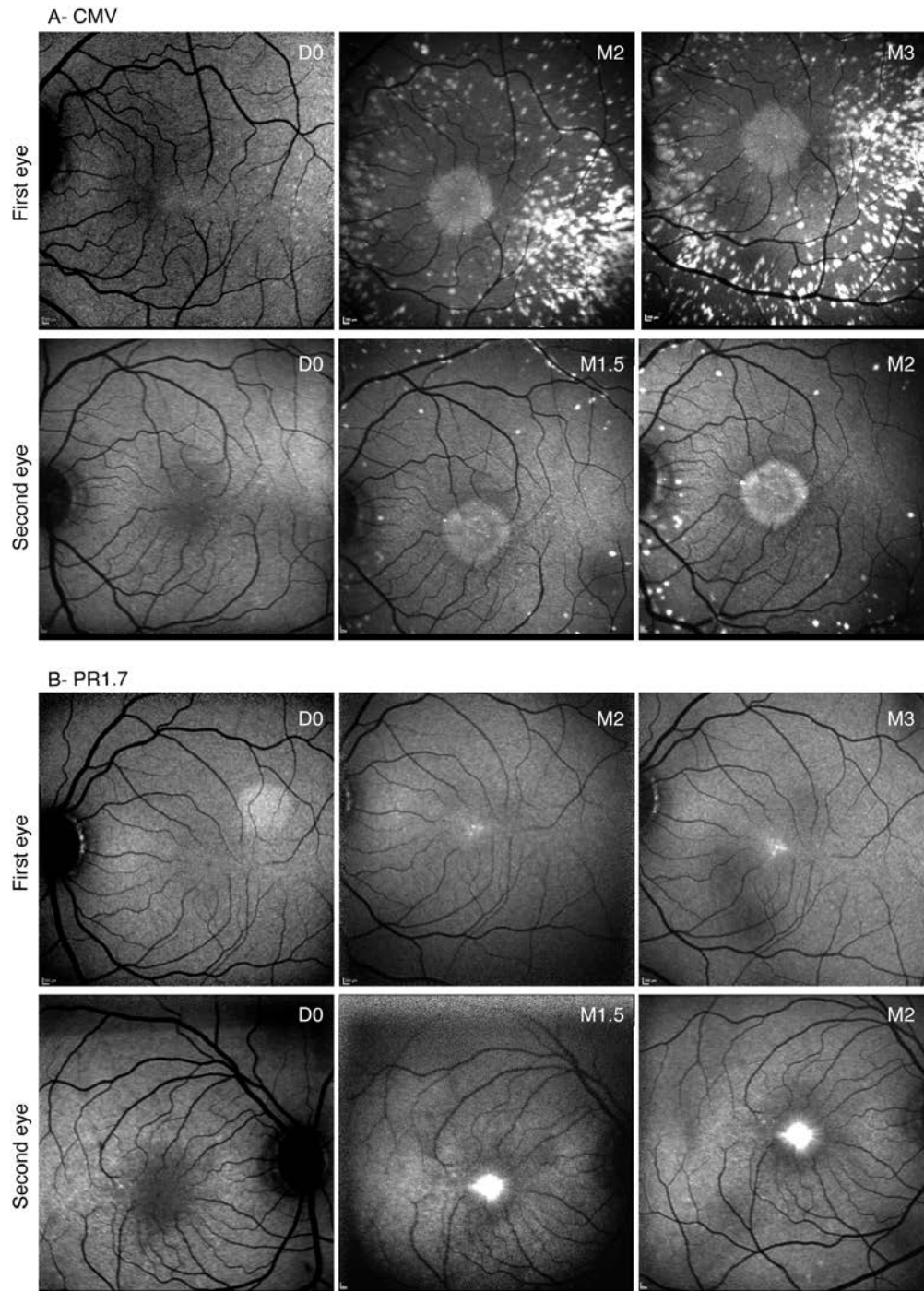
### Supplemental Figure and Figure Legends



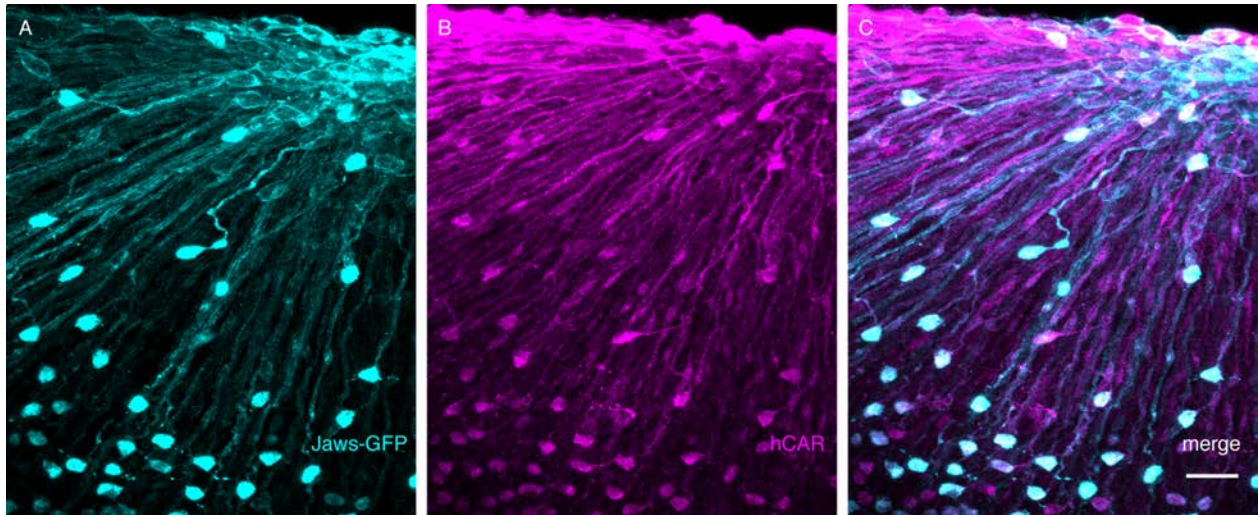
**Supplemental Figure 1: Quantification of cone transduction efficiency after intravitreal administration of AAV2-7m8-GFP in mice using mCAR, PR1.7 or PR2.1 promoters (n=4 eyes per condition).** (A) Quantification of the percentage of transduced cones based on flatmount images and colocalization of GFP and cone arrestin stainings. (B) Evaluation of the specificity of the promoters in the photoreceptor layer expressed as the ratio of number of transduced rods over the number of transduced cones. Data represent mean  $\pm$  SEM and were analyzed with ANOVA multiple comparison test. AAV: adeno-associated virus; mCAR: mouse cone arrestin promoter; PR1.7 and PR2.1: promoters of 1.7 and 2.1 kilobases in length, respectively, based on the human red opsin gene enhancer and promoter sequences.



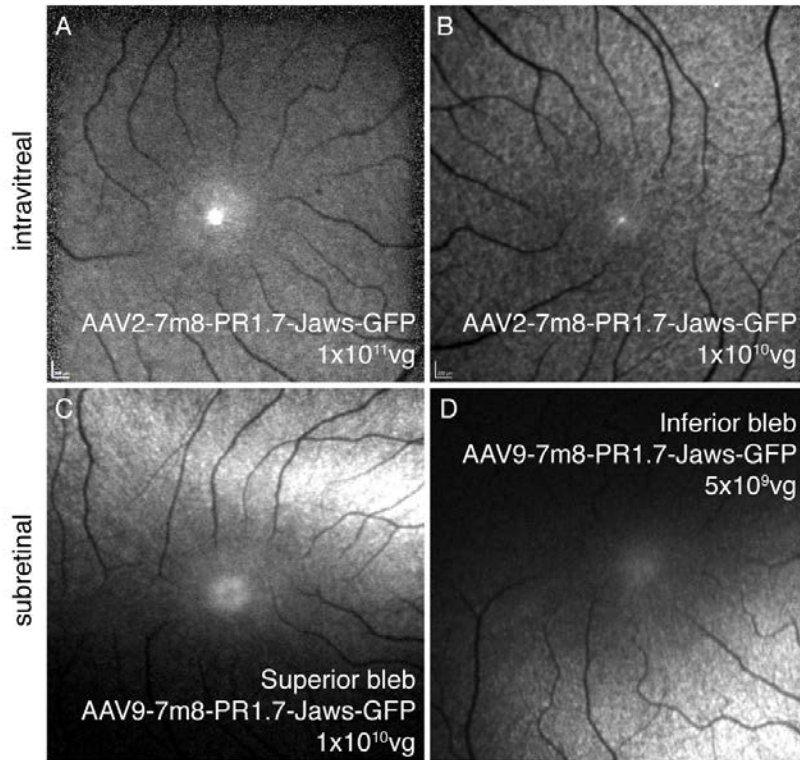
**Supplemental Figure 2: Cone transduction after intravitreal administration of AAV2-7m8-GFP in rd10 mice using PR1.7 promoter. (n=4 eyes)** (A) GFP expression in a 3-months old rd10 retinal whole-mount two months after injection. The retina is mounted with photoreceptor layer facing upwards. Scale bar is 500  $\mu\text{m}$ . (B-D) Zoom into the whole-mount retina shown in D. Scale bar is 40  $\mu\text{m}$ . (B) Cone cell bodies remaining after degeneration expressing GFP (cyan). (C) Cone arrestin immunostaining is shown in magenta. (D) Colocalization of GFP and cone arrestin stainings. AAV: adeno-associated virus; PR1.7: Promoter 1.7kilobases in length, based on the human red opsin gene enhancer and promoter sequences; rd10: retinal degeneration 10 mouse model for retinitis pigmentosa.



**Supplemental Figure 3: GFP expression follow-up after intravitreal administration of AAV2-7m8 under the control of CMV and PR1.7 promoters (n=2 per condition). (A) Eye fundus images of CMV treated eyes. (B) Eye fundus images of PR1.7 treated eyes. D0: Day of injection, pre-dose; M1.5, 2, 3: Month 1.5, 2, 3 after injection. AAV: adeno-associated virus; CMV: cytomegalovirus promoter; PR1.7: Promoter 1.7kilobases in length, based on the human red opsin gene enhancer and promoter sequences.**

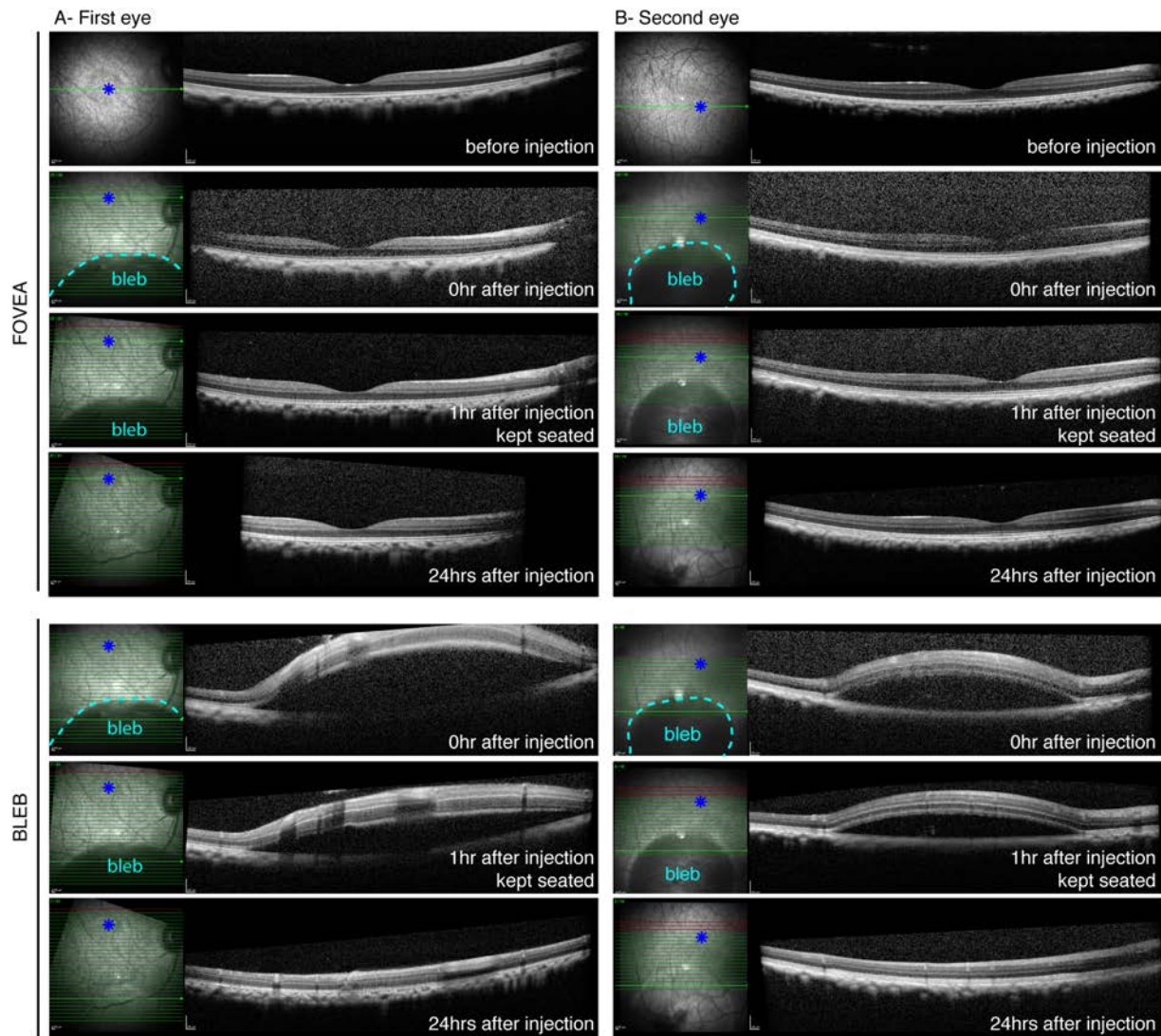


**Supplemental Figure 4: Cone transduction in the fovea after intravitreal administration of  $1 \times 10^{11}$  vg of AAV2-7m8-PR1.7-Jaws-GFP in one macaque eye (A) Jaws-GFP expression in foveal whole-mount two months after injection (cyan). (B) Human cone arrestin immunostaining is shown in magenta. (C) Colocalization of GFP and cone arrestin stainings. Scale bar is 20  $\mu\text{m}$ . AAV: adeno-associated virus; hCAR: human cone arrestin; PR1.7: Promoter 1.7kilobases in length, based on the human red opsin gene enhancer and promoter sequences.**



**Supplemental Figure 5: Macaque eye fundus images for characterization of dose response.**

Jaws-GFP expression two months after intravitreal injection of  $10^{11}$  particles (n=1 eye) (A) and  $10^{10}$  particles (B) of AAV2-7m8-PR1.7-Jaws-GFP (n=1 eye). Jaws-GFP expression two weeks after subretinal injection of  $1 \times 10^{10}$  particles (n=1 eye, superior bleb) (C) and  $5 \times 10^9$  particles (n=2 eyes, inferior blebs) (D) of AAV9-7m8-PR1.7-Jaws-GFP. AAV: adeno-associated virus, vg: viral genome; PR1.7: Promoter 1.7kilobases in length, based on the human red opsin gene enhancer and promoter sequences.



**Supplemental Figure 6: Distal inferior subretinal administration follow-up using in vivo eye fundus and optical coherence tomography (OCT) imaging.** Images were acquired before and after peripheral injection of AAV9-7m8-PR1.7-Jaws-GFP,  $5 \times 10^9$  viral particles (n=2 eyes). Eye fundus infrared image is centered on the macula and OCT image was taken at the level of the fovea or at the level of the bleb shortly before and after the injections. Follow-up images were acquired one hour after injections while the animal was kept seated. Another image was acquired 24 hours after injections. Bleb: subretinally injected fluid; hrs: hours; AAV: adeno-associated virus, PR1.7: Promoter 1.7kilobases in length, based on the human red opsin gene enhancer and promoter sequences. Dark blue asterisk: fovea; bold green arrows: OCT image of the retina highlighted with the dark green arrow, is shown on the right part of each image; dashed cyan line: delimitation of the bleb.

## Supplemental Tables

### **Supplemental Table 1: Transcription factors' binding sites analysis for red opsin gene based promoters, PR2.1 and PR1.7.**

Gene identification number	Gene title	Protein symbol	OPN1LW Promoter fragment			Probe set	Signal Intensity		
			Site number				Identification number	Robust Multi-array Average (RMA)	
			2061 bp	1724 bp	337 bp			Mean	Standard deviation
196	Aryl hydrocarbon receptor	AHR	1	1	0	202820_at	48.4	1.8	
467	Activating transcription factor 3	ATF3	2	2	0	202672_s_at	51.6	14.4	
1051	CCAAT/enhancer binding protein beta	CEBPB	55	41	14	212501_at	206.3	35.5	
1406	Cone-rod homeobox	CRX	12	11	1	217510_at	1638.3	96.4	
2002	ELK1. ETS transcription factor	ELK1	11	9	2	203617_x_at	86.8	2.6	
2353	Fos proto-oncogene. AP-1 transcription factor subunit	FOS	9	8	1	209189_at	744.1	174.7	
2969	General transcription factor Iii	GTF2I	54	44	10	210892_s_at	41.6	4.8	
3091	Hypoxia inducible factor 1 alpha subunit	HIF1A	1	1	0	200989_at	810.1	29.1	
3725	Jun proto-oncogene. AP-1 transcription factor subunit	JUN	27	23	4	201464_x_at	377.4	50.9	
4150	MYC associated zinc finger protein	MAZ	3	3	0	212064_x_at	157.3	6.9	
4205	Myocyte enhancer factor 2A	MEF2A	1	1	0	212535_at	203.8	3.5	
4782	Nuclear factor I C	NFIC	36	38	8	226895_at	195.6	11.3	
4800	Nuclear transcription factor Y subunit alpha	NFYA	4	3	1	228433_at	43.3	1.7	
10062	Nuclear receptor subfamily 1 group H member 3	NR1H3	12	11	1	217370_x_at	174.6	17.2	
7025	Nuclear receptor subfamily 2	NR2F1 /	1	0	1	209505_at	128.6	10.2	



	group F member 1	COUP-TF1						
2908	Nuclear receptor subfamily 3 group C member 1	NR3C1	173	140	33	201865_x_at	164.7	8.6
5451	POU class 2 homeobox 1	POU2F1	3	2	1	227254_at	192.6	7.2
5465	Peroxisome proliferator activated receptor alpha	PPARA	6	5	1	223437_at	232.0	19.6
5914	Retinoic acid receptor alpha	RARA	3	3	0	216300_x_at	40.0	1.9
5915	Retinoic acid receptor beta	RARB	6	6	0	205080_at	64.4	3.0
3516	Recombination signal binding protein for immunoglobulin kappa J region	RBPJ	2	2	0	211974_x_at	435.6	29.7
5970	RELA proto-oncogene. NF-kB subunit	RELA	3	3	0	201783_s_at	53.3	3.7
6256	Retinoid X receptor alpha	RXRA	26	22	4	202449_s_at	146.0	6.8
6667	Sp1 transcription factor	SP1	2	1	1	224754_at	158.2	6.6
6772	Signal transducer and activator of transcription 1	STAT1	4	4	0	200887_s_at	160.0	13.7
6908	TATA-box binding protein	TBP	14	11	3	203135_at	76.7	2.7
6925	Transcription factor 4	TCF4	2	2	0	212386_at	526.0	30.8
6934	Transcription factor 7 like 2	TCF7L2	6	5	1	212761_at	140.6	8.4
8463	TEA domain transcription factor 2	TEAD2	8	5	3	243766_s_at	53.4	2.4
7020	Transcription factor AP-2 alpha	TFAP2A	28	23	5	204653_at	264.8	29.5
7068	Thyroid hormone receptor beta	THRB	10	9	1	229657_at	106.4	5.3
7392	Upstream transcription factor 2	USF2	5	5	0	202152_x_at	176.8	9.4
7528	YY1 transcription factor	YY1	18	15	3	201901_s_at	379.0	22.4

PR1.7 and PR2.1: promoters of 1.7 and 2.1 kilobases in length, respectively, based on the human red opsin gene enhancer and promoter sequences; bp: base pairs.

**Supplemental Table 2: Transcription factors' binding sites analysis for mouse cone arrestin (mCAR) promoter.**

Gene identification number	Gene title	Protein symbol	Mouse <i>Arr3</i> Promotor fragment		Probe set	Signal Intensity		
			Site number			Identification number	Robust Multi-array Average (RMA)	
			3207 bp (-3170/+37)	521 bp (-510/+11)			Mean	Standard deviation
8546	Adaptor-related protein complex 3. beta 1 subunit	AP3B1	5	0	203142_s_at	55.3	2.1	
1386	Activating transcription factor 2	ATF2	1	0	212984_at	150.2	5.2	
467	Activating transcription factor 3	ATF3	5	0	202672_s_at	51.6	14.4	
79365	Basic helix-loop-helix family member e41	BHLHE41	5	0	221530_s_at	1083.9	64.2	
1051	CCAAT/enhancer binding protein beta	CEBPB	221	37	212501_at	206.3	35.5	
1406	Cone-rod homeobox	CRX	19	6	217510_at	1638.3	96.4	
1998	E74 like ETS transcription factor 2	ELF2	2	0	203822_s_at	91.9	2.8	
2002	ELK1. ETS transcription factor	ELK1	10	2	203617_x_at	86.8	2.6	
2353	Fos proto-oncogene. AP-1 transcription factor subunit	FOS	146	25	209189_at	744.1	174.7	
2969	General transcription factor Iii	GTF2I	3	0	210892_s_at	41.6	4.8	
3280	Hes family bHLH transcription factor 1	HES1	26	0	203394_s_at	522	71.3	
3725	Jun proto-oncogene. AP-1 transcription factor subunit	JUN	85	8	201464_x_at	377.4	50.9	
3726	JunB proto-oncogene. AP-1 transcription factor subunit	JUNB	2	0	201473_at	369.1	77.6	
3727	JunD proto-oncogene. AP-1 transcription factor subunit	JUND	20	2	203752_s_at	580.8	63.8	

4150	MYC associated zinc finger protein	MAZ	14	3	212064_x_at	157.3	6.9
4205	Myocyte enhancer factor 2A	MEF2A	4	0	212535_at	203.8	3.5
4520	Metal regulatory transcription factor 1	MTF1	2	1	227150_at	112.8	4.9
4782	Nuclear factor I C	NFIC	110	28	226895_at	195.6	11.3
4784	Nuclear factor I X	NFIX	1	0	227400_at	101	8.1
4800	Nuclear transcription factor Y	NFYA	53	0	204108_at	44.4	1.8
4801		NFYB			218127_at	104.1	6.1
4802		NFYC			202215_s_at	101	4.6
10062	Nuclear receptor subfamily 1 group H member 3	NR1H3	26	2	217370_x_at	174.6	17.2
7025	Nuclear receptor subfamily 2 group F member 1	NR2F1 / COUP-TF1	2	1	209505_at	128.6	10.2
2908	Nuclear receptor subfamily 3 group C member 1	NR3C1	297	46	201865_x_at	164.7	8.6
5080	Paired box 6	PAX6	1	0	205646_s_at	1430.4	87.3
5451	POU class 2 homeobox 1	POU2F1	3	0	227254_at	192.6	7.2
5465	Peroxisome proliferator activated receptor alpha	PPARA	6	0	223437_at	232	19.6
5914	Retinoic acid receptor alpha	RARA	3	1	216300_x_at	40	1.9
5915	Retinoic acid receptor beta	RARB	11	4	205080_at	64.4	3
3516	Recombination signal binding protein for immunoglobulin kappa J region	RBPJ	4	1	211974_x_at	435.6	29.7
5970	RELA proto-oncogene, NF-kB subunit	RELA	16	2	201783_s_at	53.3	3.7
6256	Retinoid X receptor alpha	RXRA	41	6	202449_s_at	146	6.8
6670	Sp3 transcription factor	SP3	3	1	213168_at	155.7	7.5
6722	Serum response factor	SRF	3	1	202401_s_at	58.6	4.1
6772	Signal transducer and activator of transcription 1	STAT1	15	1	200887_s_at	160	13.7
6908	TATA-box binding protein	TBP	110	17	203135_at	76.7	2.7

6925	Transcription factor 4	TCF4	2	0	212386_at	526	30.8
6934	Transcription factor 7 like 2	TCF7L2	8	1	212761_at	140.6	8.4
8463	TEA domain transcription factor 2	TEAD2	1	0	243766_s_at	53.4	2.4
7020	Transcription factor AP-2 alpha	TFAP2A	61	7	204653_at	264.8	29.5
7024	Transcription factor CP2	TFCP2	5	0	209338_at	100.1	3.6
7030	Transcription factor binding to IGHM enhancer 3	TFE3	65	3	212457_at	226.9	7
7068	Thyroid hormone receptor beta	THRB	5	0	229657_at	106.4	5.3
7528	YY1 transcription factor	YY1	67	5	201901_s_at	379	22.4

bp: base pairs.



# Abstract

Vision is our most cherished sense and its loss is a feared handicap. A highly diverse and complex array of inherited retinal degenerations leads to irreversible vision loss. Today, there is no cure for such disorders. However, in the last decade, many gene therapies entered clinical trials offering hope for the treatment of inherited retinal degenerations. In this thesis, we explored the contribution of viral vectors within the general context of retinal gene therapy. We focused on optimization of viral vectors for mutation-independent gene therapies broadly applicable across rod-cone dystrophies. We carefully designed vectors for targeting cones and studied their translational potential for optogenetic activation of cones in several relevant model systems.

Our vectors were first screened in rodents eliminating vectors lacking specificity. This allowed us to choose, a strong cone-cell specific promoter for further development. Since mice do not have a fovea, we then validated the efficacy and specificity of our promoter in combination with selected capsids and delivery routes in non-human primates. In this species we showed that AAV9-7m8 –which is 30 times more infectious than AAV9– provides efficient foveal cone transduction when injected subretinally several millimeters away from the fovea. Moreover, we showed AAV2-7m8 can target foveal cones with a well-tolerated dose administered intravitreally. Both delivery modalities resulted in high-level optogene expression leading to light responses in cones. Lastly, we validated the efficacy of these vectors on human cones, using retinal organoids derived from human induced pluripotent stem cells (iPS cells) and post-mortem human retinas. Collectively, our data support proof of concept for therapeutic potential of this gene therapy product for cone reactivation using optogenetics in late-stage RP. Our vector-promoter combinations can also be useful in future gene replacement therapy for diseases like achromatopsia where large spread of transgene expression is desirable. As a future aim, we hope to extend the toolset developed here to allow co-expression of trophic factors prolonging cone survival.

# Résumé

La vision est notre sens le plus cher et sa perte est un handicap redouté. Or, il existe un ensemble très hétérogène et complexe de dégénérescences rétiniennes héréditaires entraînant une perte de vision irréversible. Aujourd'hui, il n'y a pas de traitement pour ces maladies. Cependant, au cours de la dernière décennie, de nombreuses thérapies géniques ont été testées dans des essais cliniques, donnant de l'espoir pour le traitement des dégénérescences rétiniennes héréditaires. Dans cette thèse, nous avons exploré l'apport des vecteurs viraux dans le contexte général de la thérapie génique rétinienne. Nous avons plus particulièrement optimisé des vecteurs viraux pour des thérapies géniques indépendantes des mutations, largement applicables à toutes les dystrophies rétiniennes avec dégénérescence de bâtonnets puis cônes. Nous avons conçu des vecteurs pour cibler les cônes et étudié leur potentiel de translation pour l'activation optogénétique des cônes dans plusieurs systèmes modèles pertinents.

Nos vecteurs ont d'abord été testés sur des rongeurs, permettant d'éliminer les vecteurs non spécifiques. Cela nous a permis de choisir un promoteur fort et spécifique des cônes pour poursuivre l'étude. Comme les souris n'ont pas de fovéa, nous avons ensuite validé l'efficacité et la spécificité de notre promoteur en combinaison avec des capsides et des voies d'administration choisies pour les primates non humains. Chez cette espèce, nous avons montré que l'AAV9-7m8 - qui est 30 fois plus infectieux que l'AAV9- permet une transduction efficace des cônes fovéolaires lorsqu'il est injecté sous la rétine à plusieurs millimètres de la fovéa. De plus, nous avons montré qu'AAV2-7m8 peut cibler les cônes fovéolaires avec une dose bien tolérée et administrée par voie intravitreuse. Les deux modalités d'administration ont permis une forte expression de l'optogène, permettant la sensibilité à la lumière des cônes. Enfin, nous avons validé l'efficacité de ces vecteurs sur les cônes humains, à l'aide d'organoïdes rétiniens dérivés de cellules souches pluripotentes induites (cellules iPS) et de rétines humaines post-mortem. Collectivement, nos données soutiennent la preuve de concept du potentiel thérapeutique de ce produit de thérapie génique pour la réactivation des cônes à l'aide de l'optogénétique en phase avancée de RP. Nos combinaisons de vecteur-promoteur peuvent également être utiles dans la thérapie de remplacement génique pour des maladies comme l'achromatopsie où une large distribution de l'expression du transgène est souhaitable. Notre futur objectif est d'étendre l'ensemble des outils développés ici pour permettre la co-expression avec des facteurs trophiques prolongeant la survie des cônes.